A nature “ copy-paste ” approach for an efficient metal-free polymerization route

Leila Mezzasalma

THÈSE EN COTUTELLE PRÉSENTÉE

POUR OBTENIR LE GRADE DE

DOCTEUR DE

L'UNIVERSITÉ DE BORDEAUX

ET DE L'UNIVERSITÉ DE MONS

ÉCOLE DOCTORALE DES SCIENCES CHIMIQUES

SPÉCIALITÉ POLYMÈRES

Par Leila MEZZASALMA

A NATURE « COPY-PASTE » APPROACH FOR AN EFFICIENT METAL-FREE POLYMERIZATION ROUTE

Sous la direction de Dr. Olivier Coulembier
et de Pr. Daniel Taton

Soutenue le 07 mars 2019

Membres du jury:

M. LAZZARONI, Roberto	Professeur, Univ. de Bordeaux, France	Président
Mme. MARTIN-VACA, Blanca	Professeur, Univ. de Toulouse, France	Rapporteur
Mme. JEROME, Christine	Professeur, Univ. de Liège, Belgique	Rapporteur
M. PERUCH, Frédéric	Directeur de Recherches CNRS, France	Examinateur
M. COULEMBIER, Olivier	Chercheur FNRS, Univ. de Mons, Belgique	Invité
M. TATON, Daniel	Professeur, Univ de Bordeaux, France	Invité

A nature « copy-paste » approach for an efficient metal-free polymerization route

Abstract: Dibenzoylmethane has been investigated as organocatalyst for the bulk ring-opening copolymerization (RO*c*P) of *L*-Lactide (LA) and ε-caprolactone (CL) initiated by alcohols at high temperature. Copolymer presenting a gradient to statistical structure has been generated. Kinetic study has pointed out that DBM is a poor chain end and monomer activator, the apparent acceleration of the RO*c*P process may be due to the *in situ* generation of carboxylic acids which can catalyze the reaction as well.

Benzoic acid, a weak carboxylic acid, has then been investigated for the efficient bulk ring-opening polymerization (ROP) of LA and CL initiated by various alcohols at high temperature. The kinetic study has pointed out that LA and CL have different reactivity in presence of benzoic acid which acts as a bifunctional activator. The experimental results were supported by computational calculations.

An array of statistical copolymer of varying LA/CL compositions have been synthesized by RO*c*P of LA and CL catalyzed by BA in presence of various alcohol as initiators in bulk at high temperature. Finally, miscellaneous organocatalysts have been tested for the RO*c*P of LA and CL.

Keywords: metal-free, catalysis, lactide, caprolactone, benzoic acid, dibenzoylmethane, copolymerization, bulk, ring-opening polymerization, statistical copolymers.

Une approche « copier-coller » de la nature pour une polymérisation efficace sans métal.

Résumé : Le dibenzoylméthane (DBM) a été étudié comme catalyseur pour la copolymérisation par ouverture de cycle du *L*-lactide (LA) et du ε-caprolactone (CL) amorcée par des alcools en masse à haute température. Des copolymères présentant des structures gradient à statistique ont été formés. L'étude cinétique a mis en évidence que le DBM est un faible activateur de bout de chaîne et de monomère, l'apparente accélération de la copolymérisation étant due à la formation *in situ* d'acides carboxyliques catalysant la réaction à leur tour.

L'acide benzoïque (BA), un acide carboxylique faible, a ensuite été étudié pour les homopolymérisations par ouverture de cycle du LA et du CL amorcées par des alcools en masse à haute température. L'étude cinétique a mis en évidence un mécanisme bifonctionnel et une différence de réactivité des deux monomères en présence de BA validés par des calculs théoriques.

Une gamme de copolymères statistiques présentant différentes compositions ont été synthétisés par copolymérisation par ouverture de cycle du LA et CL catalysé par BA et amorcé par différents alcools en masse à haute température. Finalement, plusieurs catalyseurs organiques ont été testés pour la copolymérisation du LA et CL.

Mots clés : polymérisation organique, catalyse, lactide, caprolactone, acide benzoïque, dibenzoylméthane, polymérisation en masse, copolymères statistiques.

LPCM, Université de Mons, av. Maistriau 23, 7000 Mons, Belgique
LCPO (UMR 5629), ENSCBP, Université de Bordeaux, 16 av. Pey Berland 33607, Pessac, France

Résumé en Français

En moins de cent ans, les matériaux plastiques sont devenus indispensables à notre vie quotidienne. Leur application est maintenant généralisée à tous les secteurs essentiels générant une quantité de déchets considérable dans les villes, les pays, les forêts, les montagnes et les océans perturbant la vie de notre écosystème tout entier. Dans ce contexte, les industries chimiques s'efforcent de limiter leur impact en substituant les polymères issus du pétrole par des polyesters biodégradables et biosourcés tels que le poly(lactide) (PLA) et le poly(ε-caprolactone) (PCL).

Le but de ce travail est de développer des stratégies de synthèses innovantes et durables afin d'obtenir des (*co*)polymères à base de lactide (LA). La (co)polymérisation par ouverture de cycle est catalysée par des molécules organiques naturelles ou « copier-coller » de la nature, bon marché, disponible dans le commerce et biocompatibles.

Le **chapitre bibliographique** met en lumière que les catalyseurs organiques ont été considérablement étudiés tout au long de ces vingt dernières années pour la polymérisation par ouverture de cycle (POC) du *L*-lactide (*L*-LA) et du ε-caprolactone (CL). Il reste, cependant, certains défis à relever :

Le premier défi consiste en la POC du *L*-LA en masse, sans solvant toxique, qui requière des hautes températures de réaction (jusqu'à 180°C). La plupart des organocatalyseurs testés, ont en effet rencontré un succès limité d'une part dû à la dégradation thermique des catalyseurs de type basique traditionnellement étudiés pour cette polymérisation en solution. Des réactions secondaires importantes, telles que l'épimérisation qui diminue les propriétés thermomécaniques du poly(*L*-lactide) (PLLA) peuvent aussi se produire. Le diphenylphosphate, une molécule de type acide, s'est révélé être le seul organocatalyseur capable de produire un PLLA isotactique en masse à haute température mais avec une cinétique lente.

Le deuxième défis consiste à découvrir un organocatalyseur capable de mener une copolymerization statistique par ouverture de cycle du LA et du CL d'une façon contrôlée. Seulement une poignée d'organocatalyseurs ont été testés menant à une vitesse de polymérisation plus rapide soit pour le CL soit pour le LA durant la copolymérisation. En effet, les catalyseurs de type basique conduisent à la synthèse de PLA sans unité CL, tandis que les catalyseurs acides ont des comportements différents dépendant de leur nature.

Les organocatalyseurs tels que les acides carboxyliques faibles n'ont jamais été étudiés ni pour réaliser la POC du *L*-LA en masse, ni pour réaliser la copolymérisation par ouverture de cycle du LA et du CL. Ce travail a donc évalué cette classe de catalyseurs.

Dans le **deuxième chapitre**, le dibenzoylméthane (DBM), un acide faible, non toxique et naturel, a été évalué comme organocatalyseur pour la copolymérisation statistique par ouverture de cycle de *L*-LA et CL à 155 ° C initiateurs d'alcool (figure 1). Un contrôle relativement bon a été obtenu, comme en témoigne l'évolution linéaire de la masse molaire

moyenne déterminée par chromatographie d'exclusion stérique(CES) ($M_{n,SEC}$) en fonction de la conversion totale en monomères (C_{TOT}) et des valeurs de dispersité relativement faibles. Cependant, aucun copolymère de haute masse molaire n'a pu être.

Pour mieux comprendre la structure du copolymère, les rapports de réactivité du *L*-LA (r_{LA}) et de CL (r_{CL}) ont été déterminés par la méthode linéaire de Kelen-Tüdős (KT) et par la méthode non linéaire appelée « visualization of the sum of squared residual space »(VSSRS). Les structures des copolymères ont également été évaluées par RMN ^{1}H et ^{13}C et par calorimétrie différentielle à balayage (DSC). Ces analyses combinées ont révélé qu'un copolymère de type gradient était obtenu au début du processus, un copolymère statistique étant formé au dernier stade (figure 1).

L'étude de la POC du *L*-LA et du CL et leur cinétique ont mis en évidence le fait que le DBM est un pauvre activateur de monomère et de bout de chaîne, l'accélération du processus étant finalement expliquée par la survenue de réactions secondaires. Les acides carboxyliques formés *in situ* par dégradation thermique des réactifs et par le co-amorçage par de l'eau peuvent catalyser les (*co*)polymerisations, qui peuvent être considérés comme des réactions auto-catalysées.

Enfin, l'application de divers acides carboxyliques pour cette copolymérisation a montré que l'acide benzoïque (BA) est très intéressant pour déclencher la copolymérisation statistique du *L*-LA et du CL.

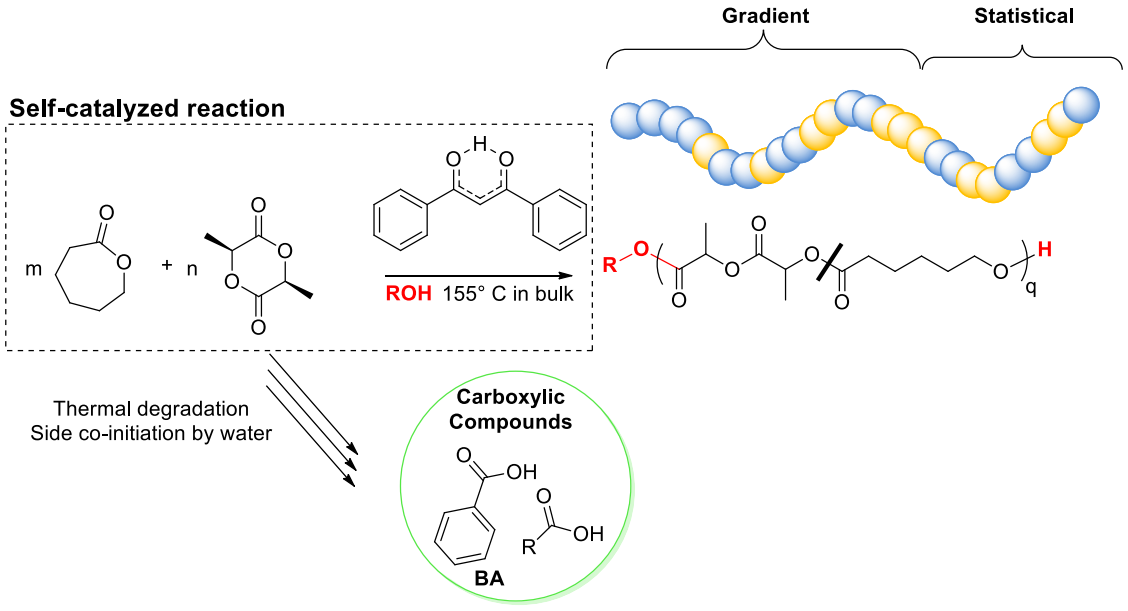

Figure 1. Copolymérisation par ouverture de cycle autocatalysée du *L*-LA et du CL - **Chapitre 2.**

Le **troisième chapitre** a été dédié à l'évaluation de l'acide benzoïque (BA) pour la POC de *L*-LA et CL avant de procéder à leur copolymérisation afin d'évaluer le contrôle et le mécanisme de ces processus. Cela a été une bonne occasion d'évaluer l'activité de BA pour la POC du *L*-LA en masse, qui est également l'un des défis de ce travail.

La POC du CL en masse catalysée par BA et amorcée par des dialcools à 155 ° C présente un bon contrôle comme l'atteste l'évolution linéaire de la $M_{n,SEC}$ en fonction de la conversion, les faibles dispersités obtenues, la haute fidélité des bouts de chaîne et la possibilité de réamorcer la polymérisation à partir des PCL (Figure 2, **2**). Amorcer cette polymérisation avec des monoalcools entre 80 et 155 ° C a toutefois montré que certaines réactions de transfert, telles que la transestérification intermoléculaire, pouvaient se produire (Figures 2, **8**). L'utilisation de dialcools a néanmoins limité les inconvénients d'un tel transfert, c'est-à-dire l'augmentation de la dispersité et l'apparition d'une seconde population dans les analyses CES.

Le POC du *L*-LA amorcée par des dialcools et des monoalcools à une température allant jusqu'à 180 ° C a montré un bon contrôle de la masse molaire et de la dispersité donnant des PLA totalement transparents (Figure 2, **6**). Toutefois, il est impossible d'atteindre des masses molaires élevées et il a été démontré que l'épimérisation du *L*-LA se produisait au cours de la polymérisation conduisant à des PLA amorphes.

La possibilité d'étendre les chaînes polymères a ensuite été correctement exploitée afin de synthétiser des copolymères triblocs, à savoir PLA-*b*-PCL-*b*-PLA à partir du butane-1,4-diol (BD, Figure 2, **1**). Cette synthèse a montré qu'aucune réaction de transfert n'a lieu sur le premier bloc PCL. En revanche, la réaction inverse, c'est-à-dire l'amorçage de la POC du CL à partir d'un précurseur de PLA, n'a pas fonctionné, car l'alcool secondaire situé à l'extrémité de la chaîne du PLA n'a pas pu amorcer efficacement la POC du CL (Figures 2, **5**).

Enfin, des études cinétiques et les calculs de théorie de la fonctionnelle de la densité (DFT) ont montré que le BA est un activateur de monomère et de chaîne fonctionnant *via* un mécanisme bifonctionnel. Globalement, le BA est vingt fois plus efficace pour la POC en masse du CL que pour la POC en masse du *L*-LA. Une telle tendance peut s'expliquer, de manière hypothétique, par une activation plus efficace du groupe carbonyle du CL (par rapport aux groupes du *L*-LA) potentiellement attribuable à la basicité supérieure du premier. Une deuxième explication pourrait être que la base conjuguée du BA est trop faible pour activer efficacement l'alcool secondaire, moins nucléophile et stériquement encombré, à l'extrémité de la chaîne du PLA.

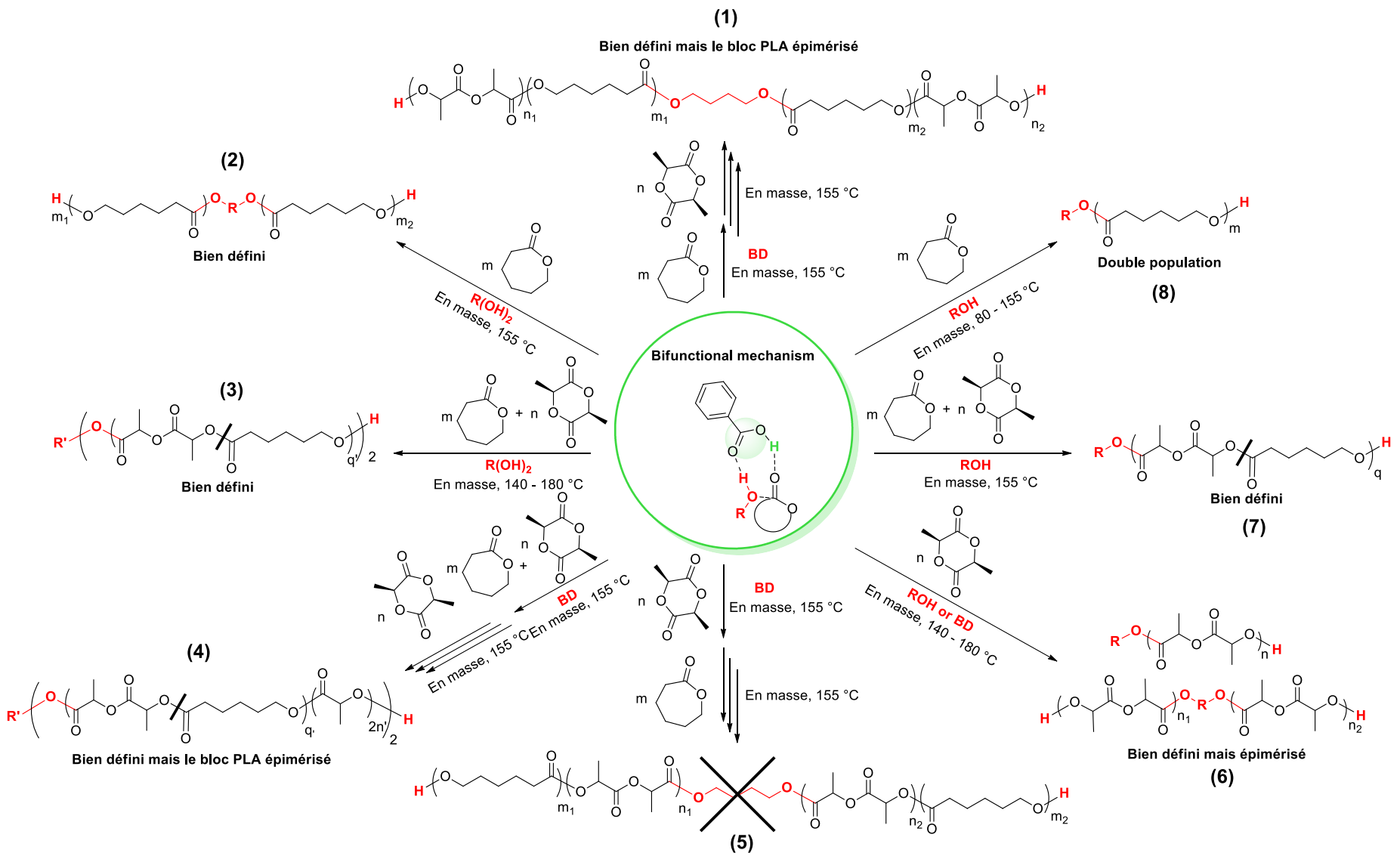

Figure 2. Homo et copolymerization par ouverture de cycle du CL et du *L*-LA en masse -**Chapitres 3 et 4** - avec q = n + m, n = n_1 + n_2, m = m_1 + m_2, 2q' = q et 2n' = n. R' = $-CH_2-CH_2-CH_2-CH_2-$.

Dans le **quatrième chapitre**, la copolymérisation par ouverture de cycle du *L*-LA et du CL à haute température (140 à 180 ° C) a été étudiée en présence d'acide benzoïque et de divers amorceurs, permettant ainsi un bon contrôle de la masse molaire et de la dispersité (Figures 2, **3** et **7**). Une gamme de copolymères de différentes compositions en *L*-LA et CL ont été synthétisée en masse à 155 ° C. Le caractère statistique des copolymères obtenus a été évalué par des techniques de caractérisation telles que la RMN ^{1}H, ^{13}C et la DOSY-RMN et par DSC. L'application de la méthode VSSRS a permis de déterminer des valeurs de rapport de réactivité plus fiables, en désaccord avec celle obtenue avec la méthode linéaire KT, certainement à cause des incertitudes dans les mesures de RMN à faibles conversions. Le calcul des taux de réactivité obtenus par la méthode VSSRS a fourni une preuve supplémentaire de la nature statistique des copolymères. La possibilité de réamorcer les chaînes de copolymères a ensuite été correctement exploitée afin de synthétiser des copolymères triblocs, à savoir PLA-*b*-P(LA-*stat*-CL) -*b*-PLA (Figure 2, **4**).

Il est important de noter qu'une nouvelle méthode de purification sans solvant a été développée dans les chapitres 3 et 4 afin d'obtenir des échantillons PCL, PLA et P(LA-*stat*-CL) extrêmement purs. Le BA récupéré pourrait donc être réutilisé pour les cycles organocatalytiques ultérieurs et, du fait de leur élimination facile, les deux monomères pourraient également être recyclés.

Enfin, la réactivité du *L*-LA et du CL en présence de différents organocatalyseurs a été évaluée. Cette étude a montré que l'acidité / la basicité de l'organocatalyseur est sûrement le principal paramètre clé influençant la copolymérisation du *L*-LA et du CL. En effet, les molécules basiques et nucléophiles insèrent préférentiellement le *L*-LA dans la chaîne copolymère alors que le contraire se produit lors de l'application de composés acides. L'acidité particulière du BA activerait plus efficacement le groupe carbonyle du CL que celle du *L*-LA, compensant ainsi la capacité plus élevée des alcools à polymériser le *L*-LA par rapport au CL à hautes températures, permettant ainsi ce processus de copolymérisation. Cependant, le caractère acide / base du catalyseur n'est pas le seul paramètre influant sur la copolymérisation et certaines fonctions peuvent avoir une influence telle que les donneurs ou les accepteurs de liaisons hydrogènes intermoléculaires: par exemple, les atomes de fluor.

Enfin, ce travail montre en arrière-plan la différence de réactivité du *L*-LA et du CL en fonction de l'organocatalyseur utilisé. D'une part, nous avons montré que la POC du *L*-LA est difficilement menée en présence d'acides faibles, peut-être parce que ses groupes carbonyles ne sont pas assez basiques pour être activés. Une autre explication possible pourrait être que l'alcool secondaire en bout de chaîne PLA est stériquement encombré et moins nucléophile doit être fortement activé pour attaquer efficacement le groupe carbonyle du LA encombré stériquement. D'autre part, il serait intéressant de comprendre pourquoi la POC du CL est difficilement réalisée sans la présence d'activateurs monomères.

À mes amis, ma famille et Florian.

Remerciements

Chaque expérience que l'on a vécu est un morceau de puzzle que le temps, en jouant le rôle de liant, imbrique les uns aux autres jusqu'à former l'histoire de notre vie. Ces trois-quatre dernières années ont formé un morceau de puzzle qui peut lui-même se diviser en plusieurs morceaux qui ont été teintés de joie, d'amour, de tristesse parfois même de désespoirs. Je ne sais pas si je me serais passée de ces trois-quatre années là, de cette expérience, mais je sais que j'ai appris énormément de choses sur moi, sur les autres et sur le monde qui nous entoure ; que finalement, cette expérience fait partie de moi et me constitue, m'a fait évoluer. Ce que j'en retire c'est qu'il me reste encore tant de choses à apprendre et à découvrir, tels que l'immensité de cette planète et les trésors qui y résident ou les belles prouesses et les horreurs que l'être humain est capable d'accomplir. Il me reste encore tant de choses à faire et de combats à mener pour espérer un jour faire changer un tant soit peu les choses. J'espère, enfin, avoir déjà ajouté ma pierre à l'édifice en travaillant sur cette thèse pour la synthèse durable de polymères biodégradables, biocompatibles et biosourcés. Ce travail n'aurait pas été possible sans l'aide de nombreuses personnes que je souhaiterais remercier ici.

Mes premiers remerciements vont à mes deux encadrants Olivier Coulembier et Daniel Taton qui m'ont d'abord permis d'intégrer leurs laboratoires respectifs. Enfin, je vous remercie de m'avoir fait confiance durant ces trois-quatre dernières années et de m'avoir donné une grande autonomie sur mes travaux tout en sachant m'aiguiller au bon moment. Je suis très reconnaissante que vous ayez eu autant de patience car je n'ai jamais été très douée pour rendre un travail à l'heure. Je vous remercie finalement pour ce travail que vous m'avez aidé à accomplir.

Il est important aussi pour moi de remercier Simon Harrison qui a fait un travail remarquable sur le chapitre 4 et qui a fait preuve de très bons conseils scientifiques. Je remercie aussi Coralie Jehanno ainsi que ces superviseurs : Dr. Fernando Ruipérez, Dr. Haritz sardon et Prof. Andrew Dove pour les calculs utilisant la théorie de la fonctionnelle de la densité. Je remercie le professeur Pascal Loyer et son doctorant, Saad Saba, pour avoir étudié la toxicité de l'acide benzoïque. Je remercie enfin Stéphanie Engelen, qui a été ma stagiaire.

Je suis très reconnaissante au professeur Blanca Martin-Vaca, au professeur Christine Jérôme et au professeur Frédéric Peruch d'avoir accepté d'évaluer mon travail et au professeur Roberto Lazzaroni d'avoir été le président du jury.

Je voudrais aussi remercier toutes les personnes qui s'occupent des deux laboratoires je vous remercie de leur permettre de fonctionner. Je remercie aussi particulièrement les personnes qui m'ont aidée en chimie et qui m'ont formée sur les différentes machines. Tout d'abord je souhaiterais remercier les collègues du SMPC à Mons. Je remercie Sébastien Moins

qui m'a formée à la paillasse sur la polymérisation par ouverture de cycle, tu as toujours été de très bons conseils et je te remercie pour ta bonne humeur au quotidien. Je souhaiterais aussi remercier Antonyia et Samira pour m'avoir formée et aidée en DSC et TGA et enfin Jérémy Odent qui m'a aidée à travailler en extrusion réactive. Au LCPO de Bordeaux, je souhaiterais remercier tout d'abord Anne Laure qui m'a formée et beaucoup aidée en RMN, Amélie en SEC et Gérard et Cédric en TGA et DSC. Je remercie aussi Romain qui m'a beaucoup aidé en paillasse.

Je souhaite remercier mes collègues du projet SUSPOL : Jin, Sofiem, Beste, Sètuhn, Andere, Coralie, Amaury, Panos, Noe.

Je remercie tous mes collègues de Mons qui ont participé à ce que mon année et demie au SMPC se passe agréablement bien. Je reremercie tout d'abord Antoniya et aussi Alexandra pour toutes les discussions et les débats endiablés, nos soirées à refaire le monde et nos barres de rire. Vous avez aussi été d'une grande aide dans les durs moments et je suis heureuse de vous compter parmi mes amis. I would like to thank you Jin, my friend, for all our discussions, the time spent together and your help in chemistry. Je remercie aussi les copains, Romain Lienard, Sébastien Delpierre, Ali Khalil, Alexandre De Neef, Nicolas Delbosc, Bastien Arrotin avec qui j'ai passé de très bons moments aussi. Mon passage au SMPC n'aurait pas été le même si vous n'aviez pas été là. Je te remercie Samira pour tous les moments partagés, pour tous nos débats et pour tes encouragements et ta bienveillance. Je remercie aussi Sutima, Benjamin, Florence, Ameni, Noémie, Laura, Bertrand et d'autres…

Merci à mes collègues du LCPO. Tout d'abord un grand merci à Nicolas, Boris et Fiona sans qui ces 1 an et demi au LCPO n'aurait pas été aussi bien. Merci Nicolas pour toutes ces discussions, à refaire le monde et ces bons moments, et surtout l'impression avec toi d'être normale. Je te remercie Boris pour toutes les discussions qu'on a pu avoir sur le monde ou la chimie et tous les bons moments qu'on a pu passer ensemble. Je te remercie aussi de m'avoir aidé à concevoir le montage pour le recyclage. Merci ma petite Fiona d'avoir été là dans les bons et les mauvais moments je suis très heureuse d'avoir pu croiser ton chemin. Je souhaite aussi remercier les collègues que j'apprécie particulièrement et avec qui j'ai passé de bons moments au LCPO tels que : Christopher, Sylwia, Léa, Cédric, Jérémy, Martin, Anne, Pauline et Benjamin. Merci Dounia pour nos discussions et bons moments. Je remercie Quentin S. pour le soutien mutuel qu'on s'est apporté, merci aussi à Camille B., David et Arthur. Je te remercie Hélène pour toutes les discussions qu'on a eues, ce fût une belle rencontre tardive… Je remercie aussi tous les autres collègues du LCPO : Cindy, Sophie, Michèle, Guillaume, Elodie, Coralie, Laura, Louis, Martin F et Monika et Quentin P et bien d'autres…

Je souhaite aussi remercier ces professeurs ou superviseurs qui ont cru en moi, m'ont soutenue et qui ont su stimuler mon envie d'apprendre et de continuer : le Professeur Anna Chrostowska, le docteur Antoine Bousquet et le professeur Maud Save.

Merci à mes ami(e)s de la fac avec qui j'ai passé énormément de bons moments et qui font partie de ces gens qui ont contribué à mon bien-être durant ces trois dernières années. Je remercie particulièrement Camille et Marion, pour tous ces bons moments, ces discussions et ces rires. Je remercie aussi Julien et Martin les vrais bons copains, toujours là dans les bons et les mauvais moments. Je remercie aussi Marie, tu es une personne formidable toujours à l'écoute, je suis heureuse d'avoir passé tous ces moments avec toi. Merci Anne-Sophie d'être toujours là rayonnante et à l'écoute. Je remercie aussi les grands copains : William, Saphir et Emile.

Surtout je ne pourrais écrire ces remerciements sans remercier mes meilleurs ami(e)s, la bande depuis dix ans et plus maintenant, ceux qui sont irremplaçables, la famille de cœur et qui ont fait ce que je suis aujourd'hui. Je remercie tout particulièrement Lisa, Maeva et Laura pour votre soutien et votre amitié depuis maintenant 12-13ans, pour tous nos bons moments, nos premières conneries, nos premières sorties. On a vécu tellement de choses ensemble que se serait maintenant impossible à énumérer. Je remercie aussi Rémi mon meilleur ami celui avec qui on a commencé par refaire le monde puis faire les mille et un coups. Je remercie Ronan, Jérémy, Tommy, Valentin, Sébastien et Thibaut pour être toujours là. Je pense très fort à Antoine.

Finalement, je souhaiterais sincèrement remercier toute ma famille. Particulièrement ma mère, tu as toujours été là pour nous et je t'en remercie. Merci à mes petites sœurs Sarah et Manon et mon petit frère Antony vous me rendez et me rendrez toujours fière de vous quoi qu'il arrive. Je remercie aussi mes grands-parents Jacqueline et Gérard qui ont toujours été là pour moi. Je remercie finalement mon père sans qui je ne serais pas qui je suis au jour d'aujourd'hui.

Je remercie enfin Florian, celui qui m'a aidé à traverser les tempêtes, je me sens si forte à tes côtés. Tu es un rayon de soleil et tu m'aides chaque jour à me sentir plus légère.

« Être libre, ce n’est pas seulement se débarrasser de ses chaînes,

c’est vivre d’une façon qui respecte et renforce la liberté des autres. »

Nelson Mandela

TABLE OF CONTENTS

Chapter 2.

Dibenzoylmethane: in situ generation of active species for the bulk ring-opening copolymerization of L-lactide and Ɛ-caprolactone

Chapter 3.

Benzoic Acid-Organocatalyzed Ring-Opening Polymerization (OROP) of L-Lactide and ε-Caprolactone Under Solvent-Free Conditions: from Simplicity to Recyclability

Chapter 4.

Bulk Organocatalytic Synthetic Access to Statistical Copolyesters from *L*-Lactide and ε-Caprolactone Using Benzoic Acid

List of Abbreviations

4m12C4imY: 4-methyl benzo-12-crown-4 imidazol-2-ylidene
ACEM: active chain end mechanism
AG: acyclic guanidine
AH: Brønsted acids
Al: aluminum
AMM: activated monomer mechanism
B: base
B_2BA: *o,o'-bis*(benzamido)benzoic acid
BA: benzoic acid
BD: butane-1,4-diol
BEMP: 2-tert-butylimino-2-diethylamino-1,3-dimethylperhydro-1,3,2-diazaphosphorine
bisTU: bis-thiourea
bisU: bis-urea
BnOH: benzyl alcohol
BNPP: bis(4-nitrophenyl)phosphate)
BPA: (R)-(−)-1,1'-Binaphthyl-2,2'-diyl hydrogen phosphate
BU: boronate-type urea
ca.: circa
CaH_2: calcium hydride
CAL-B: *Candida Antarctica* lipase B
CCl_3COOH: trichloroacetic acid
$CDCl_3$: deuterated-chloroform
$CHCl_3$: chloroform
CL: ε-caprolactone
C_M: monomer conversion
CMR: carcinogenic, mutagenic, reprotoxic
CP: cyclopropenimide
CR: creatinine
CR-A: creatinine-acetic acid
CR-G: creatinine- glycolic acid
CSA: 1R-(-)-10-camphorsulfonic acid
CTA: chain transfer agent
C_{TOT}: total monomer conversion
CTPB: cyclic trimeric phosphazene base
Đ: dispersity
Da: dalton
DABCO: 1,4-diazabicyclo[2.2.2]octane

DBM: dibenzoylmethane
DBU: 1,8-diazabicyclo[5.4.0]undec-7-ene
DCM: dichloromethane
DDO: dodecanol
DFT: density functional theory
DHBA: dihydroxybenzoic acid
DIEA: *N*-ethyldiisopropylamine
D-LA: *D*-lactide
D,*L*-LA: *D*,*L*-lactide
DMAP: 4-(*N*,*N'*-dimethylamino)pyridine
DNBA: 2,4-dinitrobenzenesulfonic acid
DOSY: Diffusion Ordered SpectroscopY
DP: degree of polymerization
$DP_{,exp}$: experimental degree of polymerization
DPP: diphenylphosphate
$DP_{,th}$: theoretical degree of polymerization
DXP: di(2,6-xylyl)phosphate
E: electrophile
EG: ethylene glycol
FB_2BA: *o,o'-bis*(4-fluorobenzamido)benzoic
f_i: co-monomer ratio
F_i: monomer fraction in the pure copolymer
$f_{i,0}$: co-monomer ratio in the initial feed
GHS: globally harmonized system
HBA: hydrogen bond acceptor
HBD: hydrogen bond donor
HBG.OAc: hexabutyl guanidinium acetate
$HCl.Et_2O$: hydrochloric acid in diethylether
HEA: 6-(2-hydroxyethyl)-aminopurine
HepOH: heptan-1-ol
HMBC: heteronuclear multiple bond correlation
HMF: hydroxymethylfurfural
HMTETA: 1,1,4,7,10,10-hexamethyltriethylenetetramine
$HNTf_2$: trifluoromethanesulfonimide
HOTf: trifluoromethane sulfonic acid
HPG: 3-[(4,5-dihydro-1H-imidazol-2-yl)amino]-propanol
HSQC: heteronuclear single quantum coherence
I: initiator
IHBD: ionic hydrogen bond donor
Im: imidazole

Imes: 1,3-Dimesitylimidazol-2-ylidene
IPA: isopropylalcohol
IpBnimY: 1-isopropyl-3-(4-methoxyphenyl) imidazol-2-ylidene
Is: isotacticity
k: rate constant
k_{app}: apparent rate constant
k_d: depropagation constant
k_i: initation rate constant
k_p: polymerization rate constant
k_t: termination rate constant
k_{tr}: transfer rate constant
L: lactoyl unit
*lac*OCA: lactic acid *O*-carboxyanhydride
$L_{i,13CNMR}$: number average block length of the lactidyl or caproyl unit determined by ^{13}C NMR.
$L_{i,1HNMR}$: number average block length of the lactidyl or caproyl unit determined by ^{1}H NMR.
$L_{i,th}$: theoretical number average block length of the lactidyl or caproyl unit.
LA: lactide
LD_{50}: median lethal dose
LL: lactidyl unit
L-LA: *L*-lactide
Ln: lanthanide
M: monomer
MA: Maleic acid
MALDI-ToF: matrix-assisted laser desorption/ionization-time of flight
meso-LA: *meso*-lactide
Me_6Tren: tris[2-(dimethylamino)ethyl]amine
M_n: number average molar mass
$M_{n,SEC}$: uncorrected number average molar mass
Mo: molybdenum
mPEG: α-methoxy(polyethylene glycol)
$M_{p,SEC}$: molar mass at the peak
MS: mass spectrometry
MSA: methanesulfonic acid
MTBD: 7-methyl-1,5,7-triazabicyclo[4.4.0]dec-5-ene
M_w: weight average molecular weight
n.a: not available
$NCyMe_2$: *N*,*N*-dimethylcyclohexylamine
n.d: non determined
NEt_3: triethylamine
NHC: *N*-heterocyclic carbene

NHO: *N*-heterocyclic olefin
NMR: Nuclear magnetic resonance
Nu: Nucleophile
ORO*c*P: Organocatalyzed ring-opening copolymerization
OROP: Organocatalyzed ring-opening polymerization
P_2BA: *o,o'-bis*(pivalamido)benzoic acid
PBA: pivalamidobenzoic acid
PC: product complex
PCL: poly(ε-caprolactone)
PDLA: poly(*D*-lactide)
PEG: poly(ethylene glycol)
PET: poly(ethylene terephthalate)
PETP: pentaerythritol
PFBA: pentafluorobenzoic acid
Ph_2PMe: methyldiphenylphosphine
PhOH: phenol
$PhPMe_2$: dimethyl(phenyl)phosphine
PLA: polylactide
PLLA: poly(*L*-lactide)
PMDTA: N,N,N',N'',N''-pentamethyldiethylenetriamine
$P(MeO)_3$: trimethyl phosphite
$P(n\text{-}Bu)_3$: tri-*n*-butylphosphine
PPA: 3-phenylpropanol
PPh_3: triphenylphosphine
PPY: 4-pyrrolidinopyridine
PS: polystyrene
$P(t\text{-}Bu)_3$: Tri-tert-butylphosphine
PyOH: 1-pyrenebutanol
RA: resorcylic acid
RC: reagent complex
REX: reactive extrusion process
RI: reflective index
r_i: reactivity ratio
RO*c*P: ring-opening copolymerization
ROP: ring-opening polymerization
r.t: room temperature
SA: salicylic acid
SEC: size exclusion chromatography
$ScCO_2$: supercritical carbon dioxide
$Sn(Oct)_2$: tin(II) 2-ethylhexanoate

SPS: solvent purification system
Sq: squaramide
SuA: succinic acid
TACN: 1,4,7-trimethyl-1,4,7-triazacyclononane
T_b: boiling point
TBD: 1,5,7-triazabicyclo[4.4.0]dec-5-ene
t-BuP_2: 1-tert-butyl-2,2,4,4,4-pentakis(dimethylamino)-2λ5,4λ5-catenadi(phosphazene)
t-BuP_4: tert-(butylimino)tris{[tris(dimethylamino)phosphoranylidene]amino}phosphorane
TCC: triclocarban
TFA: trifluoroacetic acid
T_g: glass transition temperature
THF: tetrahydrofuran
T_m: melting temperature
TMC: trimethylene carbonate
TMEDA: *N*,*N*,*N*′,*N*′-tetramethylethylenediamine
TMP: trimethylolpropane
TPTA: thiophosphorictriamide
trisTU: tris-urea
trisU: tris-thiourea
TS: transition state
TSE: twin-screw extruder
TSMR: tubular static mixing reactor
TU: thiourea
U: urea
VA: vanillic acid
VL: δ-valerolactone
VSSRS: visualization of the sum of squared residual space
VT: vacuum treatment
X: terminating agent
Y: yttrium
Zn: zinc
$\mathcal{E}_{CL/LA}$: percentage of heterodiads
ω_i : lactidyl or caproyl ω-chain end

General introduction

As a consequence of the increased demand for plastics that results from their low cost, lightweight nature, versatility and durability, production has exponentially grown from 1964 reaching 311 million metric tons in 2014 and is expected to double again in 20 years.[1] This industry provides a tremendous utility in our daily lives, however, it has a frightful impact on our environment. Between 4.8 and 12.7 million metric tons of plastic entered in the ocean in 2010[2], *i.e*. between one and four hundred kilograms of plastic entered our oceans each second. In order to reduce plastic waste, recycling and energy recovery have been implemented to a limited extent however these efforts are insufficient to deal with the ever increasing volumes of plastic that our society uses. In this respect poly(lactide) (PLA) and poly(ε-caprolactone) (PCL) and their statistical copolymers P(LA-*stat*-CL), which can be derived from biomass sources, are of special interest as a consequence of their biocompatiblity and, more importantly in this regard, biodegradability.[3,4] Synthesis of PLA and PCL is typically achieved by ring-opening polymerization (ROP), while statistical copolyesters can be obtained by ring-opening copolymerization (RO*c*P). These reactions generally employ (heavy) metal-based complexes as catalysts to achieve (co)polyesters with a high activity and selectivity. Despite their undisputable performances, those complexes are not environmentally friendly and their inherent toxicity on humans and animals is a subject of controversy.[5,6] In that context, organocatalysts of low toxicity[7] are of special interest to replace organometallic catalysts.

This PhD work will be focused on the sustainable synthesis of *L*-lactide-based (*co*)polymers. For this reason, the RO(*c*)P of *L*-lactide (*L*-LA) and ε-caprolactone (CL) will be conducted in metal- and solvent-free conditions and the organocatalysts investigated are expected to be nontoxic and "copy-paste" from nature.

The first objective of this PhD thesis is to conduct the organocatalyzed ring-opening polymerization of *L*-LA in solvent-free conditions and at high temperature in a control manner. Because of the high melting point of poly(*L*-Lactide) ($T_{m(PLLA)} \approx 180$ °C), high temperatures are needed in order to implement this polymerization in reactive extrusion, a technique highly used by industrial. The challenge will be to find thermally stable organocatalysts able to promote the controlled polymerization at such high temperature.

The second objective of this PhD thesis, which is as important as the first one, consist in performing the RO*c*P of *L*-LA with CL in a statistical manner to obtain P(LA-*stat*-CL) of controlled microstructure and tunable properties. Here again the reaction need to be perform in metal- and solvent-free conditions. The challenge will be to find out organocatalysts able to conduct this RO*c*P.

This manuscript is divided in 4 distinct chapters and is organized as summarized above:

The **first chapter** will be dedicated to the state of the art regarding the ring-opening (co)polymerization of *L*-LA and CL in solution and in bulk. The PLA, PCL and P(LA-*stat*-CL) properties and structures will be presented as well as the different techniques used to synthesize them. The different classes of organocatalysts applied over the past 20 years and the related mechanisms and side reactions will also be screened in detail.

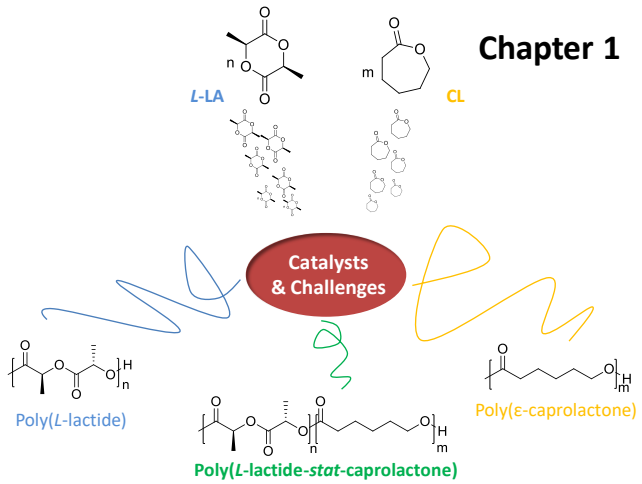

The **second chapter** aimed to investigate the activity of dibenzoylemethane, a β-diketone belonging from the flavonoid family for the bulk ROcP of *L*-LA and CL in the presence of various alcohol initiators. Deep characterization combined with the reactivity ratio calculation using the "visualization of the sum of squared residuals space" (VSSRS) method will enable to determine the structure of the copolymer obtained. Further investigations of the ROP of *L*-LA and CL and of the kinetic data will be carried out in order to further understand the mechanism of the copolymerization reaction emphazing an autocatalytic reaction. Finally, miscellaneous amino acids and carboxylic acids will be screened in order to synthesize statistical copolymers.

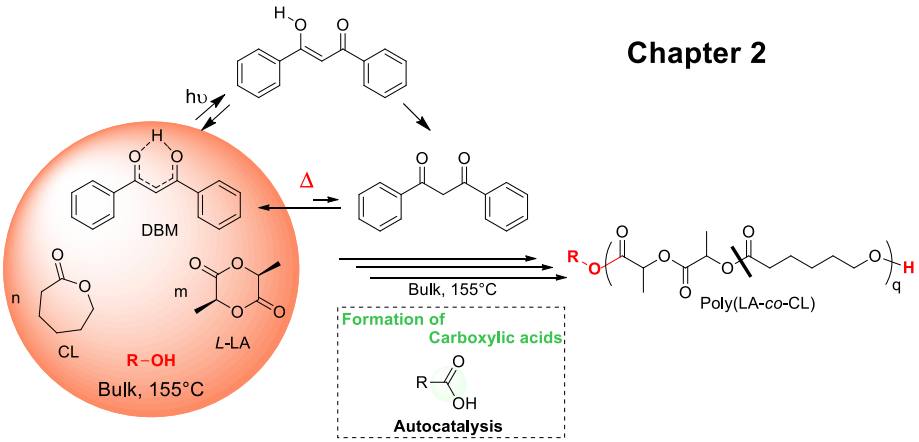

In the **third chapter**, a natural and weak carboxylic acid, namely benzoic acid will be applied for the bulk ROP of *L*-LA and CL initiated by various alcohol initiators at high temperature. The control of the polymerization will be first evaluated followed by the kinetic and mechanistic studies supported by density functional theory (DFT) calculations which will highlight a bifunctional mechanism. The synthesis of PLA- and PCL-based triblock copolymers will be then presented. Finally, a new solvent-free process enabling the recyclability and the reuse of benzoic acid catalyst and unreacted monomers will be set up.

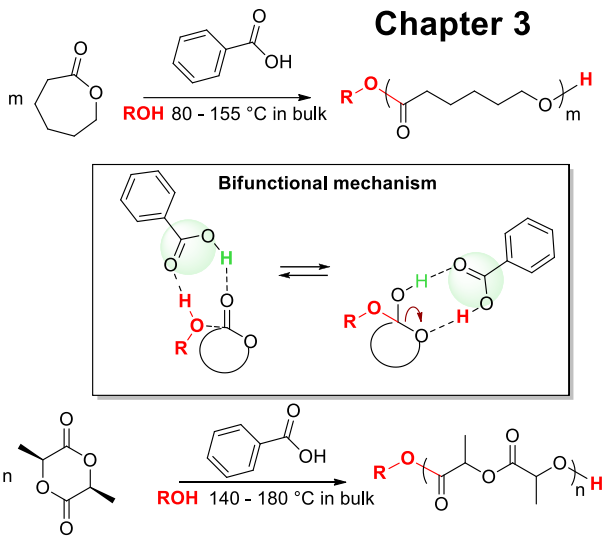

The **fourth chapter** will be dedicated to the statistical ROcP of *L*-LA and CL organocatalyzed by benzoic acid in bulk at high temperature. First the control of the polymerization will be evaluated followed by the synthesis of a library of pure statistical copolymers by varying the initial co-monomer ratios. The copolymer structures will be deeply characterized and further investigated by determining reliable reactivity ratios using the VSSRS method. Triblock copolymer, namely PLA-*b*-P(LA-*stat*-CL)-*b*-PLA will be synthesized and characterized. Finally, miscellaneous organocatalysts will be applied in order to accelerate the reaction kinetic. These experimental results will be compared to the literature data and will be discussed in order to highlight the main parameters influencing the reactivity ratios of both *L*-LA and CL. Finally the cytotoxicity of benzoic acid will be investigated.

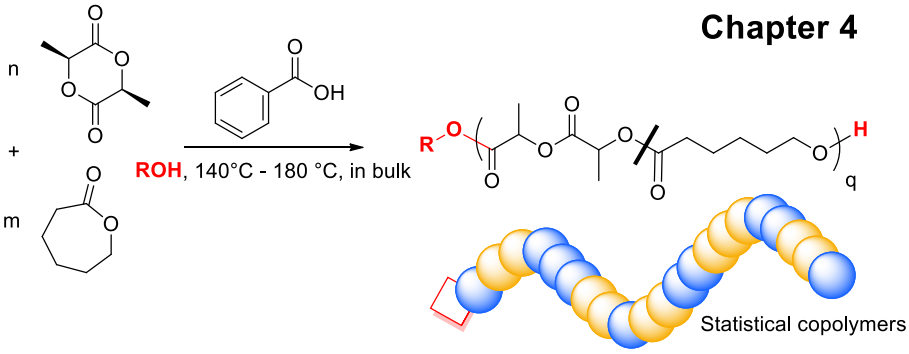

A discussion of the main results obtained throughout the last three years of this PhD work and perspectives will be presented.

This work is part of the European Joint Doctorate - SUSPOL-EJD (grant number 642671) and was supported by the EU Horizon 2020 Research and Innovation Framework Program - and by the European Commission. Several collaborations were developed, first with Dr. Simon Harrisson at the Laboratoire des Interactions Moléculaires et Réactivités Chimiques et Photochimiques (IMRCP) at the University Paul Sabatier in Toulouse. He has conducted the reactivity ratios determination using the VSSRS method. The second collaboration was carried out in order to conduct density functional theory (DFT) calculations. The calculations have been performed by Coralie Jehanno, completing her PhD between the Institute for Polymer Materials (POLYMAT) at the University of the Basque Country UPV/EHU, in San Sebastian under the supervision of Dr. Haritz Sardon and Dr. Fernando Ruipérez and the School of Chemistry at the University of Birmingham under the supervision of Prof. Dove. Finally, Prof. Pascal Loyer and Saad Saba, a PhD student working at the institute of Nutrition Metabolisms and Cancer (NUMECAN, UMR-A 1341, UMR S 1241) at the University of Rennes, have investigated the toxicity of benzoic acid catalyst.

References:

1 *World Econ. Forum*, 2016.

2 J. R. Jambeck, R. Geyer, C. Wilcox, T. R. Siegler, M. Perryman, A. Andrady, R. Narayan and K. L. Law, *Science*, 2015, **347**, 768–771.

3 E. Castro-Aguirre, F. Iñiguez-Franco, H. Samsudin, X. Fang and R. Auras, *Adv. Drug Deliv. Rev.*, 2016, **107**, 333–366.

4 M. Labet and W. Thielemans, *Chem. Soc. Rev.*, 2009, **38**, 3484–3504.

5 D. Krewski, R. A. Yokel, E. Nieboer, D. Borchelt, J. Cohen, J. Harry, S. Kacew, J. Lindsay, A. M. Mahfouz and V. Rondeau, *J. Toxicol. Environ. Health Part B*, 2007, **10**, 1–269.

6 M. C. Tanzi, P. Verderio, M. G. Lampugnani, M. Resnati, E. Dejana and E. Sturani, *J. Mater. Sci. Mater. Med.*, 1994, **5**, 393–396.

7 A. Nachtergael, O. Coulembier, P. Dubois, M. Helvenstein, P. Duez, B. Blankert and L. Mespouille, *Biomacromolecules*, 2015, **16**, 507–514.

Chapter 1.

CHALLENGES IN RING-OPENING (CO)POLYMERIZATION OF *L*-LACTIDE AND Ɛ-CAPROLACTONE

(BIBLIOGRAPHIC CHAPTER)

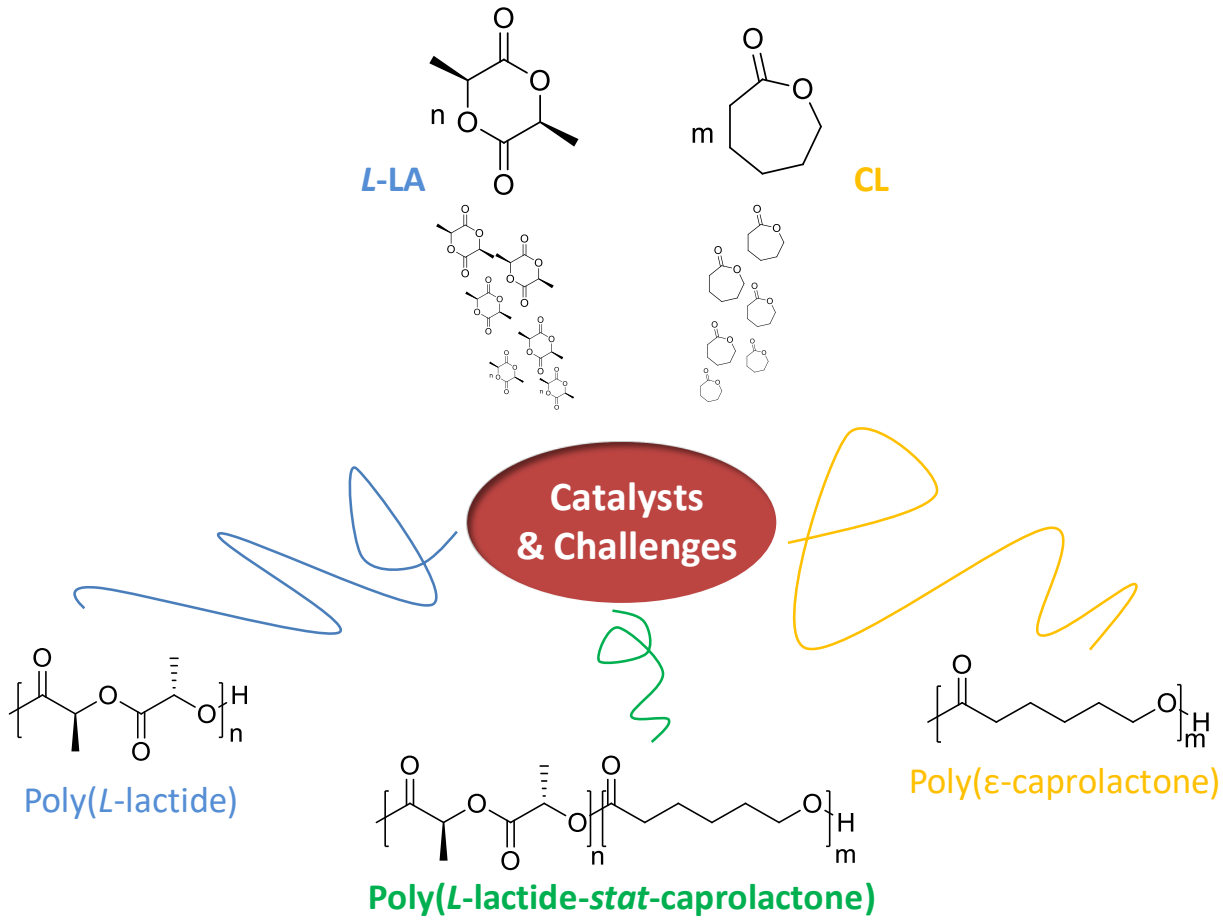

Keywords: lactide, caprolactone, polylactide, poly(ε-caprolactone) ring-opening polymerization, copolymerization, organic catalyst, statistical copolymer.

Chapter 1. CHALLENGES IN RING-OPENING (CO)POLYMERIZATION OF *L*-LACTIDE AND ε-CAPROLACTONE

Table of contents

Introduction

Poly(lactide) (PLA) and poly(ε-caprolactone) (PCL) are representative aliphatic polyesters as potential bio-sourced alternatives[1,2,3] to petroleum-based polymeric materials, which have received a considerable attention in the three past decades, as attested by the number of scientific reports published (Figure 1). Owing to their intrinsic thermal, mechanical, biodegradable, nontoxic and biocompatible properties,[1,4] both PLA and PCL have found a growing interest in a wide panel of potential applications, including in biomedical and pharmaceutical,[5,6,7,8] electronic,[9,10] or packaging[11] fields. PCL has recently been used in mechanical actuators,[12] adhesives[13] and bio-glues,[14] while PLA would be of practical use in flame retardant materials,[15]textiles[5] and automotives.[16,17]

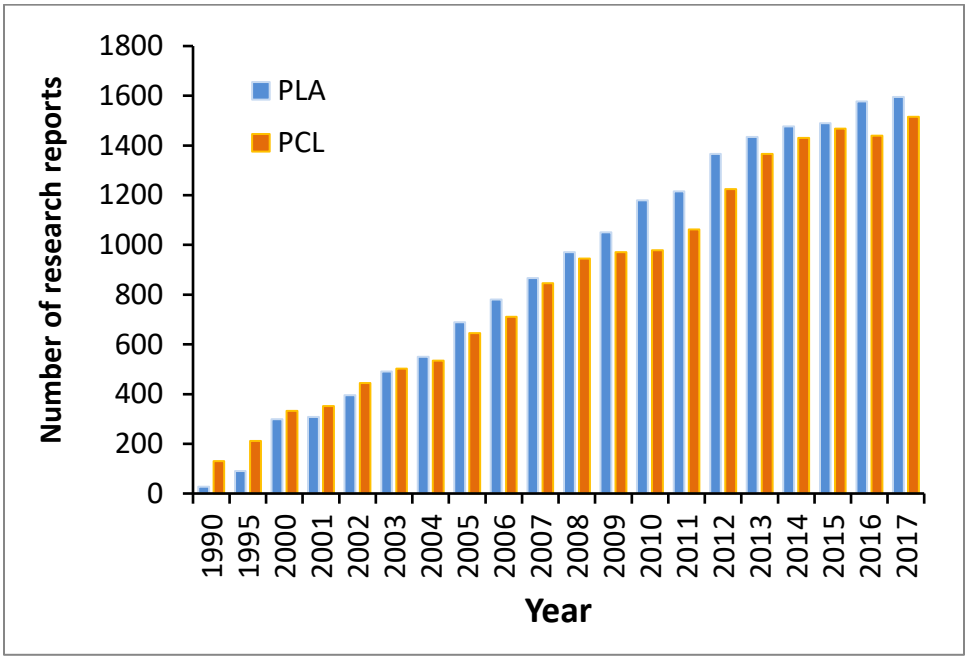

Figure 1. Evolution of the number of research reports on the topic of PLA and PCL since 1990. Data were obtained by a search in SciFinder using the keywords "poly(lactide)", "polylactide", "poly(lactic acid)"and "polylactic acid" for PLA and "polycaprolactone" and poly(caprolactone)" for PCL.

However, both polymers suffer from some drawbacks that still limit their widespread adoption in industry. For instance, PLA is a high Young modulus brittle material exhibiting poor elasticity,[18,19] high degradation rate[20] and poor drug permeability.[21] PCL shows opposite properties to PLA, with a good elasticity and permeability,[21] slow degradation rate,[20] but with poor mechanical properties.[19,4] Therefore, statistical aliphatic copolyesters based on lactide (LA) and ε-caprolactone (CL) monomer units, is often seek for to optimize thermo-mechanical and biodegradable properties of related materials, and broaden their application scope.[22,23,24,25,26,27,28]

Synthesis of PLA and PCL is typically achieved by ring-opening polymerization (ROP), while statistical copolyesters can be obtained by ring-opening copolymerization (RO*c*P). Both ROP and RO*c*P reactions generally employ heavy metal-based complexes as catalysts providing high activity and selectivity.[1,4,29,30] For instance, tin(II) 2-ethylhexanoate ($Sn(Oct)_2$) is traditionally used in *L*-lactide (*L*-LA) bulk ROP, affording isotactic poly(*L*-lactide) of hundreds of kdaltons within a few minutes.[31] Aluminum *sec*-butoxide is also highly active for the ROP of CL at 150 °C *via* reactive extrusion, which leads to PCL of predictable molar mass of 65 kDa within only 2 min.[32] Finally, the development of organometallic catalysts enabling statistical copolymerization of LA and CL is particularly challenging, owing to the highly differing reactivity between the two monomers in RO*c*P, LA being preferentially incorporated first, resulting in the formation of gradient-type copolymers.[30]

Organocatalysts have been introduced in polymer synthesis as they offer many advantages over metallic catalysts, including a reduced toxicity and cost, and easier synthesis and storage. As organocatalysts lead to metal-free polymers, this is particularly relevant in specific applications, such as microelectronics, biomedical or cosmetics. A variety of small organic molecules, including Brønsted/Lewis bases and acids, have thus been employed to catalyze the polymerization of miscellaneous monomers.[33,34,35,36,37,38,39]

The present bibliographic chapter focuses on recent synthetic developments in the field of organocatalyzed RO(*c*)P of *L*-LA and CL carried out in solution and under solvent-free conditions as well. Synthesis of CL and *L*-LA and properties of PLA and PCL will be first presented, which is followed by an overview of organocatalysts employed in the context of RO(*c*)P and underlying mechanisms will be shown. Potential side reactions occurring during these RO(*c*)P reactions will be also discussed as well as related processes developed to conduct them. Focus will be obviously put on the organocatalyzed-ROP (OROP) of both *L*-LA and CL. Finally, copolymer structures resulting from the RO*c*P of LA and CL, and related reactivity ratios, will be discussed.

1 Polymerizability of lactide (LA) and ε-caprolactone(CL)

1.1 From LA to poly(lactide) (PLA): microstructures and properties

Poly(lactic acid) can eventually be synthesized following different routes, for instance, by step-growth polymerization involving either direct azeotropic dehydration (route **1**, Figure 2) or condensation of lactic acid (route **2**, Figure 2).[11] Poly(lactic acid) synthesis can also be achieved by chain-growth polymerization processes, namely, by ROP, using different monomer substrates, including *O*-carboxyanhydride resulting from lactic acid[40] (route **3**, Figure 2) or lactide, also named 3,6-dimethyl-1,4-dioxane-2,5-dione (route **4**, Figure 2), as mentioned above. High yields of lactic acid, either of *D*- or of *L*- configuration, can be obtained by fermentation of polysaccharides or sugar, e.g. from corn and beet, using lactobacilli bacteria.[11] The cyclization (route **5**, Figure 2) consists in the condensation of either *D*-lactic acid, *L*-lactic acid or a mixture of both enantiomers, leading to low molar mass poly(lactic acid).[11] The latter can undergo a catalytic depolymerization into lactide as a white powder.

It is worth pointing out that lactide exists in the form of three isomers, namely, *(S,S)*-lactide (*L*-LA), *(R,S)*-lactide (*meso*-LA) and *(R,R)*-lactide (*D*-LA),[11] the *rac*-LA corresponding to an equimolar mixture of *L*-LA and *D*-LA.

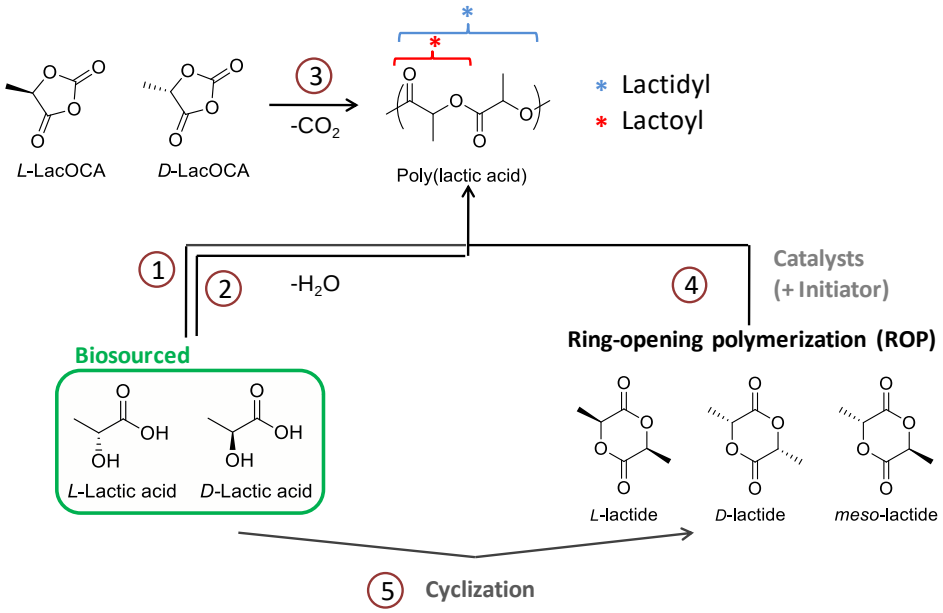

Figure 2. Preparation of poly(lactic acid) from lactic acid, O-carboxyanhydride or lactide.

PLAs are biocompatible polymers also showing biodegradable properties within a few months depending on their molar mass, crystallinity and the degradation conditions.[20,11] PLAs possess a range of properties that mainly depend on their molar masses and

stereochemistry.[11,5,41,42,43] As lactide monomer possesses two stereocenters, PLA can present different microstructures depending on the nature of the LA and of the catalyst involved during the polymerization reaction (Figure 3). Isotactic poly(*L*-lactide) (PLLA) or poly(*D*-lactide) (PDLA), which are typically synthesized by the stereocontrolled ROP of enantiopure *L*-LA or *D*-LA, contain sequential stereocenters of the same relative configuration. Syndiotactic PLAs, also called poly(*meso*-lactide) contains sequential stereocenters of opposite relative configuration and can be synthesized by the stereocontrolled ROP of *meso*-LA. Heterotactic PLAs are structured by the regular alternation of *L*- and *D*-LA units and are typically synthesized by the stereocontrolled ROP of *meso*- or *rac*-LA depending on the catalyst used. Finally, atactic PLAs are characterized by stereoirregular sequences and are obtained by the non stereocontrolled ROP of *rac*-LA or *meso*-LA or by epimerization of LA during the ROP process (see section 1.5).[41,43]

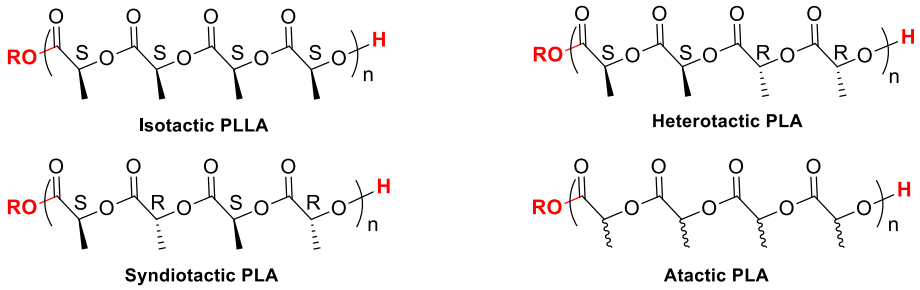

Figure 3. Different PLA's microstructures (inspired from Martin-Vaca and Bourissou *et al.*).[43]

Heterotactic and atactic PLAs are amorphous, presenting only one glass transition temperature (T_g), while stereoregular syndiotactic and isotactic PLAs are semi-crystalline, presenting higher T_g and one melting temperature (T_m, Table 1).[41]

Table 1. Thermal properties of the PLAs of various microstructures.[41]

PLA's tacticity	T_g (°C)	T_m (°C)
Isotactic	55-60	180
Syndiotactic	34	151
Stereocomplex	65-72	220-230
Heterotactic	<45	-
Atactic	44-55	-

The T_m of PLLA (170 – 180 °C) can be considerably increased by complexing PLLA with an equimolar amount of PDLA. The as-formed stereocomplex can present T_m between 220 °C and 230 °C (Table 1, Figure 4).[41] A simple way to achieve stereocomplexed PLLA and PDLA is the stereocontrolled ROP of *rac*-LA using catalyst that preferentially inserts one stereoisomer over

the other, leading to the formation of isotactic stereoblocks (Figure 4). Information about the stereocontrolled ROP of rac-LA can be found elsewhere.[44]

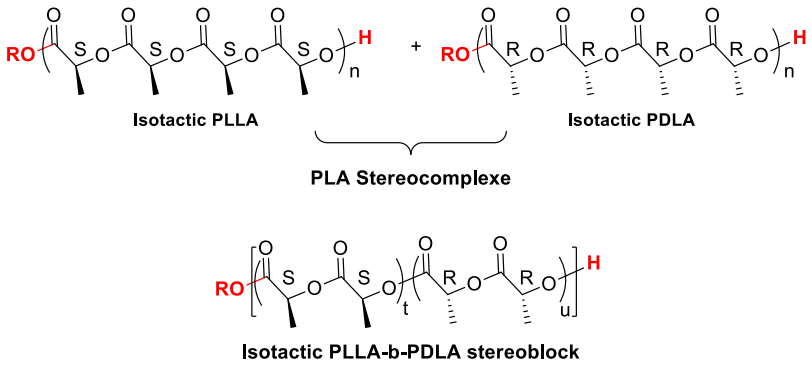

Figure 4. PLA stereocomplexe and stereoblock microstructures (inspired from Martin-Vaca and Bourissou *et al.*).[43]

Organometallic complexes are by far the most studied catalysts for the ROP of LA and are already applied in industry.[1,43,45,46,47,48,49] In this bibliographic chapter, only ROP processes involving *L*-LA and following an organocatalytic pathway will be discussed. Consequently, PLLA-based materials and related thermal and mechanical properties will be mainly discussed here. It is worth noting that fully isotactic PLLA can be hardly achieved as epimerization reactions (see section 1.5), introducing stereoerrors, can take place during ROP of the *L*-LA.

PLA comprising between 50% to 93% of *L*-lactic acid units is amorphous and exhibits poor mechanical properties.[11] These can be improved for PLLA containing 98% of *L*-lactide units. The T_m of PLLA ranges from 130 °C to 180 °C, and its glass transition temperature (T_g) is in the range 55-60 °C. PLLA is thus a brittle material with a high Young modulus (≈ 3.8 GPa), a tensile strain of about 59 MPa and poor elongation at break (4-7%).[41] PLLA shows comparable mechanical properties to polystyrene (PS), making it a promising material to replace petroleum-based polymers in various applications (Table 2).

Table 2. Comparison of the mechanical properties of PLLA, PS and poly(ethylene terephtalate) (PET).[41]

Polymer	Density	Tensile strain	Young modulus	Elongation at break
	$Kg.m^{-3}$	MPa	GPa	%
PLLA	1.26	59	3.8	4-7
PS	1.05	45	3.2	3
PET	1.40	57	2.8-4.1	300

1.2 From CL to poly(ε-caprolactone) (PCL)

Poly(ε-caprolactone) (PCL) can be synthesized by two distinct methods, namely, the direct polycondensation of 6-hydroxyhexanoic acid (route **1**, Figure 5) and the ROP of ε-caprolactone (CL) (route **2**, Figure 5).[4] The latter is the most studied because higher molar masses and, often low dispersity can be achieved under appropriate conditions.[4] ε-Caprolactone (or 6-hexanolactone) is a colorless liquid that can be prepared by Bayer-Williger reaction which consists in the oxidation of cyclohexanone by peracetic acid or hydrogen peroxide.[50] It can also be synthetized from biomass involving phenol or hydroxymethylfurfural (HMF).[2,3]

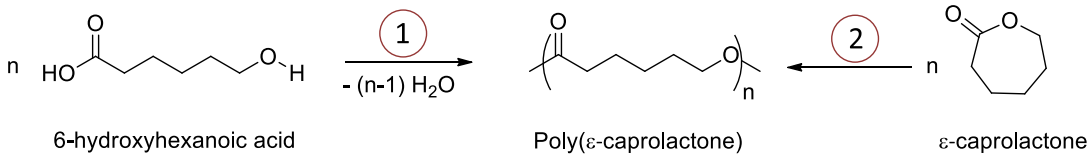

Figure 5. Preparation PCL from 6-hydroxyhexanoic acid or CL.

The ROP of CL was highly studied in the presence of organometallic catalysts and was reported elsewhere.[4,29,45,47,48] PCL is biocompatible and biodegradable as well within a few months to a few years, depending on its molar mass, crystallinity and degradation conditions implemented.[51,4] Crystallinity of PCL can reach 69%, its glass transition temperature ranges from -65 to -60 °C and its melting temperature ranges from 56 to 65 °C.[4] PCL is miscible with many other polymers, such as poly(vinyl chloride), poly(styrene-acrylonitrile), poly(carbonates), poly(ethylene), poly(propylene) and natural rubber among others.[4]

1.3 Organocatalysts applied for the bulk ROP of LA and CL

Various organic molecules have been studied for the ROP of LA and CL carried out in bulk and in solution. These organocatalysts can be classified into different families, as summarized in Figure 6, including (*i*) Brønsted and Lewis acids, (*ii*) thio(urea)s, squaramides and other hydrogen bond donors (HBDs), (*iii*) amines, pyridines, adenines, imidazoles and cyclopropenimides, (*iv*) guanidines and amidines, (*v*) phosphazenes and phosphines, and (*vi*) *N*-heterocyclic carbenes (NHCs) and *N*-heterocyclic olefins (NHOs). Distinct molecules can also be combined together in a bi-component organocatalytic system acting in a cooperative manner (= bifunctional organocatalysts).

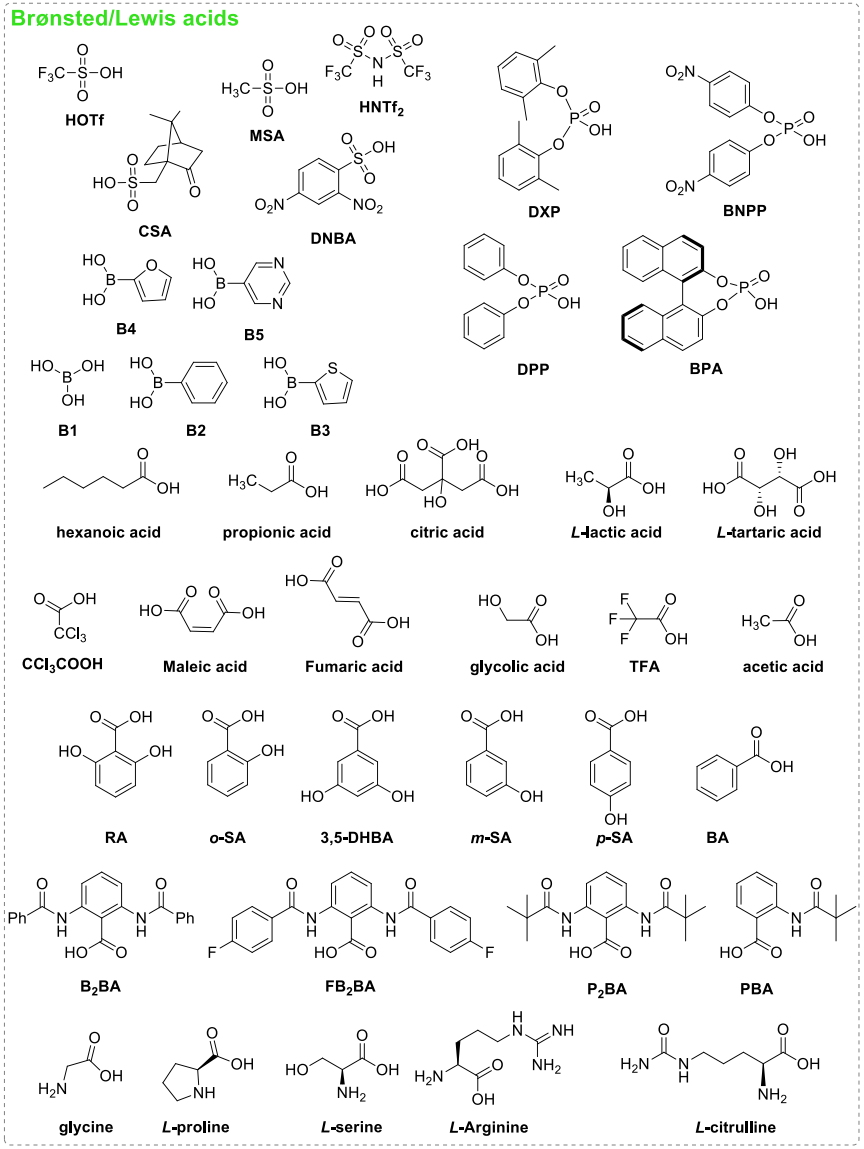
Brønsted/Lewis acids
HOTf
MSA
HNTf2
CSA
DNBA
DXP
BNPP
B4
B5
DPP
BPA
B1
B2
B3
hexanoic acid
propionic acid
citric acid
L-lactic acid
L-tartaric acid
CCl3COOH
Maleic acid
Fumaric acid
glycolic acid
TFA
acetic acid
RA
o-SA
3,5-DHBA
m-SA
p-SA
BA
B2BA
FB2BA
P2BA
PBA
glycine
L-proline
L-serine
L-Arginine
L-citrulline

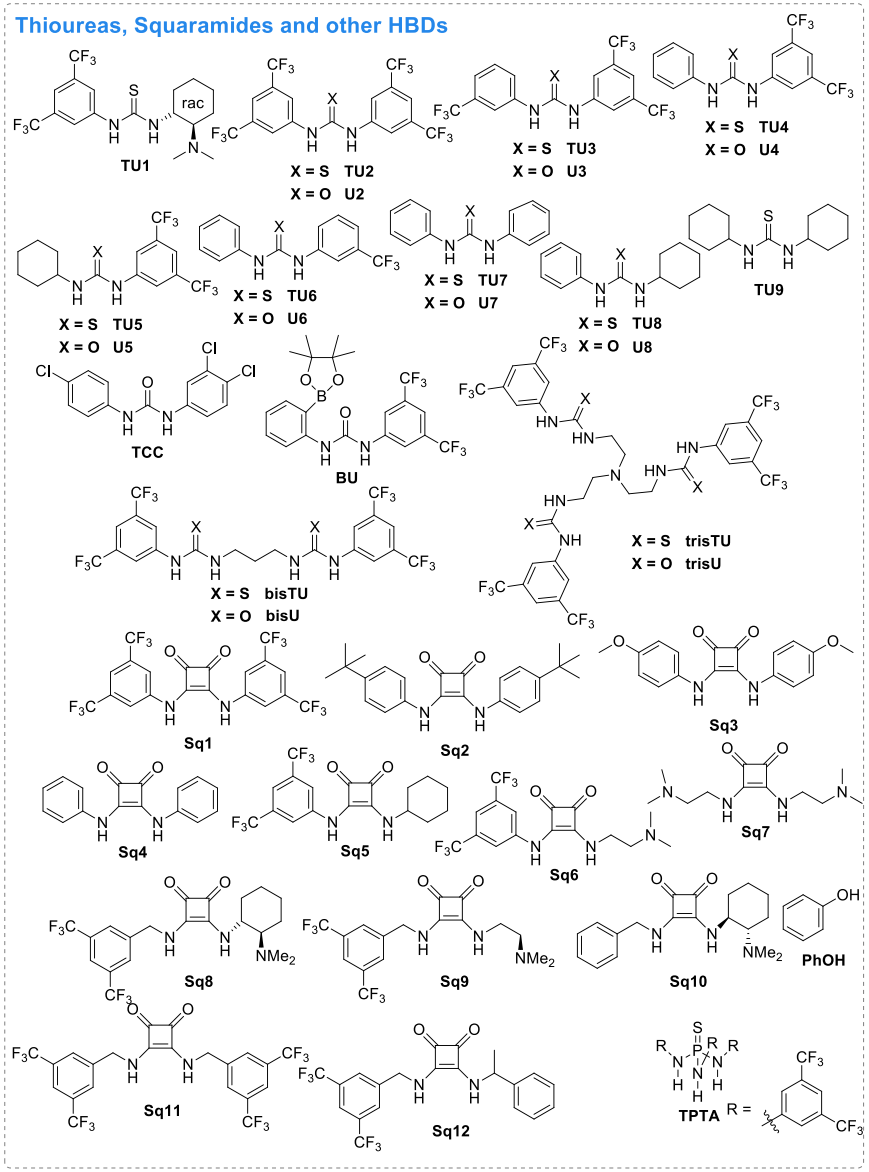
Thioureas, Squaramides and other HBDs
TU1
X = S TU2
X = O U2
X = S TU3
X = O U3
X = S TU4
X = O U4
X = S TU5
X = O U5
X = S TU6
X = O U6
X = S TU7
X = O U7
X = S TU8
X = O U8
TU9
TCC
BU
X = S bisTU
X = O bisU
X = S trisTU
X = O trisU
Sq1
Sq2
Sq3
Sq4
Sq5
Sq6
Sq7
Sq8
Sq9
Sq10
PhOH
Sq11
Sq12
TPTA

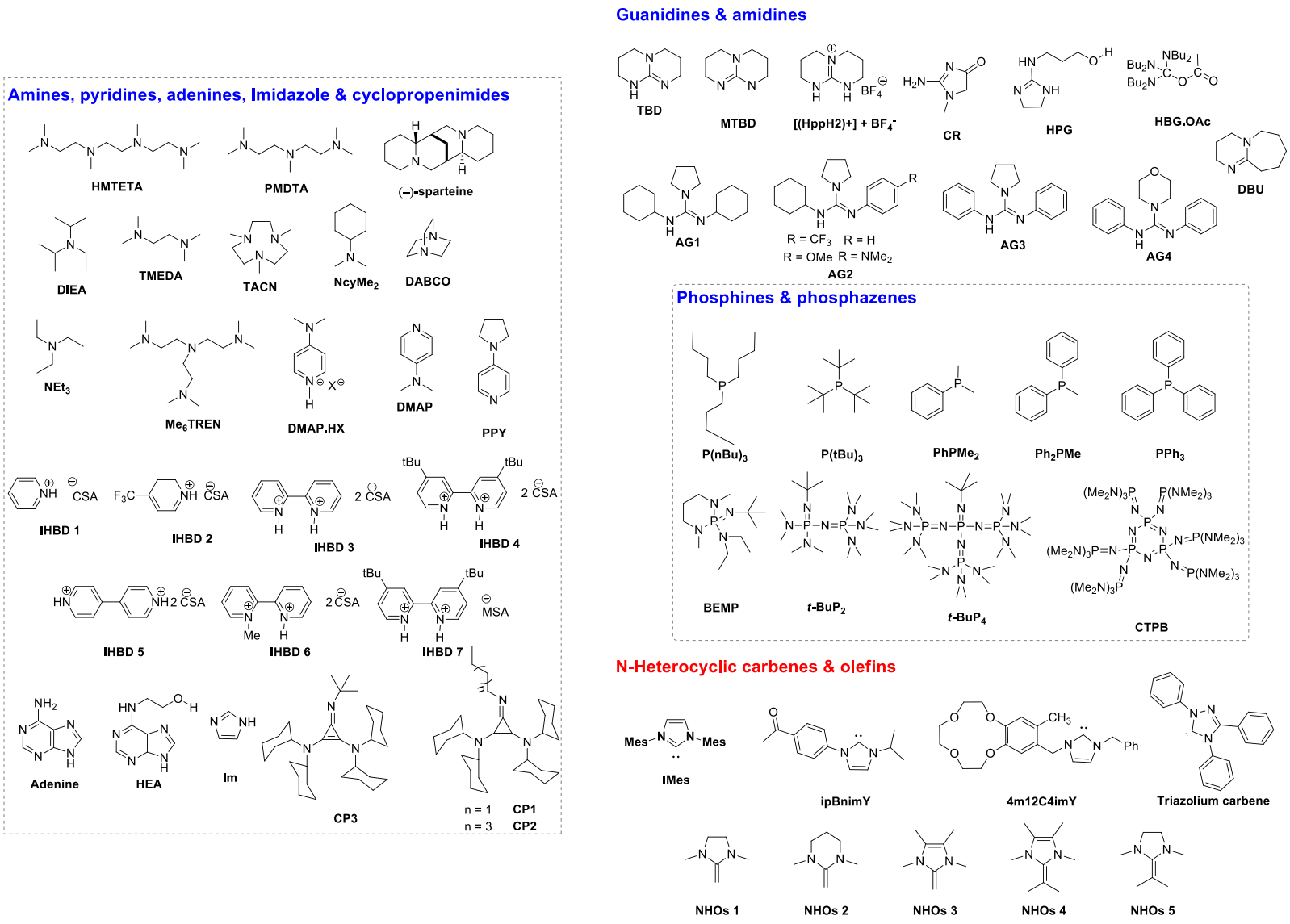

Figure 6. Organocatalysts employed for the ROP of LA and CL (Non-exhaustive) – Detachable – (Inspired from Taton *et al.*)[37]

1.4 Ring-opening polymerization mechanisms

Cyclic esters with enough ring strain can be readily polymerized by a chain-growth ROP mechanism. The ROP of cyclic esters may involve several steps, including initiation, equilibrium between propagation and depropagation, and intra- and intermolecular transesterifications. This is described in Figure 7, where I denotes the initiator, M the monomer, m the repeating unit in the polymer, m* the active species, X is the terminating agent, k_i, k_p, k_d, k_t, k_{tr} corresponding to the rate constants of initiation, propagation, depropagation, termination and transfer, respectively. Possible side reactions taking place during the ROP of cyclic esters are discussed in section1.5.

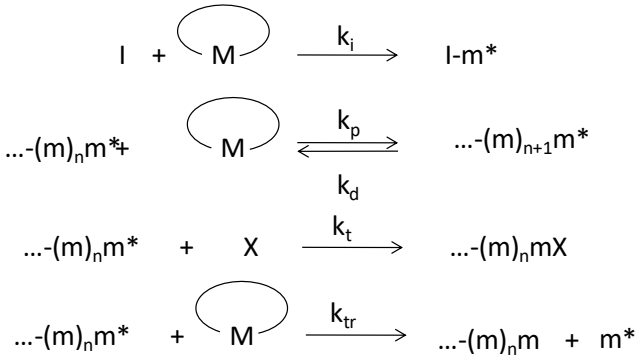

Figure 7. Elementary reactions involved in ROP of cyclic esters (reproduced from the Handbook of ROP).[52]

Possibility to achieve a "controlled/living" ROP process depends on the catalyst and the overall conditions implemented. In case of a "living" polymerization, *i.e.* in absence of irreversible termination and transfer reactions, a linear correlation between $\ln \frac{[M]_0}{[M]}$ and reaction time in the one hand, and between the number average molar mass (M_n) and the monomer conversion (C), should be observed. For the polymerization to be controlled, the initiation should be fast relatively to the rate of the propagation, leading to a low molar mass distribution, i.e. *Đ* close to unity.

Six different mechanisms have been reported, depending on the nature of the catalyst and the monomer, as highlighted in Schemes 1-6.[33,37,55]

- **'Coordination-insertion' mechanism:** A metal forms a metal alkoxide by reacting with an alcohol end group/initiator (Scheme 1, **1**). The as-formed metal alkoxide coordinates onto the carbonyl group of monomer (**2**), favoring ring-opening of the latter (**3**).

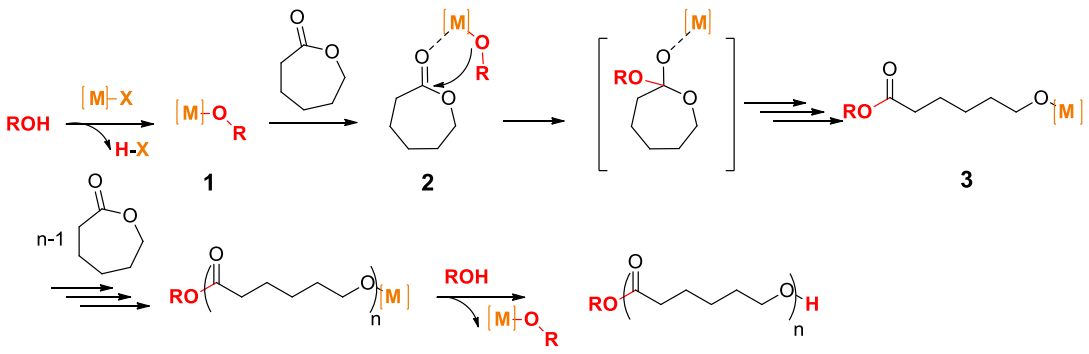

Scheme 1. Coordination-insertion mechanism in ROP of cyclic esters.[33]

- **The Activated Monomer Mechanism (AMM).**

Two mechanisms have been described in this case.

- **The electrophilic AMM.** In this mechanism, acids or electrophiles can activate the carbonyl group of the monomer (Scheme 2, **1**). The as-formed activated monomer **1** can thus undergo a nucleophilic addition of the propagating chain end/initiator (**2**). Brønsted acids, alkylating or acylating agents are representative examples of such activators/catalysts.

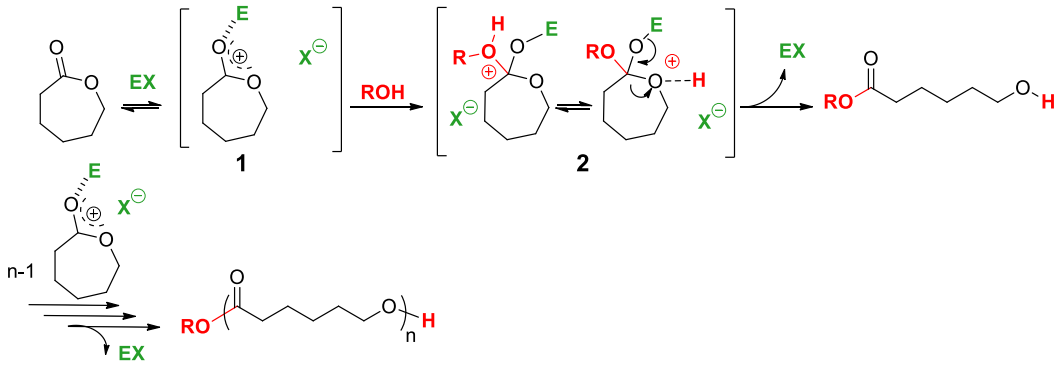

Scheme 2. Electrophilic AMM in ROP of cyclic esters.[33]

- **The nucleophilic AMM.** Nucleophiles (Nu), such as phosphines, imidazoles, pyridines and NHCs can activate the cyclic monomer by direct attack on the carbonyl moiety (Scheme 3, **1**). This leads to the formation of a zwitterionic alkoxide (**2**), which is then protonated by the alcohol initiator ROH (**3**). Acylation of the zwitterionic species by the alkoxide leads to a ring-opened alcohol monoadduct (**4**), regenerating the nucleophilic catalyst.

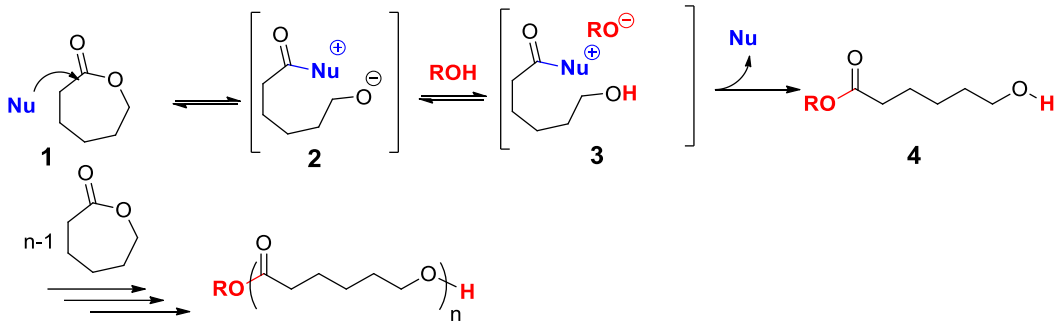

Scheme 3. Nucleophilic AMM in ROP of cyclic esters.

- **The Active Chain End Mechanism (ACEM).**

In this case also, two mechanisms have been discussed.

▪ **The anionic ACEM.** Brønsted bases (B) can activate the initiator then the propagating chain ends by hydrogen bonding or by deprotonation, generating a reactive alkoxyde **1**. In a subsequent reaction, a nucleophilic attack of the alkoxide/polarized alcohol will take place onto the carbonylated monomer (Scheme 4, **2**).

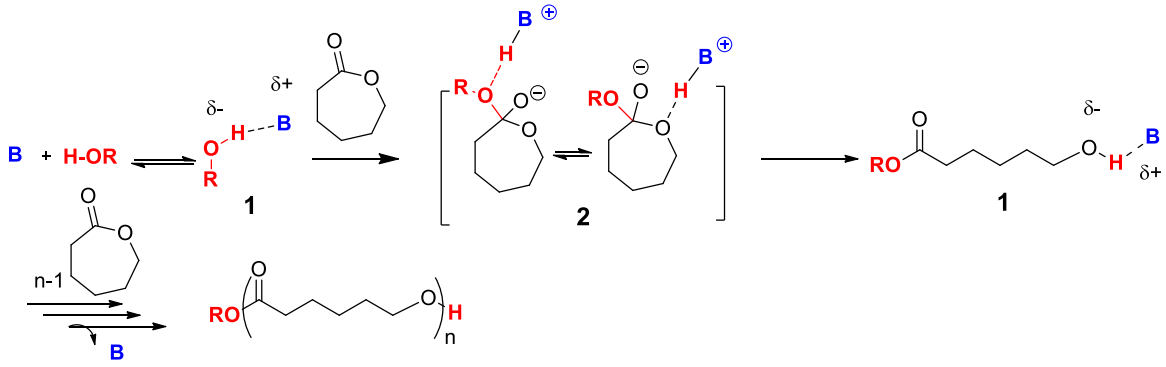

Scheme 4. Anionic ACEM in ROP of cyclic esters.

▪ **The cationic ACEM**. Brønsted acids (AH) can activate the carbonyl group of the monomer (Scheme 5, **1**) which can be further ring-opened by a second monomer by a carbon-oxygen bond scission (**2**). After completion of the ROP, the activated monomer at the ω-chain end can be neutralized by water, giving rise to a telechelic polymer presenting a carboxyl group at the α-chain end and a hydroxyl group at the ω-chain end (**3**). This mechanism was originally reported by Penczek and Kubisa for the ROP of cyclic ethers, such as ethylene oxide, THF, glycidol and epichlorohydrin.[55] Martin-Vaca, Bourissou et *al.* have further postulated that a cationic ACEM could compete with an AMM during the ROP of trimethylene carbonate (TMC) catalyzed by trifluoromethanesulfonic acid (TfOH).[56] Hedrick *et al.* have demonstrated, however, using computational calculations by density functional theory (DFT) that this mechanism is not likely to occur during the ROP of TMC.[57] Additionally, Basko and Kubisa have ruled out the possibility of ACEM during the ROP of LA.[58]

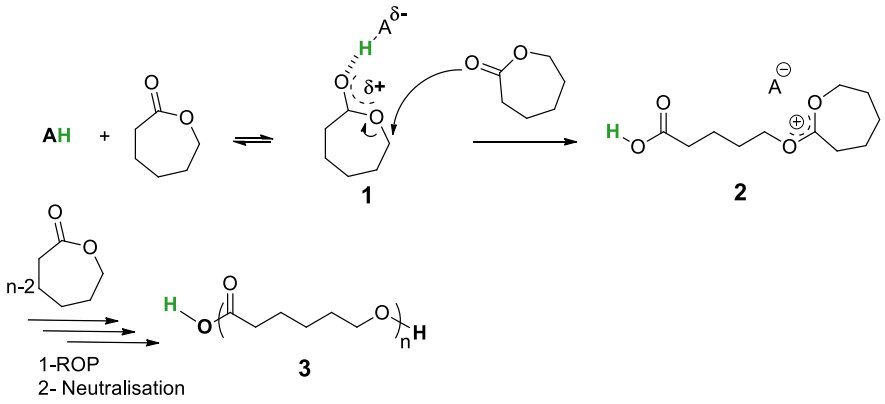

Scheme 5. Cationic ACEM in ROP of cyclic esters.

- **A bifunctional mechanism** involves a dual activation, where the base (B) can activate the initiator/chain end, while the electrophile (E) can simultaneously activate the monomer (Scheme 6). Monocomponent and bicomponent catalytic systems can be applied as bifunctional activator. For instance, the combination of a Brønsted acid such as benzoic acid (BA) and a Brønsted base such as 1,8-diazabicyclo[5.4.0]undec-7-ene (DBU) can form a bicomponent catalytic system able to activate both the monomer and the initiator/chain end.[59]

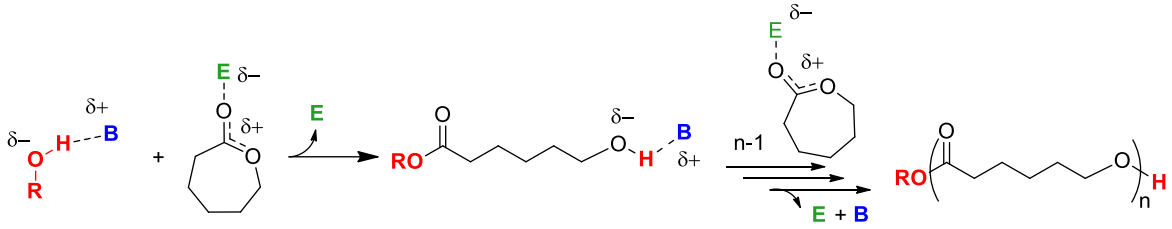

Scheme 6. Bifunctional mechanism in ROP of cyclic esters.

1.5 Potential side reactions occurring during the ROP of cyclic esters

Side reactions can occur during the ROP of LA and/or CL, namely, transesterification reactions (Scheme 7 a,b), side initiation by water (Scheme 7 c) and epimerization (Scheme 7 d).

Ester groups of polymer backbone produced by ROP can be subjected to transfer reactions. In the one hand, intramolecular transesterification causes cyclic formation along with shorter chains that can further propagate (Scheme 7 a). On the other hand, two polyester chains can undergo an intermolecular transesterification reaction, which leads to a segmental exchange (= reshuffling), the consequence of which is an increase of the dispersity of the final polyester (Scheme 7 b).

Adventious water traces –sometimes present even after careful drying the reagents- can initiate the ROP, creating a side population of chains, hampering control over the chain end fidelity by forming α-COOH polymer chain ends (Scheme 7 c).

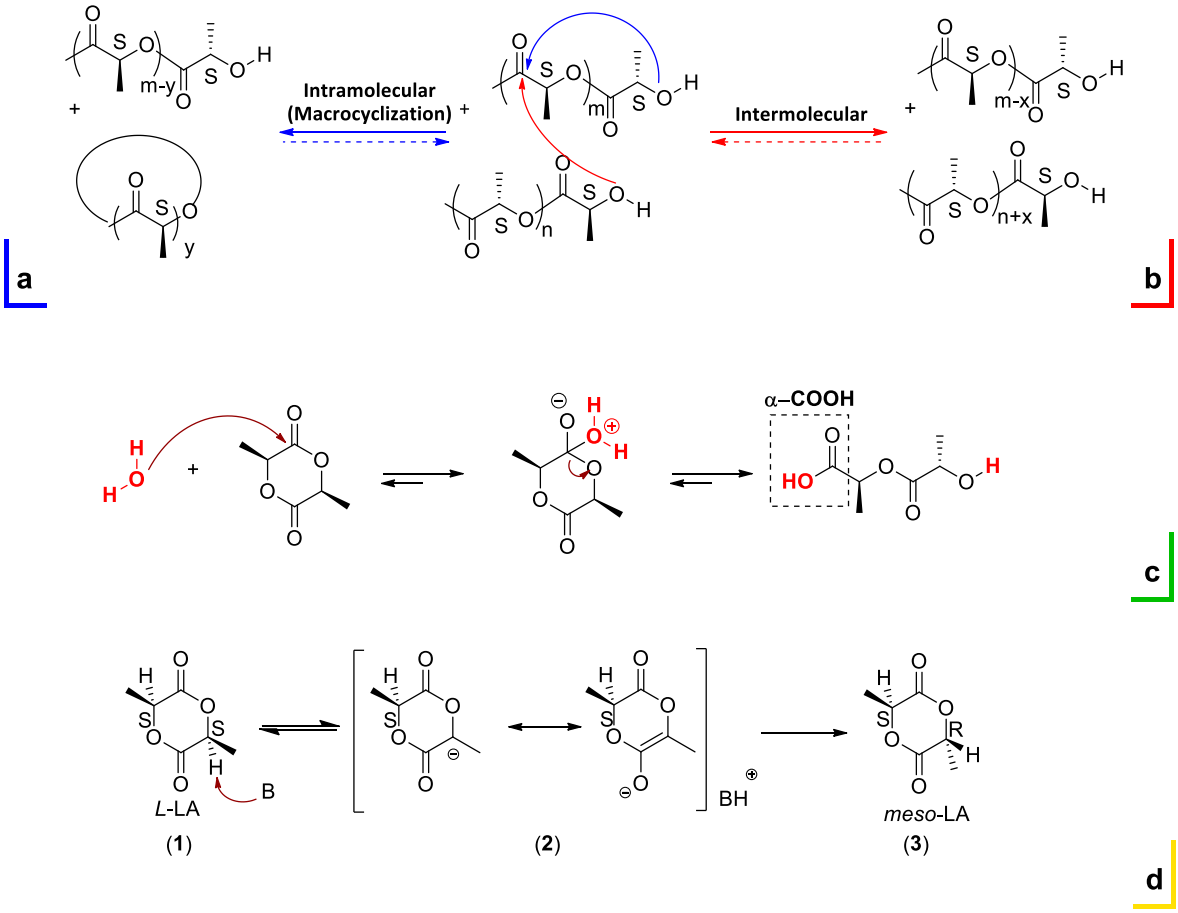

Scheme 7. Side reactions occurring during the ROP of a cyclic ester. (a) Intra- and (b) intermolecular transesterification reactions. (c) Co-initiation by water. (d) Epimerization of *L*-LA in *meso*-LA (B = Base).

Finally, in the specific case of cyclic esters featuring an asymmetric carbon, e.g. LA, epimerization can happen. This reaction consists in the reversible deprotonation of the α-methine (CH) group of *L*-LA by basic catalysts, which leads to the formation of a planar delocalized intermediate anion (Scheme 7 d). The latter is then protonated back leading to *meso*-LA.[60] Consequence of epimerization is a loss in the stereocontrol during ROP, thus decreasing the crystallinity and the thermo-mechanical properties of the obtained PLAs.

2 Processes implemented for the ROP of LA and CL

The ROP of cyclic esters requires very stringent conditions to be implemented. First of all, the reaction medium should be free of any traces of water, to avoid side initiation of the

ROP. Hence, all reagents should be dried using appropriate techniques. These include azeotropic distillation, distillation over CaH_2 or heating at high temperature under vacuum during several days. Corresponding equipement, including Schlenk-type reactors, vials and seringes are typically flamed or heated under vacuum. Finally, distilled liquids must be stored over molecular sieves and materials/reagents preferably stored in a glovebox.

Several processes have been set up to conduct the ROP of LA and CL, including solution, melt and reactive extrusion processes. Polymerization in supercritical carbon dioxide ($scCO_2$) has also been reported. Microwaves heating and continuous flow techniques are increasingly investigated in this context. Finally, emerging techniques, such as the mechanochemical ROP and the catalyst-free ROP performed under high pressure, will also be discussed.

2.1 ROP in solution and in the melt

- **ROP reactions performed in solution** have been extensively studied. This process enables to minimize the extent of side reactions, especially when ROPs are performed at ambient temperature, yielding well-defined (co)polymers. In industry, however, solvent-free techniques are much preferred, as they are cheaper, continuous and avoid the use of toxic solvents. Table 3 gathers the main solvents used for the ROP of CL and LA performed in solution, namely, chloroform ($CHCl_3$), dichloromethane (DCM), tetrahydrofuran (THF) and toluene. All these solvents are carcinogenic, mutagenic and reprotoxic (CMR). Table 3 gives their CMR classification and the globally harmonized system of classification and labeling of chemicals (GHS).

Table 3. Characteristics and toxicity of solvents used for the ROP of CL and LA.

Solvents	T_b (°C)[a]	CMR classement[b]	GHS Pictograms[c]
$CHCl_3$	61	C2, R2	
DCM	40	C2	
THF	66	C2	
Toluene	111	R2	

[a]Boiling point. [b]Carcinogenic, mutagenic, reprotoxic (CMR) substances. [c]Globally Harmonized System of Classification and Labelling of Chemicals (GHS)

- **ROP in the melt**, also referred to as bulk ROP, has been developed in order to avoid the use of toxic solvents. Because PCL chains are characterized by a low melting temperature (56 ° C < T_m < 65 °C), the bulk ROP of the liquid CL monomer is possible in mild conditions. In contrast, optically pure poly(*L*-lactide)s has a melting transition at around 180 °C, requiring to process the solid *L*-LA monomer (T_m ~ 100°C) at high temperatures. Polymerization in the solid state can yet be conducted below the melting temperature of PLA.[61,62]

2.2 Reactive extrusion process (REX) and static mode

In a batch reactor, the viscosity increases with the monomer conversion within a magnitude order of 10^5. When the viscosity is too high, the mixing and consequently the heat transfer become impossible. Reactions performed in batch can be transposed in a continuous way through a reactive extrusion process (REX, Figure 8). Twin-screw extruders (TSE) have been set up in order to solve the heat and mass transfer by increasing the mixing, to minimize the temperature gradient. Control over the residence time of the polymer within the extruder is crucial, which can be achieved thanks to the screw geometries. In this regard, REX allows for a faster polymerization kinetic and a lower residence time, enabling to minimize the thermal degradation of the polymer backbone. The process is not only cheaper and faster than ROP of LA in batch, but also operates *via* a continuous process. For these reasons, REX is preferred in industry for the synthesis of PLA or PCL.[63]

The Jérôme group in Liège has reported the REX of *L*-LA ROP catalyzed by stannous (II) octoate ($Sn(Oct)_2$).[64] Only 5 minutes are required to obtain the polymer, while 2 hours are needed in batch under the same conditions. It is noteworthy that stabilizing agents such as ultranox® (bis(2,4-di-*t*-butylphenyl)pentraerythritol diphosphite) are used in order to avoid oxidation reactions. The temperature applied for the ROP of *L*-LA and CL during REX are comprised between 130 and 180 °C.[63] Note that, to the best of our knowledge, no study has reported the use of organocatalysts for the REX of *L*-LA and CL ROP. TSE are preferentially used over single-screw extruder for REX, as they provide better control of residence time distribution and mixing, and a higher heat and mass transfer capabilities as well.[63]

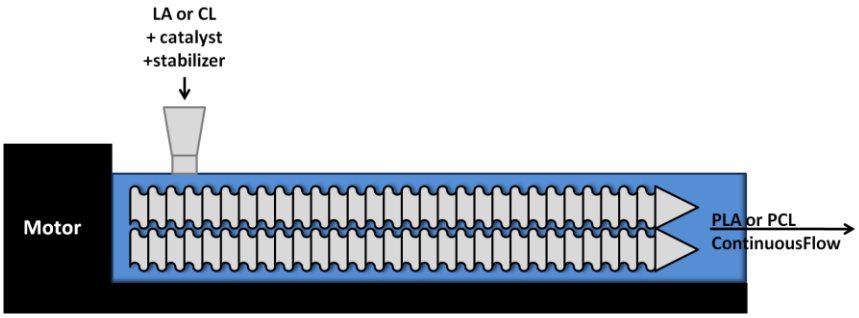

Figure 8. Twin-screw reactive extruder (inspired from Dubois *et al.*).[63]

The Shao group has compared the performances between tubular static mixing reactor (TSMR) and TSE.[65] The inner structure of the TSMR consists of four identical corrugated plate-type static mixers. The latter have many V-shaped channels, which can provide strong transversal flow. They force the polymer to flow from the center to the wall of the mixer or *vice versa* and lead to a better homogeneity of the temperature avoiding the local overheating.

The polymerization is typically conducted under the same conditions, *i.e.* at 170 °C, with an equimolar amount of $Sn(Oct)_2$ and triphenylphosphine (PPh_3) and a monomer-to-catalyst ratio of 2000/1. Even if longer polymerization time is needed in TSMR, the final PLLA exhibits better properties, such as a higher weight average molecular weight (M_w), a lower dispersity and a higher optical purity (OP) ($M_w \approx 166\,000$ g.mol^{-1}, $Đ = 1.48$ and OP = 99%), compared to the one obtained by REX under the same conditions ($M_w \approx 84\,000$ g.mol^{-1}, $Đ = 2.1$ and OP = 93%).[65]

2.3 Supercritical carbon dioxide (scCO2)

- **Supercritical carbon dioxide ($scCO_2$)** is an eco-friendly substitute of more traditional solvents; $scCO_2$ is inexpensive, non-toxic, non-flammable, recyclable, commercially available and has accessible critical parameters (T_c= 31 °C, p_c = 7.38 MPa). For the ROP of CL, different conditions can be applied, with a temperature ranging from 40 to 110 °C and pressure ranging from 8 to 24 MPa.[66,67] As PCL is not soluble and precipitates in $scCO_2$, the ROP process operates *via* a precipitation polymerization. With metallic alkoxide catalysts, a slower kinetic rate of the ROP of CL is observed in $scCO_2$, compared to bulk polymerization or reactions performed in toluene. Indeed, $scCO_2$ being a quadrupolar coordinating solvent, it can coordinate onto the alkoxide active chain ends, causing the carbonation of tin-alkoxides into dormant chain ends (Scheme 8a).[68,69] This phenomenon is also observed when aluminum (Al) IV, Al(III), lanthanide III (Ln(III)) and yttrium III (Y(III)) alkoxides are used.[67,69] Despite these issues, the use of $scCO_2$ proves convenient as CL and the metal alkoxide can be readily removed in a solvent-free process.[66,70] Furthermore, the reaction can be controlled with tin (II) and tin (IV) alkoxides.[68,69]

In the case of the ROP of *L*-LA, the working temperature can range from 65 to 80 °C, and the pressure from 24 to 30 MPa.[69,71,72,73] In these conditions, *L*-LA is in the melt state and can be dispersed in $scCO_2$, thus the ROP takes place within the *L*-LA droplets. No difference in the kinetic rates has been observed between reactions conducted in toluene or in $scCO_2$. This is due to the fact that the carbonation onto the active chain ends is possibly avoided by the formation of a five-membered coordinated structure (Scheme 8b),[69,71] the tin-based catalyst interacting with the carbonyl group of the second lactoyl unit in the lactidyl unit. The second explanation could be that the equilibrium would be shifted toward the active chains, due to the higher temperature applied (70 °C), *i.e.* above that applied for the ROP of CL (40 °C).

Enzymatic catalysts have also been applied for the ROP of CL in $scCO_2$, yielding high molar masses (up to 36 kg.mol^{-1}) with low dispersities ($1.4 < Đ < 1.6$),[66] whereas the ROP of *L*-LA, in the presence of Novozym 435 gives a molar mass of 12 kg.mol^{-1} in yields lower than 11%.[74]

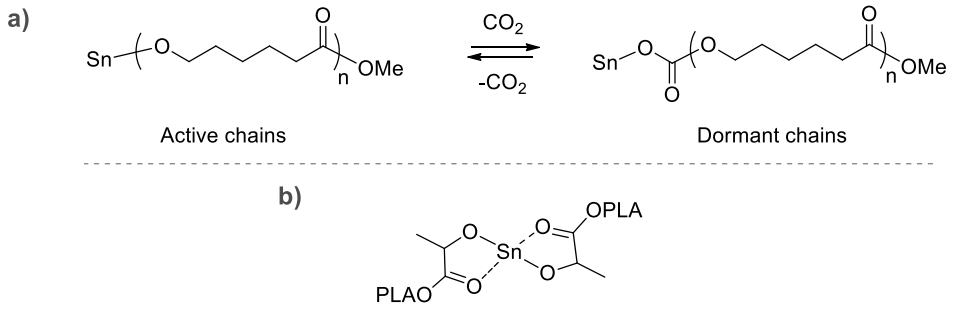

Scheme 8. a) Reversible insertion of $scCO_2$ onto the active chain ends of tin (IV) alkoxide during the ROP of CL. b) Formation of a five membered coordinated structure during the ROP of LA.[69]

Over the last decade, only two groups have described the organocatalyzed ROP (OROP) of LA in $scCO_2$,[75,76] The Thurecht group[75] has reported the use of DBU for the ROP of *D,L*-LA at 80 °C and 25 MPa, in the presence of benzyl alcohol (BnOH) as initiator with a $[DBU]_0/[BnOH]_0$ ratio of 1/1, polymerization time of 16 hours, affording PLAs with M_n up to 10 $kg.mol^{-1}$and a dispersity of 1.14. The as-obtained PLA has shown a high chain end fidelity and absence of inter- and intra-molecular transesterifications, as evidenced by MALDI-ToF mass spectroscopy. In other words, controlled ROP of LA is possible in these conditions, despite the formation of a DBU carbonate salt in equilibrium with free DBU, causing an inhibition period of the ROP process (Scheme 9).[77]

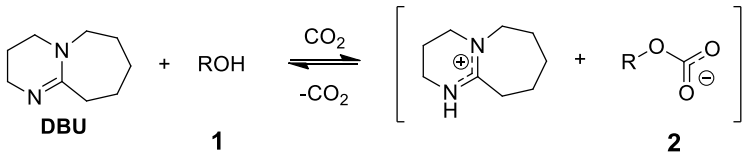

Scheme 9. Equilibrium between DBU and CO_2 in the presence of proton sources.[75]

More recently, the Detrembleur group[76] has used 1-(3,5-bistrifluoromethyl-phenyl)-3-cyclohexylthiourea/amine (TU5/amine) as a bicomponent catalytic system for the ROP of *L*-LA and *D,L*-LA. In order to avoid the formation of $RO\text{-}C(O)O^-$ (Scheme 9, **2**), which can lower the kinetic rate, only amine with low pKa values have been retained, such as *N*,*N'*-dimethylcyclohexylamine ($NCyMe_2$), N,N,N',N",N"-pentamethyldiethylenetriamine (PMDTA), 1,1,4,7,10,10-hexamethyltriethylenetetramine (HMTETA) or tris[2-(dimethylamino)ethyl]amine (Me_6TREN) (Scheme 10). Those amines are not basic enough to deprotonate the initiator/chain ends (**1**) and avoid the formation of (**2**). TU loading of 3 mol.% *vs.* monomer, $[TU5]_0/[amine]_0$= 1/1, a pressure of 30 MPa and a temperature of 80 °C have been applied. High control over the polymerization could be obtained, affording well defined PLLAs (M_n = 44 000 $g.mol^{-1}$, $Đ$ = 1.24) within 36 hours. The TU/DBU catalytic system has also been applied, but reactions have proven irreproducible.

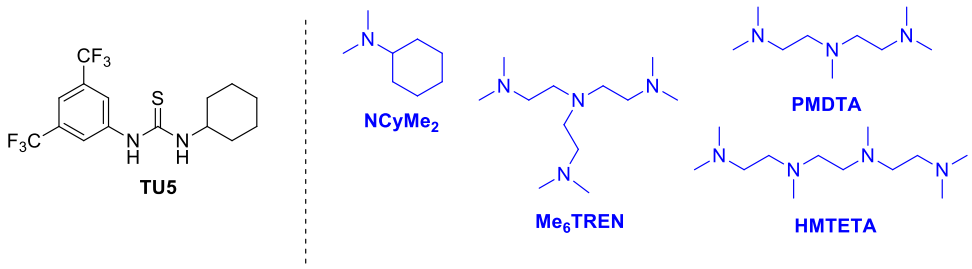

Scheme 10. Bicomponent catalytic system TU/amine.[76]

Finally, dispersion ROP of *L*-LA or CL in $scCO_2$ has been reported as a means to achieve polymeric nanoparticles.[72,73,70] To this end, perfluoropolyether-[72] and poly(dimethylsiloxane)[73] (PDMS)-based block copolymers have successfully been applied as stabilizers for the ROP of *L*-LA, while a PCL-*b*-P(heptadecafluorodecyl acrylate) diblock has been used for the ROP of CL.[70]

2.4 Miscellaneous processes

- **Microwave (MW) heating techniques** have been explored, mainly using metal alkoxide-type catalysts. Main studies about the ROP of LA or CL using microwaves have been reviewed in the book edited by Hoogenboom *et al*.[78] This process enables to easily and safely reach high temperatures. The reaction time can be decreased maintaining a high selectivity, almost quantitative yields, and with better precision than using conventional heating techniques. Several parameters can be controlled, such as pressure, temperature (continuous and ramping). The "non-thermal" microwave effect has been the topic subject of intense debates. Many researchers have thus proposed that irradiation from microwaves could influence the ROP process. In 2012 Ramier *et al.* have however shown that there is no irradiation effect, when comparing the ROP of LA in toluene heated *via* microwave dielectric heating *vs*. conventional heating. The temperature, as monitored with a connected probe, has been found the same for all experiments throughout the entire polymerization, with no significant change in monomer conversion, molar mass and dispersity noted.[79]

- **Continuous flow ROP.** Beers and Gross have transposed for the first time the ROP from a batch to a microreactor, using the continuous flow technique in order to improve the PCL synthesis process.[80,81] Guo *et al.* have reviewed the field of flow ROP in 2017.[82] An improved temperature control, a low waste generation, and safer experimental conditions are typical advantages of this process. In addition, the rapid mixing and the improved heating/mass transfer efficacy lead to in an increase of the kinetic. Finally, this technique can be conveniently scaled up, and reaction parameters can be varied easily, and more systematically.

- **Mechanochemical ROP of *D*-lactide (*D*-LA) by ball milling.**[83] Collision of small rigid stainless-steel balls inside a stainless-steel container can induce a high local pressure and mechanical energy. Such a ball milling process has been successfully applied to the ROP of *D*-LA (Figure 9). The ball collisions can be promoted by vibrations with different frequencies. However, use of a catalyst is required. In the presence of DBU as organocatalyst and BnOH as initiator, at a $[DLA]_0/[DBU]_0/[BnOH]_0$ ratio of 100/1.4/1, no polymerization has been noted after 1h at low vibration frequencies of 5 and 10 Hz. Increasing the vibration frequency from 20 to 30 Hz has enabled an increase of *D*-LA conversion, from 30 to 59%. The ball milling ROP has proven even more efficient in presence of toluene (40 µL), producing a PLA of high number average molar mass of 100 $kg.mol^{-1}$ and a dispersity of 1.64 within 4 hours.

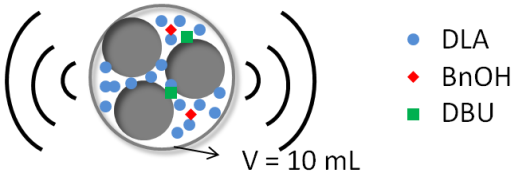

Figure 9. Mechanochemical ring-opening polymerization of *D*-lactide by ball milling.[83]

- **Catalyst-free ROP of CL initiated by water under high pressure.**[84] High pressure has been proposed to play a catalytic role during the ROP of CL initiated by water. In this case, the reaction temperatures are comprised between 80 and 120 °C, and no catalyst is needed. Two competitive phenomena have been found to occur, namely, polymerization and crystallization at high compression (1.2 GPa). To avoid the latter phenomenon, lower pressures (0.5 GPa) have been applied. Using a $[CL]_0/[H_2O]_0$ ratio of 480/1 at 80 °C and one week of reaction have provided a PCL (M_n = 19 $kg.mol^{-1}$, $Đ$ = 1.5) characterized by a carboxyl and a hydroxyl group at the α- and at the ω-chain end, respectively.

3 ROP of LA

3.1 Solution process

This section aims at providing an overview of main organocatalysts employed for the ROP of *L*-LA in solution, with a focus on reports published from May 2015 to September 2018.

BASIC AND NUCEOPHILIC CATALYSTS - Phosphazenes, NHCs, amines, amidines, guanidines and thioureas (TUs), operating *via* a nucleophilic AMM, or ACEM or by a bifunctional activation mechanism, have been extensively investigated, which have been discussed in different reviews (Scheme 11).[33,34,35,36,37,38,39,85]

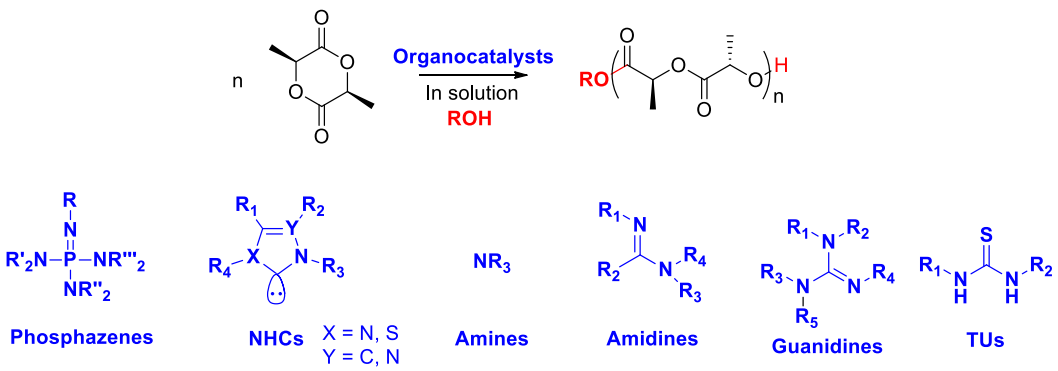

Scheme 11. Typical organocatalysts applied to the ROP of L-LA in solution.[37]

In 2016, Dove *et al*. have reported the first use of NHOs for the ROP of *L*-LA and other cyclic esters in THF at r.t (Scheme 12).[86]

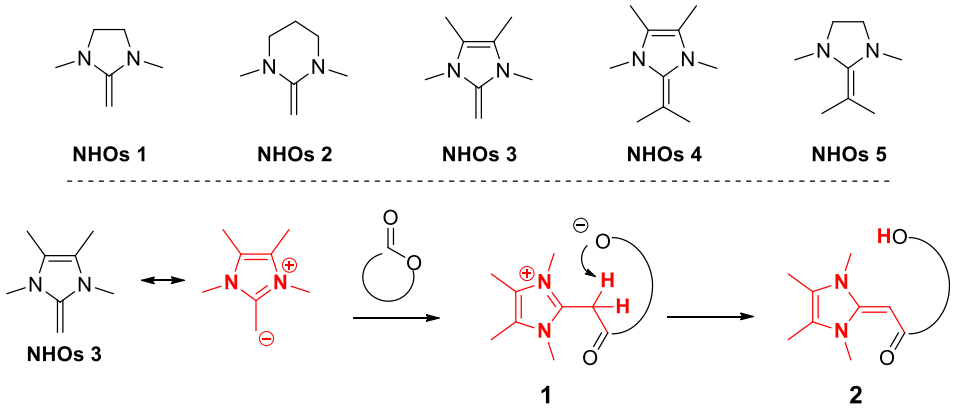

Scheme 12. NHOs for the ROP of *L*-LA in THF at r.t. (top). Deactivation of NHO **3** (bottom).[86]

NHO **1** has proven inactive in absence of alcohol, due to the saturated nature of the heterocycle. The catalytic activity in this series has been found in the following order: **3**>**2**>**1**. However, NHO **3** could not trigger the controlled ROP of *L*-LA in presence of BnOH, likely because of the formation of a zwitterionic intermediate species (**1**, Scheme 12), followed by deactivation of NHO **3** by protonation (**2**). NHO **4,** featuring a dimethyl substitution at the exocyclic carbon, has enabled the ROP of a large range of cyclic esters within a few minutes, though in a non-controlled manner. The saturated character of NHO **5** has allowed decreasing polarization of the olefinic bond, providing a faster and better controlled ROP of *L*-LA compared to NHO **4**.

The synthesis of well-defined catechol end-functionalized PLAs, as reported by Sardon *et al*.,[87] has employed the primary amine of the dopamine initiator and NEt_3 to initiate the ROP of *L*-LA in DCM at r.t (Scheme 13). PLLA with M_n up to 13 kg.mol^{-1} ($1.1 < Đ < 1.4$) has thus been

obtained. In contrast, employing DBU as organocatalyst has induced side reactions, owing to the too high basicity of DBU.

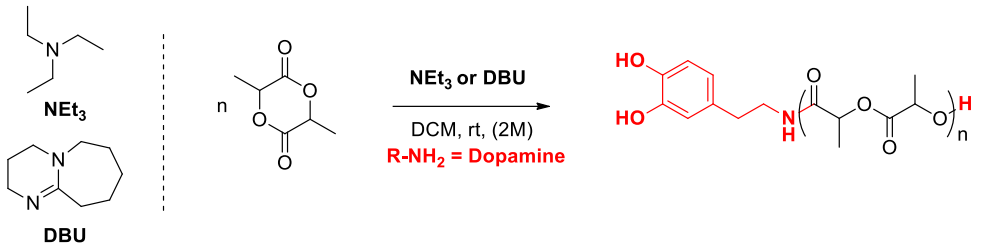

Scheme 13. Synthesis of catechol end-functionalized polylactides.[87]

In 2015, Waymouth *et al.* have used three cyclopropenimide (CP) superbases (Scheme 14) as organocatalysts.[88] The ROP of both *L*-LA and *rac*-LA has led to PLAs with molar masses up to 70 kg.mol^{-1} in DCM or benzene at r.t ($[LA]_0$ = 1 M; catalyst loadings from 1 to 5 mol.% *vs.* monomer). Nevertheless, polymerization is not controlled, as indicated by high dispersities (1.3-1.57), MALDI-ToF mass spectrum revealing transesterification reactions. Combined analyses have also shown that the lactide enolate, formed after deprotonation of LA by the superbase, can further initiate the ROP (Scheme 14). The same reaction has been postulated to occur during the ROP of *L*-LA catalyzed by 2-tertbutylimino-2-diethylamino-1,3-dimethylperhydro-1,3,2-diazaphosphorine (BEMP), a phosphazene-type organic superbase.

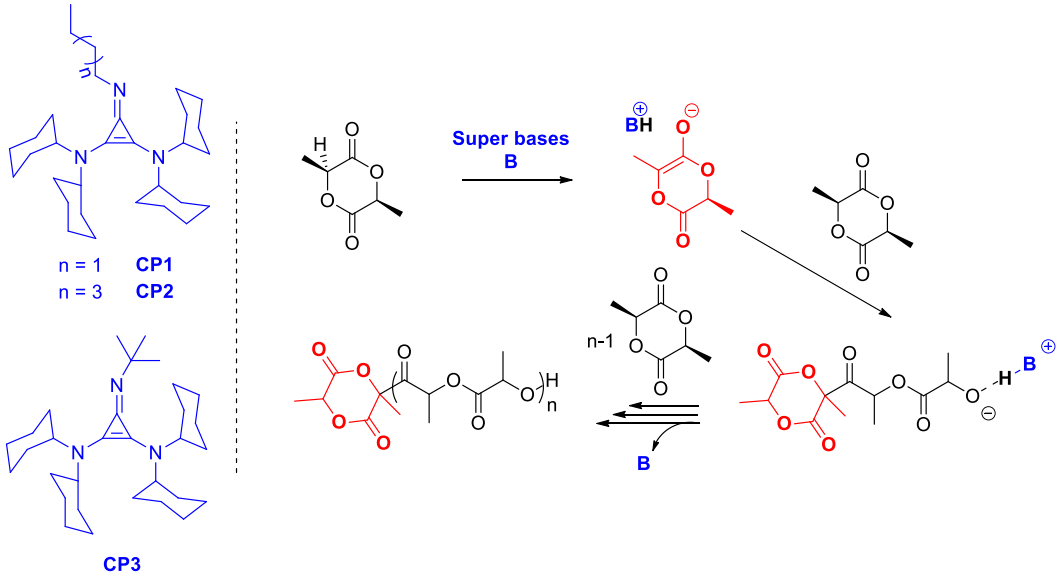

Scheme 14. Cyclopropenimide superbases. Initiation of *L*-LA ROP by LA enolate.[88]

BIFUNCTIONAL CATALYSTS – Dual (cooperative) activation through the use of mono- or bicomponent organocatalytic systems is particularly suitable to perform the ROP of cyclic esters in a controlled way. Related catalytic systems are usually composed of an acidic part that can

activate the carbonyl moiety of the monomer, and a basic part activating the hydroxyl group of the initiator/ propagating chain-end. The acid group acts as a hydrogen bond donor (HBD) while the basic group serves as a hydrogen bond acceptor (HBA) (Scheme 15).

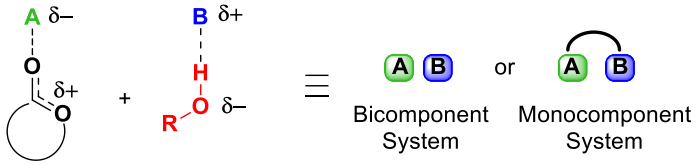

Scheme 15. Mono and bicomponent bifunctional catalytic systems.

1,5,7-Triazabicyclo[4.4.0]dec-5-ene (TBD) is a prototypal example of such bifunctional catalysts, involving accepting and donating hydrogen bondings.[89] TBD shows a very high catalytic activity for the ROP of *L*-LA (Scheme 16): within a few seconds, PLA with a high degree of polymerization (DP = 100) can be obtained with only 0.1 mol.% of TBD rel. to the monomer, in DCM at r.t.[90] Acyclic guanidine **1** (**AG1**), which has been reported by Hedrick *et al.* in 2010, exhibits a lower activity compared to TBD, which is ascribed to a lower basicity.[91] Hecht *et al.* have later developed guanidines possessing two aromatic substituents. While **AG3** has been shown poorly active, **AG4** is totally inactive for the ROP of *L*-LA in DCM at r.t.[92] The authors have thus designed acyclic guanidines, **AG2**, featuring one single aromatic moiety and giving a tunable catalytic activity. Indeed, by changing the substituent (**R**) the kinetic rate can be significantly improved, *i.e.* from 4 x 10^{-3} h^{-1} for $\mathbf{AG2_{CF3}}$ to 600 x 10^{-3} h^{-1} for $\mathbf{AG2_{NMe2}}$. The ROP process shows a "living" character with a $\mathbf{AG2_{NMe2}}$ loading of 2 mol.% *vs. L*-LA, leading to PLLAs of molar mass up to 26 kg.mol^{-1} and a *Đ* value of 1.18 within 96 hours.[92]

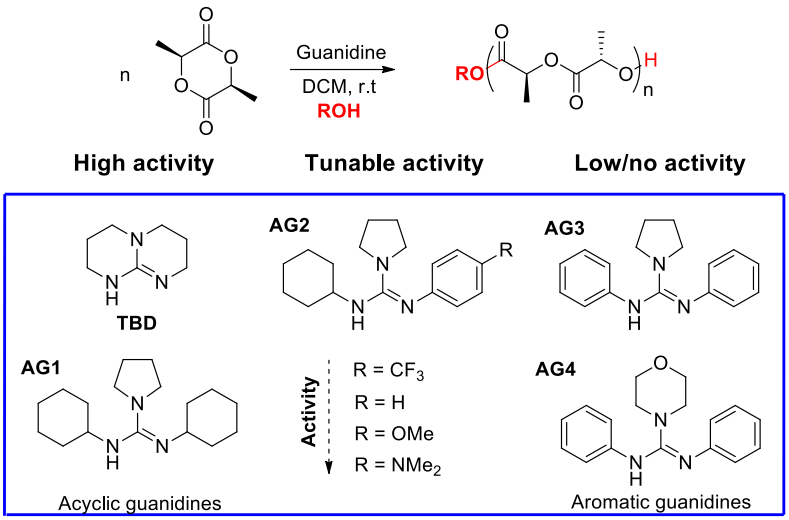

Scheme 16. Acyclic guanidines developed for the ROP of *L*-LA in solution.[90,91,92]

In 2017, Guo *et al.*[93,94] have developed a bicomponent organic catalytic system composed of an ionic HBD (guanidinium hexahydro-2Hpyrimido[1,2-a] pyrimidin-1-ium ([(HppH2)+]) and (–)-sparteine as the HBA for the ROP of *L*-LA, in presence of alcohols and secondary amines as initiators (Scheme 17). PLAs of predictable molar masses, up to 17.9 kg.mol^{-1}, and of low dispersity (*Đ* < 1.29) can thus be achieved, typically within 3h in DCM at room temperature, with a catalyst loading of 5 mol% rel. to the monomer for both HBD and HBA.

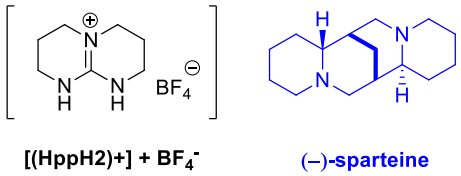

Scheme 17. Bicomponent catalytic system. HBD: [(HppH2)+]; HBA: (-)-sparteine.[93,94]

When resorting in 2005 to TU as a hydrogen bond donor (HBD), Waymouth, Hedrick *et al.* have made a real breakthrough in the context of OROP of cyclic esters. TUs indeed enable to minimize transesterification reactions,[95,96] providing a remarkable selectivity toward the carbonyl moiety of the monomer relatively to carbonyl groups also present in polymer chains.[96] As TUs are not active on their own, they are combined with a basic entity (HBA) that can activate the alcohol initiator. As mentioned, mono- (TU1) and bicomponent catalytic systems, can be employed (Scheme 18), the bicomponent TU5/ TACN being among the most efficient.[97] Despite the undisputable performances they provide in terms of selectivity, TU/amine organocatalysts are not extremely active, requiring from several hours to several days to reach completion of the ROP.[95,96,98]

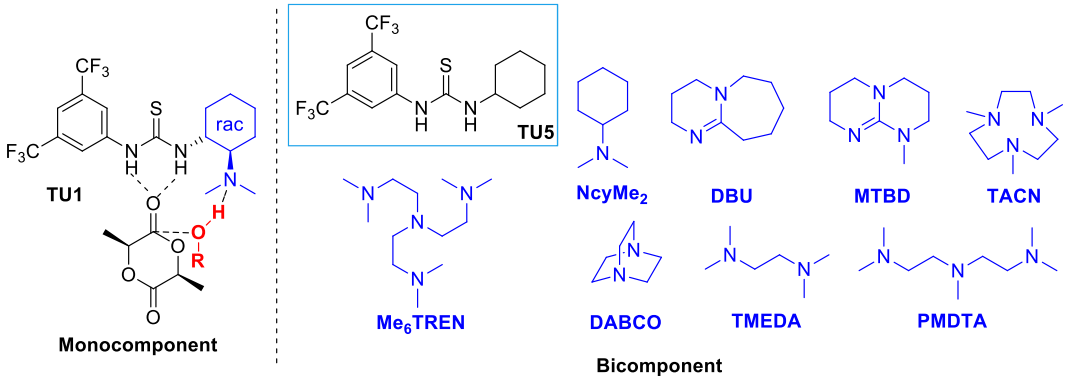

Scheme 18. Mono and Bicomponent thiourea/amine cocatalysts promote bifunctional activation.[95,96,98]

Kiesewetter *et al.* have designed bis-thiourea (bisTU) for the ROP of *L*-LA in DCM[99] By using $[LA]_0$ = 1 M and 2.5 mol% of bisTU and Me_6TREN, the ROP of *L*-LA initiated by BnOH achieves a conversion up to 95% within 20 minutes, forming well-defined PLLA ($M_{n,SEC}$ = 32 200

g.mol^{-1}, $Đ$ = 1.02). Computational calculations by DFT have evidenced that activated-TU mechanism is preferred to dual-TU activation of the monomer carbonyl (Scheme 19). During the activated-TU both TU moieties interact one to each other, favoring monomer activation while the alcohol initiator is activated by the basic cocatalyst.

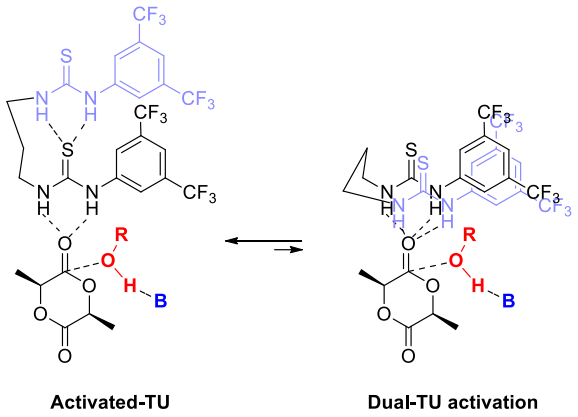

Scheme 19. Activated-TU and Dual-TU activation mechanism for bisTU/amine cocatalysts.[99]

In 2015, the Waymouth group has made a significant progress in the area of ROP by TUs. Combining TUs with organic or metallic alkoxides, the as-formed catalytic system shows both high selectivity and high reactivity for the controlled and fast ROP of *L*-LA in DCM at r.t.[100] In the presence of TU5, 1-pyrennebutanol and IMES, highly isotactic PLLAs can for instance be obtained, with M_n values up to 63 kg.mol^{-1} within only 50 min. The controlled/living nature of the ROP has been established through the production of narrowly dispersed chains ($Đ$ < 1.09) and absence of transesterification, at low catalyst loading ($[ROH]_0/[IMes]_0/[TU1]_0$ = 1/1/1). A bifunctional mechanism has been postulated, involving an imidazolium alkoxide deprotonating the thiourea to generate thioimidate. The latter would simultaneously activate the carbonyl group of the monomer and the initiator/propagating alcohol (Scheme 20).

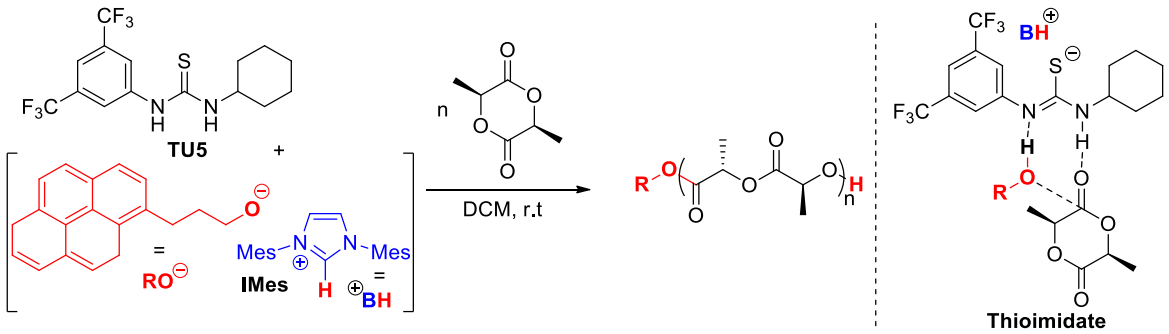

Scheme 20. Alkoxides initiated ROP of *L*-LA in solution catalyzed by TU. Thioimidate formation.[100]

In 2016, both the group of Kiesewetter and Guo have independently reported the OROP of cyclic esters through the use of bifunctional catalytic system based on urea and amine. Note

that ureas, that are the oxo-counterparts of thioureas, have not been too much considered in the context of ROP, as their NH moieties are less acidic those of thioureas. A boronate-type urea (BU) has yet been successfully applied and found more efficient than more regular ureas (U4) for the ROP of *L*-LA in DCM, in presence of tertiary amine and an alcohol as initiator (Scheme 21).[101] The boronate group would allow enhancing the HBD character of the urea. An even higher catalytic activity has been noted when combining boronate urea with (–)-sparteine. With a catalyst loading of 5 mol% rel. to monomer, PLLA with a M_n up to 18 kg.mol^{-1} has been obtained within 32 hours, the ROP showing features of a controlled/living process with low dispersity ($Đ$ < 1.14), absence of transesterification and efficient chain extension experiments.

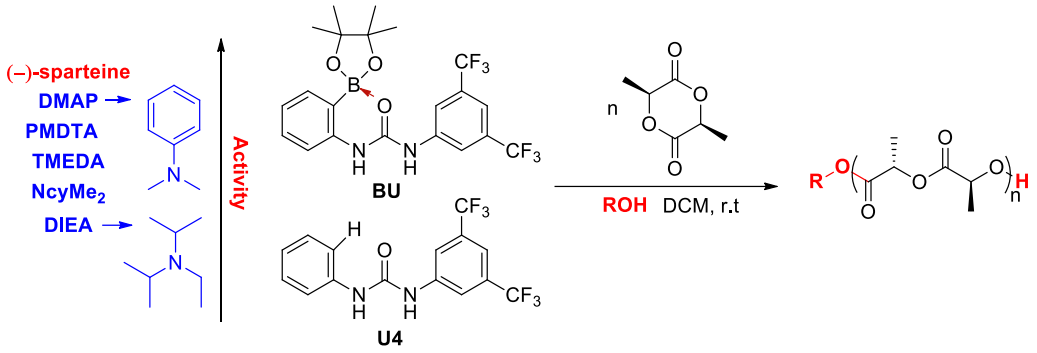

Scheme 21. Alcohol-initiated ROP of *L*-LA catalyzed by boronate urea.[101]

More insight into the ROP mechanism of δ-valerolactone (VL) utilizing (thio)ureas as HBD cocatalysts has been given in a recent study by Waymouth *et al.* (Scheme 22a).[102] The authors have combined a range of (thio)ureas with a range of organic bases. Each combination can be viewed as an acid-base couple. The catalytic activity has been correlated with pKa values of both the acidic (thio)urea and the conjugated acid of the organic base. These investigations have led the authors to the following conclusions:

- For a given thiourea or urea, the maximal catalytic activity is obtained when they are combined to the strongest base.
- For a given base, the maximal activity is obtained when the pKa of a given (thio)urea is close to the one of the conjugated acid of the base (Scheme 22a).
- When the urea and thiourea possess approximatively the same pKa value, the urea/base catalytic system is much more efficient than the thiourea/base catalytic system.

On these grounds, two mechanisms have been discussed (Scheme 22a), including an anionic mechanism if the pKa of the base is higher than that of the (thio)urea, or a cooperative mechanism if the pKa of the base is lower than that of the (thio)urea.[102]

Recently, the group of Kiesewetter has provided further insight into the mechanism involving (thio)urea combined with 7-Methyl-1,5,7-triazabicyclo[4.4.0]dec-5-ene (MTBD).[103] The authors have suggested a new pathway where the anionic (thio)urea would activate the hydroxyl of the initiator/ propagating chain-end and the protonated base would activate the carbonyl of the monomer (Scheme 22b). In addition, non-polar solvents would favor a cooperative mechanism (Scheme 22a), while polar solvents would give rise to the (thio)imidate mediated mechanism (Scheme 22b) in the case of the ROP of VL.[103]

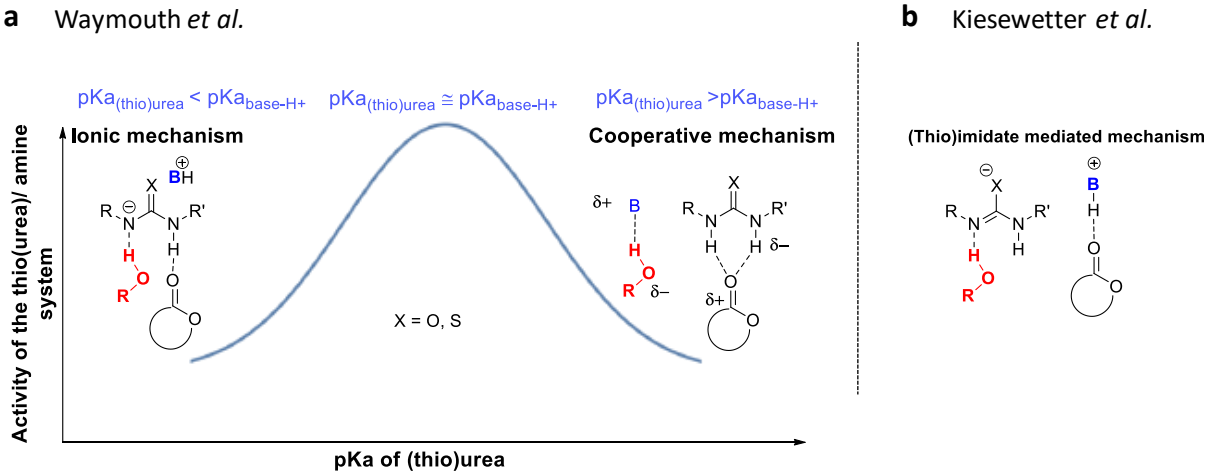

Scheme 22. (a) Ionic and cooperative mechanism proposed by Waymouth.(b) (Thio)imidate mediated mechanism proposed by Kiesewetter.[102,103]

Note that TU5 has been recently found to show a high cytotoxic.[104] Therefore, more studies are needed in the field of organocatalyzed polymerization, so as to establish the toxicity of all (thio)ureas developed in the last 15 years.

The success of bifunctional catalytic systems combining a TU and an amine, in terms of selectivity and quality of control, has driven more research efforts to find new HBAs. For instance, the group of Guo has reported the use of squaramides (Sq1, 2 & 4, Scheme 23a) for the OROP of *L*-LA in DCM at r.t.[105] To be active, squaramides also require to be combined with an amine (HBA). Thus, Sq1 that possesses electron-deficient aromatic groups in combination with *(-)*-sparteine, has been found the most efficient bicomponent system, in order to produce well-defined PLAs when using BnOH as initiator (M_n ≈ 16.2 kg.mol^{-1}; $Đ$ = 1.05) within 11 hours. Synthesis of diblock copolymers, using a pre-formed poly(trimethylenecarbonate) (PTMC) as macroinitiator for the ROP of *L*-LA and Sq1/sparteine[105]or Sq1/PMDTA[106], has been also successfully achieved.

In 2017, Specklin *et al.* have reported the OROP of *L*-LA in DCM at r.t ($[LA]_0$ = 2 M) using a monocomponent squaramide catalyst (Sq 8-10, Scheme 23b) and a bicomponent catalytic

system Sq/amine (Sq11 & 12, Scheme 23b).[107] Sq8 has for instance enabled the synthesis of PLA (M_n = 14.6 kg.mol-1, $Đ$ = 1.06) in presence of BnOH, within 72 hours with [*L*-LA]$_0$/[Sq]$_0$ = 600/1.

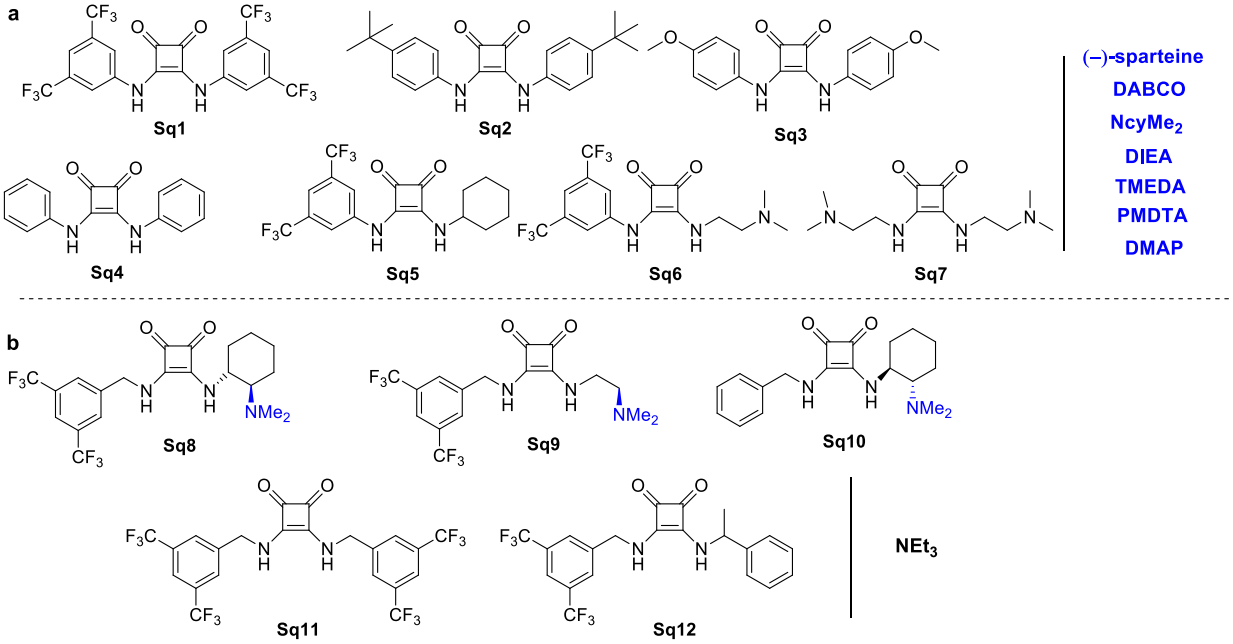

Scheme 23. Squaramide/ amine mono- and bicomponent bifunctional catalysts for the ROP of cyclic esters.[105,106,107]

Hedrick *et al.* have combined DBU and benzoic acid (BA) in the form of a salt for the subsequent ROP of *L*-LA. This dual catalytic system (1:1 eq) is indeed able to reach full conversion within 24 hours at r.t., leading to well-defined PLLA with a DP of 100.[59]

Another bicomponent catalytic system composed of a HBD and a Brønsted acid has also been proposed by Guo *et al.* to perform the ROP of LA in DCM at r.t in the presence of BnOH (Scheme 24).[108] Use of methanesulfonic acid (MSA) as Brønsted acid has not enabled the ROP of *L*-LA, in contrary to thiophosphorictriamide (TPTA). The reaction has been found to be accelerated by combining both MSA and TPTA, achieving PLLA with molar masses up to 16 kg.mol^{-1} and dispersity bellow 1.22 ([BnOH]$_0$/[TPTA]$_0$/[MSA]$_0$= 1/1/1]). Nevertheless, long reaction times are needed, *i.e.* 120 hours for a targeted DP of 100. In addition, side initiation by water has been evidenced. An AMM has been proposed, where TPTA would stabilize the sulfonate anion by triple hydrogen bonds, enhancing proton release of MSA for activation of the monomer.

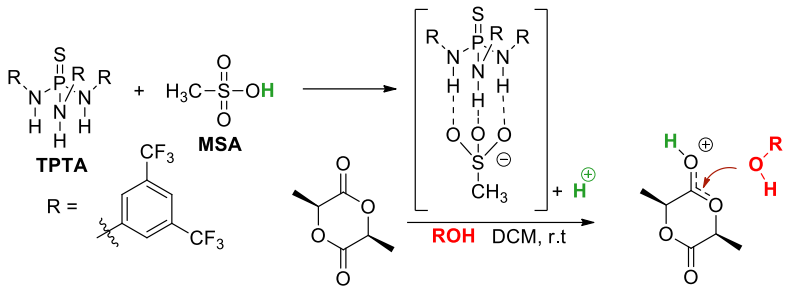

Scheme 24. Bicomponent catalytic system composed of TPTA and MSA.[108]

Finally, it is worth mentioning that there is only one acidic-type organic catalyst that has been reported to efficiently trigger the ROP of *L*-LA in solution, namely, trifluoromethane sulfonic acid (HOTf) *(pKa = -12)*.[109,110,111,58] Controlled ROP of *L*-LA can be achieved in DCM at r.t with a catalyst-to-initiator ratio of $[HOTf]_0/[ROH]_0 = 1$ and an initial *L*-LA concentration, $[LA]_0 = 1$ M. PLLAs with a molar mass (M_n) up to 16.4 kg.mol^{-1} and a dispersity between 1.13 and 1.48 have thus been obtained within several hours, depending on the targeted degree of polymerization ($DP_{,th}$).[110]

Sulfonic acids, such as TfOH and MSA, have originally been presented as strong Brønsted organic acids operating *via* an AMM. However, Bourissou, Martin-Vaca *et al*. and Hedrick *et al.* have reconsidered this statement and, on the basis of DFT calculations, the authors have postulated that sulfonic acids would behave as bifunctional catalysts (Scheme 25). These acids would thus act as a proton shuttle *via* the acidic hydrogen atom and the basic oxygen atom of the sulphonate group.[112,57]

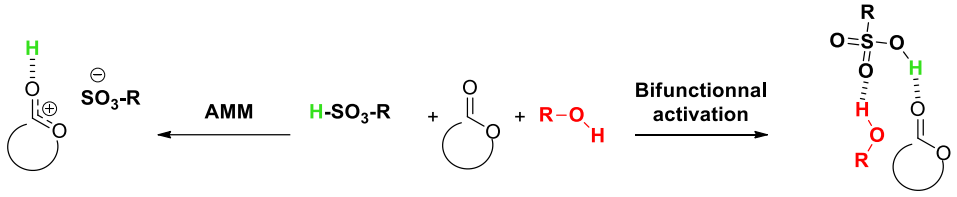

Scheme 25. Activated monomer mechanism *vs.* bifunctional activation for sulfonic acid catalysts.[112,57]

Intermediate conclusions- The use of basic and nucleophilic compounds for the organocatalyzed ROP of *L*-LA in solution under rather mild conditions is very well documented. With the noticeable exception of trifluomethanesulfonic acid, which has enabled on its own to perform the ROP of *L*-LA, other Brønsted acidic catalysts require a co-activation with a basic compound, or with a HBD, to be efficient. Besides this, mono- and bicomponent dual catalytic systems have gained an increasing interest over the last three years. Among them, (thio)ureas combined with Brønsted bases appear as the most promising catalytic systems, affording well-defined and high molar mass polyesters within few seconds or minutes.

3.2 ROP in the melt

Bulk polymerization requires the use of temperatures as high as 180 °C, *i.e.* above the melting temperature of PLLA,[42] in order to produce PLLA chains by reactive extrusion processes. Beyond the possibility to achieve PLLAs at such high temperatures without the occurrence of epimerization, transesterification and macrocyclization side reactions, use of organic catalysts in this context is challenging as they generally show a low thermal stability, hence they have rapidly deactivated under such conditions. The next chapter discusses the efforts to synthesize PLLAs under solvent free conditions and at high temperature (bulk). Basic-type, acidic-type and bicomponent catalysts, some of them being naturally occurring, have been investigated for this purpose.

ENZYMES - First attempts at conducting the metal-free ROP of *L*-LA in bulk have been reported by Matsumura *et al.* using enzymes as catalysts.[113,114] Among several lipases tested, *Lipase pseudomonas PS* has led to the most promising results for the ROP of *L*-LA at 100 °C, affording high molecular weight PLLA (M_w = 48kg.mol^{-1}; $Đ$ = 1.2). However, the ROP process cannot be carried out at too high temperatures because the enzyme would be susceptible to degradation; hence long polymerization times are needed -up to 7 days- to reach a monomer conversion of 82%. Furthermore, low polymer yields of 10% are obtained as a consequence of the removal of the major oligomeric *L*-LA fraction by precipitation. Similar results have been reported with other lipases, such as Novozym 435[115] and *Candida Antarctica* lipase B (CAL-B)[116,117] limiting the potential of such enzymatic catalysts for the ROP of *L*-LA in bulk.

BASIC AND NUCLEOPHILIC CATALYSTS -In 2001, Hedrick *et al.* have reported the the OROP of *L*-LA at 185 °C using 4-(*N*,*N*'-dimethylamino)pyridine (DMAP)[118] in presence of BnOH (DMAP/BnOH=2/1; Scheme 26). Predictable DP values, up to 60, and low dispersities ($Đ$ < 1.2) have been achieved in less than 10 minutes. According to the authors, the polymerization would operate *via* the AMM, involving the nucleophilic attack of DMAP onto the monomer, generating an acyl pyridinium alkoxide zwitterionic intermediate species. DMAP has also been used for the ROP of *L*-LA in presence of pyrenemethanol at 140 °C.[119] This organocatalyst, however, is recognized as being highly toxic (median lethal dose (LD_{50}) in rats, intravenous: 56 mg/kg)[120] and only PLLA of molar mass lower than 10 kg.mol^{-1} could be obtained. Alternatively, 4-pyrrolidinopyridine (PPY) can be employed to catalyze the bulk ROP of *D,L*-LA at 135 °C, as reported by Hedrick *et al.*.[118] This has also been shown by Katiyar *et al.* who have used PPY for the bulk ROP of *L*-LA at 120 °C.[121] In absence of added protic initiator, polymers with M_n values up to 18 kg.mol^{-1} have been achieved. MALDI-ToF MS analysis has revealed that PPY acts as both catalyst and initiator. Under these conditions, however, significant transesterification side reactions have been noted. Notably, increasing the temperature, from 120 to 160 °C, has allowed increasing the

polymerization rate, as expected, though at the expense of the control since M_n has been found to decrease at 160 °C as conversion has increased.

Beyond the use of DMAP and PPY, other nucleophilic catalysts have been studied for the bulk ROP of *L*-LA. In 2002, the group of Hedrick has reported the controlled ROP of *L*-LA catalyzed by phosphines.[122] Reactions have been conducted in bulk at 135 °C or at 180 °C in the presence of BnOH as initiator, with targeted DP between 30 and 60. A linear correlation between the DP and the monomer conversion has been observed and polymers displaying low dispersities (for bulk polymerization) from 1.11 to 1.40. P(*n*-Bu)$_3$ has been shown very active, enabling the polymerization within 10 min, phosphine activity eventually decreasing with decreasing the basicity and the nucleophilicity as follows: P(*n*-Bu)$_3$> P(*t*-Bu)$_3$> PhPMe$_2$> Ph$_2$PMe > PPh$_3$> P(MeO)$_3$ (unreactive). Thus, the electron availability at phosphorous atom appears as a dominant variable, as expected in the nucleophilic catalysis mechanism. Nevertheless, phosphines are flammable (flash point = 37 °C) and susceptible to undergo oxidation[123] since phosphorous has a strong oxygenophilic character. In fact, it has been noted that the reaction media turns to amber color after long polymerization times when the less nucleophile catalysts are used, which is especially notable at 180 °C.

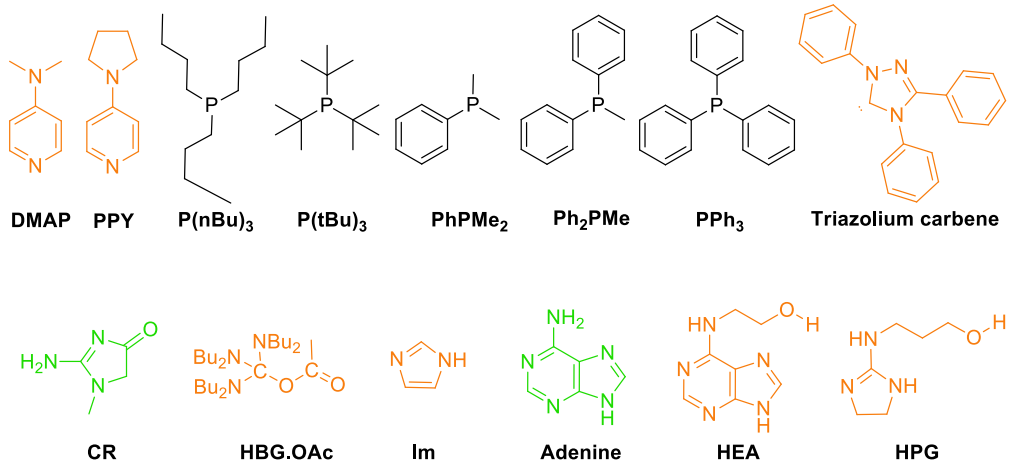

Scheme 26. Basic and nucleophilic organocatalysts applied for the ROP of *L*-LA in bulk. With the natural catalysts drawn in green, the Nature-inspired ones in orange, while the others in black.

NHCs have also been widely studied as potent nucleophilic catalysts for the ROP of cyclic esters (and for other monomers as well) on account of their highly reactive nature and tunability of the catalyst structure.[34] Despite the large number of studies, the only statement of using NHCs for ROP of *L*-LA in bulk has been reported in 2007.[124] Using 1,3,4-triphenyl-4,5-dihydro-1*H*-1,2,4-triazol-5-ylidene carbene, and alcohol initiators at 135 °C, highly isotactic PLLAs have been achieved with experimental M_n values, up to 10 kg.mol^{-1}($Đ$ ~ 1.15), comparable with theoretical

values. Notably, however, increasing the temperature of the polymerization reaction has led to a loss of control as a result of a thermal decomposition of the triazolylidene-type NHC.

In 2004, the group of Zhao has studied two guanidine-like organocatalysts in this process. Creatinine (CR),[125] a naturally-sourced compound, and hexabutyl guanidinium acetate (HBG.OAc),[126] a synthetic analogue, have thus been studied for the bulk ROP of *L*-LA (Scheme 26). Creatinine produces PLLA with M_n= 15.6 kg.mol^{-1}in 96h at 165 °C, but the controlled/living nature of the polymerization has been not reported. In contrast, use of guanidinium acetate enables a highly-controlled polymerization at 110 °C, yielding PLLA with DPs up to 150 and narrow dispersity (*ca*. 1.09) within 24h. However, none of these organocatalysts can be applied at temperatures as high as 180 °C, epimerization of the monomer being observed.

Acyclic guanidines[119] have been found to efficiently catalyze the ROP of *L*-LA at 140 °C, the most promising one being 1,1,3,3-tetramethyl-guanidine, achieving 45% monomer conversion within 30 min to give a polymer with a M_n of 12 kg.mol^{-1}. However, no detailed study has been provided with this catalyst.

Imidazole (Im) and imidazole-based catalysts have also proven attractive for the synthesis of PLLAs. Kricheldorf *et al.* have reported the synthesis of cyclic PLLAs using Im catalysis.[60] The polymerization of *L*-LA has been conducted in the absence of protic initiator, at 100 °C, with a *L*-LA-to-Im ratio of 20. The polymerization process has been postulated to occur *via* a combination of a chain-growth ROP with PLA chains containing an imidazole α-chain end, and a step-growth polymerization forming cyclic polymers *via* a kinetically controlled end-to-end cyclisation involving the subsequent Im elimination. Transesterification side-reactions and extensive epimerization have been observed during the *L*-LA polymerization, leading to amorphous atactic PLAs.

Adenine end-capped PLLAs have been synthesized by Nogueira *et al.*[127] This naturally occurring compound featuring pyrimidine and imidazole moieties has served both as catalyst and initiator at 135 °C under solvent-free conditions. However, the polymerization is not controlled and leads to oligomers of high dispersity (1.48 < *Đ* < 2.05) and non-predictable chain length. Analysis of the resultant polymers by MALDI-ToF MS has revealed that transesterification reactions occur. Three distinct populations of chains have been identified, including (*i*) PLA initiated by adenine (*ii*) PLA containing carboxylic acid at the α-chain end due to adenine initiation followed by displacement by water and (*iii*) cyclic PLA. At higher monomer conversions and at high polymerization temperature, the proportion of PLA macrocycles has been found to increase. The presence of cyclic PLAs has suggested that the imidazole moiety of adenine initiates the polymerization, consistently with previous findings by Kricheldorf *et al*.[60] Increasing the polymerization temperature up to 180 °C causes the degradation of the polymer, which is characterized by a deep brown color. In order to avoid the generation of cyclic PLAs and

to reach higher M_n, the group of Penczek[128] has developed a hydroxyl-alkylated adenine, 6-(2-hydroxyethyl)-aminopurine (HEA). This strong base, which has a structure very close to that of adenine, also acts as both catalyst and initiator for the ROP of *L*-LA in bulk at 120 °C. High molar mass PLAs up to 56 kg.mol^{-1} have been achieved in this way with relatively narrow dispersity (*Đ* < 1.31) within 30.5 h. No transesterification has been noted, and only HEA end-capped PLLAs have been observed by MALDI ToF MS analysis. The absence of PLA macrocycles may result from the steric hindrance around the imidazole moiety generated by the hydroxyalkyl group. A hydroxyalkylated imidazole, namely, 3-[(4,5-dihydro-1H-imidazol-2-yl)amino]-propanol (HPG), has also been designed for the bulk polymerization of *L*-LA, enabling shorter reaction times at 120 °C.[128] However, PLLAs with lower molar masses *ca*. 13 kg.mol^{-1}and broad dispersity *ca*. 1.63 have been obtained. In this case initiation occurs from both the -OH and -NH groups leading to two PLA arms per HPG molecule. For both catalysts, epimerization of the monomer has been evidenced, limiting their applicability in bulk ROP.

ACIDIC CATALYSTS –Brønsted organic acids have been little explored for the ROP of *L*-LA in bulk.[129,130] Bednarek *et al.*[129] have used TfOH in combination with amine-type initiators for the ROP of *L*-LA in bulk at 120 °C (Scheme 27). However, only oligomers with high dispersities (between 1.87 and 3.8) have been achieved. This has been in part explained by side initiation by water. Diphenylphosphate (DPP), which acts as a very efficient bifunctional organocatalyst for the ROP of lactones, is not suitable for the ROP of *L*-LA in solution.[131] In contrast, Saito *et al.* [130] have shown that DPP – 2eq rel. to the initiator for a DP = 50 – can activate the ROP of *L*-LA at 130 °C, yielding a highly isotactic PLLA within 22 h with a relatively good control over molar mass and dispersity.

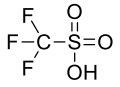

HOTf

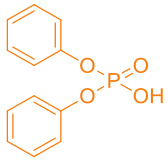

DPP

Scheme 27. Acidic catalysts applied for the ROP of *L*-LA in bulk. With the non natural catalysts drawn in black and the Nature-inspired ones in orange.

AMINO ACID CATALYSTS – They are interesting organic compounds as they contain both carboxylic and amine groups probably enabling a bifunctional mechanism. For instance, *L*-citrulline and *L*-arginine[132] have been studied as α-amino acid-type organocatalysts (Scheme 28), for the ROP of *L*-LA in bulk. While analysis of polymers resulting from polymerization performed in bulk at 160 °C has revealed a good correlation between the $M_{n,th}$ and $M_{n,exp}$ up to 14 kg.mol^{-1}, significant transesterification reactions has been noted. Three populations of PLLA chains have been

identified, including two linear structures bearing either a carboxylic acid or α-amino acid as α-chain ends, and cyclic PLLAs.

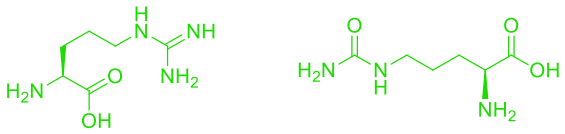

Scheme 28. Amino acids catalysts applied for the ROP of *L*-LA in bulk. With the natural catalysts drawn in green.

Bicomponent catalytic systems- Association of a basic- and an acidic-type molecule usually forms a salt of improved thermal stability. Furthermore, bicomponent catalytic systems are known to activate both the monomer and the initiator/chain end (Scheme 29). For instance, creatinine combined with acetic acid (CR-A) and glycolic acid (CR-G) have been employed by Zhao *et al.* for the bulk ROP of *L*-LA at 130 °C (for CR-A) and 110 °C (for CR-G).[133] Rather good control over the polymerization can be achieved, polymers with M_n up to 15 kg.mol^{-1} being obtained within four days. However, the ROP process is characterized by extensive epimerization of *L*-LA. Moreover, creatinine also contributes to initiation of the ROP before being removed by residual water.

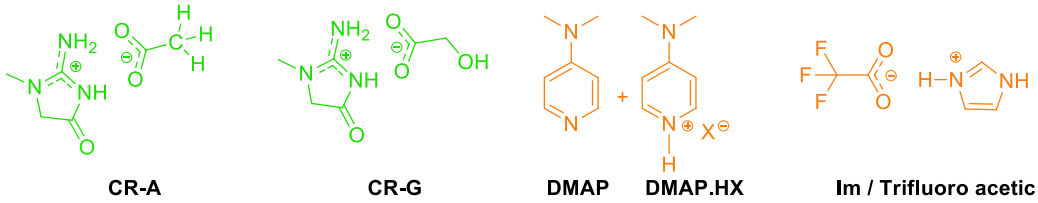

Scheme 29. Bicomponent catalytic systems applied for the ROP of *L*-LA in bulk. With natural catalysts drawn in green and the Nature-inspired ones in orange

A bifunctional catalytic system composed of imidazole and trifluoro acetic acid in the presence of BnOH has been studied by Coulembier group.[134] The combination of the bicomponent system to the exogenous alcohol actually mimics the catalytic triad of an enzyme active in ROP and enables the ROP of *L*-LA to proceed at 140 °C. The high activity of this catalyst system has been established by the achievement of a 84% monomer conversion after 3.7h ([*L*-LA]$_0$/[Im salt]$_0$/[BnOH]$_0$ = 70/5/1) with the resultant polymers being produced in a controlled manner. However, transesterification reactions have been observed to some extent, as well as a low molar mass population initiated by water. In addition, TGA analysis of the catalytic salt has revealed a thermal degradation at 170 °C, which would limit its application under industrially-relevant bulk polymerization conditions.

Guillerm *et al.*[119] and Peruch *et al.*[61] have combined DMAP with its conjugated acid in the form DMAP.HX, in a bicomponent catalytic system (2:1 mol% rel. to the monomer) in the presence of protic initiators at 100 °C. This system exhibits a high organocatalytic activity and a high selectivity, producing PLLAs of *ca*. 14kg.mol^{-1}within only 1 h using DMAP:DMAP.HOTf.[61] The absence of transesterification reactions during the course of the polymerization up to 90% monomer conversion and narrow dispersities characterize this ROP process. However, base-catalyzed epimerization has been evidenced, as attested by the rather low melting temperature of 130 °C of as-synthesized PLLA.

Kiesewetter *et al.* have reported the solvent-free ROP of *L*-LA in the presence of (T)U/amine co-catalyst, in the solid state at 100 °C (Scheme 30).[62] When PMDTA base cocatalyst is used, the order of catalytic activity should be as follows: bisTU > tris-thiourea (trisTU) > TCC > tris-urea (trisU) > TU5 > bis-urea(bisU) > U5. All thioureas employed have proven more active than their urea counterparts. For instance, bisTU proves more active than bisU. When a mixture of bisTU and PMDTA (1/1 mol% each rel. to the monomer) is employed as catalytic system, well defined PLLA (M_n= 10700 g.mol^{-1}, $Đ$ = 1.06) with high isotacticity (Is = 0.94) is obtained within only 5 minutes (isotacticity is the number of isotactic enchainment divided by the total number of enchainment). When bisTU is applied in presence of different amines, the catalytic activity varies in the order: *t*-TACN > Me_6TREN > PMDTA > (+)-sparteine >DMAP > TMEDA > pyridine (no activity). PMDTA represents a good compromise between catalytic activity and isotacticity. However, a higher temperature (140 °C) induces a loss of control of stereochemistry, and the final material evolves from transparent to yellowish.

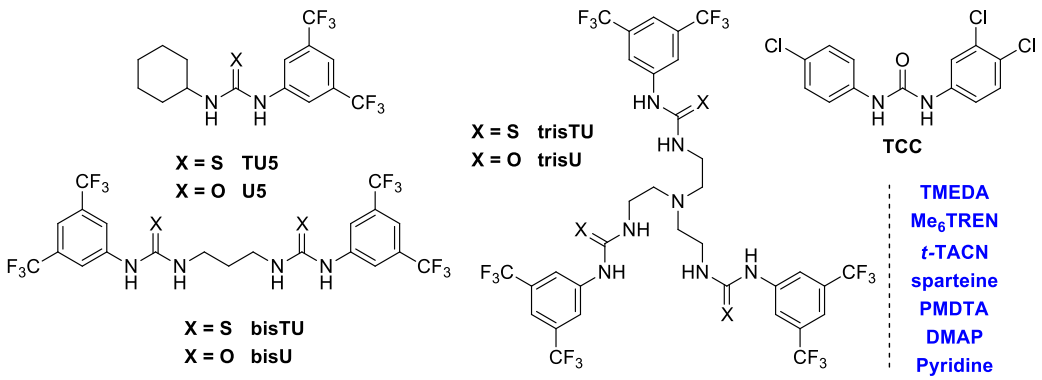

Scheme 30. Bicomponent catalytic systems – (Thio)urea amines applied for the bulk ROP of *L*-LA.[62]

Intermediate conclusions- Naturally occurring compounds have been an important source of inspiration in the context of polymerization by organocatalysis. Low cost Brønsted bases have been widely used and enable moderate to good control over ROP processes. However, increasing the temperature up to 180 °C can lead to deleterious side reactions, such as inter- and intramolecular transesterification reactions and/or epimerization. In addition, these

catalysts exhibit a poor thermal stability and that polymer can degrade as shown by brown coloration of the polymers. For instance, the bis-thiourea/PMDTA bicomponent catalytic system appears powerful for the ROP of LA in the solid state at 100 °C but cannot be applied at temperature above 140 °C because of the epimerization reactions. Acidic compounds, which are more thermally stable, have received much less attention in this context. Diphenylphosphate has been shown to lead to highly isotactic PLLAs. However, its low activity requiring long reaction times for ROP is a limitation towards its wide application in an industrial-scale process. Bicomponent catalytic systems hold great promise also, in particular in the form of salts showing a higher thermal stability. Yet, there is still room for improvement in particular to find appropriate organocatalytic sytems that would combine high thermal stability and high catalytic activity, which remains an unsolved challenge in ROP of LA at high temperature.

4 ROP of CL

This section gives an overview of main organocatalysts employed for the ROP of CL in solution and in bulk, with a focus on reports published from May 2015 to September 2018. Information about previous studies in this area can be found elsewhere.[33,34,35,36,37,38,39]

BASIC AND NUCLEOPHILIC CATALYSTS– As in the case of the ROP of *L*-LA, a distinction should be made between acidic, basic and nucleophilic molecules for the ROP of CL. While basic compounds, such as DBU or MTBD, operating by the ACEM are particularly efficient for the ROP of *L*-LA in solution (*vide supra*), they show a very poor –if any- catalytic activity for the ROP of CL.[96]

Brønsted "super strong" organic bases, such as phosphazenes,[85] can trigger the ROP of CL in the presence of a protic alcohol (Scheme 31).[135,136,137] Note however that BEMP exhibits a poor activity, for instance when used in presence of 1-pyrenebutanol in bulk at 80 °C ($[CL]_0/[BEMP]_0/[OH]_0 = 100/1/1$). Indeed, after 10 days the conversion reached barely 14%.[138]

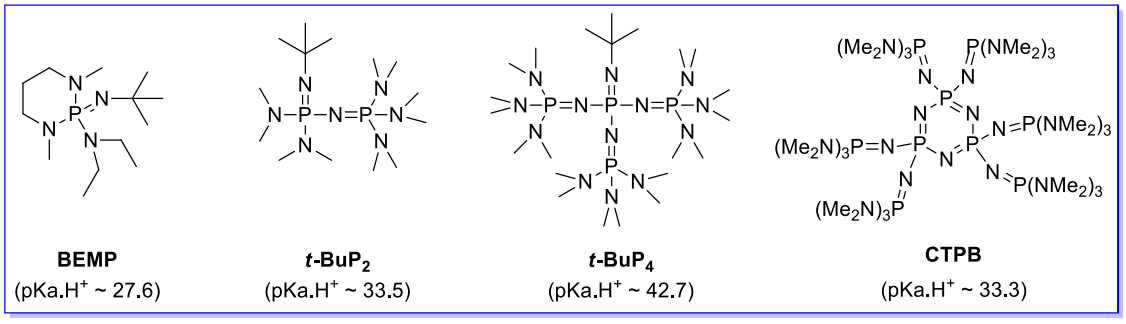

Scheme 31. Phosphazene bases; pKa.H$^+$values are given in acetonitrile.[139,85]

Synthesis of well-defined polyether-*b*-polyester block copolymers has been achieved by one pot synthesis involving a catalyst switch, as reported by Hadjichristidis *et al.* (Scheme 32).[137]

The first block, namely, poly(styrene oxide) is synthesized using *t*-BuP$_4$, before quenching by addition of an excess of acidic DPP. This is followed by the synthesis of PCL as the second block, using in this case *t*-BuP$_2$ under the following conditions: [CL]$_0$/[*t*-BuP$_2$]$_0$/[OH]$_0$ = 100/1/1 at r.t. The reaction can be accelerated using toluene as solvent, with a conversion of 90% reached after only 5 hours, but a bimodal SEC trace is observed due to a slow initiation. The slower rate noted in THF is explained by a competitive coordination of this solvent with alkoxide-type propagating chains.[137] In a previous study, the authors have shown that the kinetic is faster in DCM rel. to toluene, due to a higher dissociation of the [*t*-BuP$_2$, H$^+$]; however, transesterification reactions have been observed in DCM.[136]

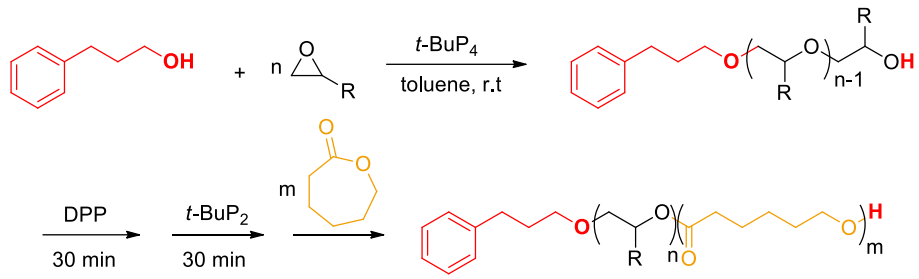

Scheme 32. One pot sequential ROP of styrene oxides and CL using the "catalyst switch" strategy from *t*-BuP$_4$ to *t*-BuP$_2$.[137]

A similar strategy has been applied for the synthesis of block copolymers derived from macrolactones and CL.[140] However the kinetic has been found slower for the ROP of CL in toluene at 80 °C, under the following conditions: [CL]$_0$/[*t*-BuP$_2$]$_0$/[OH]$_0$ = 100/5/1. With BnOH serving as initiator, up to 48 hours are needed to obtain a PCL with molar mass of 10.9 kg.mol^{-1} and a dispersity of 1.16. According to the authors, the *t*-BuP$_4$, which is the strongest phosphazene base, is not appropriate for the ROP of CL as it promotes extensive inter- and intramolecular transesterification reactions,[136] as reflected by the high dispersity values (1.45-1.5).[135]

Recently, a cyclic trimeric phosphazene base (CTPB) has been applied to produce a PCL with a molar mass up to 112 kDa, within few minutes.[141] The ROP of CL can be typically carried out in toluene at r.t in presence of BnOH as initiator, in the following conditions: [CL]$_0$/[CTPB]$_0$/[BnOH]$_0$ = 1000/1/1], reaching 75% conversion within 8 minutes, and affording a PCL with a M_n = 84.8 kDa, but with a high dispersity (*Đ* = 1.92).

Some nucleophilic NHCs have also shown a potent catalytic activity toward the ROP of CL.[142,143,144] Use of NHCs in the general context of organocatalyzed polymerizations can be found elsewhere[35,38,145] Early investigations on NHC-OROP of CL, and underlying mechanisms, have been reported by Waymouth *et al.* Occurrence of the two main mechanisms,[146] namely, AMM and ACEM, has been postulated. As already mentioned, AMM would involve the direct

nucleophilic attack of NHC onto the monomer (Scheme 33a,c), while ACEM takes place by activation of the alcohol initiator by hydrogen bonding (Scheme 33b). In the presence of an alcohol initiator, ACEM seems more likely to occur rather than AMM, as suggested by the 6 kcal.mol^{-1} difference calculated by DFT in favor of the former mechanism. Nevertheless, both mechanisms can occur simultaneously in a competitive manner, in particular at low alcohol concentration (high monomer-to-initiator ratios).[146]

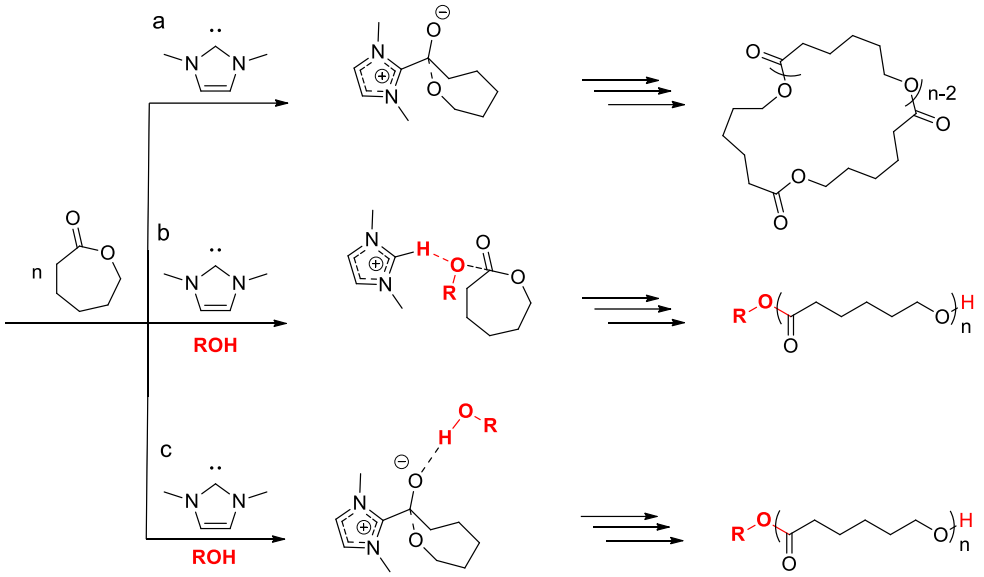

Scheme 33. Possible mechanisms involved during the NHC-OROP of CL in the presence or in the absence of alcohol initiator.[146]

NHO **4** has also been applied to catalyze the ROP of CL in THF at r.t ($[CL]_0/[NHO\ 4]_0/[BnOH]_0$ = 100/1/2; Figure 6). A PCL of M_n= 6500 g.mol^{-1} has thus been synthesized within 240 min, but poor control has been noted, as mirrored by the high dispersity obtained ($Đ$ = 2.15).[86]

HYDROGEN BOND DONORS + BASIC CO-CATALYSTS - Amidine, such as DBU or MTBD, can be combined with thioureas, ureas or squaramides for efficient ROP of CL by an organocatalysis pathway.[96,102,106, 147,148] As in the case of the ROP of LA, squaramides require long polymerization time (days).[106] Squaramides **8** and **9** are inefficient for the ROP of CL in solution (Figure 6).[107]

The development of bis- and tris-(thio)ureas by the group of Kiesewetter has enabled to significantly improve the ROP of lactones (Scheme 34).[99,148] Thus, trisU has offered best performances in the ROP of lactones in C_6D_6 at r.t. ($[CL]_0$ = 2 M; MTBD and trisU employed at 1.67mol% each), achieving 93% within 166 min for a monomer-to-initiator ratio of 500, leading to a well-defined PCL ($M_{n,SEC}$= 58600 g.mol^{-1}, $Đ$ = 1.03).[148] The tris-U/MTBD bicomponent catalytic system has been proposed to operate similarly to bis-thiourea, with a simultaneous

activation of the alcohol initiator by the basic cocatalyst and activation of the monomer by the urea moieties.

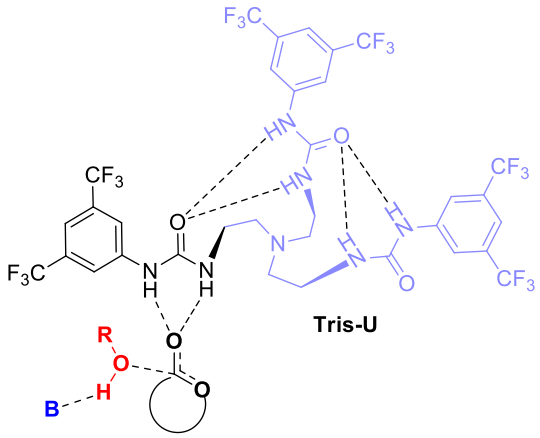

Scheme 34. Activated-urea mechanism combined with a chain end activation (B = Base).[148]

The group of Waymouth has proposed to combine a monourea (U7, Figure 6) to IMes in order to conduct the ROP of CL in THF at r.t. with $[CL]_0$ = 2.5 M.[102] Impressive kinetic rate has been observed when 1-pyrenebutanol initiated the ROP, with a conversion reaching 90 % within only 1 min for a monomer-to-initiator ratio of 100 leading to well-defined PCL ($M_{n,SEC}$= 9700 g.mol^{-1}, $Đ$ = 1.05).

Finally, the solvent-free OROP of CL has been conducted in the presence of BnOH initiator ($[CL]_0/[BnOH]_0$ = 500) and TCC/BEMP cocatalytic system (0.3 mol% each related to the monomer) at r.t (see Figure 6).[62] A well-defined PCL ($M_{n,SEC}$= 85000 g.mol^{-1} and $Đ$= 1.22) with a conversion reaching 60% was obtained in 98 min. Importantly, in this study urea/amine co-catalysts have been found more efficient than their TU/amine counterparts for the ROP of lactones. In contrast, the TU/amine co-catalysts are more effective for the ROP of *L*-LA.

HYDROGEN BOND DONORS + ACIDIC CO-CATALYSTS – TU2 as HBD has been combined with a carboxylic acid, namely, trifluoroacetic acid (TFA), to carry out the OROP of CL in solution at r.t ($[CL]_0$ = 1 M).[149] This enables a better control than in the case of TFA-OROP of CL. PCL of M_n= 12 000 g.mol^{-1} and $Đ$ = 1.19 has indeed been obtained within 195 hours (8 days and 3 h), although analysis by MALDI-ToF MS has evidenced a co-initiation by adventitious water. Synthesis of PCL-*b*-PV block copolymers can also be achieved using this TU2/TFA organocatalytic system. An AMM has been postulated, where TU HBD would stabilize the carboxylate ion, leading to an improvement of the proton release and increasing its acidity (Scheme 35).

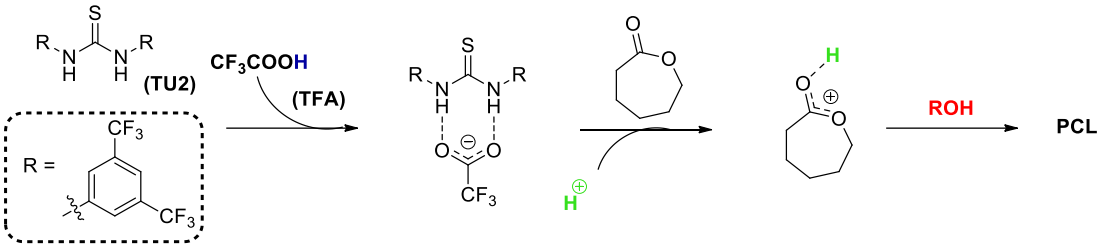

Scheme 35. Thiourea HBD binding with carboxylic acid for the ROP of lactones.[149]

Organic salts deriving from the mixture of acid and base have been studied by Bourissou, Martin-Vaca *et al*. for the ROP of CL in solution. The authors have evaluated whether the monomer could be activated by (bis)pyridinium/ acid salts during the ROP of CL in absence of a basic co-catalyst (Scheme 36).[150] Two acids have thus been used, namely, 1R-(-)-10-camphorsulfonic acid (CSA) and methanesulfonic acid (MSA). Best performances have been achieved with IHBD 7 in C_6D_6 at 75 °C, the conversion in CL reaching 97% within 8h20 in the following conditions: $[CL]_0$ = 1 M and $[CL]_0/[BnOH]_0/[Salt]_0$ = 150/1/1. Well-defined PCL can thus be obtained with M_n up to 13000 g.mol^{-1} and $Đ$ = 1.09.

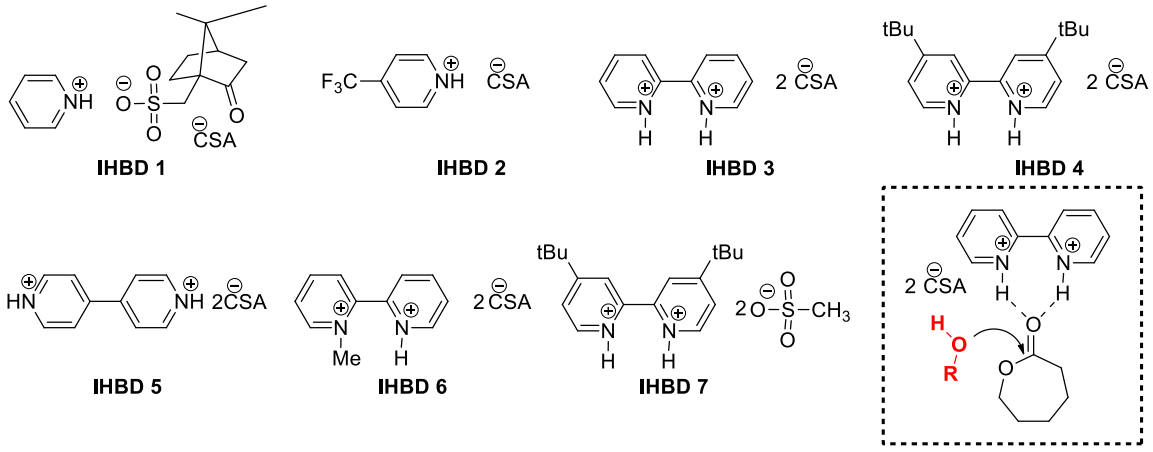

Scheme 36. (Bis)pyridiniums salts, ionic hydrogen bond donors (IHBDs), for CL activation.[150]

Guo *et al.* have reported a bicomponent catalytic system composed of TPTA/MSA (HBD + acid) for the ROP of LA and CL in DCM at r.t.[108] A higher rate of proton release can be achieved with this organic catalytic system (Scheme 24, section 3.1), a higher activity being observed for CL (< 5 h) than for LA ROP (a few days).[108] Well defined PCL (M_n = 12 000 g.mol^{-1} and $Đ$ = 1.18) can be synthesized in this way.

Peruch *et al.* [61] have found that DMAP/DMAP.HOTf (Figure 6) is poorly efficient for the ROP of CL in bulk at 100 °C. Indeed, with a catalyst loading of 5 mol%, conversion reaches 92% but after 135h (6 days) affording PCL of M_n = 10800 g.mol^{-1} and $Đ$= 1.45. In the same conditions

the ROP of *L*-LA proceeds during only 1h leading to well-defined PLLA (M_n = 13900 g.mol^{-1}, $Đ$= 1.16).

Brønsted Acids – Contrary to the ROP of *L*-LA, the OROP of CL utilizing acid-type organocatalysts has often been considered.[33,34,36,37] Sulfonic- and sulfonamide-type,[151,152,153,154,155,156,157,158] and phosphoric and phosphoramide acids[131,159,160,130,161,162,163,130,158,164] have been the most studied for this purpose. On the basis of DFT calculations, phosphoric (Scheme 37) and sulfonic acids (Scheme 25, section 3.1) have been confirmed to act as proton shuttles *via* their acidic hydrogen atom and their basic oxygen atoms.[57, 112, 131]

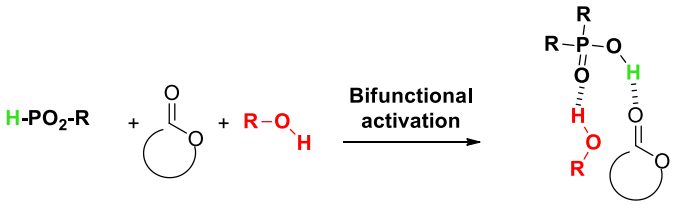

Scheme 37. Bifunctional activation for the phosphoric acid-OROP of cyclic esters. [131]

Guo *et al.* have employed a commercial organocatalyst, namely, 2,4-dinitrobenzenesulfonic acid (DNBA) (Figure 6) for the OROP of CL at r.t. in acetonitrile.[155] Under the following conditions, $[CL]_0/[BnOH]_0/[DNBA]_0$ = 40/1/1 and for a $[CL]_0$ = 1 M, DNBA has been shown as efficient as DPP, HOTf and trifluoromethanesulfonimide.($HNTf_2$, see Figure 6), affording well-defined PCL (M_n= 4580 and M_n = 16580 g.mol^{-1}, $Đ$ < 1.16) within 4 and 20 h respectively. Furthermore, functionalized PCLs and star shaped PCLs have been achieved by initiating the DNBA-OROP of CL from appropriate functional initiators. PCL-*b*-PVL & PCL-*b*-PTMC diblock copolymers have also been synthesized. MALDI-ToF analysis has shown that some PCL chains have been initiated by water. Guo *et al.* have claimed that a "simple" AMM occurs during this DNBA-OROP of CL.

Sulfonic acids have mainly been applied for PCL synthesis in solution, while phosphoric acids[166, 161,130, 164] can catalyze the reaction both in solution and in bulk. Saito *et al.* have employed DPP as catalyst for the bulk ROP of cyclic esters in the presence of various alcohol initiators, for instance, 3-phenyl-1-propanol (PPA, Scheme 38).[130] Performing the DPP-OROP of CL in bulk at 80 °C offers the advantage of short polymerization time and low catalyst loading. Under the following conditions, $[CL]_0/[PPA]_0/[DPP]_0$ = 50/1/1, the monomer conversion reaches 86.2% within 12 min, against 83.6% within 300 min in solution. The catalyst loading can be reduced ($[PPA]_0/[DPP]_0$ = 1/0.05) maintaining short reaction times (250 min) and control of the polymerization ($M_{n,\,NMR}$= 5500 g.mol^{-1}, $Đ$ = 1.08). Polymerization kinetic can also be increased by adding an electron withdrawing group onto the organophosphate (Scheme 38). Finally, the bulk

ROP of CL at 80 °C has been found much faster than that of LA carried out in bulk at 130 °C, (250 min *vs*. 22 hours), for $[M]_0/[PPA]_0$ = 50/1 and ten times less catalyst for the ROP of CL.[130]

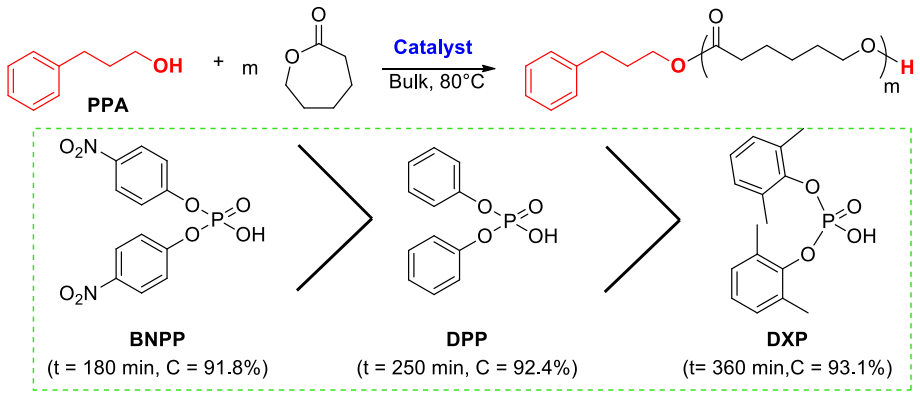

Scheme 38. Phosphoric acid derivatives for the bulk ROP of CL at 80°C BNPP: bis(4-nitrophenyl)phosphate), DXP: Di(2,6-xylyl)phosphate.[130]

PCLs of high molar mass can be achieved using phosphoric acids. For instance, Zhou *et al.* have shown that the bulk ROP of CL can be conducted at 85 °C using (R)-(−)-1,1′ -binaphthyl-2,2-diyl hydrogen phosphate (BPA) as organocatalyst and 1-octanol as initiator. PCLs with M_n = 43500 g.mol^{-1}and $Đ$ = 1.2 for a conversion of 52% within 24 h have been synthesized in this way.[161]

Carboxylic acids will be highly investigated in this PhD thesis, consequently, they are discussed here in detail. These weak Brønsted acid organocatalysts have been first reported by the group of Endo in 2002.[167] The ROP of CL initiated by pentaerythritol (PETP) requires high temperature to proceed homogeneously. Yet, hydrochloric acid in diethylether ($HCl.Et_2O$), which is effective for the living ROP of CL at r.t in solution,[168] has proven inappropriate at elevated temperature.[167] It has thus been attempted to perform the bulk ROP of CL at 70 °C in presence of TFA, trichloroacetic acid (CCl_3COOH), maleic acid at 90 °C and fumaric acid at 70 °C, with a monomer-to-initiator ratio of 100 (Scheme 39). TFA and CCl_3COOH have been shown too active at 70 °C, affording PCLs of high dispersity ($Đ$ = 1.67 and $Đ$ = 1.98, respectively).[167] Maleic acid, and most of all fumaric acid, have given the best results, leading to well defined PCLs (M_n= 9500 g.mol^{-1} and $Đ$ = 1.09). In addition, well defined linear and star-shaped PCL constituted of three and four arms have been synthesized from trimethylolpropane (TMP) and PETP respectively (Scheme 39).

Later on, the groups of Iversen and Cordóva have also used a carboxylic acid, namely *L*-lactic acid (Figure 6), to initiate the ROP of CL in bulk at 120 °C from several naturally occurring molecules as initiators, namely, β-D-glucopyranoside, sucrose, or raffinose.[169] Synthesis of a dendrimer-like PCL has also been reported.[169] In the same vein, Oledzka *et al.* have described

the synthesis of lipid-functionalized PCLs by a carboxylic acid-OROP of CL,[170] the reaction taking place *via* an AMM according to the authors.

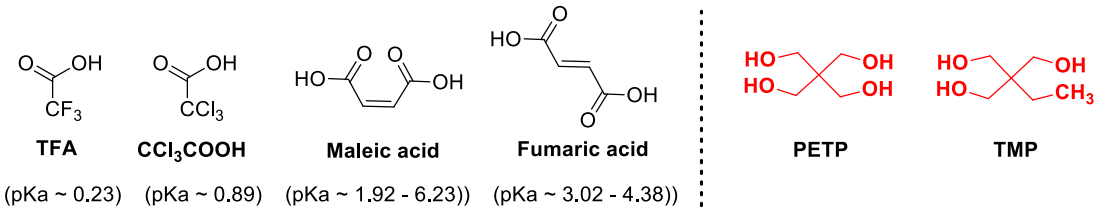

Scheme 39. Carboxylic acids used for the bulk ROP of CL.[167]

The groups of Cordóva and Iversen have applied several carboxylic acids and amino acids as well for the bulk ROP of CL at 120 °C, using 10 mol% of catalyst rel. to the monomer, in the presence of BnOH as initiator (Scheme 40).[171] They have found that these weak acids (3 < pKa < 5) afford PCL of low M_n up to (2800 g.mol^{-1}) and with fairly low dispersity (1.2 < $Đ$ < 1.3) within few hours under solvent-free conditions. The order of catalytic activity has been found to be: *L*-tartaric acid > citric acid > *L*-lactic acid > *L*-proline. *L*-lactic acid and amino acids have also been shown to directly initiate the ROP of CL in absence of any alcohol as initiator. Oledzka *et al.* have taken advantage of this property to synthesize amino acid end-functionalized PCLs and PLAs. The ROP of CL has been conducted in bulk at 160 °C in the presence of *L*-citrulline or *L*-arginine (Figure 6), affording PCLs of predictable M_n but of high dispersity (1.38 < $Đ$ < 1.54).[132]

High molar mass PCLs can be obtained using salicylic acid (*o*-SA) as carboxylic acid organocatalyst (Figure 6).[172] For this purpose, the BnOH-initiated SA-OROP of CL is conducted at 80 °C producing PCLs of predictable molar mass (1 300 g.mol^{-1}< M_n < 41 000 g.mol^{-1}) and low dispersity (1.03 < $Đ$ < 1.16) within a few hours. The highest M_n value is achieved within 80 hours with a conversion reaching 70% for a monomer-to-initiator ratio of 500. Various functional initiators have been used, and synthesis of PCL-*b*-PVL diblock copolymers has also been reported.[172]

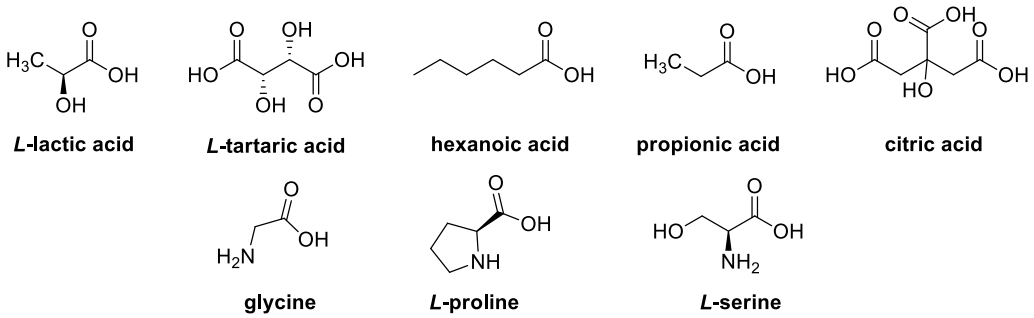

Scheme 40. Carboxylic acids (top) and amino-acids (bottom) applied for the bulk ROP of CL at 120°C.[171]

Weak carboxylic acids are usually employed in bulk as they are usually not efficient to conduct the ROP of CL at r.t in solution.[59,57] In order to enable BA to be active in solution, the group of Guo has shown that intramolecular hydrogen bond can enhance the acid-like character, hence the catalytic activity, of benzoic acid (BA).[173,174] This would be due to a stabilization of the carboxylate anion improving proton release, as illustrated in Scheme 41 and Scheme 42.

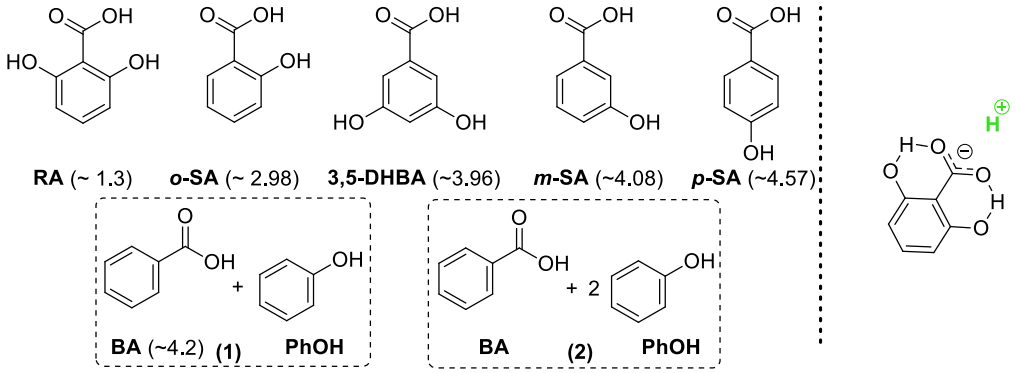

Scheme 41. Benzoic and its derivatives for the ROP of VL and CL. Stabilization of the carboxylate anion by intramolecular hydrogen bond. PhOH = phenol. pKa values under brackets.[173]

They have thus reported the use of γ-resorcylic acid (RA) to catalyze the ROP of CL in DCM at r.t., with $[CL]_0$ = 3 M and $[CL]_0/[BnOH]_0/[RA]_0$ = 30/1/1 (Scheme 41).[173] The conversion reaches 93% within 24 hours, affording a PCL with an molar mass higher than the theoretical value ($M_{n,NMR}$= 4320 g.mol^{-1} > $M_{n,th}$= 3290 g.mol^{-1}) and low dispersity ($Đ$ = 1.06). MALDI ToF analysis has shown that some PCL chains have been initiated by water. SA alone has proven poorly efficient, and other catalytic systems (*p*-SA, *m*-SA, 3,5-DHBA, 1 and 2) have been found inactive for the ROP of cyclic esters in solution. These results indicate that only one intramolecular or even several intermolecular hydroxy hydrogen bonds are not sufficient to stabilize the carboxylate anions and enhance the proton release.

The same authors have also designed BA derivatives bearing amido groups, namely, *o,o'-bis*(pivalamido)benzoic acid (P_2BA), pivalamidobenzoic acid (PBA), *o,o'-bis*(benzamido)benzoic acid (B_2BA) and *o,o'-bis*(4-fluorobenzamido)benzoic (FB_2BA) (Scheme 42).[174] P_2BA has been found more active than the previously reported RA for the ROP of VL. PBA has been found less active to promote the ROP in comparison to P_2BA. As B_2BA and FB_2BA, they are totally inactive due to their poor solubility in DCM, THF, toluene and acetonitrile. The P_2BA-OROP of CL initiated by BnOH in the following conditions, in toluene at r.t., with $[CL]_0$ = 3 M and $[CL]_0/[BnOH]_0/[RA]_0$ = 30/1/1, has afforded PCL within 20h of predictable M_n values and low dispersity ($Đ$ = 1.08). Here again, MALDI-ToF MS analysis has evidenced co-initiation by traces of water. The living

nature of the P_2BA-OROP has been established through the synthesis of diblock copolymers deriving from VL, CL and TMC.

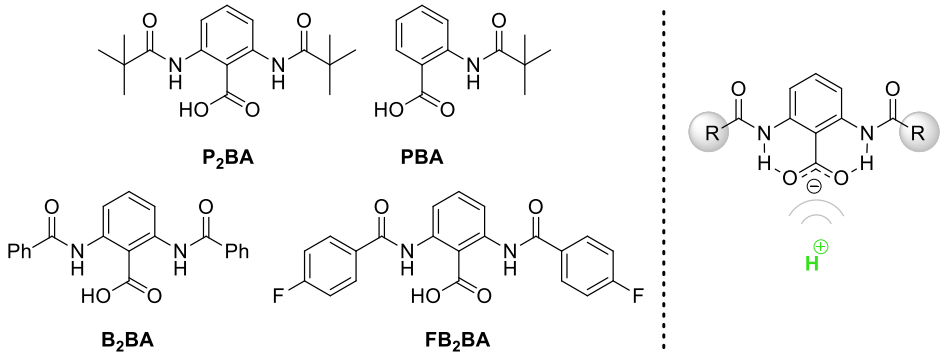

Scheme 42. *Ortho*-amido benzoic acid derivatives with tunable acidity.[174]

Lewis acids – Non-metallic boron derivatives B1 to B5 shown in Scheme 43 have proved potent organocatalysts when used at 130 °C in bulk under the following conditions $[CL]_0/[BnOH]_0/[B]_0$ = 50/1/0.5.[175] The catalytic activity increases in the following order: B1 > B3 > B4 > B2 > B5, in accordance with the Lewis acidity and steric hindrance of the different catalysts. For instance, the B1-OROP of CL proceeds during 10h to reach a conversion of 98.6%, leading to PCL of M_n= 5200 g.mol^{-1} and $Đ$ = 1.27. B2 enables to achieve high molar mass, M_n = 42500 g.mol^{-1}, with a dispersity of $Đ$ = 1.44 within 90 hours. Boron derivatives have been proposed to operate *via* an AMM, due to the Lewis acidity of boron atom (Scheme 43).

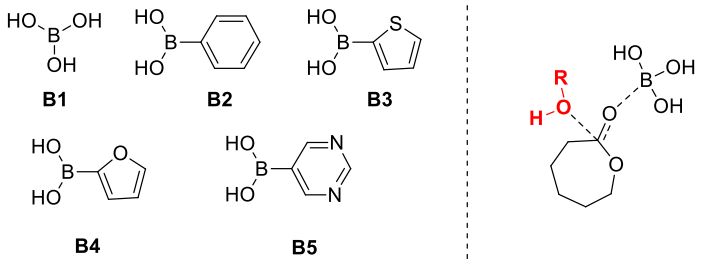

Scheme 43. Boric acids (B1) and its derivatives: phenylboronic acid (B2), 2-thienylboronic acid (B3), 2-furanylboronicacid (B4), 5-pyrimidinylboronic acid (B5). Monomer activation by boric acid catalyst.[175]

Intermediate conclusions- Phosphazene bases display best performances towards the ROP of CL, affording well-defined PCLs of high molar mass (M_n up to 100 000 g.mol^{-1}). (Thio)urea/base co-catalytic systems also prove highly active and selective for this purpose. Nevertheless, the latter components have been found cytotoxic. Hydrogen bond donors combined with acidic co-catalysts provide mitigated results. As for sulfonic, sulfonamide and phosphoramic acids, they have mainly been employed in solution, although efficiency of phosphoric acids has been established when used in bulk as well. Carboxylic acids appear as

promising alternatives as their Brønsted acidity can be tuned for an efficient use both in solution and in bulk.

5 Ring-opening copolymerization (ROcP) of LA and CL

As biodegradable, nontoxic and biocompatible polymers, polylactide (PLA) and poly(ε-caprolactone) (PCL) are attractive biosourced surrogates for petroleum-based polymers. Both PLA and PCL have been intensively investigated in applications ranging from pharmaceutics to packaging and electronics.[5,1,6,14] Yet, both PLA and PCL show some limitations in these applications. For instance, PLA is brittle, exhibits a poor elasticity,[18] a low thermal stability and a modest permeability to drugs. PCL has higher thermal stability and elasticity than PLA, with a glass transition temperature (T_g) around -60 °C *vs.* 45-65 °C for PLA,[19,4,41] but suffers from poor mechanical properties. PCL has also a higher permeability to drugs[21] and a half time *in vivo* of 1 year,[51] *vs.* a few weeks for PLA.[20] As a result, statistical copolymers of lactide (LA) and CL, *i.e.* P(LA-*stat*-CL) aliphatic copolyesters, are highly sought-after materials as they combine the strengths and minimize the weaknesses of both homopolymers. P(LA-*stat*-CL) have thus attracted a great deal of attention in the biomedical and pharmaceutical fields,[23,24,25,26,22] and as compatibilizers for PLA/PCL blends.[27] In order to obtain desirable properties, the ring-opening copolymerization (ROcP) of LA and CL must be controlled.

The following part overviews the synthetic tools enabling to study the copolymer microstructure and composition and will briefly present the organometallic catalysts, while organic catalysts will be described in more detail for this purpose.

5.1 Copolymer structures and reactivity ratios determination

The relative reactivity of the two comonomers has an influence on the structure of the final copolymers, thereby it influences the thermal and mechanical properties. In ROP, this relative reactivity depends on the nature of the catalyst used and the nature of both monomers. They can be appreciated through the determination of the reactivity ratios. These represent the relative reactivity of the monomer units at the chain end towards monomer of the same nature and monomer of a different nature.

In the present study, r_{CL} represents the tendency of a caproyl unit at the chain end to ring-open a CL or LA monomer while r_{LA} represents the tendency of a lactidyl unit at the chain end to ring-open a LA or a CL monomer. The assumption that the terminal model describes the copolymerization kinetics is made meaning that the penultimate units of the chain end have no effect on the reactivity.[176] Furthermore, in order to simplify the calculation, depropagation of both monomers is neglected. The following equations (**1**) show the relationship between

reactivity ratios and the rate constants (k_{M-M}) of the four elementary propagation reactions as described in Figure 10.

$$r_{CL} = k_{CL-CL}/k_{CL-LA} \text{ and } r_{LA} = k_{LA-LA}/k_{LA-CL} \quad \textbf{(1)}$$

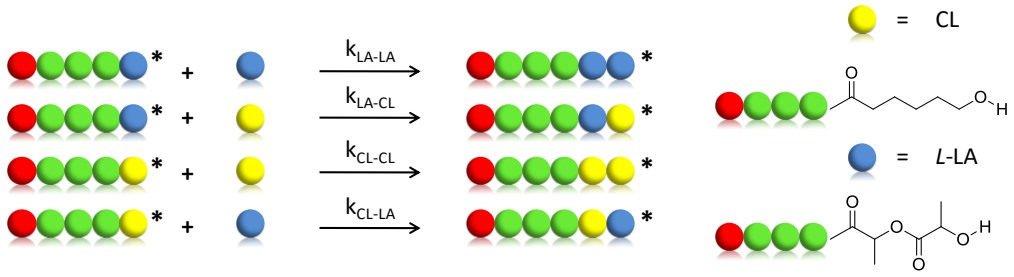

Figure 10. Rate constants in the ROcP of LA and CL.

For r_{CL}> 1, the CL units at the chain end are more reactive toward CL monomer than toward LA monomer. A value of r_{CL}= 1 means that a CL unit at the chain end will have the same reactivity toward both monomers. Consequently, the structure of the copolymers depends on the values of the reactivity ratios (Figure 11):

- $r_{CL} \approx r_{LA} \approx 0$ will lead to the formation of alternating copolymers.
- r_{CL} x $r_{LA} \approx 1$, the two different chain ends have the same ability to ring open both monomers leading to random/statistical copolymers. Note that a random copolymer is a kind of statistical copolymer ($r_1 = r_2 = 1$)
- $r_{CL} > r_{LA}$ (or $r_{CL} < r_{LA}$) this combination leads to the formation of gradient copolymers.
- $r_{CL} >> r_{LA}$, (or $r_{CL} << r_{LA}$) tapered or block copolymers can be formed.

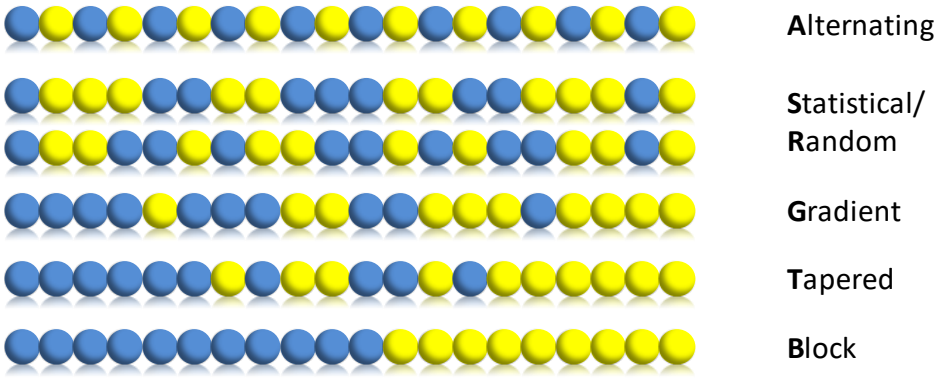

Figure 11. Different types of copolymers.

Several models can be applied for the calculations of the reactivity ratios. In the following lines, the Kelen-Tüdős linear method and a nonlinear method "the visualization of the sum of squared residuals space" (VSSRS) will be briefly discussed. The two methods arises from

the **Mayo–Lewis** equations.[177] The specific polymerization rate of each monomer (R_{LA} and R_{CL}) can be written as follow (**2**) and (**3**):

$$R_{LA} = -\frac{d[LA]}{dt} = k_{LA-LA}[PLA*][LA] + k_{CL-LA}[PCL*][LA] \quad (\mathbf{2})$$

$$R_{CL} = -\frac{d[CL]}{dt} = k_{CL-CL}[PCL*][CL] + k_{LA-CL}[PLA*][CL] \quad (\mathbf{3})$$

With [LA] and [CL] the concentration of LA or CL monomers respectively and [PLA*] and [PCL*] the concentration of the propagating species terminated with a LA or CL unit respectively.

By combining equations (**2**) and (**3**) the equation (**4**) is obtained:

$$\frac{d[CL]}{d[LA]} = \frac{k_{CL-CL}[PCL*][CL] + k_{LA-CL}[PLA*][CL]}{k_{LA-LA}[PLA*][LA] + k_{CL-LA}[PCL*][LA]} \quad (\mathbf{4})$$

Then the system is assumed to be in the stationary state giving equation (**5**)

$$\frac{d[PCL*]}{dt} = k_{LA-CL}[PLA*][CL] - k_{CL-LA}[PCL*][LA] = 0 \quad (\mathbf{5})$$

By combining (**4**) and (**5**) followed by rearrangements the differential form of Mayo-Lewis equation (**6**) is obtained:

$$\frac{d[CL]}{d[LA]} = \left(\frac{[CL]}{[LA]}\right) \times \frac{(r_{CL}[CL] + [LA])}{([CL] + r_{LA}[LA])} \quad (\mathbf{6})$$

The following equations (**7** & **8**) are then considered:

$$[M] = [CL] + [LA],$$

And (**7a**) $f_{CL} = \frac{[CL]}{[M]}$ (**7b**) $f_{LA} = \frac{[LA]}{[M]}$ (**7c**) $f_{CL} + f_{LA} = 1$

Finally (**8a**) $F_{CL} = \frac{d[CL]}{d[M]}$ (**8b**) $F_{LA} = \frac{d[LA]}{d[M]}$ (**8c**) $F_{CL} + F_{LA} = 1$

With [M] the instantaneous concentration of total comonomers, f_i the instantaneous composition in monomer *i* in the polymerizing mixture (mole fraction of unreacted monomer), F_i the instantaneous mole fraction of monomer unit *i* incorporated into the copolymer.

Finally, the Mayo-Lewis equation can be written as followed (**9**):

$$\frac{F_{CL}}{F_{LA}} = \left(\frac{f_{CL}}{f_{LA}}\right) \times \frac{(r_{CL}f_{CL} + f_{LA})}{(f_{CL} + r_{LA}f_{LA})} \quad (\mathbf{9})$$

Kelen-Tüdős (KT) method:[178]

Where $x = \frac{f_{CL}}{f_{LA}}$, $y = \frac{F_{CL}}{F_{LA}}$

$$G = \frac{x\,(y-1)}{y}, F = \frac{x^2}{y}$$

$$\eta = \frac{G}{\alpha + F}, \varepsilon = \frac{F}{\alpha + F} \text{ with } \alpha = \sqrt{F_{min}.F_{max}}$$

By rearranging (**9**), equation below –representing η = f(ε) (**10**) - can be plotted in order to determine the reactivity ratios.

$$\eta = \left(r_{CL} + \frac{r_{LA}}{\alpha}\right)\varepsilon - \frac{r_{LA}}{\alpha} \quad \textbf{(10)}$$

Nevertheless, these linear methods derived from the Mayo-Lewis equation may unduly weight some data points while giving less weight to others and thus provide biased estimates of reactivity ratios. Furthermore, low monomer conversions are needed to implement them. All these issues may impede the obtention of reliable values of reactivity ratios.

For this purpose the VSSRS method[179,180], developed by Van den Brink *et al.* has been applied. The use of VSSRS method presents the advantage of being able to estimate the reactivity ratios even at higher conversion and to study the conversion effects. Furthermore, the model takes into account the error on both the monomer conversion and the fraction of unreacted monomer, providing unbiased estimates and joint confidence regions. The conversion, the copolymer composition *(F)* and monomer fraction *(f)* data are fitted to the integrated form of the copolymerization equation (**11**):

$$C_{TOT} = 1 - \left(\frac{f_{CL}}{f_{CL,0}}\right)^{\alpha} \times \left(\frac{f_{LA}}{f_{LA,0}}\right)^{\beta} \times \left(\frac{f_{CL,0}-\delta}{f_{CL}-\delta}\right)^{\gamma} \quad \textbf{(11)}$$

With C_{TOT} the monomer conversion, f_i the instantaneous fraction of unreacted monomer, $f_{i,0}$ the initial fraction of monomer and:

$$\alpha = \frac{r_{LA}}{1-r_{LA}} \quad \beta = \frac{r_{CL}}{1-r_{CL}} \quad \gamma = \frac{1-r_{CL}\times r_{LA}}{(1-r_{CL})\times(1-r_{LA})} \quad \delta = \frac{1-r_{LA}}{2-r_{CL}-r_{LA}}$$

Easy to implement in Microsoft Excel software the (VSSRS) method consists in minimizing the sum of squares (SS) as described in equation (**12**).[179]

$$\boldsymbol{SS(r_{CL}, r_{LA}) = \sum_{i=1}^{n} w_i \times \left(z_{i,exp} - z_{i,th}\right)^2} \quad \textbf{(12)}$$

In equation 13, w_i represent the weighting factors (here a constant absolute error was considered, *i.e.*, w_i= 1), $z_{i,exp}$ are the experimental values of the variable *z* for the experiment *i* and $z_{i,th}$ are the theoretical values of the variable *z* for the experiment *i*. The best estimate for the reactivity ratios is set for the minimum value of SS.

5.2 Statistical ROcP of LA and CL in the presence of organometallic catalysts

The ROcP of LA and CL in a statistical fashion have shown to be particularly challenging using organometallic catalysts.[30] In most cases, LA is preferentially incorporated owing to its higher reactivity ratio.[96,136,144,181,182,183,184,185,186,187,188,189,190] Visseaux et *al.* have recently reviewed metal-based catalysts applied for the ROcP of LA and CL in a statistical manner.[30] To date, aluminum-based organometallic catalysts have been shown the most efficient for a true controlled statistical ROcP of LA and CL[188,191,192,193,194,195] and only two other studies using less toxic metal-based catalyst (zinc= Zn[196] and molybdenum = Mo[197] complexes) have succeeded in "controlling" the reaction (Scheme 44).

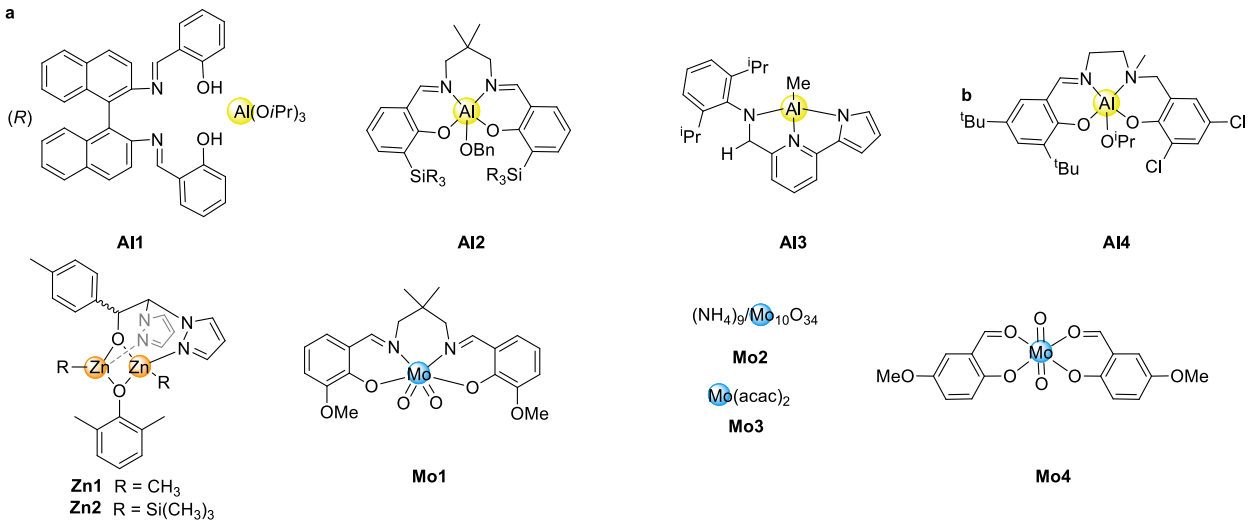

Scheme 44. Organometallic complexes applied for the ROcP of LA and CL.[188,191,192,193,194,196,197]

From a kinetic viewpoint, the ROP of CL is usually much faster than that of the ROP of LA by several orders of magnitude. However, as stated before LA is often incorporated first in the copolymer chain. The LA ability to coordinate on the metal alkoxide center (Scheme 8b, section 2.3), which has been postulated by the group of Jérôme[185]and later established by Lewinski *et al.*,[198] may play an important role in the higher r_{LA} value. This stabilization phenomenon disfavors the CL insertion in favor of LA on the metal-PLA growing chain. Nanok *et al.* have then evidenced by DFT calculations the higher affinity of LA toward the propagating species in the case of salen-type aluminum complexes.[199] The ways to reduce the difference in the reactivity ratio values are listed here after:

- Nomura *et al.* have first proposed organometallic catalysts with ligands presenting a high steric hindrance reducing the coordination of LA on the metal center, thus enabling the statistical ROcP of LA and CL.[191]

- The use of catalysts highly reactive toward CL.
- The insertion of an alcohol as a chain transfer agent (CTA).

Finally, Nanok *et al.* have shown that electron withdrawing groups on the ligand may favor the insertion of LA being detrimental for the statistical RO*c*P of LA and CL.[199]

5.3 Statistical organocatalyzed ROcP of LA and CL

Over the last twenty years, the copolymerization of miscellaneous monomers has been conducted in the presence of various organocatalysts,[200] but only few studies have reported the organocatalyzed ring-opening copolymerization (ORO*c*P) of LA and CL added simultaneously in the media. [62,96,136,144,181,182,161,183]

BASIC AND NUCLEOPHILIC CATALYSTS - Basic and nucleophilic organocatalysts such as guanidine base,[96] phosphazene,[136] NHCs[144,183] and TCC/TACN[62] have been found inappropriate to copolymerize LA and CL in a statistical manner. LA is indeed totally consumed in the early stage of the reaction, CL monomer remaining as a "spectator" (Scheme 45).

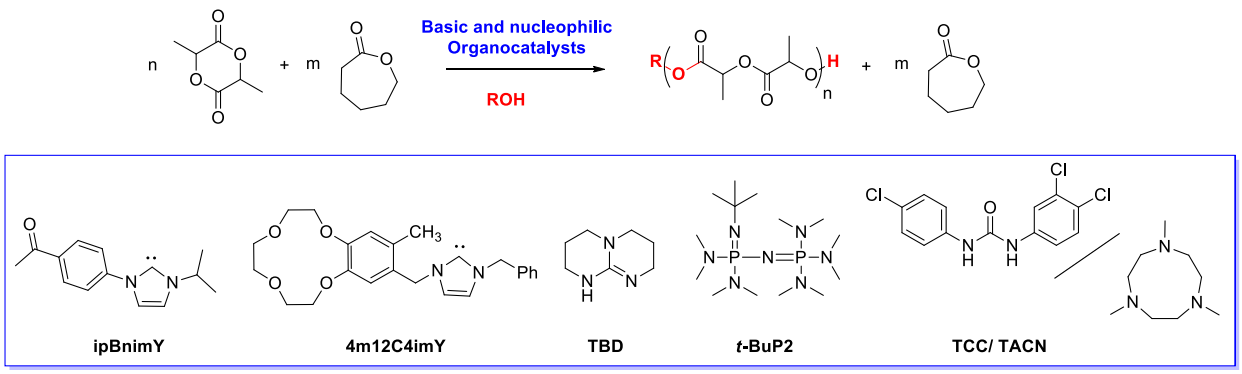

Scheme 45. Organocatalyzed ring-opening copolymerization (ORO*c*P) of LA and CL catalyzed by basic and nucleophilic compounds.[62,96,136,144,183]

Hedrick, Waymouth *et al.* have first reported, in 2006, the use of TBD for the ORO*c*P of LA and CL added simultaneously in solution at r.t. After full consumption of LA, the as-obtained PLA (M_n = 8700 g.mol^{-1}, M_w/M_n= 1.09) starts being transesterified without incorporating the CL monomer in the polymer backbone (M_n= 10 600 g.mol^{-1}, M_w/M_n = 1.33).[96]

Alamri *et al.* have used a phosphazene base (*t*-BuP_2) for the synthesis of PCL-*b*-PLLA block copolymers in solution at r.t.[136] They have first conducted the *t*-BuP_2-OROP of CL in the presence of 1-pyrenebutanol as initiator in toluene, toluene/THF (46/1 v/v) and THF during 8 hours under the following conditions: $[CL]_0/[t\text{-BuP}_2]_0/[PyOH]_0$ = 100/1/1. After incomplete polymerization, PCL macroinitiators of 4400 < $M_{n,NMR}$ < 10 300 g.mol^{-1}and 1.07 < M_w/M_n < 1.12 have been obtained and THF solutions containing *L*-LA monomer ($[L\text{-LA}]_0/[t\text{-BuP}_2]_0/[PCL]_0$ =

50/1/1) hahe then directly inserted in the different media. The *L*-LA has been found to be consumed in less than 10 min while the remaining CL in the solution behaves as a "spectator". PCL-*b*-PLLA diblocks are thus eventually achieved, with 9 700< $M_{n,NMR}$ < 17 300 g.mol^{-1} and 1.09 < M_w/M_n < 1.15 in the presence of residual CL monomers.[136]

Two NHCs, namely, 1-isopropyl-3-(4-methoxyphenyl) imidazol-2-ylidene (IpBnimY) and 4-methyl benzo-12-crown-4 imidazol-2-ylidene (4m12C4imY) have been employed for the ORO*c*P of LA and CL in THF at r.t. In both cases, only *L*-LA has been inserted in the polymer chain.[144,183]

Kiesewetter *et al*. have recently attempted the ORO*c*P of LA and CL in bulk using TCC/TACN co-catalytic system in the following conditions: $f_{CL,0}$ = 0.75, 2.5 mol% of each co-catalyst with a targeted DP of 100 in solvent-free conditions at 100°C. LA has achieved full conversion within only 2 minutes but CL has not been incorporated over the next 24 hours.[62]

ACIDIC CATALYSTS - In 2006, Kubisa and Baśko have found that TfOH is able to conduct the ORO*c*P of LA and CL in the presence of isopropylalcohol (IPA) in DCM at 35 °C within 50 hours (Scheme 46).[181] During the copolymerization of a mixture containing $f_{CL,0}$ = 0.66, the LA monomer is consumed slightly faster than CL one traducing a higher LA reactivity ratio compared to the reactivity ratio obtained for CL ($r_{LA} > r_{CL}$). As already observed with organometallic catalysts, the ROP of CL is much faster than the *L*-LA ROP. In another study, they have synthesized α,ω-telechelic P(LA-*co*-CL) diols from ethylene glycol (EG) initiator in the same conditions.[182]

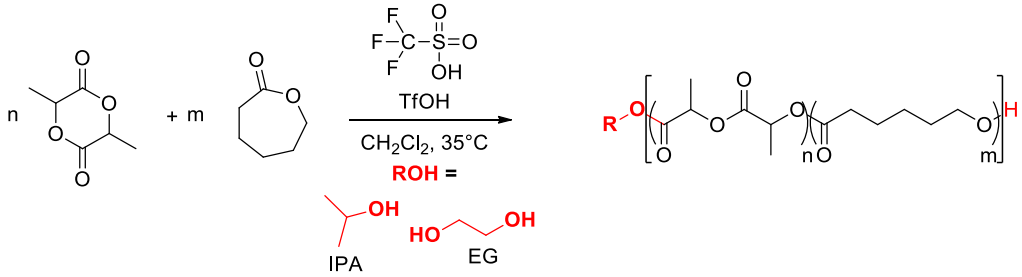

Scheme 46. TfOH-ORO*c*P of LA and CL in the presence of various initiators.[181,182]

As detailed by Kasperczyk and Bero, because LA is composed by two lactoyl units (L), two possible modes of transesterification reactions may happen during a LA-based copolymerization (Figure 12).[201] The second mode of transesterification, which gives rise to "anomalous" CL-L-CL sequences (L, representing one lactoyl unit) at 170.8 ppm has been shown to be absent on the ^{13}C NMR.[181] Kubisa and Baśko have demonstrated, however, that lactoyl (L) units are present at the chain ends. [182]

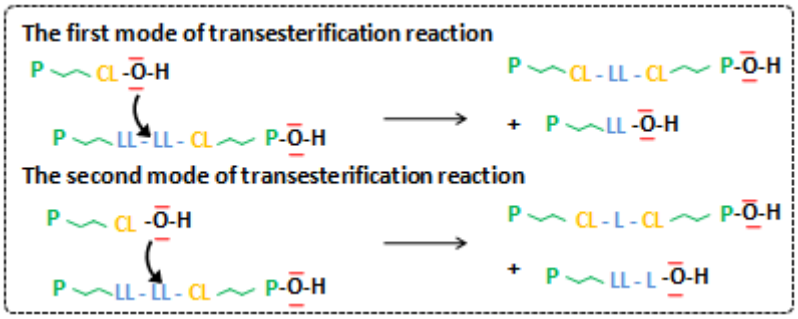

Figure 12. The two modes of transesterification reactions during *the* ROcP of *L*-LA and CL. With L: lactoyl unit and LL: lactidyl unit.[201]

(R)-(−)-1,1'-Binaphthyl-2,2'-diyl hydrogen phosphate (BPA) an acidic compound has been studied by Zhou *et al.* in 2013, for the ROcP of an equimolar mixture of LA and CL in the presence of octanol initiator, in toluene at 85 °C, with $[CL]_0/[LA]_0/[BPA]_0/[octanol]_0$ = 56/56/0.5/1 (Scheme 47).[161] CL monomers are inserted preferentially into the chain ends, leading to a copolymer containing only 8% of LA units after 39 hours in those conditions. This result indicates a r_{CL} well higher than the r_{LA}. Nevertheless, BPA is not able to homopolymerize LA in those conditions, which may explain why LA units are not efficiently incorporated in the copolymer.

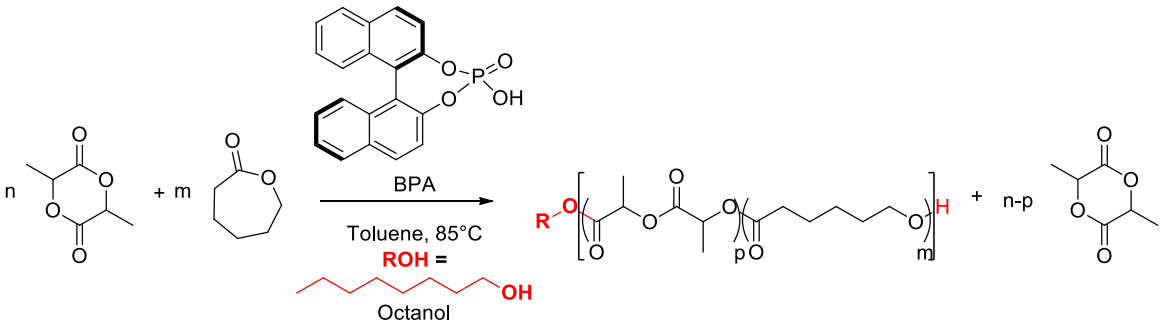

Scheme 47. BPA-ROcP of LA and CL in the presence of octanol.[161] p = n *0.08

Intermediate conclusions- During ROcP of LA and CL the nature of the catalyst has a strong influence on the microstructure of the final copolymers. These microstructures are related to the reactivity ratios which can be calculated by several methods. It thus appears that the ROcP of LA and CL in a statistical fashion is particularly challenging, using both organometallic and organic catalysts. Only aluminum-based and two other organometallic catalysts succeed in the statistical ROcP of LA and CL. None of the organocatalysts enabled the ROcP of LA and CL in a truly statistical fashion and only trifluoromethane sulfonic acid gave "satisfactory" results.

6 Conclusion and project presentation

This chapter has provided an overview of the main organocatalysts applied over the last 20 years for the ring-opening (co)polymerization (RO(*c*)P) of *L*-lactide (*L*-LA) and ε-caprolactone (CL), emphasizing the recent studies reported. Both ROP of LA and CL have shown different behaviors depending on the nature of the organocatalysts used. While, the ROP of *L*-LA is mainly conducted by basic and nucleophilic organocatalysts, acidic organocatalysts hardly trigger this reaction. In contrast, the ROP of CL is mainly conducted in the presence of acidic compounds and is arduously conducted in the presence of simple bases, working through activated chain end mechanism. “Super strong” phosphazene bases and (thio)ureas-amines bifunctional co-catalysts have witnessed their very high activity and/or selectivity in the ROP of both LA and CL. These two classes of organocatalysts are very promising and approach the activity of some organometallic catalysts, however, such organocatalysts have been found to be cytotoxic that is also blamed on organometallic catalysts.

Nevertheless, some challenges still need to be tackled such as the controlled OROP of *L*-LA in bulk at high temperature, close to 180 °C, in order to produce highly statistical PLLA and then to transpose the reaction in reactive extrusion processes (Figure 13). The second key challenge is to controlled the RO*c*P of *L*-LA and CL to produced statistical copolymer (P(LA-*stat*-CL)).

The main objective of the present PhD thesis is to find out new organocatalysts able to solve one or both of the aforementioned challenges. The green aspect of the poly(*L*-lactide), poly(ε-caprolactone) and poly(lactide-*stat*-caprolactone) synthesis is highly desirable. The organocatalysts has to be natural or “copy-paste” from nature, cheap, commercially available and biocompatible (Figure 13). Their thermal stability is required to conduct the polymerization reactions in solvent-free conditions (in bulk). In the next chapter dibenzoylmethane organocatalyst will be applied for the bulk RO*c*P of *L*-LA and CL. Chapter 3 will discuss the ROP of LA and CL in the presence of benzoic acid, as recyclable, cheap and non toxic acidic catalyst. Chapter 4 is related to the statistical RO*c*P of *L*-LA and CL in the presence of benzoic acid catalyst and to the understanding of the *L*-LA and CL reactivity.

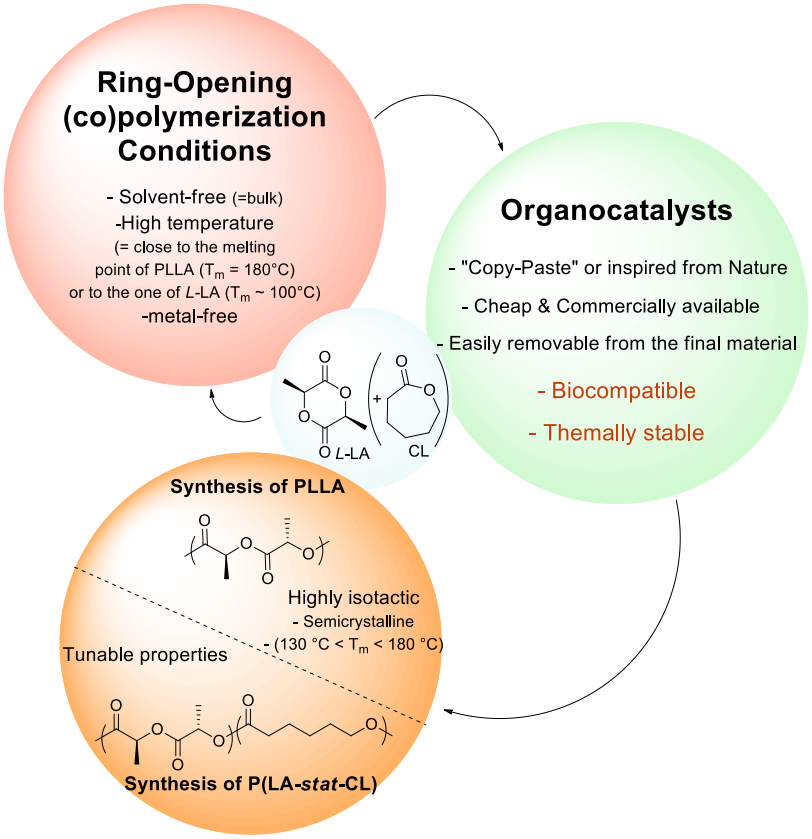

Figure 13. Main objectives and challenges of this present PhD work.

References

1 A. P. Gupta and V. Kumar, *Eur. Polym. J.*, 2007, **43**, 4053–4074.

2 T. Buntara, S. Noel, P. H. Phua, I. Melián-Cabrera, J. G. de Vries and H. J. Heeres, *Angew. Chem. Int. Ed.*, 2011, **50**, 7083–7087.

3 S. Wedde, P. Rommelmann, C. Scherkus, S. Schmidt, U. T. Bornscheuer, A. Liese and H. Gröger, *Green Chem.*, 2017, **19**, 1286–1290.

4 M. Labet and W. Thielemans, *Chem. Soc. Rev.*, 2009, **38**, 3484–3504.

5 E. Castro-Aguirre, F. Iñiguez-Franco, H. Samsudin, X. Fang and R. Auras, *Adv. Drug Deliv. Rev.*, 2016, **107**, 333–366.

6 T. K. Dash and V. B. Konkimalla, *J. Controlled Release*, 2012, **158**, 15–33.

7 K. E. Washington, R. N. Kularatne, V. Karmegam, M. C. Biewer and M. C. Stefan, *Wiley Interdiscip. Rev. Nanomed. Nanobiotechnol.*, 2017, **9**, e1446.

8 B. J. Kim, H. Cheong, E.-S. Choi, S.-H. Yun, B.-H. Choi, K.-S. Park, I. S. Kim, D.-H. Park and H. J. Cha, *J. Biomed. Mater. Res. A*, 2017, **105**, 218–225.

9 Y. Ren, Z. Zhou, G. Yin, G.-X. Chen and Q. Li, *RSC Adv.*, 2016, **6**, 31351–31358.

10 X. Wu, Y. Ma, G. Zhang, Y. Chu, J. Du, Y. Zhang, Z. Li, Y. Duan, Z. Fan and J. Huang, *Adv. Funct. Mater.*, 2015, **25**, 2138–2146.

11 R. Auras, B. Harte and S. Selke, *Macromol. Biosci.*, 2004, **4**, 835–864.

12 U. H. Choi, A. Mittal, T. L. Price, R. H. Colby and H. W. Gibson, *Macromol. Chem. Phys.*, 2016, **217**, 1270–1281.

13 S. A. Estrada A. and H.-R. Lin, *Polym. Eng. Sci.*, 2017, **57**, 283–290.

14 J. H. Kim and I. Han, *J. Adhes. Sci. Technol.*, 2017, **31**, 1328–1337.

15 W. S. Chow, E. L. Teoh and J. Karger-Kocsis, *Express Polym. Lett.*, 2018, **12**, 396–417.

16 D. Notta-Cuvier, M. Murariu, J. Odent, R. Delille, A. Bouzouita, J.-M. Raquez, F. Lauro and P. Dubois, *Macromol. Mater. Eng.*, 2015, **300**, 684–698.

17 A. Bouzouita, C. Samuel, D. Notta-Cuvier, J. Odent, F. Lauro, P. Dubois and J.-M. Raquez, *J. Appl. Polym. Sci.*, 2016, **133**, n/a-n/a.

18 O. Martin and L. Avérous, *Polymer*, 2001, **42**, 6209–6219.

19 K. Van de Velde and P. Kiekens, *Polym. Test.*, 2002, **21**, 433–442.

20 C. G. Pitt, M. M. Gratzl, G. L. Kimmel, J. Surles and A. Schindler, *Biomaterials*, 1981, **2**, 215–220.

21 C. G. Pitt, A. R. Jeffcoat, R. A. Zweidinger and A. Schindler, *J. Biomed. Mater. Res.*, 1979, **13**, 497–507.

22 S. H. Kim, S. H. Kim and Y. Jung, *J. Controlled Release*, 2015, **206**, 101–107.

23 D. W. Grijpma, G. J. Zondervan and A. J. Pennings, *Polym. Bull.*, 1991, **25**, 327–333.

24 Y. Jung, M. S. Park, J. W. Lee, Y. H. Kim, S.-H. Kim and S. H. Kim, *Biomaterials*, 2008, **29**, 4630–4636.
25 J. I. Lim, S. il Kim and S. H. Kim, *Colloids Surf. B Biointerfaces*, 2013, **103**, 463–467.
26 K. J. Cha, E. Lih, J. Choi, Y. K. Joung, D. J. Ahn and D. K. Han, *Macromol. Biosci.*, 2014, **14**, 667–678.
27 L. Calandrelli, A. Calarco, P. Laurienzo, M. Malinconico, O. Petillo and G. Peluso, *Biomacromolecules*, 2008, **9**, 1527–1534.
28 M. Rizzuto, A. Mugica, M. Zubitur, D. Caretti and A. J. Müller, *CrystEngComm*, 2016, **18**, 2014–2023.
29 A. Arbaoui and C. Redshaw, *Polym. Chem.*, 2010, **1**, 801–826.
30 E. Stirling, Y. Champouret and M. Visseaux, *Polym. Chem.*, 2018, **9**, 2517–2531.
31 S. Jacobsen, H. G. Fritz, P. Degée, P. Dubois and R. Jérôme, *Polymer*, 2000, **41**, 3395–3403.
32 J.-M. Raquez, P. Degée, Y. Nabar, R. Narayan and P. Dubois, *Comptes Rendus Chim.*, 2006, **9**, 1370–1379.
33 M. K. Kiesewetter, E. J. Shin, J. L. Hedrick and R. M. Waymouth, *Macromolecules*, 2010, **43**, 2093–2107.
34 N. E. Kamber, W. Jeong, R. M. Waymouth, R. C. Pratt, B. G. G. Lohmeijer and J. L. Hedrick, *Chem. Rev.*, 2007, **107**, 5813–5840.
35 M. Fèvre, J. Pinaud, Y. Gnanou, J. Vignolle and D. Taton, *Chem. Soc. Rev.*, 2013, **42**, 2142–2172.
36 C. Thomas and B. Bibal, *Green Chem*, 2014, **16**, 1687–1699.
37 W. N. Ottou, H. Sardon, D. Mecerreyes, J. Vignolle and D. Taton, *Prog. Polym. Sci.*, 2016, **56**, 64–115.
38 S. Naumann and A. P. Dove, *Polym. Int.*, 2016, **65**, 16–27.
39 A. P. Dove, *ACS Macro Lett.*, 2012, **1**, 1409–1412.
40 B. Martin Vaca and D. Bourissou, *ACS Macro Lett.*, 2015, **4**, 792–798.
41 J. M. Becker, R. J. Pounder and A. P. Dove, *Macromol. Rapid Commun.*, 2010, **31**, 1923–1937.
42 L.-T. Lim, R. Auras and M. Rubino, *Prog. Polym. Sci.*, 2008, **33**, 820–852.
43 O. Dechy-Cabaret, B. Martin-Vaca and D. Bourissou, *Chem. Rev.*, 2004, **104**, 6147–6176.
44 M. J. Stanford and A. P. Dove, *Chem Soc Rev*, 2010, **39**, 486–494.
45 J. Wu, T. Yu, C. Chen and C. Lin, *Coord. Chem. Rev.*, 2006, **250**, 602–626.
46 A. Sauer, A. Kapelski, C. Fliedel, S. Dagorne, M. Kol and J. Okuda, *Dalton Trans.*, 2013, **42**, 9007.
47 S. Dagorne, M. Normand, E. Kirillov and J.-F. Carpentier, *Coord. Chem. Rev.*, 2013, **257**, 1869–1886.
48 T. Fuoco and D. Pappalardo, *Catalysts*, 2017, **7**, 64.

49 A. B. Kremer and P. Mehrkhodavandi, *Coord. Chem. Rev.*, 2019, **380**, 35–57.
50 A. Arbaoui and C. Redshaw, *Polym. Chem.*, 2010, **1**, 801.
51 C. G. Pitt, F. I. Chasalow, Y. M. Hibionada, D. M. Klimas and A. Schindler, *J. Appl. Polym. Sci.*, 1981, **26**, 3779–3787.
52 A. Duda and A. Kowalski, in *Handbook of Ring-Opening Polymerization*, eds. P. Dubois, O. Coulembier and J.-M. Raquez, Wiley-VCH Verlag GmbH & Co. KGaA, Weinheim, Germany, 2009, pp. 1–51.
53 M. K. Kiesewetter, E. J. Shin, J. L. Hedrick and R. M. Waymouth, *Macromolecules*, 2010, **43**, 2093–2107.
54 W. N. Ottou, H. Sardon, D. Mecerreyes, J. Vignolle and D. Taton, *Prog. Polym. Sci.*, 2016, **56**, 64–115.
55 P. Kubisa and S. Penczek, *Prog. Polym. Sci.*, 1999, **24**, 1409–1437.
56 D. Delcroix, B. Martín-Vaca, D. Bourissou and C. Navarro, *Macromolecules*, 2010, **43**, 8828–8835.
57 D. J. Coady, H. W. Horn, G. O. Jones, H. Sardon, A. C. Engler, R. M. Waymouth, J. E. Rice, Y. Y. Yang and J. L. Hedrick, *ACS Macro Lett.*, 2013, **2**, 306–312.
58 M. Baśko and P. Kubisa, *J. Polym. Sci. Part Polym. Chem.*, 2008, **46**, 7919–7923.
59 D. J. Coady, K. Fukushima, H. W. Horn, J. E. Rice and J. L. Hedrick, *Chem. Commun.*, 2011, **47**, 3105–3107.
60 H. R. Kricheldorf, N. Lomadze and G. Schwarz, *Macromolecules*, 2008, **41**, 7812–7816.
61 J. Kadota, D. Pavlović, H. Hirano, A. Okada, Y. Agari, B. Bibal, A. Deffieux and F. Peruch, *RSC Adv.*, 2014, **4**, 14725.
62 J. U. Pothupitiya, N. U. Dharmaratne, T. M. M. Jouaneh, K. V. Fastnacht, D. N. Coderre and M. K. Kiesewetter, *Macromolecules*, 2017, **50**, 8948–8954.
63 J.-M. Raquez, R. Narayan and P. Dubois, *Macromol. Mater. Eng.*, 2008, **293**, 447–470.
64 S. Jacobsen, H. G. Fritz, P. Degée, P. Dubois and R. Jérôme, *Polym. Eng. Sci.*, 1999, **39**, 1311–1319.
65 P. Liu, J. Wu, G. Yang and H. Shao, *Mater. Lett.*, 2017, **186**, 372–374.
66 F. C. Loeker, C. J. Duxbury, R. Kumar, W. Gao, R. A. Gross and S. M. Howdle, *Macromolecules*, 2004, **37**, 2450–2453.
67 V. Bergeot, T. Tassaing, M. Besnard, F. Cansell and A.-F. Mingotaud, *J. Supercrit. Fluids*, 2004, **28**, 249–261.
68 D. Bratton, M. Brown and S. M. Howdle, *Macromolecules*, 2005, **38**, 1190–1195.
69 F. Stassin and R. Jérôme, *Macromol. Symp.*, 2004, **217**, 135–146.
70 B. Grignard, F. Stassin, C. Calberg, R. Jérôme and C. Jérôme, *Biomacromolecules*, 2008, **9**, 3141–3149.
71 F. Stassin and R. Jérôme, *J. Polym. Sci. Part Polym. Chem.*, 2005, **43**, 2777–2789.

72 D. Bratton, M. Brown and S. M. Howdle, *J. Polym. Sci. Part Polym. Chem.*, 2005, **43**, 6573–6585.
73 H. S. Ganapathy, H. S. Hwang, Y. T. Jeong, W.-K. Lee and K. T. Lim, *Eur. Polym. J.*, 2007, **43**, 119–126.
74 R. García-Arrazola, D. A. López-Guerrero, M. Gimeno and E. Bárzana, *J. Supercrit. Fluids*, 2009, **51**, 197–201.
75 I. Blakey, A. Yu, S. M. Howdle, A. K. Whittaker and K. J. Thurecht, *Green Chem.*, 2011, **13**, 2032.
76 B. Grignard, J. De Winter, P. Gerbaux, B. Gilbert, C. Jérôme and C. Detrembleur, *Eur. Polym. J.*, 2017, **95**, 635–649.
77 O. Coulembier, S. Moins, R. Todd and P. Dubois, *Macromolecules*, 2014, **47**, 486–491.
78 R. Hoogenboom, U. S. Schubert and F. Wiesbrock, Eds., *Microwave-assisted Polymer Synthesis*, Springer International Publishing, Cham, 2016, vol. 274.
79 J. Ramier, E. Renard and D. Grande, *Macromol. Chem. Phys.*, 2012, **213**, 784–788.
80 S. Kundu, A. S. Bhangale, W. E. Wallace, K. M. Flynn, C. M. Guttman, R. A. Gross and K. L. Beers, *J. Am. Chem. Soc.*, 2011, **133**, 6006–6011.
81 A. S. Bhangale, K. L. Beers and R. A. Gross, *Macromolecules*, 2012, **45**, 7000–7008.
82 X. Hu, N. Zhu, Z. Fang and K. Guo, *React. Chem. Eng.*, 2017, **2**, 20–26.
83 N. Ohn, J. Shin, S. S. Kim and J. G. Kim, *ChemSusChem*, 2017, **10**, 3529–3533.
84 A. Dzienia, P. Maksym, M. Tarnacka, I. Grudzka-Flak, S. Golba, A. Zięba, K. Kaminski and M. Paluch, *Green Chem.*, 2017, **19**, 3618–3627.
85 S. Liu, C. Ren, N. Zhao, Y. Shen and Z. Li, *Macromol. Rapid Commun.*, 2018, **39**, 1800485.
86 S. Naumann, A. W. Thomas and A. P. Dove, *ACS Macro Lett.*, 2016, **5**, 134–138.
87 N. Sadaba, M. Salsamendi, N. Casado, E. Zuza, J. Muñoz, J.-R. Sarasua, D. Mecerreyes, D. Mantione, C. Detrembleur and H. Sardon, *Polymers*, 2018, **10**, 155.
88 T. S. Stukenbroeker, J. S. Bandar, X. Zhang, T. H. Lambert and R. M. Waymouth, *ACS Macro Lett.*, 2015, **4**, 853–856.
89 A. Chuma, H. W. Horn, W. C. Swope, R. C. Pratt, L. Zhang, B. G. G. Lohmeijer, C. G. Wade, R. M. Waymouth, J. L. Hedrick and J. E. Rice, *J. Am. Chem. Soc.*, 2008, **130**, 6749–6754.
90 R. C. Pratt, B. G. G. Lohmeijer, D. A. Long, R. M. Waymouth and J. L. Hedrick, *J. Am. Chem. Soc.*, 2006, **128**, 4556–4557.
91 L. Zhang, R. C. Pratt, F. Nederberg, H. W. Horn, J. E. Rice, R. M. Waymouth, C. G. Wade and J. L. Hedrick, *Macromolecules*, 2010, **43**, 1660–1664.
92 F. Eisenreich, P. Viehmann, F. Müller and S. Hecht, *Macromolecules*, 2015, **48**, 8729–8732.
93 S. Chen, Y. Liu, Z. Li, X. Wang, H. Dong, H. Sun, K. Yang, H. Gebru and K. Guo, *Eur. Polym. J.*, 2017, **97**, 389–396.

94 X. Zhi, J. Liu, Z. Li, H. Wang, X. Wang, S. Cui, C. Chen, C. Zhao, X. Li and K. Guo, *Polym. Chem.*, 2016, **7**, 339–349.

95 A. P. Dove, R. C. Pratt, B. G. G. Lohmeijer, R. M. Waymouth and J. L. Hedrick, *J. Am. Chem. Soc.*, 2005, **127**, 13798–13799.

96 B. G. G. Lohmeijer, R. C. Pratt, F. Leibfarth, J. W. Logan, D. A. Long, A. P. Dove, F. Nederberg, J. Choi, C. Wade, R. M. Waymouth and J. L. Hedrick, *Macromolecules*, 2006, **39**, 8574–8583.

97 O. I. Kazakov and M. K. Kiesewetter, *Macromolecules*, 2015, **48**, 6121–6126.

98 R. C. Pratt, B. G. G. Lohmeijer, D. A. Long, P. N. P. Lundberg, A. P. Dove, H. Li, C. G. Wade, R. M. Waymouth and J. L. Hedrick, *Macromolecules*, 2006, **39**, 7863–7871.

99 S. S. Spink, O. I. Kazakov, E. T. Kiesewetter and M. K. Kiesewetter, *Macromolecules*, 2015, **48**, 6127–6131.

100 X. Zhang, G. O. Jones, J. L. Hedrick and R. M. Waymouth, *Nat. Chem.*, 2016, **8**, 1047–1053.

101 S. Xu, H. Sun, J. Liu, J. Xu, X. Pan, H. Dong, Y. Liu, Z. Li and K. Guo, *Polym. Chem.*, 2016, **7**, 6843–6853.

102 B. Lin and R. M. Waymouth, *Macromolecules*, 2018, **51**, 2932–2938.

103 J. U. Pothupitiya, R. S. Hewawasam and M. K. Kiesewetter, *Macromolecules*, 2018, **51**, 3203–3211.

104 A. Nachtergael, O. Coulembier, P. Dubois, M. Helvenstein, P. Duez, B. Blankert and L. Mespouille, *Biomacromolecules*, 2015, **16**, 507–514.

105 J. Liu, C. Chen, Z. Li, W. Wu, X. Zhi, Q. Zhang, H. Wu, X. Wang, S. Cui and K. Guo, *Polym. Chem.*, 2015, **6**, 3754–3757.

106 J. Liu, J. Xu, Z. Li, S. Xu, X. Wang, H. Wang, T. Guo, Y. Gao, L. Zhang and K. Guo, *Polym. Chem.*, 2017, **8**, 7054–7068.

107 D. Specklin, F. Hild, L. Chen, L. Thévenin, M. Munch, F. Dumas, F. Le Bideau and S. Dagorne, *ChemCatChem*, 2017, **9**, 3041–3046.

108 X. Li, Q. Zhang, Z. Li, S. Xu, C. Zhao, C. Chen, X. Zhi, H. Wang, N. Zhu and K. Guo, *Polym. Chem.*, 2016, **7**, 1368–1374.

109 E. Raamat, K. Kaupmees, G. Ovsjannikov, A. Trummal, A. Kütt, J. Saame, I. Koppel, I. Kaljurand, L. Lipping, T. Rodima, V. Pihl, I. A. Koppel and I. Leito, *J. Phys. Org. Chem.*, 2013, **26**, 162–170.

110 D. Bourissou, B. Martin-Vaca, A. Dumitrescu, M. Graullier and F. Lacombe, *Macromolecules*, 2005, **38**, 9993–9998.

111 M. Baśko and P. Kubisa, *J. Polym. Sci. Part Polym. Chem.*, 2010, **48**, 2650–2658.

112 N. Susperregui, D. Delcroix, B. Martin-Vaca, D. Bourissou and L. Maron, *J. Org. Chem.*, 2010, **75**, 6581–6587.

113 S. Matsumura, K. Mabuchi and K. Toshima, *Macromol. Rapid Commun.*, 1997, **18**, 477–482.

114 S. Matsumura, K. Mabuchi and K. Toshima, *Macromol. Symp.*, 1998, **130**, 285–304.

115 M. Fujioka, N. Hosoda, S. Nishiyama, H. Noguchi, A. Shoji, D. S. Kumar, K. Katsuraya, S. Ishii and Y. Yoshida, *FIBER*, 2006, **62**, 63–65.

116 M. Yoshizawa-Fujita, C. Saito, Y. Takeoka and M. Rikukawa, *Polym. Adv. Technol.*, 2008, **19**, 1396–1400.

117 M. Mena, A. López-Luna, K. Shirai, A. Tecante, M. Gimeno and E. Bárzana, *Bioprocess Biosyst. Eng.*, 2013, **36**, 383–387.

118 F. Nederberg, E. F. Connor, M. Möller, T. Glauser and J. L. Hedrick, *Angew. Chem. Int. Ed.*, 2001, **40**, 2712–2715.

119 B. Guillerm, V. Lemaur, B. Ernould, J. Cornil, R. Lazzaroni, J.-F. Gohy, P. Dubois and O. Coulembier, *RSC Adv.*, 2014, **4**, 10028.

120 Sweet,D.V., *Regist. Toxic Eff. Chem. Subst.*, 1985.

121 V. Katiyar and H. Nanavati, *Polym. Chem.*, 2010, **1**, 1491.

122 M. Myers, E. F. Connor, T. Glauser, A. Möck, G. Nyce and J. L. Hedrick, *J. Polym. Sci. Part Polym. Chem.*, 2002, **40**, 844–851.

123 S. A. Buckler, *J. Am. Chem. Soc.*, 1962, **84**, 3093–3097.

124 P. Dubois, O. Coulembier and C. Delcourt, *Open Macromol. J.*, 2007, **1**, 1–5.

125 C. Wang, H. Li and X. Zhao, *Biomaterials*, 2004, **25**, 5797–5801.

126 H. Li, C. Wang, J. Yue, X. Zhao and F. Bai, *J. Polym. Sci. Part Polym. Chem.*, 2004, **42**, 3775–3781.

127 G. Nogueira, A. Favrelle, M. Bria, J. P. Prates Ramalho, P. J. Mendes, A. Valente and P. Zinck, *React Chem Eng*, 2016, **1**, 508–520.

128 P. Lewinski, S. Sosnowski and S. Penczek, *Polymer*, 2017, **108**, 265–271.

129 M. Bednarek, M. Basko, T. Biedron, E. Wojtczak and A. Michalski, *Eur. Polym. J.*, 2015, **71**, 380–388.

130 T. Saito, Y. Aizawa, K. Tajima, T. Isono and T. Satoh, *Polym Chem*, 2015, **6**, 4374–4384.

131 D. Delcroix, A. Couffin, N. Susperregui, C. Navarro, L. Maron, B. Martin-Vaca and D. Bourissou, *Polym. Chem.*, 2011, **2**, 2249–2256.

132 E. Oledzka, K. Sokolowski, M. Sobczak and W. Kolodziejski, *Polym. Int.*, 2011, **60**, 787–793.

133 H. Li, S. Zhang, J. Jiao, Z. Jiao, L. Kong, J. Xu, J. Li, J. Zuo and X. Zhao, *Biomacromolecules*, 2009, **10**, 1311–1314.

134 O. Coulembier, T. Josse, B. Guillerm, P. Gerbaux and P. Dubois, *Chem. Commun.*, 2012, **48**, 11695–11697.

135 H. Yang, J. Xu, S. Pispas and G. Zhang, *Macromolecules*, 2012, **45**, 3312–3317.

136 H. Alamri, J. Zhao, D. Pahovnik and N. Hadjichristidis, *Polym Chem*, 2014, **5**, 5471–5478.

137 H. Alamri and N. Hadjichristidis, *Polym. Chem.*, 2016, **7**, 3225–3228.
138 L. Zhang, F. Nederberg, R. C. Pratt, R. M. Waymouth, J. L. Hedrick and C. G. Wade, *Macromolecules*, 2007, **40**, 4154–4158.
139 T. Ishikawa, Ed., *Superbases for Organic Synthesis*, John Wiley & Sons, Ltd, Chichester, UK, 2009.
140 V. Ladelta, J. D. Kim, P. Bilalis, Y. Gnanou and N. Hadjichristidis, *Macromolecules*, 2018, **51**, 2428–2436.
141 H. Li, N. Zhao, C. Ren, S. Liu and Z. Li, *Polym. Chem.*, 2017, **8**, 7369–7374.
142 G. W. Nyce, T. Glauser, E. F. Connor, A. Möck, R. M. Waymouth and J. L. Hedrick, *J. Am. Chem. Soc.*, 2003, **125**, 3046–3056.
143 N. E. Kamber, W. Jeong, S. Gonzalez, J. L. Hedrick and R. M. Waymouth, *Macromolecules*, 2009, **42**, 1634–1639.
144 Y. Wang, J. Niu, L. Jiang, Y. Niu and L. Zhang, *J. Macromol. Sci. Part A*, 2016, **53**, 374–381.
145 S. Naumann and M. R. Buchmeiser, *Macromol. Rapid Commun.*, 2014, **35**, 682–701.
146 G. O. Jones, Y. A. Chang, H. W. Horn, A. K. Acharya, J. E. Rice, J. L. Hedrick and R. M. Waymouth, *J. Phys. Chem. B*, 2015, **119**, 5728–5737.
147 P. P. Datta, J. U. Pothupitiya, E. T. Kiesewetter and M. K. Kiesewetter, *Eur. Polym. J.*, 2017, **95**, 671–677.
148 K. V. Fastnacht, S. S. Spink, N. U. Dharmaratne, J. U. Pothupitiya, P. P. Datta, E. T. Kiesewetter and M. K. Kiesewetter, *ACS Macro Lett.*, 2016, **5**, 982–986.
149 X. Li, Q. Zhang, Z. Li, X. Wang, J. Liu, S. Cui, S. Xu, C. Zhao, C. Chen and K. Guo, *Polymer*, 2016, **84**, 293–303.
150 G. Gontard, A. Amgoune and D. Bourissou, *J. Polym. Sci. Part Polym. Chem.*, 2016, **54**, 3253–3256.
151 J. M. Jonté, R. Dunsing and H. R. Kricheldorf, *J. Macromol. Sci. Part - Chem.*, 1985, **22**, 495–514.
152 B. C. Wilson and C. W. Jones, *Macromolecules*, 2004, **37**, 9709–9714.
153 S. Gazeau-Bureau, D. Delcroix, B. Martín-Vaca, D. Bourissou, C. Navarro and S. Magnet, *Macromolecules*, 2008, **41**, 3782–3784.
154 N. Stanley, G. Bucataru, Y. Miao, A. Favrelle, M. Bria, F. Stoffelbach, P. Woisel and P. Zinck, *J. Polym. Sci. Part Polym. Chem.*, 2014, **52**, 2139–2145.
155 H. Wang, W. Wu, Z. Li, X. Zhi, C. Chen, C. Zhao, X. Li, Q. Zhang and K. Guo, *RSC Adv*, 2014, **4**, 55716–55722.
156 K. Makiguchi, S. Kikuchi, T. Satoh and T. Kakuchi, *J. Polym. Sci. Part Polym. Chem.*, 2013, **51**, 2455–2463.
157 Y. Jin, Y. Ji, X. He, S. Kan, H. Xia, B. Liang, J. Chen, H. Wu, K. Guo and Z. Li, *Polym. Chem.*, 2014, **5**, 3098–3106.

158 X. Wang, J. Liu, S. Xu, J. Xu, X. Pan, J. Liu, S. Cui, Z. Li and K. Guo, *Polym. Chem.*, 2016, **7**, 6297–6308.
159 K. Makiguchi, T. Satoh and T. Kakuchi, *Macromolecules*, 2011, **44**, 1999–2005.
160 P. Malik and D. Chakraborty, *Inorganica Chim. Acta*, 2013, **400**, 32–41.
161 X. Zhou and L. Hong, *Colloid Polym. Sci.*, 2013, **291**, 2155–2162.
162 S. Kan, Y. Jin, X. He, J. Chen, H. Wu, P. Ouyang, K. Guo and Z. Li, *Polym. Chem.*, 2013, **4**, 5432.
163 L.-H. Yao, S.-X. Shao, L. Jiang, N. Tang and J.-C. Wu, *Chem. Pap.*, 2014, **68**, 1381–1389.
164 C. Chen, R. Xu and B. Li, *Sci. China Chem.*, 2012, **55**, 1257–1262.
165 N. Susperregui, D. Delcroix, B. Martin-Vaca, D. Bourissou and L. Maron, *J. Org. Chem.*, 2010, **75**, 6581–6587.
166 Y. Miao, Y. Phuphuak, C. Rousseau, T. Bousquet, A. Mortreux, S. Chirachanchai and P. Zinck, *J. Polym. Sci. Part Polym. Chem.*, 2013, **51**, 2279–2287.
167 F. Sanda, H. Sanada, Y. Shibasaki and T. Endo, *Macromolecules*, 2002, **35**, 680–683.
168 Y. Shibasaki, H. Sanada, M. Yokoi, F. Sanda and T. Endo, *Macromolecules*, 2000, **33**, 4316–4320.
169 P. V. Persson, J. Casas, T. Iversen and A. Córdova, *Macromolecules*, 2006, **39**, 2819–2822.
170 E. Oledzka and S. S. Narine, *J. Appl. Polym. Sci.*, 2011, **119**, 1873–1882.
171 J. Casas, P. V. Persson, T. Iversen and A. Córdova, *Adv. Synth. Catal.*, 2004, **346**, 1087–1089.
172 J. Xu, J. Song, S. Pispas and G. Zhang, *J. Polym. Sci. Part Polym. Chem.*, 2014, **52**, 1185–1192.
173 J. Xu, J. Liu, Z. Li, X. Li, C. Chen, C. Zhao, S. Xu, X. Pan, J. Liu and K. Guo, *Polym Chem*, 2016, **7**, 1111–1120.
174 J. Xu, K. Yang, Z. Li, J. Liu, H. Sun, S. Xu, H. Wang, T. Guo, H. Dong and K. Guo, *Polym Chem*, 2017, **8**, 6398–6406.
175 Y. Ren, Z. Wei, X. Leng, Y. Wang and Y. Li, *Polymer*, 2015, **78**, 51–58.
176 T. Fukuda, K. Kubo and Y.-D. Ma, *Prog. Polym. Sci.*, 1992, **17**, 875–916.
177 F. R. Mayo and F. M. Lewis, *J. Am. Chem. Soc.*, 1944, **66**, 1594–1601.
178 T. Kelen and F. Tüdös, *J. Macromol. Sci. Part - Chem.*, 1975, **9**, 1–27.
179 M. Van Den Brink, A. M. Van Herk and A. L. German, *J. Polym. Sci. Part Polym. Chem.*, 1999, **37**, 3793–3803.
180 S. Harrisson, F. Ercole and B. W. Muir, *Polym Chem*, 2010, **1**, 326–332.
181 M. Baśko and P. Kubisa, *J. Polym. Sci. Part Polym. Chem.*, 2006, **44**, 7071–7081.
182 M. Baśko and P. Kubisa, *J. Polym. Sci. Part Polym. Chem.*, 2007, **45**, 3090–3097.
183 L. Zhang, N. Li, Y. Wang, J. Guo and J. Li, *Macromol. Res.*, 2014, **22**, 600–605.
184 D. W. Grijpma and A. J. Pennings, *Polym. Bull.*, 1991, **25**, 335–341.
185 P. Vanhoorne, P. Dubois, R. Jerome and P. Teyssie, *Macromolecules*, 1992, **25**, 37–44.

186 Y. Shen, K. J. Zhu, Z. Shen and K.-M. Yao, *J. Polym. Sci. Part Polym. Chem.*, 1996, **34**, 1799–1805.
187 J. Contreras and D. Dávila, *Polym. Int.*, 2006, **55**, 1049–1056.
188 M. Florczak and A. Duda, *Angew. Chem. Int. Ed.*, 2008, **47**, 9088–9091.
189 D. Pappalardo, L. Annunziata and C. Pellecchia, *Macromolecules*, 2009, **42**, 6056–6062.
190 Z. Wei, L. Liu, C. Qu and M. Qi, *Polymer*, 2009, **50**, 1423–1429.
191 N. Nomura, A. Akita, R. Ishii and M. Mizuno, *J. Am. Chem. Soc.*, 2010, **132**, 1750–1751.
192 G. Li, M. Lamberti, D. Pappalardo and C. Pellecchia, *Macromolecules*, 2012, **45**, 8614–8620.
193 Y. Wang and H. Ma, *Chem. Commun.*, 2012, **48**, 6729–6731.
194 A. Pilone, N. De Maio, K. Press, V. Venditto, D. Pappalardo, M. Mazzeo, C. Pellecchia, M. Kol and M. Lamberti, *Dalton Trans*, 2015, **44**, 2157–2165.
195 T. Shi, W. Luo, S. Liu and Z. Li, *J. Polym. Sci. Part Polym. Chem.*, 2018, **56**, 611–617.
196 M. Honrado, A. Otero, J. Fernández-Baeza, L. F. Sánchez-Barba, A. Garcés, A. Lara-Sánchez and A. M. Rodríguez, *Organometallics*, 2016, **35**, 189–197.
197 Y. Maruta and A. Abiko, *Polym. Bull.*, 2014, **71**, 989–999.
198 J. Lewiński, P. Horeglad, K. Wójcik and I. Justyniak, *Organometallics*, 2005, **24**, 4588–4593.
199 D. Chandanabodhi and T. Nanok, *Mol. Catal.*, 2017, **436**, 145–156.
200 Q. Song, S. Hu, J. Zhao and G. Zhang, *Chin. J. Polym. Sci.*, 2017, **35**, 581–601.
201 J. Kasperczyk and M. Bero, *Makromol. Chem.*, 1993, **194**, 913–925.

Chapter 2.

Dibenzoylmethane: *in situ* generation of active species for the bulk ring-opening copolymerization of *L*-lactide and ε-caprolactone

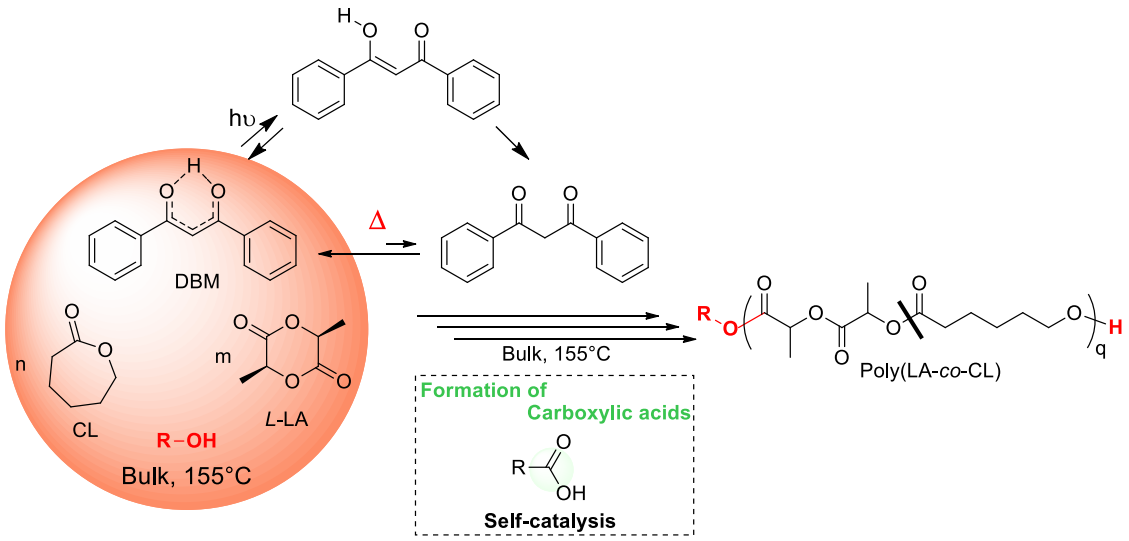

Keywords: bulk, catalysis; copolymerization; ε-caprolactone; diketone; lactide; organocatalysis; polyesters, organic catalysts, ring-opening.

Chapter 2. Dibenzoylmethane: *in situ* generation of active species for the bulk ring-opening copolymerization of *L*-lactide and ε-caprolactone

Table of contents

Introduction

As emphasized in the previous chapter, the organocatalyzed ring-opening copolymerization (ORO*c*P) of lactide (LA) and ε-caprolactone (CL) is a key challenge in polymer chemistry that needs to be addressed. Attempts utilizing basic organocatalysts, such as phosphazenes,[1] *N*-heterocycliccarbenes,[2] guanidine "superbases" 1,5,7-triazabicyclo[4.4.0]dec-5-ene[3] (TBD) or urea/amine cocatalysts[4] have met with limited success in the insertion of CL monomer in the polymer chain. Acidic organocatalysts, such as trifluoromethane sulfonic acid (TfOH) and (R)-(−)-1,1'-binaphthyl-2,2'-diyl hydrogen phosphate (BPA) have also been employed for this purpose.[5,6,7] When using TfOH in solution at low temperatures, a statistical distribution of LA and CL units has been evidenced,[5,6] LA has being consumed faster in the course of the RO*c*P process. In this regard, TfOH shows a similar trend to that observed from most of the organometallic catalysts (Table 1), *i.e*. a CL reactivity ratio (r_{CL}) lower than that of LA (r_{LA}).[8] In contrast, attempts at copolymerizing LA and CL by BPA have led to the incorporation of a limited fraction of LA (8 mol%) into the final copolymer[7], suggesting a r_{CL} higher than r_{LA} in these peculiar conditions.

Table 1. Reactivity ratio (*r*) values of *L*-LA and CL towards various organometallic catalysts.

Entry	Catalysts	r_{LA}	r_{CL}	Ref
1	$Sn(oct)_2$ [a]	42	0.4	9
2	$Mg(oct)_2$ [b]	23	0.2	10
4	$Al(O^iPr)$ + Ligand[c]	112	7.2	11
5	Diphenylzinc	14.4	0.36	12
6	Al + ligand[d]	2.68	0.29	13
7	Al + ligand[d]	2.13	0.43	13

[a] Tin (II) octoate, [b] Magnesium (II) octoate, [c] ligand = Schiff base, [d] Phenoxyimine Aluminum system

Dibenzoylmethane (DBM) is a 1,3-diketone, cheap and commercially available belonging to the flavonoid family (Scheme 1). This molecule is nontoxic and is known to exhibit interesting anti-tumor promoting activities.[14,15]

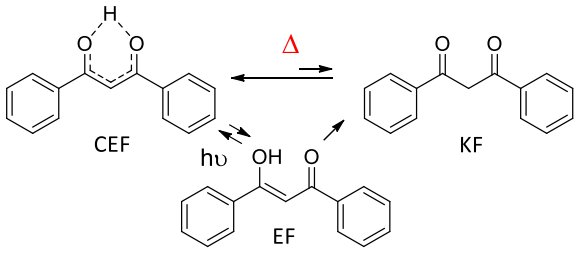

Scheme 1. The three different forms of DBM

In the context of polymer synthesis, DBM has been served as efficient ligand of Sn(II)-based complex for the bulk ring-opening polymerization (ROP) of (*L*-lactide) *L*-LA at 180 °C (Scheme 2).[16] Complex (**2**) in the presence of dodecanol (DDO) has afforded PLAs with molar mass (M_n) up to 176 000 g.mol^{-1} and a dispersity of 1.91, using the following conditions [*L*-LA]$_0$/[DDO]$_0$/[**2**]$_0$ = 40000/40/1.

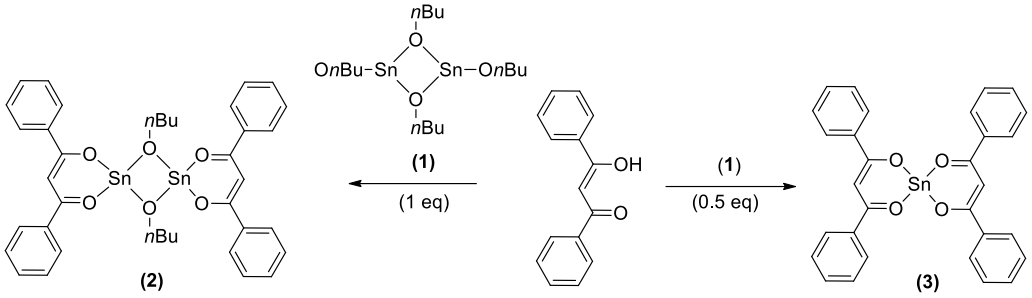

Scheme 2. Sn(II) complexes used for the bulk ROP of *L*-LA at 180°C.

Dibenzoylmethane compound can eventually exist in three different forms, depending on the analytical conditions: a chelated enol form (CEF) and a diketone form (KF) in tautomeric equilibrium and a short lived non-chelated enol form (EF) (Scheme 1).[17] The chelated enol form, predominant at r.t in several solvents[18] (11 < K_e=[CEF]/[KF] < 98, with K_e the equilibrium constant), is expected to be relatively inert toward its environment, due to a strong stabilization by intramolecular hydrogen bonds (Scheme 1). This leads to a conjugated system that is extended over the whole molecule. It is worth mentioning that Moriyasu *et al.* have highlighted that K_e is higher in non-polar solvent, and is also higher at lower concentrations in DBM. The lower K_e value, hence the higher content of the KF form, is achieved in acetonitrile as solvent (Table 2). In the present work bulk conditions will be used. CL monomer is also an aprotic and polar molecule possessing almost the same permittivity constant to that of acetonitrile at r.t ($\varepsilon_{0,CL}$= 36.5 *vs.* $\varepsilon_{0,CH3CN}$= 35.8).[19,20] Furthermore, the permittivity constant of LA being unknown, its value will be assumed to be relatively the same like that of CL. As a matter of fact, DBM is thus expected to be predominantly in its CEF form.

Table 2. Equilibrium constant (K_e = [CEF]/[KF]) for keto-enol tautomerism of DBM at r.t in several solvents

Solvent	ε_0[a]	K_e (0.01 mol.L^{-1})	K_e (0.1 mol.L^{-1})
Hexane	1.88	98	n.a
Chloroform	4.8	24	23
Acetonitrile	37.5	12	11
Methanol	32.7	24	16

[a] Dielectric constants[21].

In the present study, we reasoned that DBM could be thermally activated by disruption of the intramolecular hydrogen bonds of the CEF form at high temperature. Indeed, the non-chelated intermediate, which can interact more strongly with proton acceptors and/or donors, is known to be generated under UV stimulation, reverting to the original chelated form or tautomerizing to the diketone form.[17] Folkendt *et al.* have also evidenced, on the basis of NMR investigations, an increase of the diketone form of acetylacetone when increasing the temperature.[22] One can thus hypothesize that the non-chelated enol and diketone isomers could be generated when the temperature is increased up to 155 °C. Thus, the non-chelated enol isomer could activate both the monomer and the propagating alcohol whereas the resulting diketone isomer might activate the propagating alcohol. A bifunctional mechanism involving the three co-existing isomers acting as proton shuttles- without any hydrogen bond formation- between the initiator and the monomers can be expected.

In this chapter, dibenzoylmethane is studied as a potential organocatalyst for the preparation of statistical-like P(LA-*co*-CL) copolyesters under solvent-free conditions at 155 °C (Scheme 3). The ring-opening copolymerization of *L*-LA and CL in the presence of benzyl alcohol has thus been evaluated. Reactivity ratios of CL and *L*-LA have then been determined using the Kelen-Tüd*ő*s linear method. However, a nonlinear method referred to as "the visualization of the sum of squared residual space" (VSSRS) has also been applied to have a better insight into the copolymer structure. Dibenzoylmethane has been associated to two different initiators, including butane-1,4-diol and poly(ethylene glycol), in order to produce α,ω- telechelic P(LA-*co*-CL) diols. In a subsequent part, ring-opening polymerizations of *L*-LA and CL have been conducted. Finally, miscellaneous carboxylic acids and amino acids have been evaluated in the RO*c*P of *L*-LA and CL because DBM is suspected to *in situ* generate RCOOH species that could play the role of the real organocatalyst.

The VSSRS investigations have been conducted in collaboration with Dr. Simon Harrisson at the Laboratoire des Interactions Moléculaires et Réactivités Chimiques et Photochimiques (IMRCP, UMR 5623) in Toulouse.

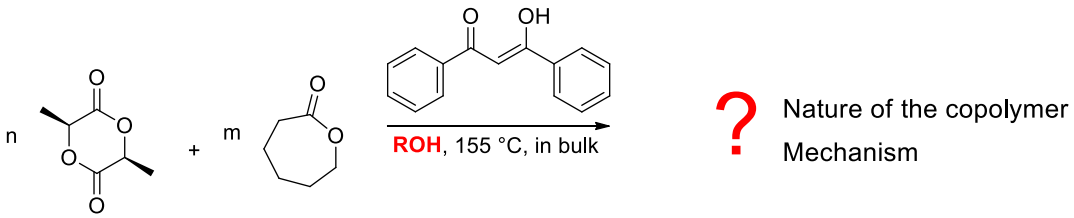

Scheme 3. DBM-ORO*c*P of *L*-LA and CL in the presence of several initiators.

1 Dibenzoylmethane-organocatalyzed ring-opening copolymerization (DBM-ORO*c*P) of *L*-lactide (*L*-LA) and ε-caprolactone (CL)

As mentioned above, the ring-opening copolymerization (RO*c*P) of *L*-LA and CL was carried out in solvent-free and metal-free conditions. Dibenzoylmethane (DBM) was selected not only owing to its thermal stability (Figure S 2, in supporting information, SI) but also because of its ability to conduct these copolymerizations at high temperature in the melt. Exogenous alcohol initiators, such as benzyl alcohol (BnOH), butane-1,4-diol (BD) and poly(ethylene glycol) (PEG_{1000}), were used to initiate the DBM-organocatalyzed RO*c*P (ORO*c*P) of *L*-LA and CL (Scheme 4). All these experiments are summarized in Table 3. Reactions were carried out in bulk at 155 °C, using 5mol% of DBM and with an initial comonomer-to-initiator ratio of 30 ($[M]_0/[I]_0$= 30, *i.e.* a $[L\text{-LA}]_0/[I]_0 = [CL]_0/[I]_0$ = 15), a ratio of 50 was also attempted (Entry 8).

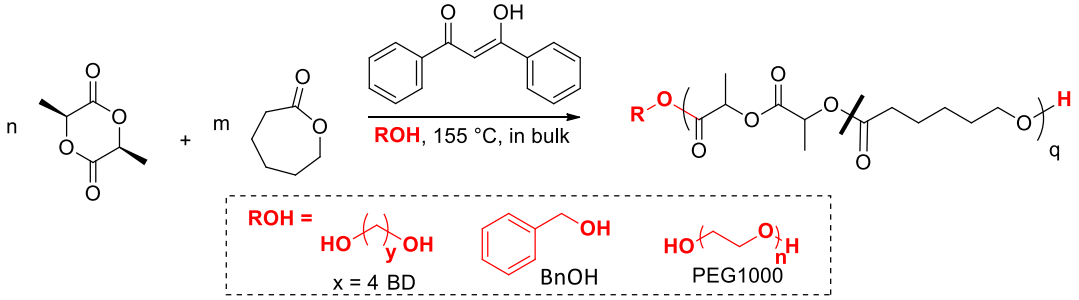

Scheme 4. General scheme of the DBM-ORO*c*P of *L*-LA and CL in the presence of various alcohols (n+m = q).

Table 3. Results and conditions of the DBM-ORO*c*P of *L*-LA and CL in bulk.[a]

Entry	I[b]	Cat[c] (%)	Time (h)	C_{CL}/C_{LA}[d] (%/%)	F_{CL}[e] (%)	$M_{n,SEC}$[f] (g.mol^{-1})	$M_{p,SEC}$[f] (g.mol^{-1})	$Đ$[f]	$DP_{,th}$[g]	$DP_{,exp}$[h]
1	No	0	41	0/0	-	-	-	-	-	-
2	BnOH	5	24	14/39	26	1000	1280	1.3	7.6	5.6
3	BnOH	5	48	52/72	41	2200	3010	1.36	18.6	13.1
4	BnOH	5	51	65/78	46	2750	n.a	1.32	21.6	n.a
5	BnOH	5	68	90/91	50	3450	4350	1.4	27.2	20
6	BnOH	5	70	93/94	50	3600	4770	1.48	28.3	18
7	BnOH	5	72	99/96	51	3300	4900	1.72	29.3	21.9
8	BnOH[i]	5	72	81/85	49	3730	5070	1.46	41.6	25.8
9	BD	5	48	51/70	44	3850	5720	1.34	18.1	24.4
10	PEG	5	38	86/92	51	4100	7000	1.55	n.a	n.a

[a]All reactions were carried out in bulk under nitrogen atmosphere at 155°C with reaction conditions: n_{CL}= n_{LA}=1.4mmol with $[M]_0/[I]_0$= 30, *i.e.* a $[L\text{-LA}]_0/[I]_0 = [CL]_0/[I]_0 = 15$; [b]Initiator used: benzyl alcohol (BnOH), butane-1,4-diol (BD) and poly(ethylene glycol) (PEG_{1000}, M_w≈1000g.mol-1); [c]Catalyst loading in mol% rel. to the monomers [d]CL and *L*-LA conversions determined by ^{1}H NMR analysis; [e] CL fraction in the pure copolymer formed; [f]Uncorrected average molar mass ($M_{n,SEC}$) and molar mass at the peak ($M_{p,SEC}$) and dispersity ($Đ$) of crude copolymers determined by SEC chromatography (Polystyrene standards), THF/NEt_3 (2w%) as eluent at 35°C; [g]Theoretical degree of polymerization $DP_{,th} = \frac{[LA]_0}{[I]_0} \times C_{LA} + \frac{[CL]_0}{[I]_0} \times C_{CL}$; [h]Degree of polymerization calculated from the chain ends determined by ^{1}H NMR (*cf.* experimental part for calculations); n.d= not determined. [i]$[M]_0/[I]_0$= 50, i.e. a $[L\text{-LA}]_0/[I]_0 = [CL]_0/[I]_0 = 25$; n.a = not available.

1.1 Copolymerization reactions initiated by benzyl alcohol

DBM enabled the consumption of both *L*-LA and CL comonomers, in presence of benzyl alcohol as initiator (Table 3, Entries 2-7). As attested by ^{1}H NMR spectroscopy, 93-94% of both comonomers were polymerized after 70 hours of reaction (Figure 1, Table 3, Entry 6). Since the copolymerization required long reaction times, the catalyst activity was further demonstrated through a blank experiment with no catalyst or initiator (Table 3, Entry 1, Figure S 3). As expected, no reaction took place after 41h.

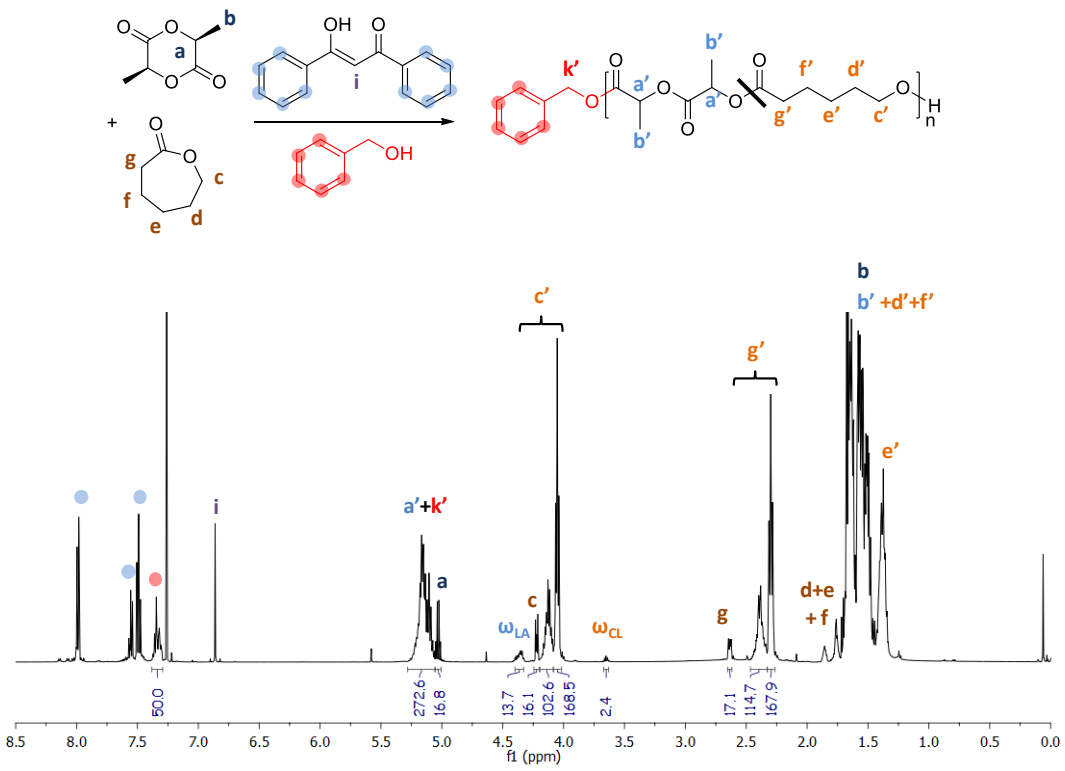

Figure 1. ^{1}H NMR spectrum of the crude copolymers (Table 3, Entry 6). With ω_{LA} and ω_{CL} the ω-chain ends of *L*-LA and CL units, respectively ($CDCl_3$, 500MHz, r.t).

Integral values of the *L*-LA and CL units at the ω-chain end (ω_{LA} and ω_{CL}, respectively) determined by ^{1}H NMR were found slightly higher than those expected from the feed molar ratio of the comonomers. This led to a lower experimental degree of polymerization ($DP_{,exp}$) than that expected theoretically ($DP_{,th}$, Table 3), suggesting that another protic residue such as water traces might have initiated the DBM-ORO*c*P of *L*-LA and CL (Scheme 5). The presence of water could be explained as follows:

1) It may be contained in the reagents, despite extensive efforts to dry them. Typically, CL and BnOH were distillated over CaH_2 and stored over molecular sieves while *L*-LA was recrystallized three times from toluene in inert atmosphere and dried under vacuum at 35°C for two days. As for DBM, it was dried *via* three azeotropic distillations of toluene. All reagents were stores in glove box and no protic residues were detected by ^{1}H NMR analysis.

2) The thermal degradation of the reagents at 155 °C.

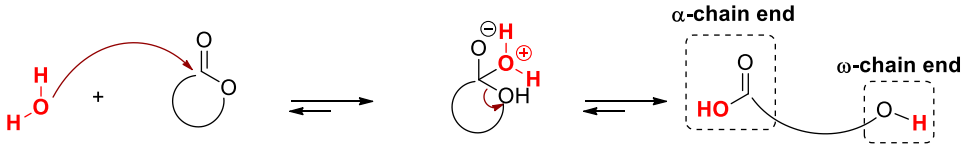

Scheme 5. Side initiation by water leading to a higher amount of ω-chain end in the medium.

Despite co-initiation occured, the BnOH-initiated ROcP exhibited an acceptable level of control, as attested by the linear correlation between the uncorrected average molar mass ($M_{n,SEC}$) and the total monomer conversion (C_{TOT}) (Figure 2a) in the one hand, and on the other hand the relatively narrowly distributed copolymers ($Đ = M_w/M_n$ < 1.5, Figure 2a,b). At almost completion of the reaction (> 98%), however, the lowering of the molar mass along with an increase in disperisty were noted ($Đ$ = 1.72, Table 3, Entry 7) very likely due to intermolecular transesterification reactions.

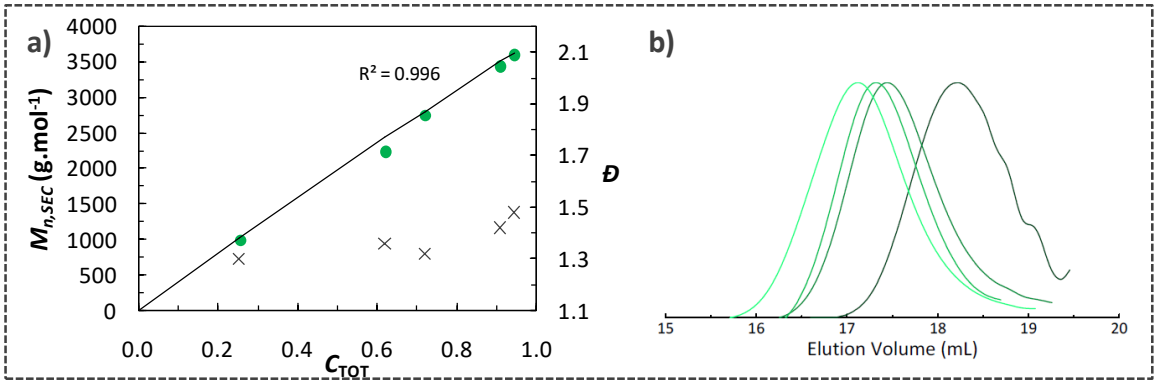

Figure 2. (a) Evolution of the uncorrected $M_{n,SEC}$ (●)and $Đ$ (x) with total monomer conversion for the crude copolymers synthesized using DBM in bulk at 155°C (Table 3, Entries 2 to 6).(b) SEC traces of the crude copolymers (Table 3, Entries 2 to 5).

Finally, attempts to perform the bulk ROcP of *L*-LA and CL at 155 °C, targeting a higher DP $[L\text{-LA}]_0/[CL]_0/[DBM]_0/[BD]_0$= 25/25/2.5/1 met with limited success (Table 3, Entry 8). Indeed, the $DP_{,exp}$ of the as-obtained copolymer did not match to the $DP_{,th}$ ($DP_{,exp}$ = 25.8 ≠ $DP_{,th}$ = 41.6). Moreover, the brown color of the final copolymer strongly suggested that many side reactions occurred during the copolymerization. DBM was not enough active to enable the ROcP of *L*-LA and CL for higher targeted degree of polymerization.

1.2 Determination of the reactivity ratios

Of particular interest, both monomers were inserted almost simultaneously in the copolymer chain during this DBM-ROcP process. This could be evidenced by ^{1}H NMR analyses of the crude mixtures (Figure 3, Table 3, Entries 2 to 6).

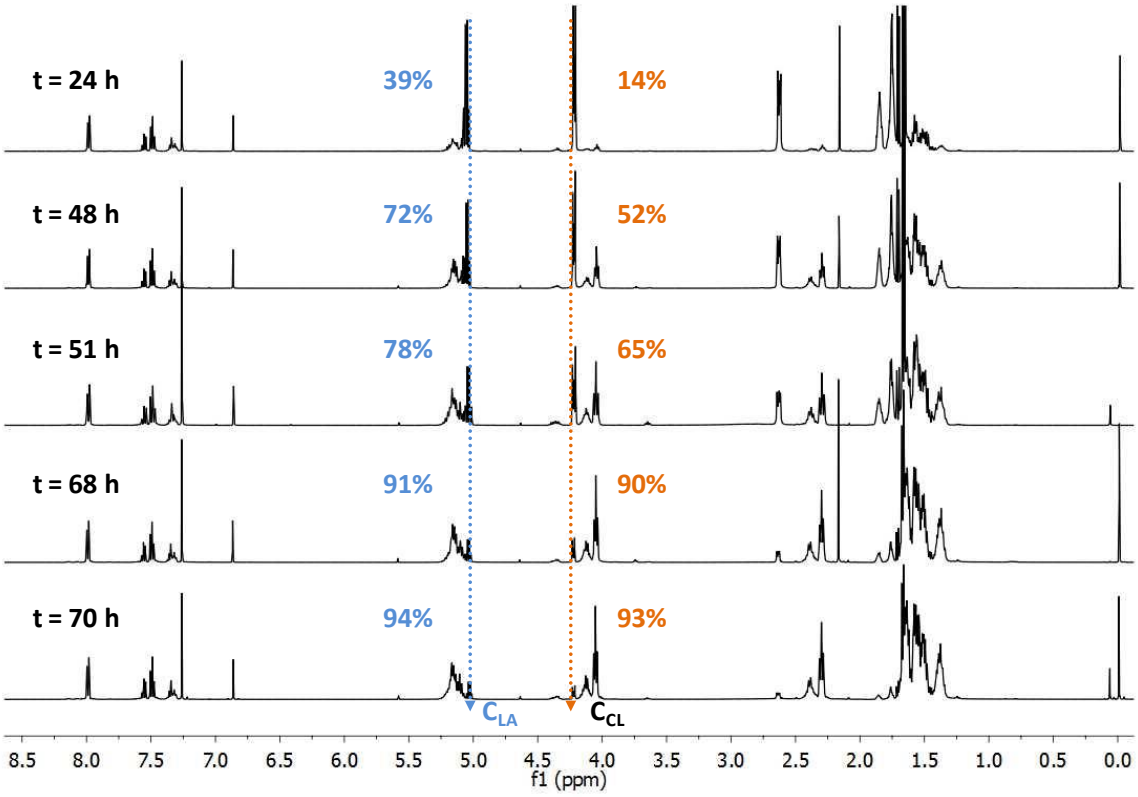

Figure 3. Stack of the ^{1}H NMR spectra of the crude copolymers, (Table 3, Entries 2 to 6) from top to bottom ($CDCl_3$, 500MHz, r.t).

In order to account of the copolymer microstructure, the reactivity ratios were assessed using the Kelen-Tüdős linear method. For this purpose, the DBM-ORO*c*P of *L*-LA and CL with different chosen compositions ($f_{LA,0}$: $f_{CL,0}$ ≈ 15:85, 30:70, 40:60, 50:50, 60:40, 70:30) were performed and the monomer compositions (F_{LA} and F_{CL}) in the obtained oligomers were examined at low conversion. This method led to a value of 1.81 for r_{LA} and 0.08 for r_{CL} (Table S 1, Figure S 4, Equations **1**).[23,24]

$$r_{CL} = \frac{k_{CL-CL}}{k_{CL-LA}} \qquad r_{LA} = \frac{k_{LA-LA}}{k_{LA-CL}} \qquad (1)$$

As discussed in the bibliographic chapter, the linearized Kelen-Tüdős method, which derives from the Mayo-Lewis equation and requires that monomer conversion be kept very low, may unduly weight some data points while giving less weight to others. It thus provide biased estimates of reactivity ratios. This prompted us to implement a more reliable method, namely, the VSSRS nonlinear method [25,26] that was developed by Van den Brink *et al.* This VSSRS method not only allows for an estimate of reactivity ratios at high conversion, but also takes into account errors both on the monomer conversion and the co-monomer ratios, thus providing unbiased estimates of the reactivity ratios as well as joint confidence regions. Data related to

monomer conversion, copolymer composition (*F*) and co-monomer ratio (*f*) were fitted to the integrated form of the Mayo-Lewis copolymer composition equations (**2**):

$$\boldsymbol{C_{TOT} = 1 - \left(\frac{f_{CL}}{f_{CL,0}}\right)^{\alpha} \times \left(\frac{f_{LA}}{f_{LA,0}}\right)^{\beta} \times \left(\frac{f_{CL,0}-\delta}{f_{CL}-\delta}\right)^{\gamma}} \qquad (\mathbf{2})$$

$$\boldsymbol{\alpha = \frac{r_{LA}}{1-r_{LA}}, \quad \beta = \frac{r_{CL}}{1-r_{CL}}, \quad \gamma = \frac{1-r_{CL}\times r_{LA}}{(1-r_{CL})\times(1-r_{LA})}, \qquad \delta = \frac{1-r_{LA}}{2-r_{CL}-r_{LA}}}$$

The reactivity values determined with this method, r_{LA}= 1.80 and r_{CL} = 0.05, were eventually in good agreement with values determined from the linear method. Figure 4a shows the point estimates and the confidence regions associated to the VSSRS method applied. The 95% confidence intervals are narrow: r_{CL} (0.04 – 0.06) and r_{LA} (1.70 – 1.90).

It is worth mentioning that these reactivity ratios were determined without taking into account values of F_{CL} and f_{CL} obtained after 60% of conversion, because after this stage the gap between both reactivity ratios seemed to be reduced. This statement is supported by the fact that experimental data (Figure 4b,c, black dots: k) deviate from the theoretical plots of f_{CL} and F_{CL} as a function of the total conversion (C_{TOT}), modeled from the reactivity ratio values obtained by the VSSRS method (Figure 4b,c, red line). This phenomenon could be explained by the possible occurrence of side reactions, e.g. water initiation leading to carboxylic acids α-chain ends which may catalyze the RO*c*P reaction. Another explanation could be that there are some uncertainties in the NMR measurements at low conversions.

Values thus determined by the VSSRS method revealed that caproyl chain-end units are twenty times more reactive towards *L*-LA than towards CL. As for lactidyl chain-end units, they are found twice as reactive towards *L*-LA as towards CL. This explains why, at the first stage of the RO*c*P process (Table 3, Entries 2-3), *L*-LA monomers were consumed faster than CL. After 60% of conversion, *i.e*. in the second stage of the reaction, CL monomers were consumed faster than expected (Figure 4b,c) hence the gap between r_{CL} and r_{LA} is reduced. All these data support the formation of a gradient copolymer at the early stage of the RO*c*P process, a statistical copolymer being generated at the later stages (Scheme 6). Such a rearrangement of the microstructure also explains why $M_{n,SEC}$ does not evolve linearly with the *L*-LA and CL conversions.

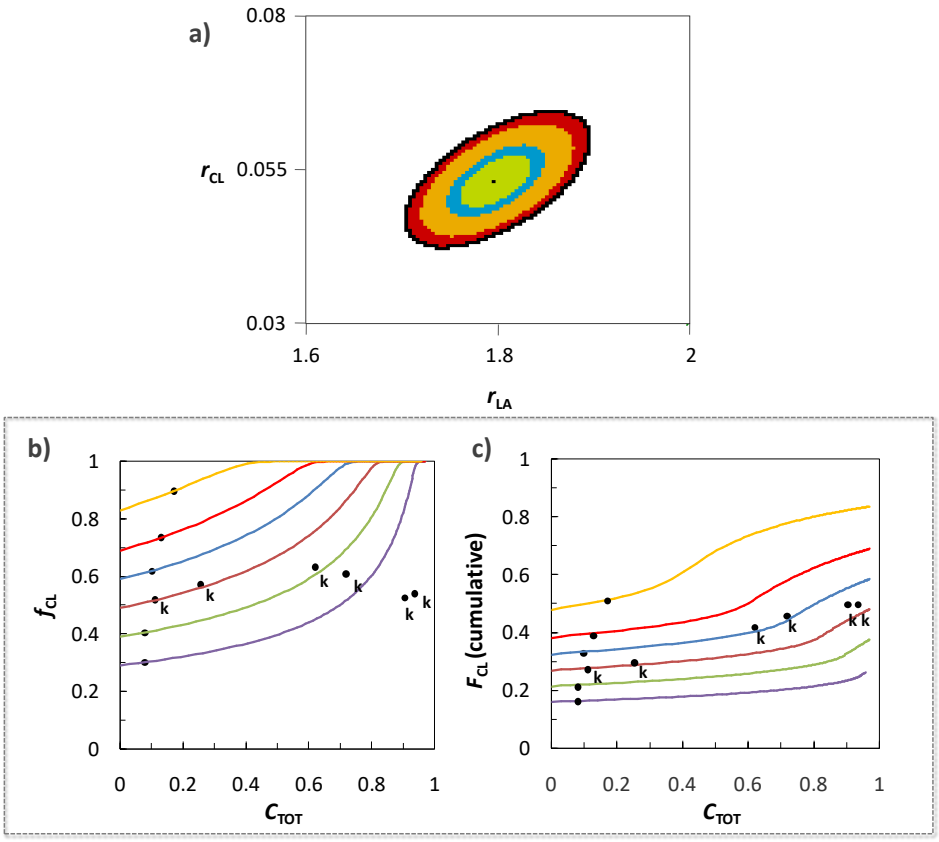

Figure 4. (a) 95% Joint confidence interval (JCI) for reactivity ratios with point estimate (r_{CL}= 0.05, r_{LA} = 1.80). Internal contours indicate 50% (green), 70% (yellow), and 90% (red) JCIs.(b) Prediction of the co-monomer ratio f_{CL} (solid lines) as a function of conversion *vs.* experimental points (black dots). (c) Prediction of the cumulative copolymer composition (solid lines) as a function of conversion versus experimental points (black dots). k: experimental datas of the DBM-ORO*c*P kinetic of an equimolar mixture of *L*-LA and CL (Table 3, Entries 2 to 6).

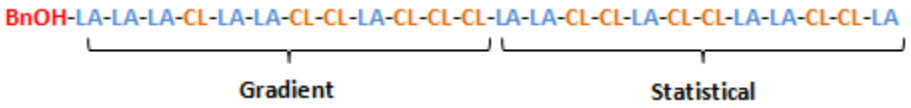

Scheme 6. Copolymer structure obtained during the DBM-ORO*c*P of *L*-LA and CL initiated by BnOH.

1.3 Copolymer structure

Since DBM was still present in the crude medium at the end of the RO*c*P reaction (Figure 1), copolymers were purified by precipitation in cold methanol. The ^{1}H NMR spectrum of a typical copolymer (Table 3, Entry 6) allowed us to determine an overall composition that was found in good agreement with that engaged in the co-monomer feed ratio (LA:CL = 49:51, Figure 5a & Figure S 5). While homo- and heterodiads were clearly identified by ^{1}H NMR spectroscopy,

the amount of CL-CL homosequences was estimated to be 1.7 times higher than CL-LA heterosequences (Figure 5a).

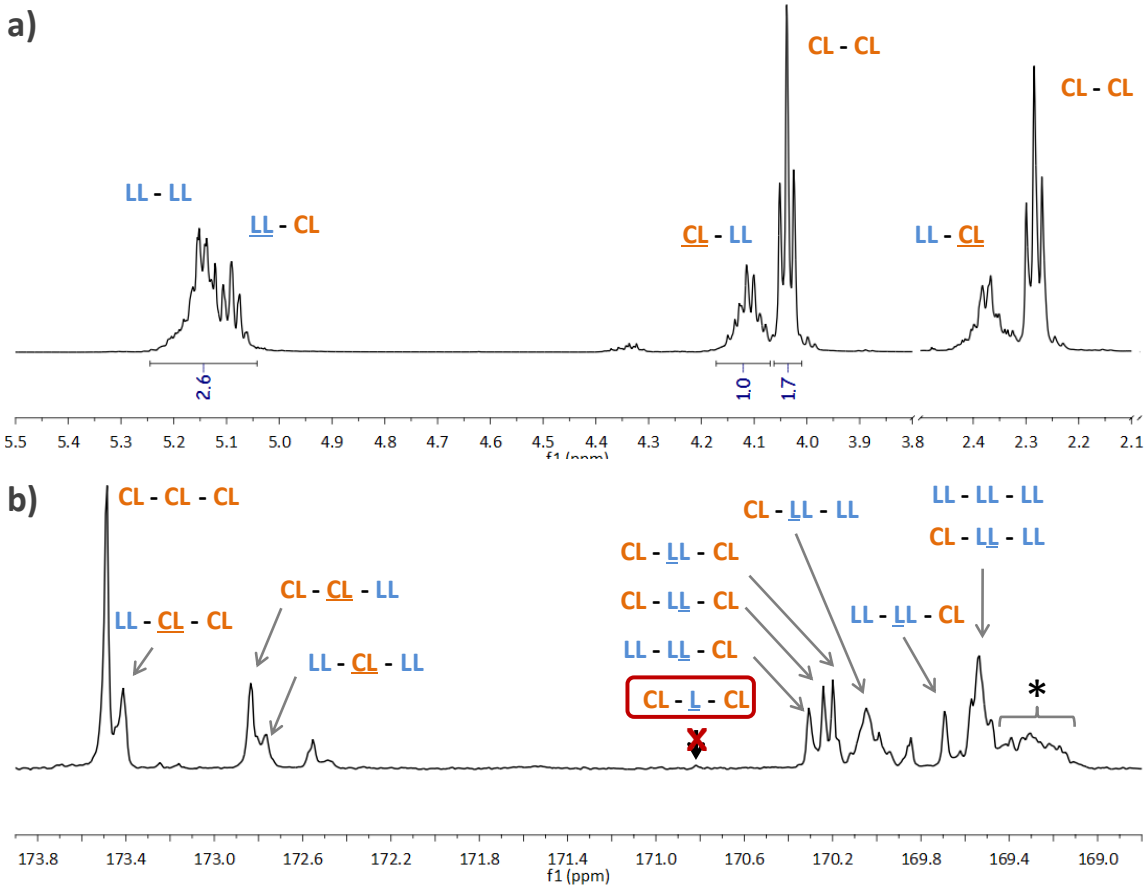

Figure 5. (a) ^{1}H ($CDCl_3$, 500 MHz, r.t.) and (b) ^{13}C NMR ($CDCl_3$, 100 MHz, r.t.) spectra of a P(LA-*co*-CL) copolymer (Table 3, Entry 6) [LL and L refer to lactidyl and lactoyl units, respectively], * stereoirregular LL-LL-LL,[27] ($CDCl_3$, 500 MHz, r.t.).

The microstructure of the copolymer was also assessed by ^{13}C NMR analysis (Figure 5b), attesting to the presence of all expected triads, as already reported in the literature.[28] As detailed by Kasperczyk and Bero, because *L*-LA is composed of two lactoyl units, two possible modes of transesterification reactions may happen during copolymerization involving LA as monomer (Figure 6).[29] Importantly, the second mode of transesterification, which gives rise to "anomalous" CL-L-CL sequences (L representing one lactoyl), was not observed within the limits of detection of NMR spectroscopy, as reflected by the absence of a peak at 170.8 ppm in the ^{13}C NMR analysis (Figure 5b). Thus, only the first mode of transesterification might have occured, which was mirrored by the slight increase of the dispersity during the copolymerization process (*Đ* from 1.3 to 1.48).

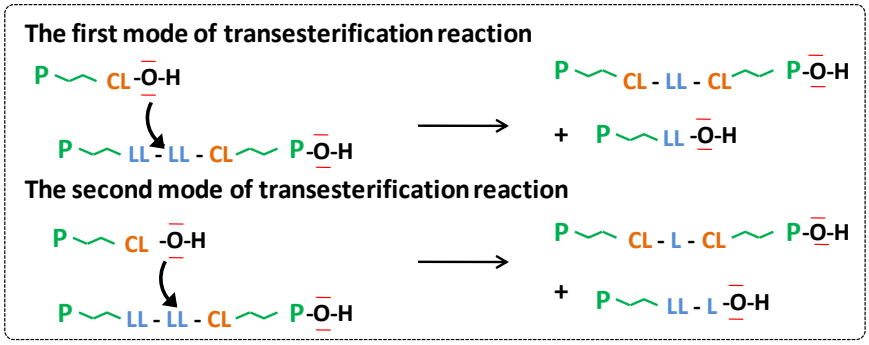

Figure 6. The two modes of transesterification reactions during *the* ROcP of *L*-LA and CL (L = lactoyl unit LL = one lactidyl unit).

Finally, and in agreement with previously reported results[27], thermal analysis carried out by differential scanning calorimetry (DSC) revealed a single glass transition temperature, T_g, at around -19 °C consistent with the formation of a gradient to statistical copolymer <<<(Figure S 6).

1.4 Copolymerization reactions initiated by butane-1,4-diol (BD) and poly(ethylene glycol) (PEG)

The BD-initiated DBM-ORO*c*P of *L*-LA and CL was also conducted in bulk at 155 °C under the following conditions $[L\text{-LA}]_0/[CL]_0/[DBM]_0/[BD]_0$= 15/15/1.5/1 (Table 3, Entry 9). The ^{1}H NMR spectrum of the pure P(LA-*co*-CL) thus initiated by BD showed the presence of both homo- and heterodiads (Figure 7) and enabled to calculate a $DP_{,exp}$ of 24.4. This latter value was slightly higher than $DP_{,th}$ of 18.1 (Figure 7). This discrepancy could be due to a slow or partial initiation. Note that the peak due to protons of BD methylene oxycarbonyl (k', Figure 7) is found to overlap with peaks due to protons of PCL (c'$_1$ and c'$_2$) in the NMR spectrum, impeding the determination of the degree of polymerization from the intensity of initiator.

The molar mass determined by ^{1}H NMR ($M_{n,NMR}$ = 3300 g.mol^{-1}) was found in good agreement to the one determined by MALDI-ToF analysis, *i.e.* 3127 g.mol^{-1} (Figure 8). This thus indicates that BD would be the main initiator during this ROcP process involving *L*-LA and CL, leading to telechelic α,ω- P(LA-*co*-CL) diols.

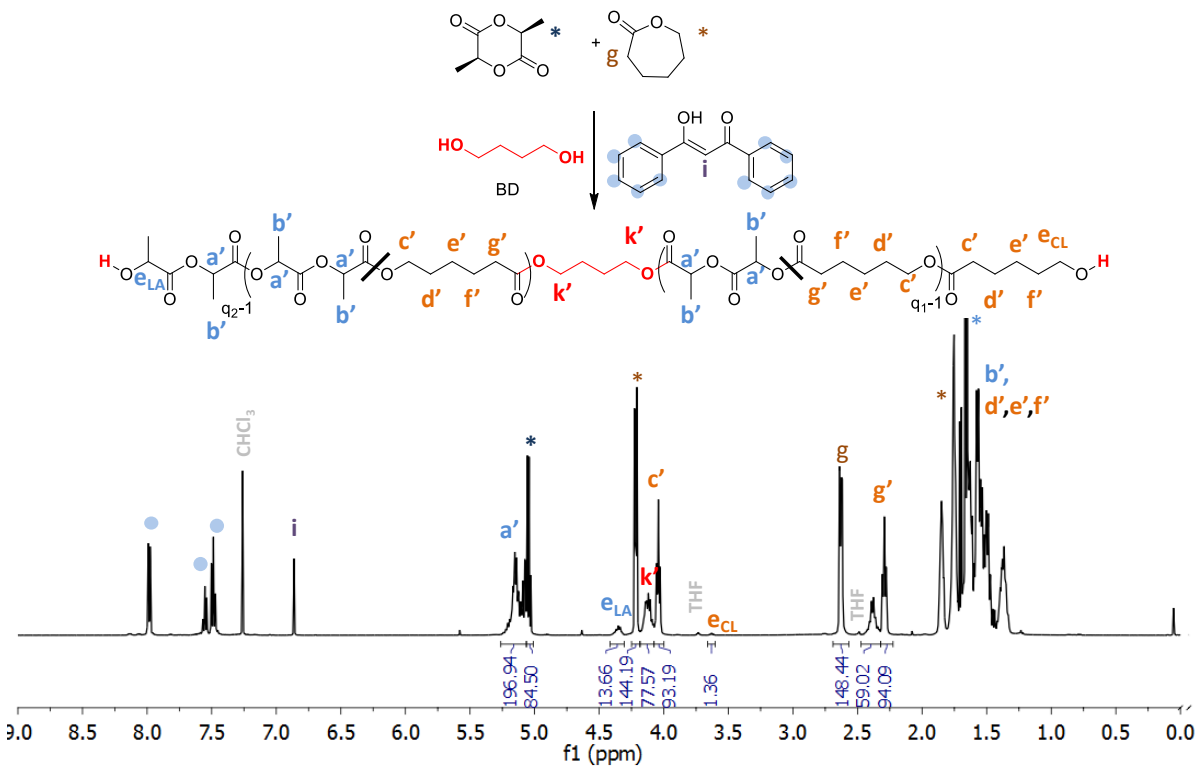

Figure 7. ^{1}H NMR spectrum of the crude copolymer initiated by BD (Table 3, Entry 9). ($CDCl_3$, 500MHz, r.t)

The MALDI-ToF MS spectrum of the pure P(LA-*co*-CL) initiated by BD (Table 3, Entry 9) exhibited a Gaussian-like distribution, as illustrated in Figure 8a. A difference of 30 mass units (u) is clearly visible and corresponds to the difference of mass between both *L*-LA (M_{LA}) and CL (M_{CL}) monomers (mass difference: M_{LA} - M_{CL} = 144 g.mol^{-1} – 114 g.mol^{-1} = 30 u). Three different populations cationized with sodium (Na^+) were found to be overlapped (Figure 8b):

A. Initiated by BD [*m/z* = 90 (M_{BD}) + n x 144 (M_{LA}) + m x 114 (M_{CL}) + 23 (M_{Na+})].

B. Initiated by water (H_2O) [m/z = 18 (M_{H20}) + n x 144 (M_{LA}) + p x 72 (M_{LA}/2) + m x (M_{CL}) + 23 (M_{Na+})].

C. Cyclics polymers [m/z =n x 144 (M_{LA}) + m x 114 (M_{CL}) + 23 (M_{Na+})]

With n the number of lactidyl units (LL), p the number of lactoyl units (L), which is the half of a lactidyl unit (LL) and m the number of CL units in the copolymer chain, M_{BD} and M_{H2O} the molar masses of BD and water initiators.

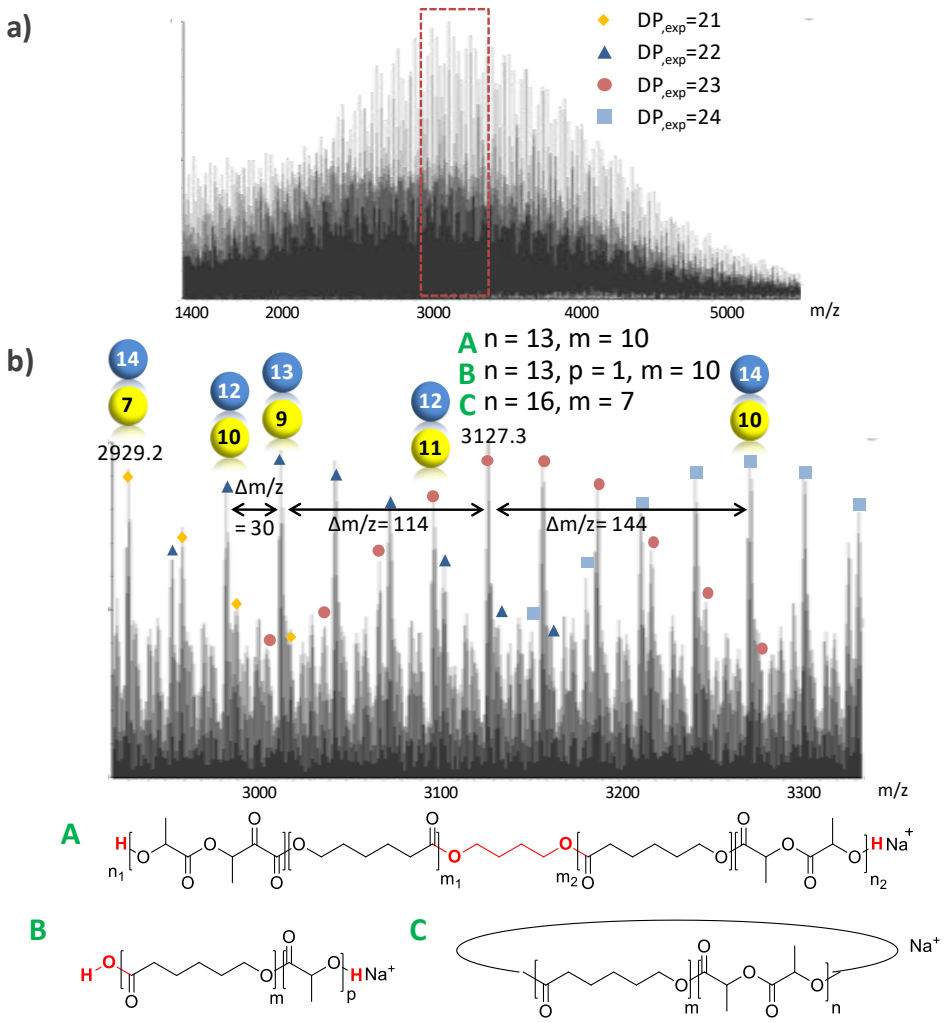

Figure 8. MALDI-ToF MS spectrum of pure P(LA-*co*-CL) initiated by BD (Table 3, Entry 9). *L*-LA =blue circles, CL = yellow circles with n and m values for population A. With M_{LA}=144.13 g.mol^{-1};M_{CL}=114.14 g.mol^{-1}; M_{LA}-M_{CL}=30 g.mol^{-1}.

Population **A** was the one expected and was the more likely to occur, as the ^{1}H NMR analysis revealed that the copolymer chains are principally initiated by BD. However, water initiation represented by population **B** could not be totally discarded; MALDI-ToF MS analysis did not enable to differentiate any of such signals. Similarly, inter- and intramolecular transesterifications represented by populations **B** and **C** respectively, cannot be ruled out.

On the MALDI-ToF spectrum, chains exhibiting the same degree of polymerization ($DP_{,exp}$) initiated from BD, for instance population $DP_{,exp}$ = 23 represented by red circles, depicts a Gaussian-like distribution (Figure 8b).

As compared to BD, initiating the ROcP of *L*-LA and CL with an oligoPEG induced an unexpected synergetic effect. Indeed, 90% of both comonomers were converted in only 38 hours of reaction under otherwise identical conditions $[L\text{-LA}]_0/[CL]_0/[DBM]_0/[PEG]_0$ = 15/15/1.5/1 at 155 °C (Table 3, Entry 10). The PEG effect on the ROcP kinetic might be explained as follows:

1) The presence of oxygen atoms throughout the PEG backbones which can act as H-bonding acceptors (Scheme 7).
2) Modification of the polarity of the reaction medium favoring solvation of the monomers.
3) Viscosity of the medium that evolves in the course of the reaction might improve the diffusion of small molecules.

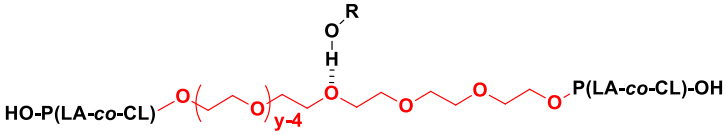

Scheme 7. Hydrogen bonding between the oxygen atoms of PEG_{1000} and the hydrogen of protic species.

Analysis of the corresponding ^1H spectrum confirmed the formation of a P(LA-*co*-CL)-*b*-PEG_{1000}-*b*-P(LA-*co*-CL) copolymer (Figure 9a) and displayed characteristic peaks of each repetitive units, in particular those due to methylene protons of PEG at 3.6 ppm. The latter signals, however, overlapped with peaks due to methylene hydroxy of the CL terminal unit (-CH_2-OH), preventing the calculation of the $DP_{,exp}$.

In order to account for the initiation from the PEG_{1000} macroinitiator, SEC traces were recorded in the course of ROcP process. The shift to lower elution volumes, *i.e*. to higher molar masses, of the resulting triblock copolymer confirmed the efficient chain extension from the PEG_{1000} precursor (Figure 9b). To further attest on the effective initiation from the PEG_{1000}, the amphiphilic nature of the as-obtained triblock copolymer ($M_{n,SEC}$ = 4100 g.mol^{-1}, F_{CL} = 51%, Table 3, Entry 10) was compared to a fully hydrophobic P(LA-*co*-CL) obtained from a benzyl alcohol initiator ($M_{n,SEC}$ = 3600 g.mol^{-1}, F_{CL} = 50%, Table 3, Entry 6). For this purpose, 20 mg of both the latter hydrophobic copolymer and amphiphilic copolymer were introduced in 2 mL of dionized water. After 10 min of an ultrasonication, the unsolubilized hydrophobic copolymer initiated by BnOH collapsed (Figure 9c, vial A), while the P(LA-*co*-CL) obtained from the PEG_{1000} hydrophilic block was dispersed in water owing to its amphiphilic nature (Figure 9c, vial B).

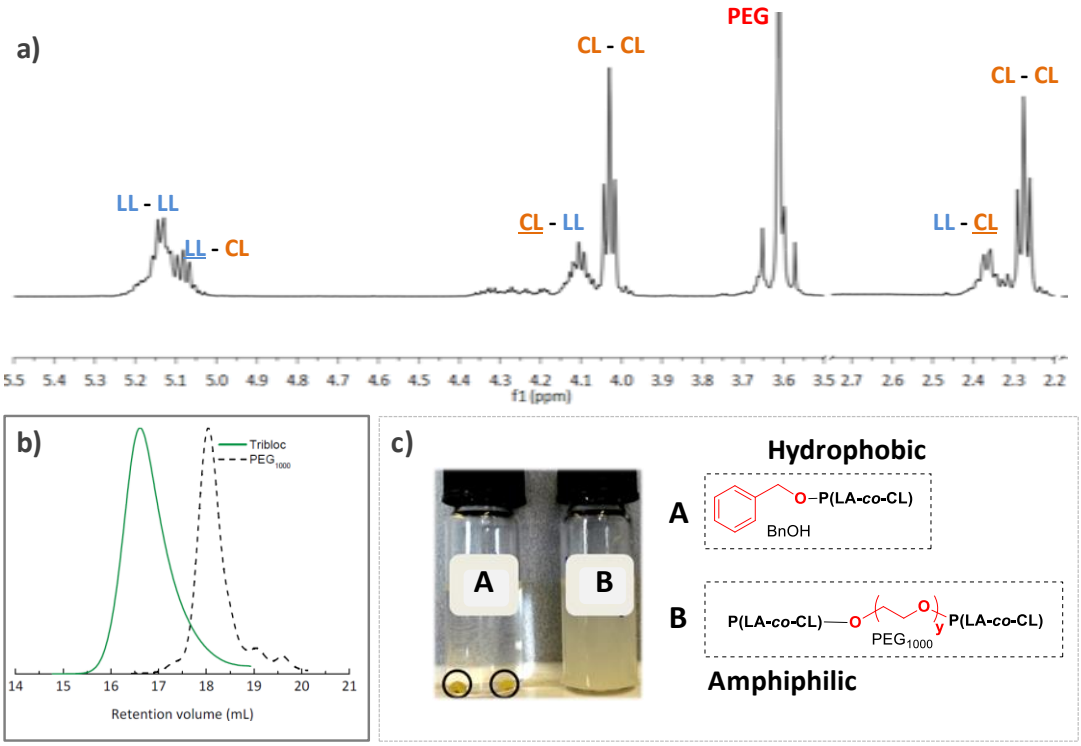

Figure 9. (a) ^{1}H NMR spectrum ($CDCl_3$, r.t, 500 MHz), (b) SEC traces (THF/NEt_3 (2w%) as eluent, 308K) of the PEG(-*b*-P(LA-*co*-CL))$_2$ triblock copolymer obtained from a PEG_{1000} (Table 3, Entry 10). (c) Picture of P(LA-*co*-CL) initiated from (**A**) BnOH (Table 3, Entry 6) and (**B**) PEG_{1000} (Table 3, Entry 10) in deionized water (10 mg.mL^{-1}) after 10 min of ultrasonication.

In conclusion DBM was demonstrated to efficiently trigger the bulk ORO*c*P of *L*-LA and CL at 155 °C in the presence of alcohol-type initiators affording copolymer evolving from a gradient to a statistical microstructure.

2 DBM organocatalyzed ring-opening polymerization (OROP) of *L*-LA and CL

To gain more insight into these DBM-ORO*c*P reactions, the DBM-organocatalyzed ring-opening polymerization (DBM-OROP) of each of the two monomers, *L*-LA and CL, were investigated using BnOH initiator under the same experimental conditions.

2.1 Case of *L*-LA

The DBM-OROP of *L*-LA initiated by BnOH was carried out in bulk at 155 °C for a [*L*-LA]$_0$/[DBM]$_0$/[BnOH]$_0$ initial ratio of 30/1.5/1 (Scheme 8). The results are summarized in Table 4 (Entries 1 to 4).

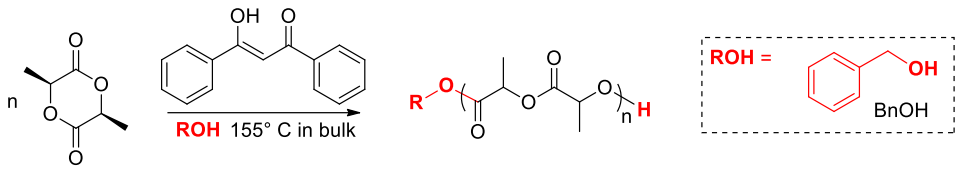

Scheme 8. DBM-OROP of *L*-LA initiated by BnOH.

Table 4. Results and conditions of DBM-OROP of *L*-LA in bulk and in solution.[a]

Entry	Solvent[b]	Temp (°C)	Time (h)	C_{LA}[c] (%)	$M_{n,SEC}$[d] (g.mol^{-1})	$M_{p,SEC}$[d] (g.mol^{-1})	$DP_{,th}$[e]	$DP_{,exp}$[f]	$Đ^d$
1	no	155	29	28	870	950	8.5	5.3	1.25
2	no	155	48	53	1300	1780	16.0	8.7	1.47
3	no	155	81	91	1700	2940	27.4	13.1	1.73
4	no	155	96	96	1800	3190	28.8	13.8	1.88
5[g]	THF	35	96	0	-	-	-	-	-
6[g]	DCM	35	96	0	-	-	-	-	-
7[g]	Toluene	90	96	0	-	-	-	-	-

[a]Reactions were performed under nitrogen atmosphere with reaction conditions: m_{LA}= 300 mg $[M]_0/[I]_0$ = 30 and with a DBM loading of 5mol% *vs* monomer; [b]If a solvent is used for the DBM-OROP of *L*-LA, $[LA]_0$ is equal to 0.9 or 4 M; [c]LA conversions determined by ^{1}H NMR analysis; [d]Uncorrected number average molar mass ($M_{n,SEC}$), molar mass at the peak ($M_{p,SEC}$) and dispersity ($Đ$) of crude polymers as determined by SEC chromatography (polystyrene standards) at 308 K and THF/NEt_3 (2w%) as eluent; [e]Theoretical degree of polymerization $\boldsymbol{DP_{,th} = [LA]_0/[I]_0 \times C_{LA}}$; [f]Experimental degree of polymerization calculated from PLA *ω*-chain ends as determined by ^{1}H NMR.

The DBM-OROP of *L*-LA reached almost full conversion (C_{LA} = 96%) after 96 hours (Table 4, Entry 4). The ^{1}H NMR spectrum of the crude PLA initiated by BnOH in presence of DBM enabled to determinate the values of the degree of polymerization from the ω-chain ends ($\omega_{LA,}$ Figure 10). At the early stage of the polymerization, a discrepancy between the $DP_{,exp}$ and $DP_{,th}$ was noticed (Table 4, Entries 1 to 4), which might be due to a side co-initiation by adventitious water.

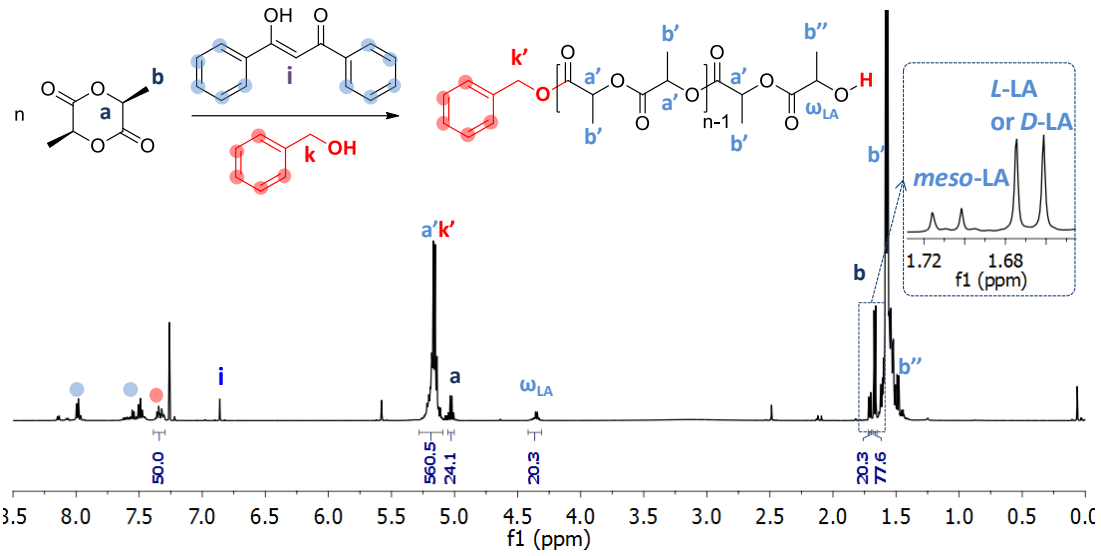

Figure 10. ^{1}H NMR spectrum of the crude PLA initiated by BnOH- Table 4, Entry 4 -($CDCl_3$, 500MHz, r.t).

In addition, plot of $M_{n,SEC}$ as a function of C_{LA} did not evolve linearly and dispersity values were found to increase throughout the ROP process reaching 1.88 at the end of the reaction (Figure 11a&b). One can thus conclude that the OROP of *L*-LA is not controlled in presence of DBM as activator.

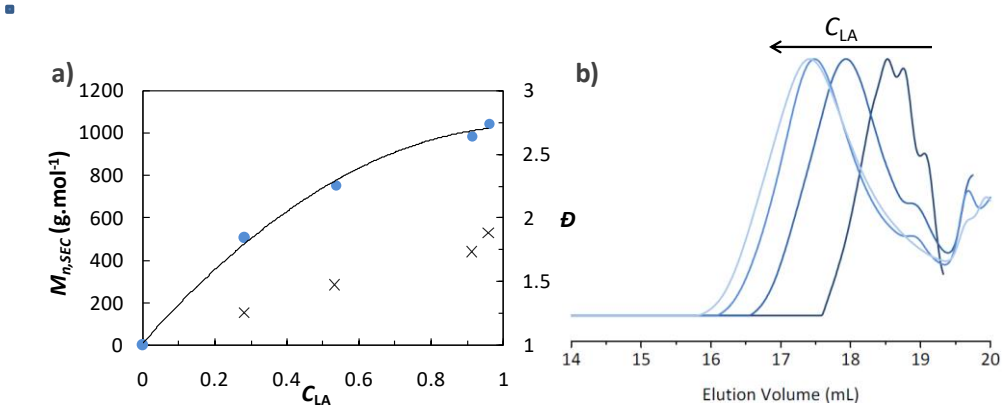

Figure 11. (a) Evolution of the uncorrected $M_{n,SEC}$ (●)and $Đ$ (x) with LA conversion for the DBM-OROP of *L*-LA initiated by BnOH in bulk at 155°C. (b) SEC traces of crude PLAs recorded in THF/NEt_3 (2 w%) as eluent, 308K.(Table 4, Entries 1 to 4).

A close look at the ^{1}H NMR spectrum of a PLA (Table 4, Entry 4), revealed the presence of *meso*-lactide (*meso*-LA, (**2**), Scheme 9, Figure 10) as indicated by the signal observed at 1.72 ppm.[30] Formation of *meso*-LA can be explained by the occurrence of epimerization of *L*-LA (**1**) in presence of DBM at 155 °C. As discussed in the previous chapter, this side reaction causes damage to the thermal and mechanical properties of the PLLA. Epimerization generally occurs in presence of basic-type organocatalysts (*cf*. Chapter 1, section 1.5). It was yet not expected to

occur here, *i.e.* in presence of our acidic-type organocatalyst. For instance, OROP of *L*-LA in bulk triggered by diphenylphosphate leads to a highly isotactic PLLA. [31] In our case, one can hypothesize that DBM may be able to deprotonate the proton in alpha position of the carbonyl moiety. This epimerization side reaction was not investigated further here, but a more detailed study will be presented in the following chapter regarding the use of benzoic acid as organocatalyst.

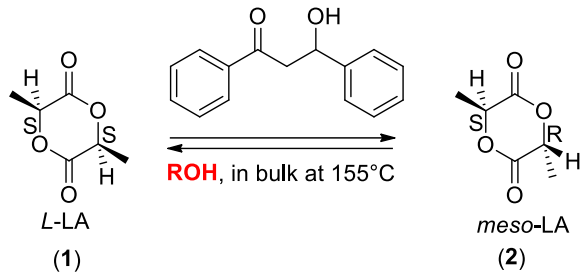

Scheme 9. Epimerization of *L*-LA in *meso*-LA in the presence of DBM.

Finally, attempts to initiate the DBM-OROP of *L*-LA monomer in solution failed (Table 4, Entries 5-7) whatever the solvent used (THF, DCM and toluene), the temperature of the reaction (35 or 90 °C) and the relative concentration in monomer (0.9 and 4 M). These results are eventually not surprising as dibenzoylmethane can be viewed as a less acidic specie (pKa ≈ 8.7)[32] than carboxylic acids (pKa ≈ 4) used in ROP requiring high temperatures to be active. [33,34,35,36,37]

To conclude, dibenzoylemethane was found to be non-active for the OROP of *L*-LA in mild conditions. Even at 155 °C in bulk, DBM was shown to be poorly active and did not allowed to control the ROP of *L*-LA.

2.2 Case of CL

The DBM-OROP of CL was similarly initiated using BnOH in bulk at 155 °C, for a $[CL]_0/[DBM]_0/[BnOH]_0$ initial ratio of 30/1.5/1 (Scheme 10). The results are summarized in Table 5 (Entries 1 to 5).

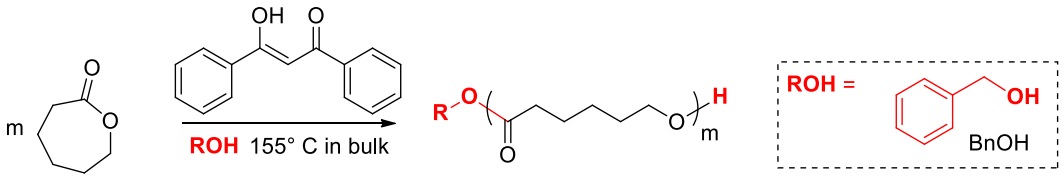

Scheme 10. DBM-OROP of CL initiated by BnOH.

Table 5. Results and conditions of the DBM-OROP of CL in bulk and in solution.[a]

Entry	Solvent[b]	Temp (°C)	Time (h)	C_{CL}[c] (%)	$M_{n,SEC}$[d] (g.mol-1)	$M_{p,sec}$[d] (g.mol-1)	Đ[d]	$DP_{,th}$[e]	$DP_{,exp}$[f]
1	no	155	39	13	905	1050	1.24	3.9	3.9
2	no	155	40.5	44	1977	2330	1.2	13	10.6
3	no	155	42	64	2715	3190	1.22	19.3	16.3
4	no	155	43	78	3295	3750	1.21	23.3	18.5
5	no	155	44	98	4475	5520	1.53	29.5	25
6	THF	35	96	0	-	-	-	-	-
7	DCM	35	96	0	-	-	-	-	-

[a]Reactions were performed under nitrogen atmosphere with reaction conditions: m_{CL}= 300 mg $[M]_0/[I]_0$ = 30 and with a DBM loading of 5mol% *rel. to the* monomer; [b]If a solvent is used for the DBM-OROP of CL, the initial concentration of CL ($[CL]_0$) is equal to 0.9 or 4 M; [c]CL conversions determined by ^{1}H NMR analysis; [d]Uncorrected number average molar mass ($M_{n,SEC}$) and dispersity (*Đ*) of crude polymers as determined by SEC chromatography (polystyrene standards) at 308 K and THF as eluent; [e]Theoretical degree of polymerization $\boldsymbol{DP_{,th} = [CL]_0/[I]_0 \times C_{CL}}$; [f]Experimental degree of polymerization calculated from PCL ω-chain ends as determined by ^{1}H NMR.

The DBM-OROP of CL at 155 °C did showed an induction period as the reaction started after 39 hours (Table 5, Entry 1). Interestingly, only 5 hours were needed to reach completion of the polymerization. ^{1}H NMR analyses revealed that, from the early stage of the ROP process, 99% of BnOH initiated the ROP of CL. This was established through the disappearance of the BnOH methylene protons (k, Figure 12) at 4.68 ppm, and the concomitant appearance of the methylene oxycarbonyl protons at 5.2 ppm (Ph-C**H$_2$**-OC(O), k'). $DP_{,exp}$ values were found in good agreement with $DP_{,th}$ at the beginning of the process (Table 5, Entry 1, Figure 12). At 98% conversion, however, the $DP_{,exp}$ of 25 was barely lower than the theoretical one ($DP_{,th}$ = 29.5) likely due to some extent of co-initiation by water (Table 5, Entry 5). As the water co-initiation led to the formation of a carboxyl group at the α-chain end of the PCL (Scheme 11), the peak characteristic of methylene protons of the CL unit (**α_{CL}**) at 2.36 ppm could be observed in the ^{1}H NMR spectrum (Figure 12 & Figure S 8).

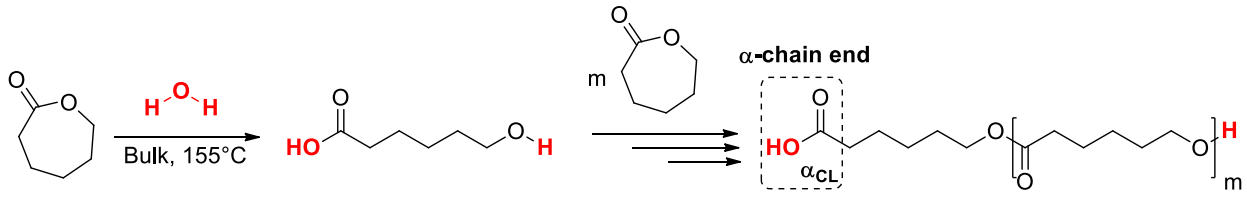

Scheme 11. Carboxyl group generated during the DBM-OROP of CL initiated by water.

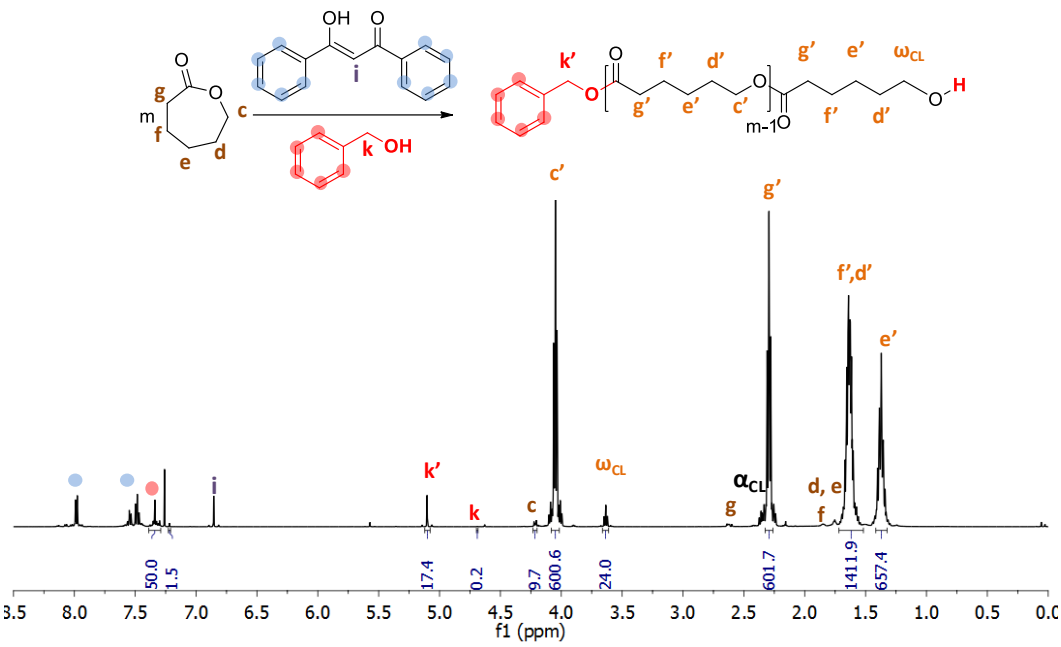

Figure 12. ^{1}H NMR spectrum of the crude PCL initiated by BnOH- Table 5, Entry 5 -($CDCl_3$, 500MHz, r.t).

Nevertheless, the linear evolution of the molar mass with CL conversion (C_{CL}) and the relatively narrow dispersities obtained (< 1.55) attested that DBM enables a rather good level of control of the OROP of CL (Figure 13a & b).

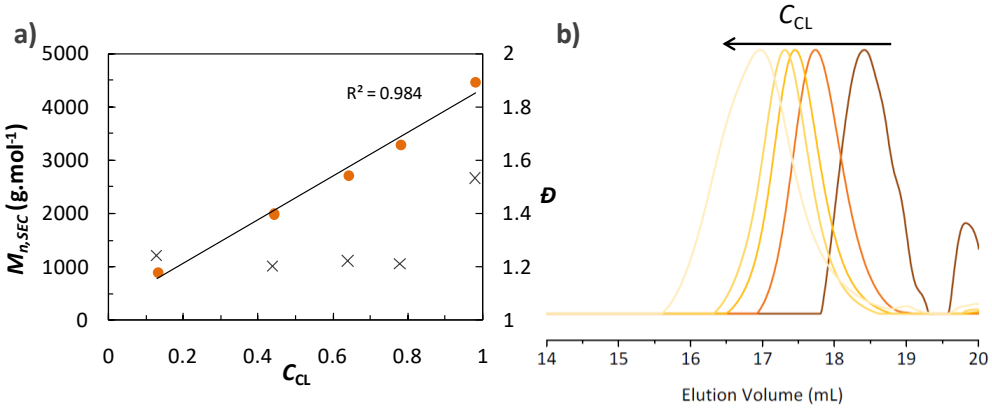

Figure 13. (a) Evolution of the uncorrected $M_{n,SEC}$ (●)and $Đ$ (x) with CL conversion for the crude PCLs synthesized using DBM in bulk at 155°C (Entries 1 to 5).(b) SEC traces of crude copolymers (Entries 1 to 5, Table 5).

Similarly to the case of *L*-LA discussed above, the potential for DBM to activate the ROP of CL in mild conditions was also evaluated by performing reaction in solution. The ROPs of CL were conducted in THF and DCM solvent at 35 °C in the presence of 5mol% catalyst rel. to the

monomer, and with a monomer concentration of 0.9 and 4 M (Table 5, Entries 6 & 7). However, no polymerization took place after 96 hours of reaction.

DBM organocatalyst is therefore not effective enough to trigger the ROP of CL in solution. In contrast, ROP of CL could be trigger in bulk at 155°C but only after a rather long induction period (39h). Overall, DBM is thus not a very performing catalyst for metal-free PCL synthesis.

3 Investigation into the kinetics and related mechanisms

To get some insight into the reaction mechanism, kinetic analyses were studied. For this purpose, the semi-logarithmic kinetic plots of the DBM-ORO(*c)*P of *L*-LA and CL are presented in Figure 14.

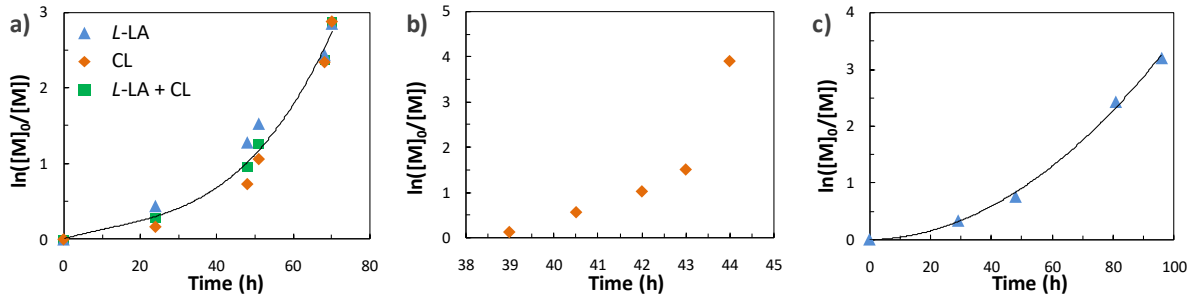

Figure 14. Semi-logarithmic kinetic plots of (a) the RO*c*P of *L*-LA and CL (Table 3, Entries 2 to 6); (b) the ROP of CL (Table 5, Entries 1 to 5) and (c) the ROP of *L*-LA (Table 4, Entries 1 to 4) initiated by BnOH in the presence of DBM in bulk at 155°C for a targeted degree of polymerization of 30.

These plots show upward curvatures for both ROP reactions as well as for the RO*c*P of *L*-LA and CL (Figure 14). Such a deviation from a pseudo-first order dependence on monomer has already been observed by Kubisa and Baśko for the TfOH-OROP of CL.[5] The authors have stated that the rate of polymerization is not related to the monomer concentration ($[M]_t$), but to the protonated monomer concentration ($[MH^+]_t$). They have also claimed that, when the basicity of the monomer carbonyl is higher than that of the polymer carbonyl, that is, in the case of the ROP of CL, the ratio $[MH^+]_t/[M]_t$ should increase during the course of the polymerization. This leads to an acceleration of the polymerization. However, in the case of *L*-LA ROP, the basicity of both carbonyl moieties should be similar, hence a pseudo-first order kinetic is expected. Besides the lack of information in the literature on the basicity of the carbonyl groups of *L*-LA and CL and of their corresponding polymer units, this statement is founded on the assumption that acidic OROP proceeds *via* an activated monomer mechanism (AMM) only. The authors have thus neglected the effect of the counter ion arising from the catalyst. Later on, Martin-Vaca,

Bourissou and Maron *et al.*[38] have shown, by density functional theory (DFT) calculations, that sulfonic acids eventually behave as bifunctional activators, *i.e.* acting as proton shuttles both *via* their acidic hydrogen and their basic oxygen atoms (see Scheme 25 in section 3.1 in the bibliographic chapter). Analogously, DBM could also act as a bifunctional organocatalyst, thanks to the aforementioned non-chelated enol form and the diketone form (Scheme 12).

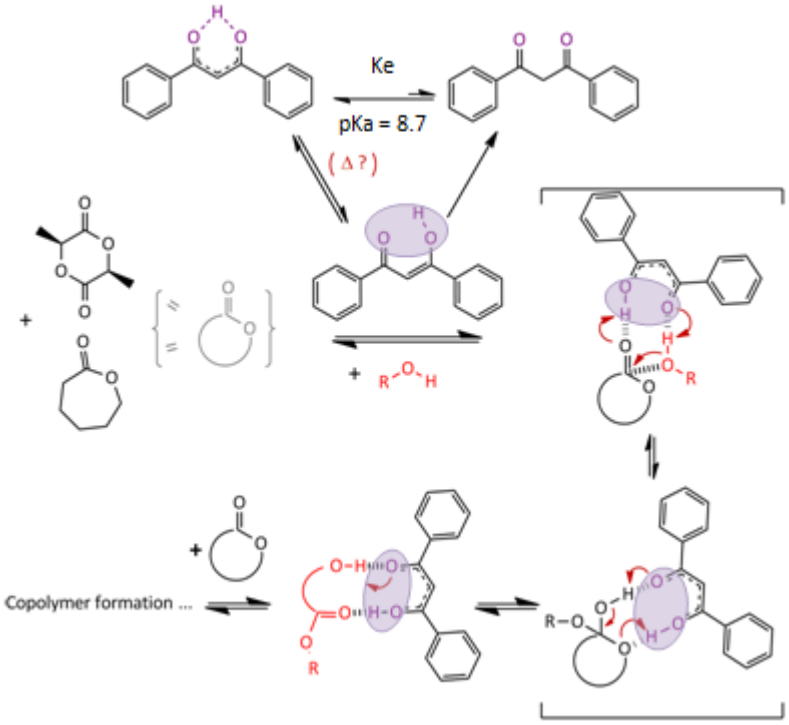

Scheme 12. Possible mechanism involved during the DBM-ORO*(c)*P of *L*-LA and CL.

Model experiments consisting in mixing equimolar amounts of DBM and CL were thus analysed at r.t (Figure 15) and at 55 °C by ^{13}C NMR in $CDCl_3$. No shift of the carbonyl carbon atom of both CL and DBM was observed, meaning that no interactions have been developed between the reaction partners in these conditions. It is worth reminding that, in chloroform, the equilibrium constant (K_e= [CEF]/[KF]) is equal to 24, meaning that the chelated enol form, which is inert toward its environment, is predominant. Therefore, no conclusions can be drawn from these NMR analyses as very different reaction polymerization conditions were used. However, considering kinetic of the ROP of CL performed in bulk at 155 °C, one can assume that even if the non-chelated enol form was generated at high temperature, DBM poorly interacts with the carbonyl group of CL. Indeed, the ROP of CL is known to be efficiently conducted in presence of a monomer activator, such as a weak carboxylic acid.[33,36,35,34,39] One can thus hypothesize that DBM is not a good monomer activator.

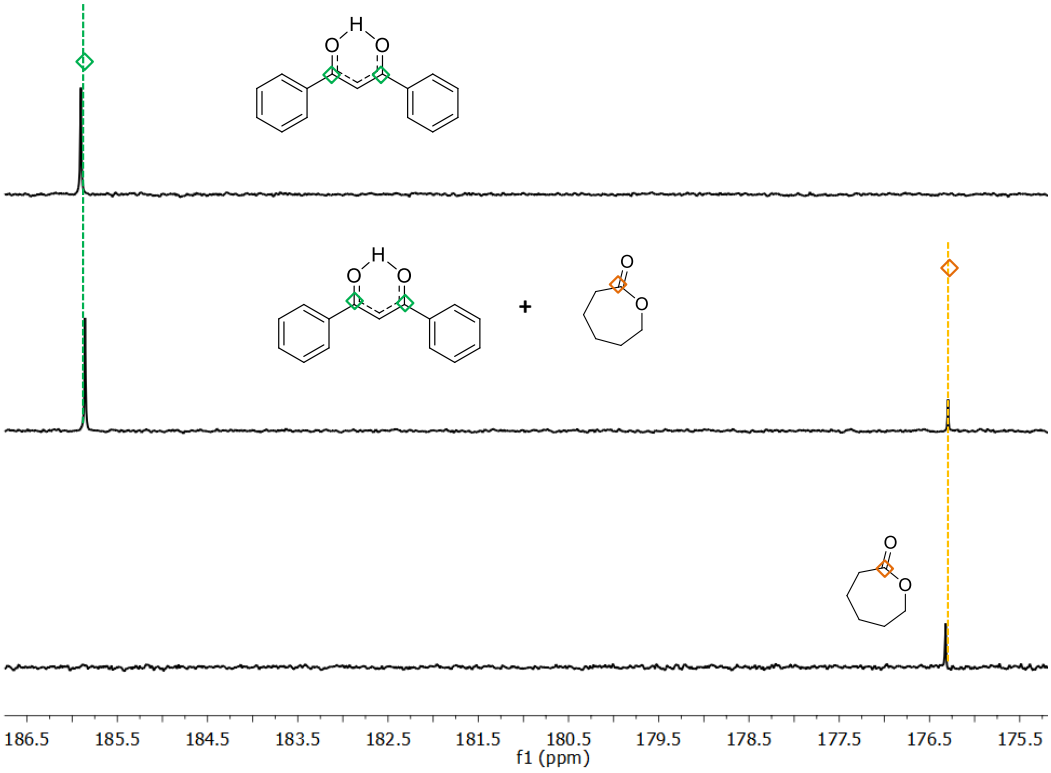

Figure 15. ^{13}C NMR spectra of the carbonyl region of DBM, DBM/CL (1/1) and CL ($CDCl_3$, 100MHz, r.t).

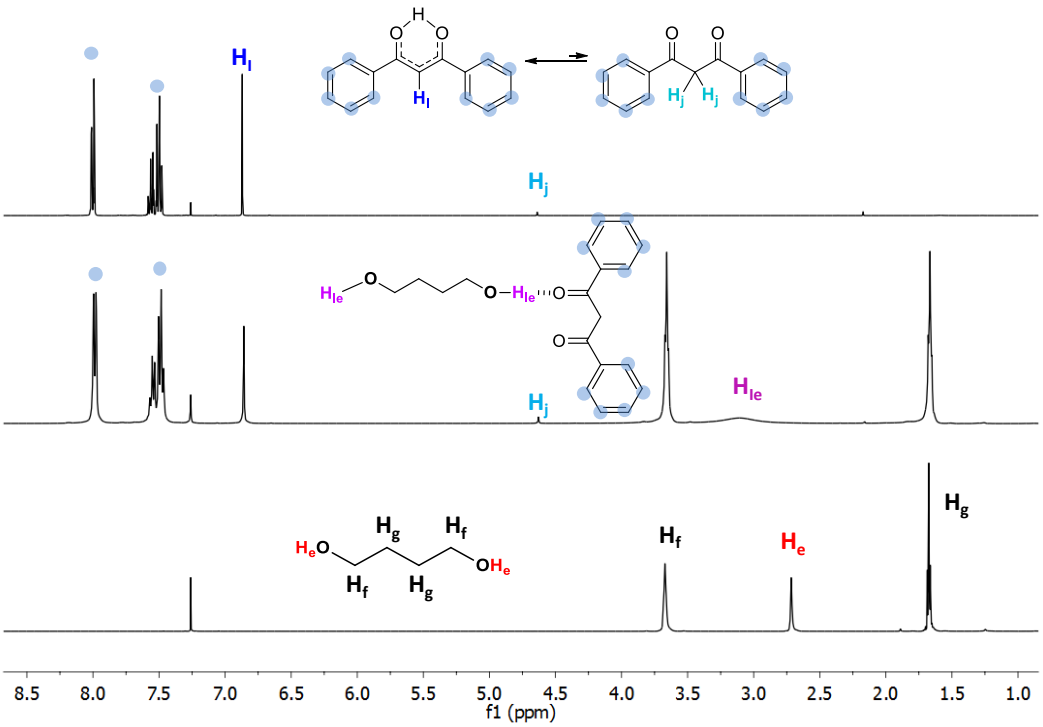

Figure 16. ^{1}H NMR spectra of DBM, DBM + BD 1/1 and BD ($CDCl_3$, 500MHz, r.t).

Model reactions consisting in mixing equimolar amount of DBM and BD were yet analyzed by ^{1}H NMR at r.t in $CDCl_3$ (Figure 16). A downfield shift of the signal due to the BD hydroxyl group (**H_e to H_{ei}**) can be noted. This would indicate that DBM could activate the propagating alcohol at the chain ends. However, the ROP of *L*-LA being very sluggish, DBM is certainly a poor chain end activator.

Finally, the apparent acceleration of the kinetic may be ascribed to the increase of the concentration in active species, [-OH] = [I], due to *co*-initiation by water, the polymerization kinetic rate (v_p) being expressed as the propagation kinetic rate from the following equation (**3**):

$$v_p = -\frac{d[M]}{dt} = k_p \times [M]^{\alpha} \times [I]^{\beta} \times [DBM]^{\gamma} \quad (\mathbf{3})$$

With [M] the concentration in monomer, t the reaction time, k_p the polymerization rate constant, [DBM] the concentration of catalyst and α, β, γ the kinetic partial orders.

Another explanation could be an self-catalysis of the DBM-ORO(*c*)P of *L*-LA and CL initiated by BnOH. Indeed, water initiation leads to carboxyl moiety at the α-chain end of the (*co*)polymers, which may be able to further catalyze polymerization reactions. The concentration of carboxylic acids [αCOOH] produced at the α-chain ends may be equal to the concentration of water that initiated the copolymerization and should be expressed by equation (**4**):

$$[\boldsymbol{\alpha COOH}] = [\mathbf{Water}] = \frac{[\mathbf{M}]_0 \times \mathbf{C_{TOT}}}{\mathbf{DP_{exp}}} - [\boldsymbol{BnOH}] \quad (\mathbf{4})$$

We could thus determinate [αCOOH] in the medium when the reaction time reached 48h (Table 3, Entry 3). Value of [αCOOH] ($9.7 * 10^{-2}$ mM) was estimated to be around 28% of the total concentration of catalyst ($[DBM]_0 = 3.44 \times 10^{-1}$ mM), which cannot be neglected as this part could also catalyze the reaction.

To conclude, DBM proved a rather poor initiator/chain end activator. Its capability to interact/activate the carbonyl group of the monomer could not be established by NMR analyses. The apparent increase of the kinetic of the DBM-ORO(*c*)P of *L*-LA and CL may thus be due to side reactions, in particular to water initiation by increasing the concentration of active species and the concentration of carboxylic groups in the medium. Consequently, the DBM-ORO(*c*)P of *L*-LA and CL may be viewed as a self-catalyzed reactions.

4 First attempts to copolymerize *L*-LA and CL using carboxylic acid-containing organocatalysts

4.1 Carboxylic acids

From the previous observations, we reasoned that the bulk statistical ROcP of *L*-LA and CL could be catalyzed by carboxylic acids as minute amount of such species might form *in situ* from DBM. The ROcP of *L*-LA and CL was thus conducted in bulk at 155 °C using benzoic acid (BA), simply because the structure of BA (Scheme 13) is similar to that of DBM, BA being also produced from the thermal degradation of DBM (*cf.* Figure S 9, Scheme S 1). The results are summarized in Table 6.

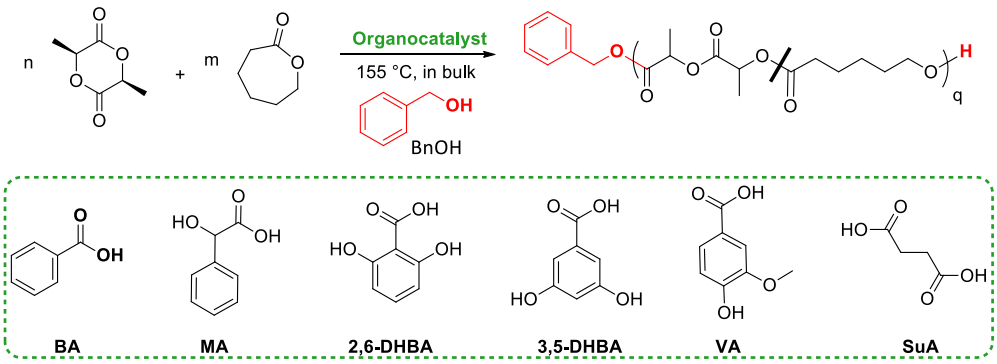

Scheme 13. Carboxylic acids-OROcP of *L*-LA and CL in bulk at 155°C.

In presence of BnOH as initiator, BA was found to incorporate both monomers in a simultaneous manner using the following conditions: $[CL]_0/[L\text{-}LA]_0/[BA]_0/[BnOH]_0$ = 25/25/2.5/1 at 155°C in bulk. After 24 hours, both monomer conversions reached approximatively 68-69%, with copolymers displaying quite a narrow dispersity for bulk reaction ($Đ \approx 1.36$), demonstrating the potential of BA as organocatalyst.

Use of other carboxylic acids, including maleic acid (MA), 2,6-dihydroxybenzoic acid (2,6-DHBA), 3,5-dihydroxybenzoic acid (3,5-DHBA), vanillic acid (VA) or succinic acid (SuA), was also attempted in the same conditions. However, all of them either incorporated *L*-LA (3,5-DHBA and VA) or CL preferentially (2,6-DHBA, SuA) in the copolymer chain. In other words, no statistical copolymers can be expected from all those catalysts. In addition, much higher dispersities ($1.31 < Đ < 1.81$) were noted mirroring a higher amount of intermolecular transesterifications. The copolymer obtained from the MA-ROcP of *L*-LA and CL initiated by BnOH was not analyzed by ^{1}H NMR because of its low molar mass ($M_{n,SEC} < 1790$ g.mol^{-1}) and its high dispersity (up to 2.02, Table 6, Entry 3). This significant loss of control may be due to the co-initiation of the copolymer chains from the secondary alcohol of MA (Scheme 13).

Table 6. Results and conditions of the bulk ROcP of *L*-LA and CL at 155°C.[a]

Entry	Cat[b]	Time (h)	C_{CL}/C_{LA}[c] (%/%)	$M_{n,SEC}$[d] (g.mol^{-1})	$M_{p,SEC}$[d] (g.mol^{-1})	$Đ^{d}$	$DP_{,th}$[e]	$DP_{,exp}$[f]
1	BA	24	68/69	3570	5070	1.36	34.3	18.2
2	MA	4	n.d/n.d	1100	1690	1.57	n.d	n.d
3	MA	24	n.d/n.d	1790	3390	2.02	n.d	n.d
4	2,6-DHBA	4	86/22	4040	5930	1.53	27	19.3
5	2,6-DHBA	24	90/59	3550	6280	1.69	38.2	16.3
6	3,5-DHBA	4	10/36	1090	1460	1.31	11.5	5.9
7	3,5-DHBA	24	95/98	3720	6130	1.81	48.2	22.5
8	VA	4	7/79	1040	1410	1.41	6.7	3
9	VA	24	19/96	4900	7440	1.55	43.8	25.07
10	SuA	4	n.d/n.d	890	n.a	1.36	n.d	n.d
11	SuA	24	89/79	2260	3360	1.52	42.1	24.1

[a]All reactions were carried out in bulk under nitrogen atmosphere at 155°C with reaction conditions: $n_{CL}= n_{LA} = 1.4$ mmol with BnOH as initiator: $[M]_0/[I]_0= 50$; [b]Organocatalyst used; [c]CL and *L*-LA conversions determined by ^{1}H NMR analysis; [d] Uncorrected average molar mass ($M_{n,SEC}$), molar mass at the peak ($M_{p,SEC}$) and dispersity ($Đ$) of crude copolymers determined by SEC chromatography (Polystyrene standards), THF/NEt_3(2w%) as eluent; [e]Theoretical degree of polymerization $\boldsymbol{DP_{,th}} = \frac{[\boldsymbol{LA}]_0}{[\boldsymbol{I}]_0} \times \boldsymbol{C_{LA}} + \frac{[\boldsymbol{CL}]_0}{[\boldsymbol{I}]_0} \times \boldsymbol{C_{CL}}$; [f]Degree of polymerization calculated from the chain ends determined by ^{1}H NMR; n.d= not determined.

Whatever the catalyst used, copolymers displayed a discordance between the $DP_{,exp}$ and the $DP_{,th}$. This could be attributed to co-initiation by water and to the fact that the copolymers were not purified. In the case of hydroxybenzoic acids, water might arise from dehydration of the hydroxyl groups, as such compounds have been showed to be poorly thermostable.[40] In the following chapters, the reactions will be carried out in Schlenks under argon atmosphere and the reagents will be drastically dried in order to prevent co-initiation by water.

Finally, the copolymer obtained using VA catalyst was found to be brown, while that obtained from MA was yellowish (Figure 17). By using SuA, the copolymer was totally transparent.

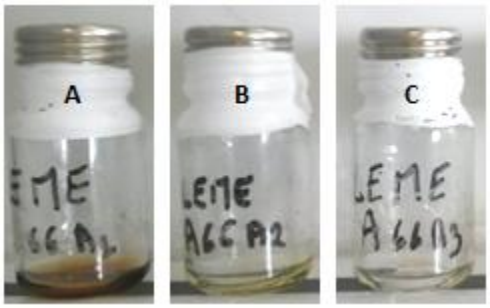

Figure 17. Pictures of the copolymers obtained using (A) VA, (B) MA and (C) SuA organocatalysts.

4.2 Amino-acids

In order to speed up the reaction, amino acids such as *D,L*-aspartic acid (AA) and picolinic acid (PA) were exploited as organocatalysts for the bulk RO*c*P of *L*-LA and CL at 155°C (Scheme 14). The results are summarized in Table 7.

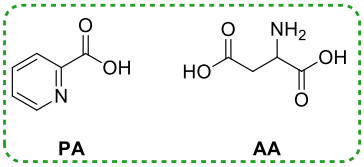

Scheme 14. Amino acids tested for the ORO*c*P of *L*-LA and CL in bulk at 155°C.

Amino acids were selected because they possess carboxylic group(s) and amino functions and can form a salt. As stated in the bibliographic chapter, organic salts were shown to be more thermally stable during the bulk ROP of *L*-LA at high temperature than basic-type catalysts. Additionally, picolinic acid was expected to behave as a bifunctionnal activator(Scheme 15a), such as the DBU/BA salt developed by Coady *et al.* (Scheme 15b).[41] These authors have conducted computational studies using DFT showing that the carboxylate anion is able to activate the initiator/chain end hydroxyl moiety, while the protonated amine activates the monomer by hydrogen bonding. In the present study, the AA- and PA-RO*c*P of *L*-LA and CL were conducted in bulk at high temperature, meaning that such hydrogen bonding would be weak and favor instead proton exchange.

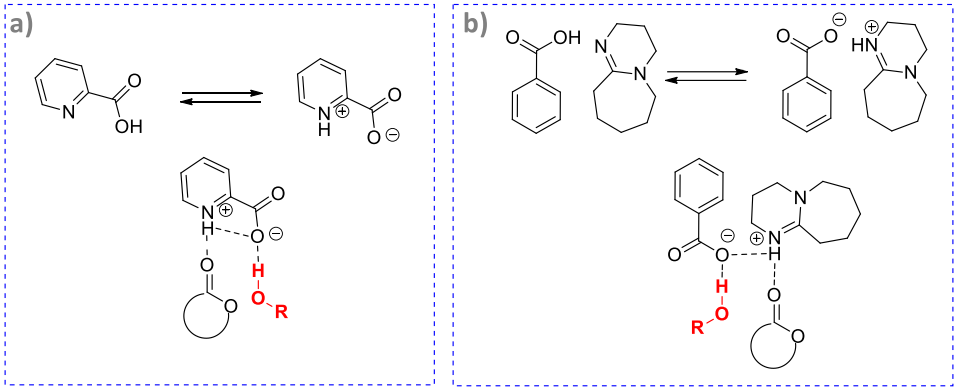

Scheme 15. (a) Proposed bifunctional activation of a lactone-alcohol mixture by picolinic acid, (b) bifunctional activation of a lactone-alcohol mixture by a BA/DBU salt revealed by DFT calculations.[41]

Table 7. Results and conditions of the bulk RO*c*P of *L*-LA and CL at 155°C.[a]

Entry	Cat[b]	Time (h)	C_{CL} / C_{LA}[c] (%/%)	$M_{n,SEC}$[d] (g.mol^{-1})	$M_{p,SEC}$[d] (g.mol^{-1})	$Đ$[d]	$DP_{,th}$[e]	$DP_{,exp}$[f]
1	PA	4	n.d / n.d	900	n.a	1.34	n.d	n.d
2	PA	24	n.d /n.d	3280	5050	1.75	n.d	n.d
3	AA	4	- / -	-	-	-	-	-
4	AA	24	n.d/n.d	1790	3250	1.77	n.d	n.d

[a]All reactions were carried out in bulk under nitrogen atmosphere at 155°C with reaction conditions: n_{CL}= n_{LA} = 1.4 mmol with BnOH as initiator: $[M]_0/[I]_0$= 50; [b] Organocatalyst used; [c]CL and *L*-LA conversions determined by ^{1}H NMR analysis; [d]Uncorrected average molar mass ($M_{n,SEC}$), molar mass at the peak ($M_{p,SEC}$) and dispersity ($Đ$) of crude copolymers determined by SEC chromatography (Polystyrene standards), THF/NEt_3(2w%) as eluent; [e]Theoretical degree of polymerization $DP_{,th} = \frac{[LA]_0}{[I]_0} \times C_{LA} + \frac{[CL]_0}{[I]_0} \times C_{CL}$; [f] Degree of polymerization calculated from the chain ends determined by ^{1}H NMR; n.d= not determined.

The AA- and PA-RO*c*P of *L*-LA and CL in bulk at 155 °C afforded brown copolymers, as previously observed for the bulk ROP of *L*-LA in the presence of *N*-containing catalysts.[42] This brown coloration of the copolymer likely mirrored the thermal degradation of the catalyst in the course of the copolymerization (Figure 18). Additionally, the high dispersities obtained, up to 1.77, dissuade us working with these amino-acids.

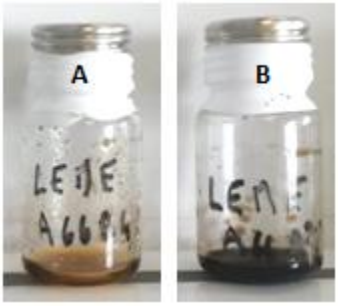

Figure 18. Pictures of the materials obtained using (A) AA (Table 7, Entries 3 & 4) and (B) PA (Table 7, Entries 1 & 2) organocatalysts.

Conclusions and outlooks

The ring-opening copolymerization (RO*c*P) of *L*-Lactide (*L*-LA) and ε-caprolactone (CL) initiated by benzyl alcohol (BnOH) as initiator and organocatalyzed by dibenzoylmethane (DBM) in solvent-free conditions, at 155°C, have been investigated. Despite a discrepancy between the experimental and the theoretical degree of polymerization ascribed to water co-initiation, the copolymerization reaction displayed an acceptable level of control, as attested by a relatively low dispersity and a linear correlation between the SEC molar masses *vs.* total monomer conversion. The versatility of DBM has been demonstrated by initiating the RO*c*P from two other initiators, namely butane-1,4-diol and poly(ethylene glycol).

To further evaluate the copolymer structure, the reactivity ratios of both *L*-LA (r_{LA}) and CL (r_{CL}) have been determined using the Kelen-Tüd*ő*s (KT) linear method and the nonlinear method called "the visualization of the sum of squared residual space" (VSSRS). Both techniques enable to determine the reactivity ratios and are found in good agreement (KT: r_{LA} = 1.81, r_{CL} = 0.08, VSSRS: r_{LA} = 1.8, r_{CL} = 0.05). Calculations from the VSSRS method take into account the data obtained at low conversion and up to 60% of conversion. After this stage some side reactions seem to influence the copolymerization by reducing the gap between both reactivity ratios. Indeed, the consumption rate of CL seems to be faster at the end of the reaction after 60% of conversion. The structure of the copolymer has been assessed by ^{1}H and ^{13}C NMR and by DSC, and combined with the reactivity ratio study, proves to be of gradient-type first and further evolving to a statistical-type microstructure.

The ring-opening polymerizations of *L*-LA and CL have been then evaluated in the presence of BnOH initiator and DBM as organocatalyst. The ROP of *L*-LA and CL catalyzed by DBM needs to be conducted at 155 °C in bulk. While the ROP of *L*-LA is not controlled, with a loss of chain end fidelity due to important co-initiation by water, the ROP of CL exhibits an acceptable level of control, but displays an important induction period of 39 hours.

Investigations into the kinetic have highlighted an acceleration of the polymerization rate of the DBM-organocatalyzed RO(*c*)P (DBM-ORO(c)P) of *L*-LA and CL during the course of the reaction. As DBM has been shown to be a poor monomer activator and a poor initiator/chain end activator, the (*co*)polymerization acceleration has been ascribed to the formation of carboxylic acids during the course of the reaction. The carboxylic moieties of the as-formed compounds may catalyze the reaction in such conditions meaning that the DBM-ORO(*c*)P of *L*-LA and CL may be viewed as self-catalyzed reactions.

Part of this work has been published in JPSA.[43]

This finally prompts us to evaluate miscellaneous carboxylic acid- and amino acid-type compounds for the DBM-ORO*c*P of *L*-LA and CL in bulk at 155°C. While amino acids do not control the copolymerization and lead to brownish copolymers, carboxylic acids appear more promising differently depending on the molecule. In the one hand, *L*-LA is consumed faster than CL during the RO*c*P when using 3,5-dihydroxybenzoic acid or vanillic acid. On the other hand, CL is consumed faster than *L*-LA when using 2,6-dihydroxybenzoic acid or succinic acid. In contrast, use of benzoic acid as organocatalyst proves very interesting toward the synthesis of statistical copolymers, as both monomers are inserted in the copolymer chain with the same rate.

The next chapters will discuss in depth the exact role of benzoic acid during the bulk RO(*c*)P of *L*-LA and CL.

Experimental part

Materials *L*-Lactide (*L*-LA, 99%, Corbionpurac) was recrystallized three times from toluene and dried under vacuum. ε-Caprolactone (CL, 99%, VWR), benzyl alcohol (BnOH, 99%, VWR) butane-1,4-diol (BD, 99%, VWR) and heptanol (HeptOH, 98%, Sigma Aldrich) were dried over CaH_2 for 48 hours prior to their distillation under reduced pressure and were stored on molecular sieves. Poly(ethylene glycol) (PEG_{1000}) (Fluka, Mw ~ 1000 $g.mol^{-1}$) and 1,3-diphenyl-1,3-propanedione (DBM, 98%,Sigma Aldrich) were dried via three azeotropic distillations of tetrahydrofuran (THF) and toluene, respectively. Compounds were stored in a glove box ($O_2 \leq 6$ ppm, $H_2O \leq 1$ ppm). Tetrahydrofuran and toluene solvents were dried using a MBraun Solvent Purification System (model MB-SPS 800) equipped with alumina drying columns.

Characterizations ^1H and ^{13}C nuclear magnetic resonance (NMR) spectra were recorded using a Bruker AM 500 MHz spectrometer at 298 K in $CDCl_3$. The δ-scale is referenced to residual $CHCl_3$ in $CDCl_3$ as internal standard.

Size exclusion chromatography (SEC) measurements were performed on a Polymer Laboratories PL-GPC 50 Plus Integrated System, comprising a PLgel 10 µm guard column followed by two PLgel 10 µm Mixed-B columns and a differential refractive index detector using THF/ triethylamine (NEt_3, 2wt%) as the eluent at 308 K with a flow rate of 1 $mL.min^{-1}$. The SEC system was calibrated using linear polystyrene (PS) standards.

Differential scanning calorimetry (DSC) measurements were carried out with a DSC Q2000 apparatus from T.A. Instruments under nitrogen flow. The purified copolymers were dried in an oven at 40 °C and were kept on the working bench at least 1 week before measurements. The sample was heated for the first run from -70 to 200 °C, then cooled again to -70 °C and heated again for the second run to 200 °C (heating and cooling rate 10 °C/min). Glass transition temperatures (T_g) and melting temperatures (T_m) were measured from the second and first heating run respectively. DBM was heated from room temperature to 300 °C with a rate of 10 °C/min.

Positive-ion MALDI-Mass Spectrometry (MALDI-MS) experiments were recorded using a Waters QToF Premier mass spectrometer equipped with a Nd:YAG (third harmonic) operating at 355 nm with a maximum output of 65 µJ delivered to the sample in 2.2 ns pulses at 50 Hz repeating rate. Time-of-flight mass analyses were performed in the reflectron mode at a resolution of about 10,000. All the samples were analyzed using trans-2-[3-(4-tert-butylphenyl)-2-methylprop-2-enylidene]malononitrile (DCTB) as matrix. That matrix was prepared as 40 $mg.mL^{-1}$ solution in $CHCl_3$. The matrix solution (1 µL) was applied to a stainless steel target and air-dried. Polymer samples were dissolved in THF to obtain 1 $mg.mL^{-1}$ solutions and 50 µL of 2 $mg.mL^{-1}$ NaI solution in acetonitrile has been added to the polymer solution. Therefore, 1 µL of

this solution was applied onto the target area already bearing the matrix crystals, and air-dried. For the recording of the single-stage MS spectra, the quadrupole (rf-only mode) was set to pass all the ions of the distribution, and they were transmitted into the pusher region of the time-of-flight analyzer where they were mass analyzed with 1s integration time. Data were acquired in continuum mode until acceptable averaged data were obtained.

DBM-OROP of *L*-LA or CL in bulk at 155°C

In a glove box, previously dried 10 mL vials were charged with the DBM catalyst (5mol% compared to the monomer), followed by the introduction of *L*-LA (0.3 g, 2.1 mmol) or CL (0.3 g, 2.6 mmol). Then the initiator (BnOH, BD or PEG_{1000}) was added in order to target a $[M]_0/[I]_0 = 30$. The vials were carefully sealed with polytetrafluoroethylene (PTFE) tape before being introduced in a graphite bath into an oven preheated at 155 °C. From time to time, one vial was removed from the oven to follow the kinetic of polymerization by ^{1}H NMR and the average molar mass ($M_{n,SEC}$) and dispersity ($Đ$) by SEC.

DBM-OROP of *L*-LA or CL in solution

In a glove box, previously dried 10 mL vials, containing a stirring bar each, were charged with the DBM catalyst (5 mol% compared to the monomer), followed by the introduction of *L*-LA (0.3 g, 2.1 mmol) or CL (0.3 g, 2.6 mmol). Then the initiator (BnOH, BD or PEG_{1000}) was added in order to target a $[M]_0/[I]_0 = 30$. The solvents, *i.e.* dichloromethane, THF or Toluene, were subsequently added using glass pipettes in order to reach 0.9 or 4 M. The vials were carefully sealed with polytetrafluoroethylene (PTFE) tape before being introduced in an oil bath preheated at 35 °C for dichloromethane and THF and at 90 °C for toluene.

RO*c*P of *L*-LA and CL using miscellaneous organocatalysts in bulk at 155°C in vials

In a glove box, previously dried 10 mL vials were charged with the chosen organocatalyst (5mol% compared to the monomer) and the same molar amount of *L*-LA (0.2 g, 1.4 mmol) and CL (0.16 g, 1.4 mmol). Then the initiator (BnOH, BD or PEG_{1000}) was added in order to target a $[M]_0/[I]_0 = 30$ with $[CL]_0/[I]_0 = [L\text{-LA}]_0/[I]_0 = 15$. The vials were carefully sealed with polytetrafluoroethylene (PTFE) tape before being introduced in a graphite bath into an oven preheated at 155°C. From time to time, one vial was removed from the oven to follow the kinetic of polymerization by ^{1}H NMR and the average molar mass ($M_{n,SEC}$) and dispersity ($Đ$) by SEC.

Detailed calculations for section 1.1:

Determination of the monomer conversions: $C_{CL} = \frac{I_{c\prime}}{I_{c\prime} + I_c}$, $C_{L-LA} = \frac{I_{a\prime}}{I_{a\prime} + I_a}$

Determination of the composition in the copolymers: $F_{CL} = \frac{I_{c\prime}}{I_{a\prime} + I_{c\prime}}$, $F_{L-LA} = \frac{I_{a\prime}}{I_{a\prime} + I_{c\prime}}$

Determination of the ω-chain end: $DP_{,exp} = \frac{\frac{I_{a\prime} + I_{c\prime}}{2}}{I_{\omega LA} + \frac{I_{\omega CL}}{2}}$

Determination of the number average molar mass from ω-chain end by NMR:

$$M_{n,NMR} = \frac{\frac{I_{a\prime}}{2}}{I_{\omega LA} + \frac{I_{\omega CL}}{2}} \times M_{LA} + \frac{\frac{I_{c\prime}}{2}}{I_{\omega LA} + \frac{I_{\omega CL}}{2}} \times M_{CL}$$

Detailed calculations for section 1.4:

Determination of the ω-chain end: $DP_{,exp} = \frac{(\frac{I_{a\prime} + I_{g\prime}}{2})}{(\frac{I_{eLA}}{2} + \frac{I_{eCL}}{4})}$

Detailed calculations for section 2.1:

Determination of the ω-chain end: $DP_{,exp} \approx \frac{(\frac{I_{a\prime}}{2})}{I_{\omega LA}}$

Detailed calculations for section 2.2:

Determination of the ω-chain end: $DP_{,exp} \approx \frac{(\frac{I_{c\prime}}{2})}{(\frac{I_{\omega CL}}{2})}$

Supporting information

Figure S 1. ^{1}H ($CDCl_3$, 500 MHz, r.t.) and ^{13}C NMR ($CDCl_3$, 100 MHz, r.t.) spectra of dibenzoylmethane. ^{1}H NMR attribution.[44]

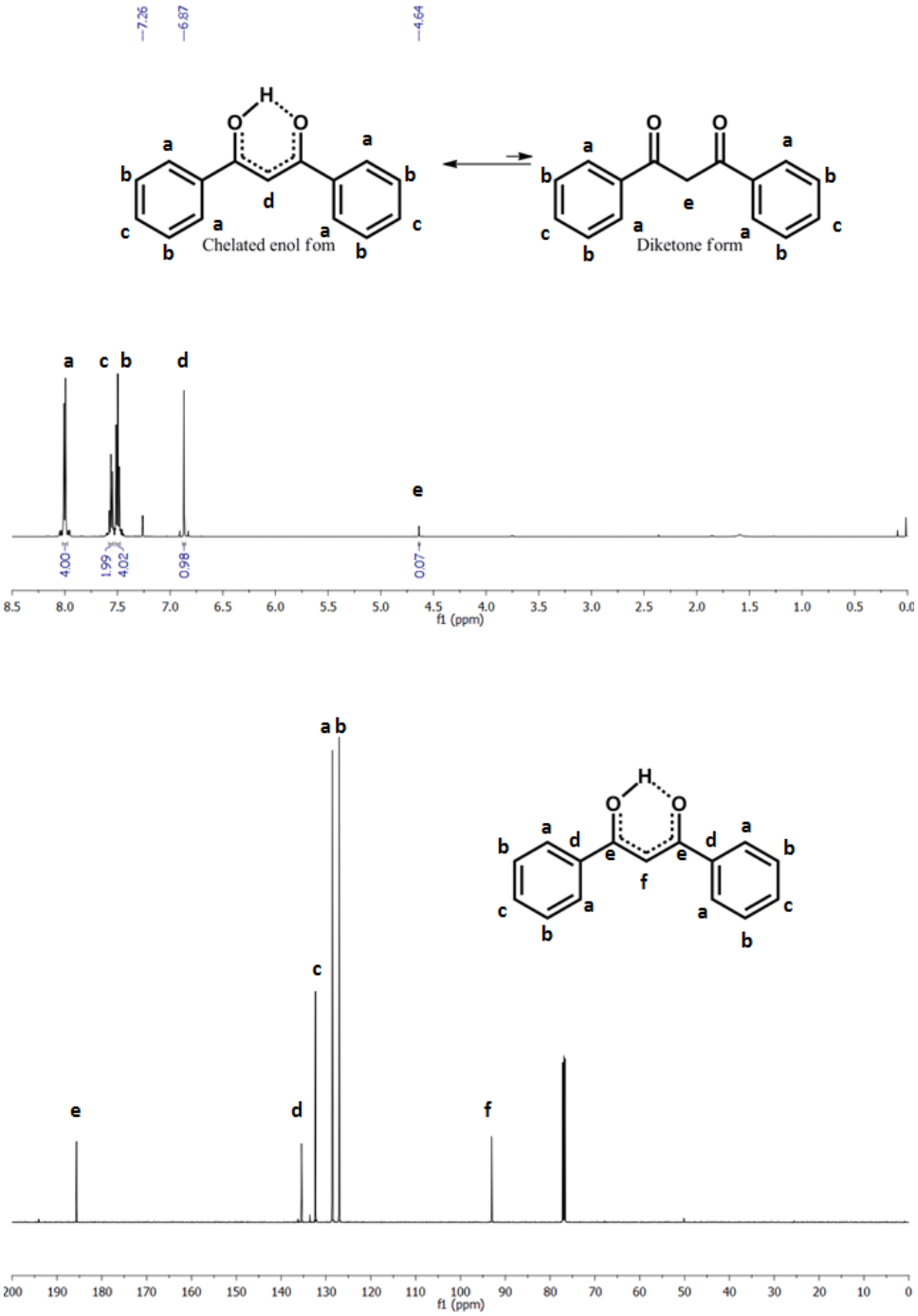

Figure S 2. DSC spectrum of dibenzoylmethane.

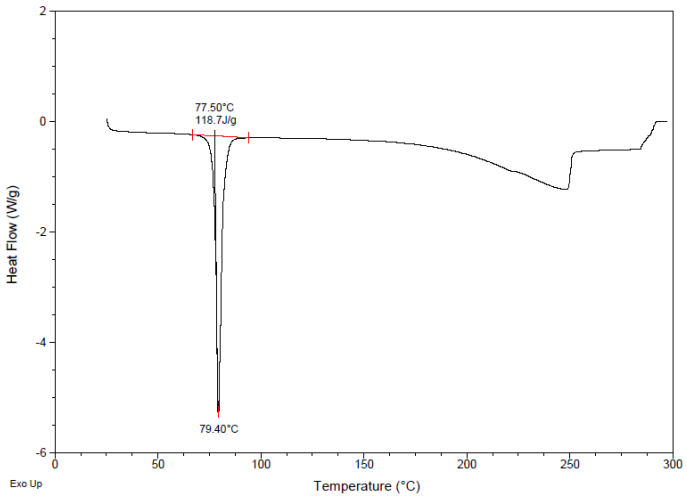

Figure S 3. ^{1}H NMR spectrum ($CDCl_3$, 500 MHz, r.t) of DBM-ORO*c*P of CL and *L*-LA without any catalyst and initiator after 41h: Blank experiment (Table 3, Entry 1).

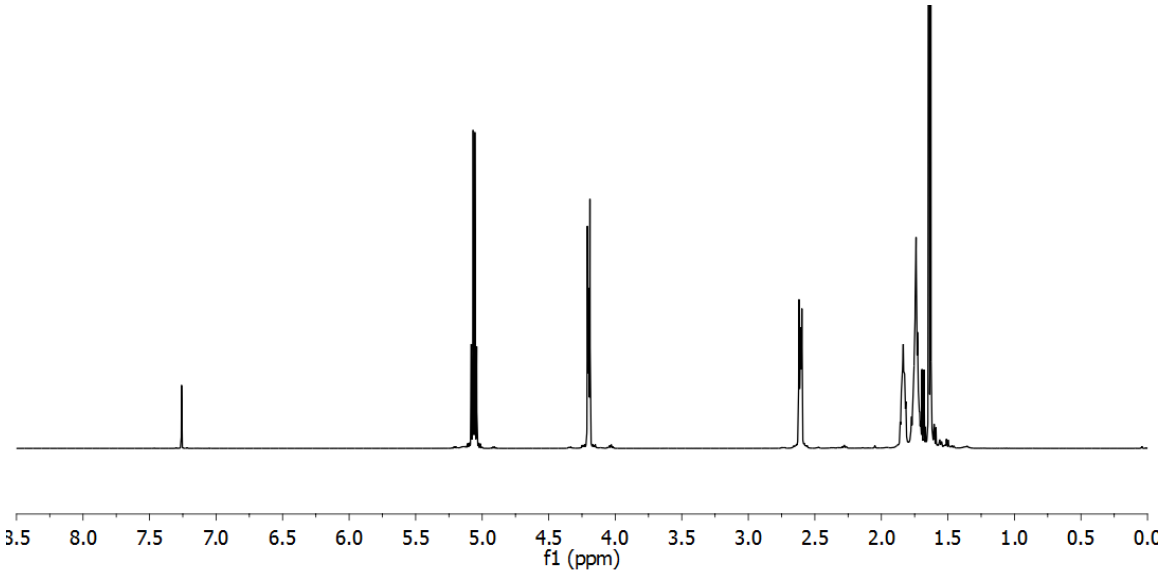

Determination of Reactivity Ratios:

The reactivity ratios were calculated using the Kelen-Tüdös[23] linear method which can be used in ROP.[45] For this purpose, the copolymerization of the monomer with different chosen compositions ($f_{LA,0}$: $f_{CL,0}$ ≈ 15:85, 30:70, 40:60, 50:50, 60:40, 70:30) were performed and the monomer composition (F_{LA} and F_{CL}) in the obtained oligomers was examined at low conversion.

Kelen-Tüdös: Where $x = \frac{f_{CL}}{f_{LA}}$, $y = \frac{F_{CL}}{F_{LA}}$

$$G = \frac{x\,(y-1)}{y}, \quad F = \frac{x^2}{y}$$

$$\eta = \frac{G}{\alpha + F}, \varepsilon = \frac{F}{\alpha + F} \quad \text{with} \quad \alpha = \sqrt{F_{min}.F_{max}}$$

$$\eta = \left(r_{CL} + \frac{r_{L-LA}}{\alpha}\right)\varepsilon - \frac{r_{L-LA}}{\alpha}$$

Table S 1. Mole fraction of each monomer in the initial reaction mixture ($f_{LA,0}$, $f_{CL,0}$) and in the copolymer ($F_{LA,}$ F_{CL}) and the total conversion (C_{TOT}).

$f_{LA,0}$ (%)	$f_{CL,0}$ (%)	C_{TOT} (%)	F_{LA} (%)	F_{CL} (%)
0.17	0.83	17	0.49	0.51
0.31	0.69	13	0.61	0.39
0.41	0.59	10	0.67	0.33
0.51	0.49	11	0.73	0.27
0.61	0.39	08	0.79	0.21
0.71	0.29	08	0.84	0.16

Figure S 4. Graph of the Kelen-Tüdös method.

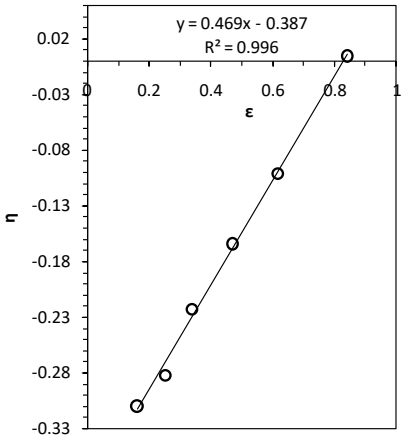

DBM-ORO*c*P initiated by BnOH: Copolymer structure.

Figure S 5. ^{1}H NMR spectrum ($CDCl_3$, 500 MHz, r.t) of a P(LA-co-CL) copolymer (Table 3, Entry 6).

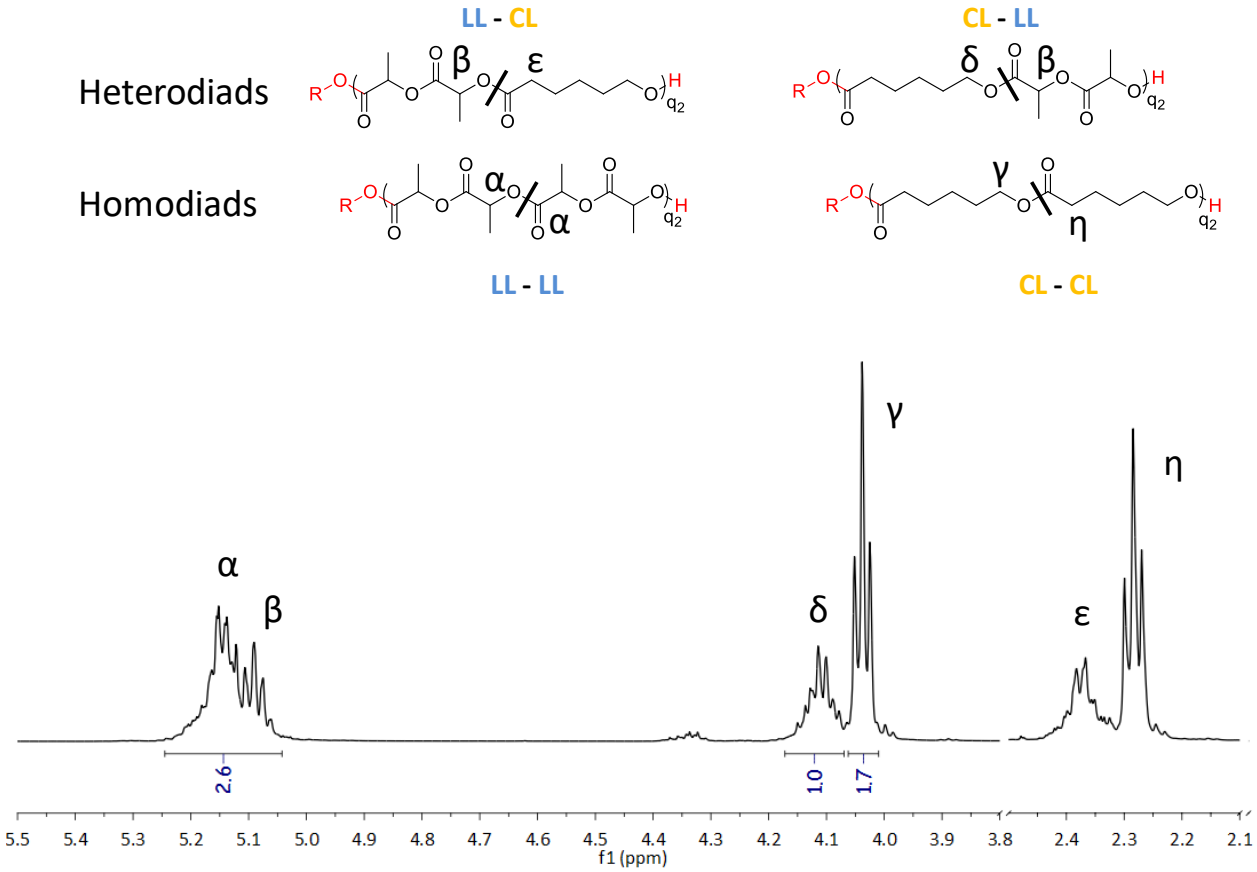

Figure S 6. DSC spectrum of the final pure copolymer P(CL-*co*-LA) (Table 3, Entry 6).

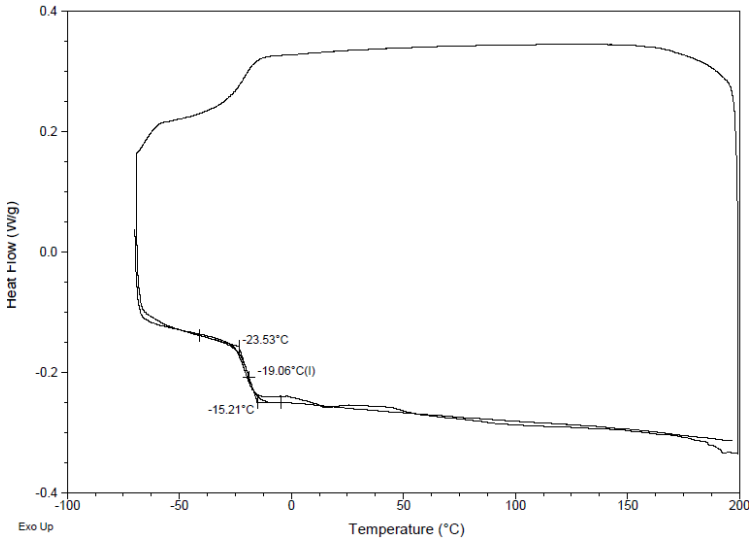

DBM-ORO*c*P initiated by BD:

Figure S 7. ^{1}H NMR spectrum of crude P(LA-*co*-CL) initiated by BD (Table 3, Entry 9) ($CDCl_3$, r.t, 500 MHz). * Monomer peaks. Peak of methylene oxycarbonyl of BD (k') attribution.[46]

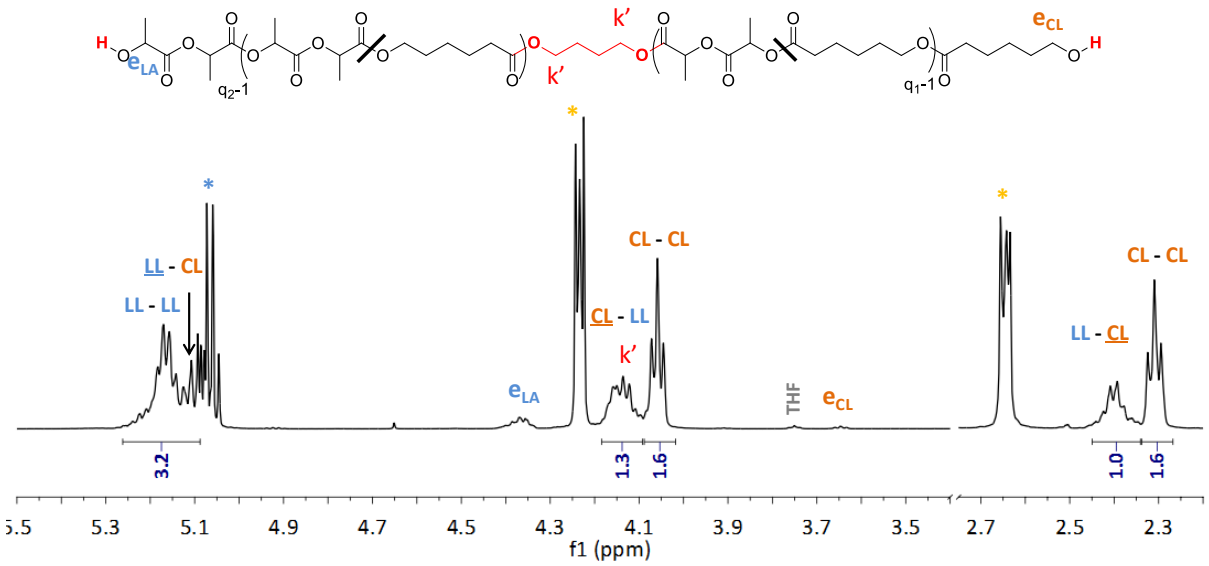

DBM-OROP of CL:

Figure S 8. ^{1}H NMR spectra of PCL (Table 5, Entries 1 to 5).

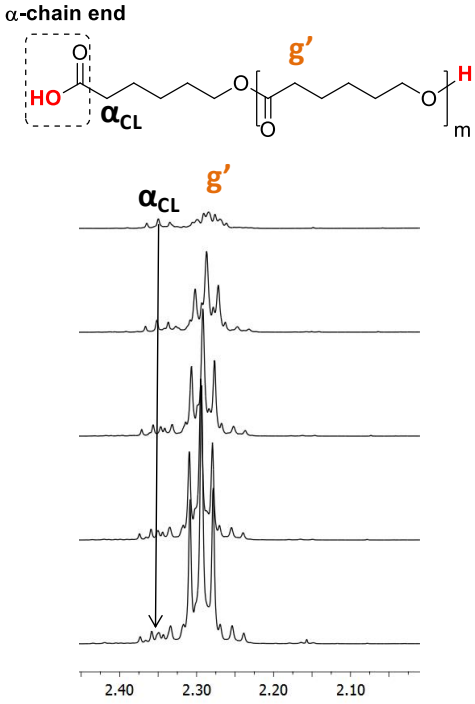

Thermal degradation of DBM

Figure S 9. ^{1}H NMR spectra of mixture of DBM and BnOH (1/1) (a) before thermal treatment (b) after thermal treatment at 155°C for 72 hours.

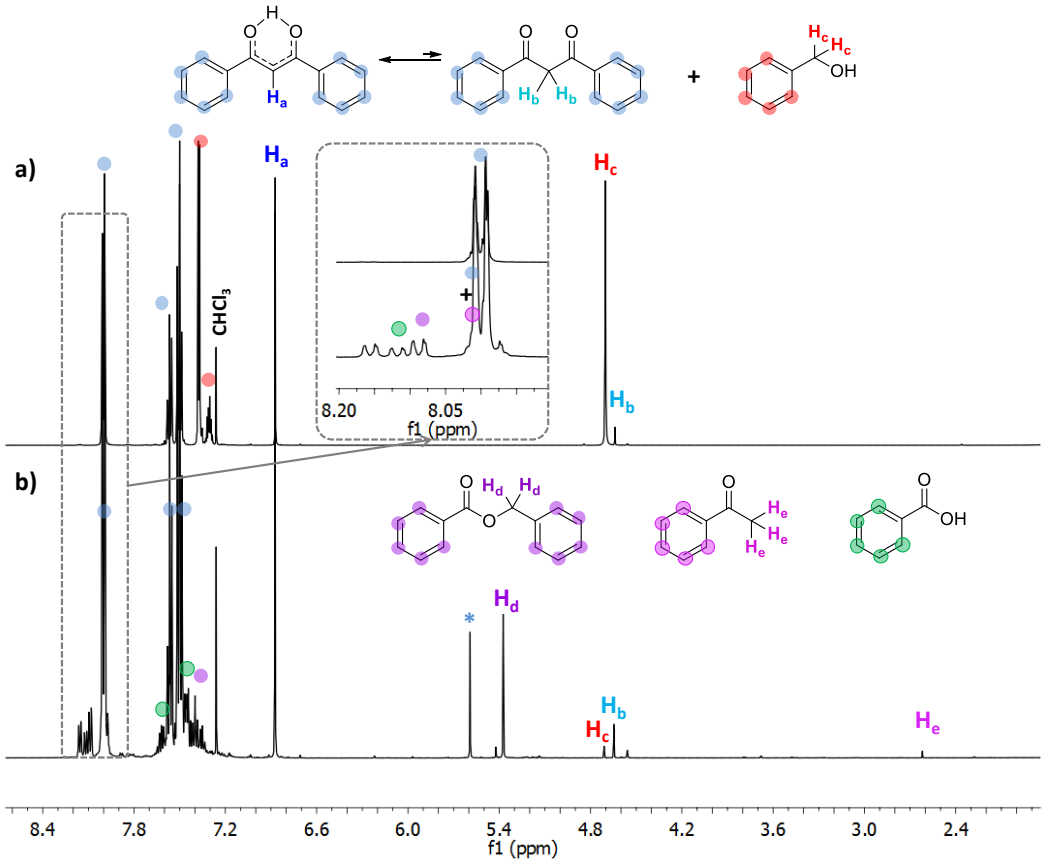

Scheme S 1. Hydrolysis of DBM leading to the generation of benzoic acid.

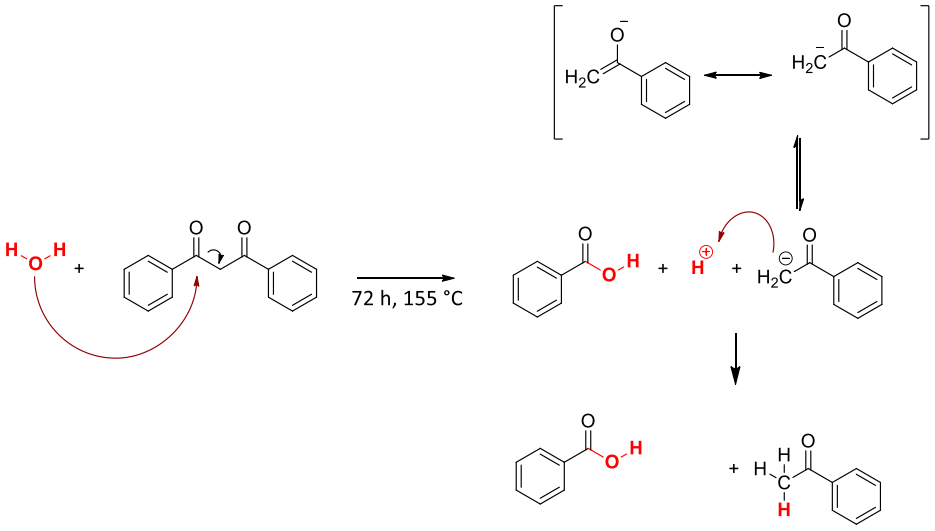

References

1 H. Alamri, J. Zhao, D. Pahovnik and N. Hadjichristidis, *Polym Chem*, 2014, **5**, 5471–5478.

2 L. Zhang, N. Li, Y. Wang, J. Guo and J. Li, *Macromol. Res.*, 2014, **22**, 600–605.

3 B. G. G. Lohmeijer, R. C. Pratt, F. Leibfarth, J. W. Logan, D. A. Long, A. P. Dove, F. Nederberg, J. Choi, C. Wade, R. M. Waymouth and J. L. Hedrick, *Macromolecules*, 2006, **39**, 8574–8583.

4 J. U. Pothupitiya, N. U. Dharmaratne, T. M. M. Jouaneh, K. V. Fastnacht, D. N. Coderre and M. K. Kiesewetter, *Macromolecules*, 2017, **50**, 8948–8954.

5 M. Baśko and P. Kubisa, *J. Polym. Sci. Part Polym. Chem.*, 2006, **44**, 7071–7081.

6 M. Baśko and P. Kubisa, *J. Polym. Sci. Part Polym. Chem.*, 2007, **45**, 3090–3097.

7 X. Zhou and L. Hong, *Colloid Polym. Sci.*, 2013, **291**, 2155–2162.

8 E. Stirling, Y. Champouret and M. Visseaux, *Polym. Chem.*, 2018, **9**, 2517–2531.

9 D. W. Grijpma and A. J. Pennings, *Polym. Bull.*, 1991, **25**, 335–341.

10 Z. Wei, L. Liu, C. Qu and M. Qi, *Polymer*, 2009, **50**, 1423–1429.

11 M. Florczak and A. Duda, *Angew. Chem. Int. Ed.*, 2008, **47**, 9088–9091.

12 J. Contreras and D. Dávila, *Polym. Int.*, 2006, **55**, 1049–1056.

13 T. Shi, W. Luo, S. Liu and Z. Li, *J. Polym. Sci. Part Polym. Chem.*, 2018, **56**, 611–617.

14 K. M. Jackson, M. DeLeon, C. R. Verret and W. B. Harris, *Cancer Lett.*, 2002, **178**, 161–165.

15 Y.-F. Liao, Y.-M. Tzeng, H.-C. Hung and G.-Y. Liu, *Mol. Med. Rep.*, 2015, **11**, 4597–4604.

16 S. C. Yoon, K. M. Lee, M. H. Lee and S. Y. Park, *Bull. Korean Chem. Soc.*, 2015, **36**, 340–345.

17 D. Veierov, T. Bercovici, E. Fischer, Y. Mazur and A. Yogev, *J. Am. Chem. Soc.*, 1977, **99**, 2723–2729.

18 M. Moriyasu, A. Kato and Y. Hashimoto, *J Chem Soc Perkin Trans 2*, 1986, 515–520.

19 C. Wohlfarth, in *Supplement to IV/6*, ed. M. D. Lechner, Springer Berlin Heidelberg, Berlin, Heidelberg, 2008, vol. 17, pp. 345–345.

20 C. Wohlfarth, in *Supplement to IV/6*, ed. M. D. Lechner, Springer Berlin Heidelberg, Berlin, Heidelberg, 2008, vol. 17, pp. 117–121.

21 B. S. Furniss, A. J. Hannaford, P. W. G. Smith and A. R. Tatchell, *Vogel's Textbook of practical organic chemistry - 5th ed.*, John Wiley & Sons, New York, Fifth., 1989.

22 M. M. Folkendt, B. E. Weiss-Lopez, J. P. Chauvel and N. S. True, *J. Phys. Chem.*, 1985, **89**, 3347–3352.

23 T. Kelen and F. Tüdös, *J. Macromol. Sci. Part - Chem.*, 1975, **9**, 1–27.

24 M. Fineman and S. D. Ross, *J. Polym. Sci.*, 1950, **5**, 259–262.

25 M. Van Den Brink, A. M. Van Herk and A. L. German, *J. Polym. Sci. Part Polym. Chem.*, 1999, **37**, 3793–3803.
26 S. Harrisson, F. Ercole and B. W. Muir, *Polym Chem*, 2010, **1**, 326–332.
27 N. Nomura, A. Akita, R. Ishii and M. Mizuno, *J. Am. Chem. Soc.*, 2010, **132**, 1750–1751.
28 J. Kasperczyk and M. Bero, *Makromol. Chem.*, 1991, **192**, 1777–1787.
29 J. Kasperczyk and M. Bero, *Makromol. Chem.*, 1993, **194**, 913–925.
30 J.-B. Zhu and E. Y.-X. Chen, *J. Am. Chem. Soc.*, 2015, **137**, 12506–12509.
31 T. Saito, Y. Aizawa, K. Tajima, T. Isono and T. Satoh, *Polym Chem*, 2015, **6**, 4374–4384.
32 J. W. Bunting, J. P. Kanter, R. Nelander and Z. Wu, *Can. J. Chem.*, 1995, **73**, 1305–1311.
33 F. Sanda, H. Sanada, Y. Shibasaki and T. Endo, *Macromolecules*, 2002, **35**, 680–683.
34 J. Casas, P. V. Persson, T. Iversen and A. Córdova, *Adv. Synth. Catal.*, 2004, **346**, 1087–1089.
35 P. V. Persson, J. Schröder, K. Wickholm, E. Hedenström and T. Iversen, *Macromolecules*, 2004, **37**, 5889–5893.
36 P. V. Persson, J. Casas, T. Iversen and A. Córdova, *Macromolecules*, 2006, **39**, 2819–2822.
37 P. Domínguez de María, *ChemCatChem*, 2010, **2**, 487–492.
38 N. Susperregui, D. Delcroix, B. Martin-Vaca, D. Bourissou and L. Maron, *J. Org. Chem.*, 2010, **75**, 6581–6587.
39 J. Xu, J. Song, S. Pispas and G. Zhang, *J. Polym. Sci. Part Polym. Chem.*, 2014, **52**, 1185–1192.
40 E. Lindquist and Y. Yang, *J. Chromatogr. A*, 2011, **1218**, 2146–2152.
41 D. J. Coady, K. Fukushima, H. W. Horn, J. E. Rice and J. L. Hedrick, *Chem. Commun.*, 2011, **47**, 3105–3107.
42 G. Nogueira, A. Favrelle, M. Bria, J. P. Prates Ramalho, P. J. Mendes, A. Valente and P. Zinck, *React Chem Eng*, 2016, **1**, 508–520.
43 L. Mezzasalma, J. De Winter, D. Taton and O. Coulembier, *J. Polym. Sci. Part Polym. Chem.*, 2018, **56**, 475–479.
44 J. Zawadiak and M. Mrzyczek, *Magn. Reson. Chem.*, 2013, **51**, 589–594.
45 A. Duda and A. Kowalski, in *Handbook of Ring-Opening Polymerization*, eds. P. Dubois, O. Coulembier and J.-M. Raquez, Wiley-VCH Verlag GmbH & Co. KGaA, Weinheim, Germany, 2009, pp. 1–51.
46 O. Coulembier, T. Josse, B. Guillerm, P. Gerbaux and P. Dubois, *Chem. Commun.*, 2012, **48**, 11695–11697.

Chapter 3.

Benzoic Acid-Organocatalyzed Ring-Opening Polymerization (OROP) of *L*-Lactide and ε-Caprolactone Under Solvent-Free Conditions: from Simplicity to Recyclability

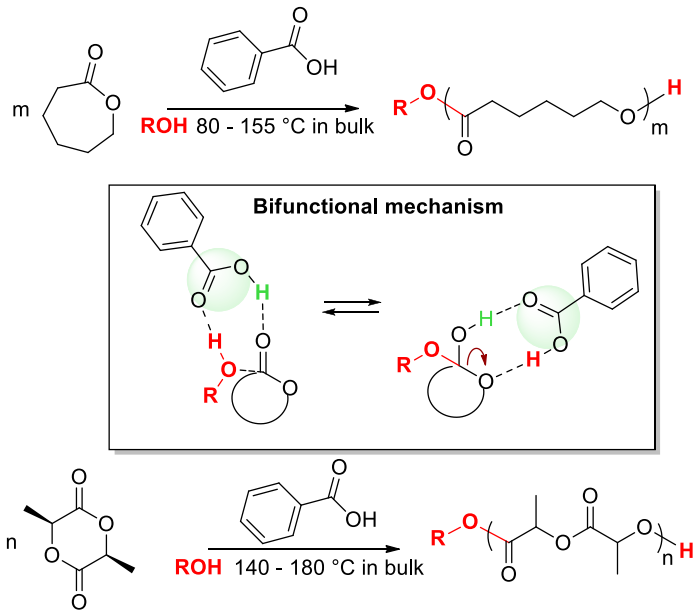

Keywords: lactide, ε-caprolactone, bulk, catalysis, organocatalysis, acids, benzoic acid, polymerization, ring-opening.

Chapter 3. Benzoic Acid-Organocatalyzed Ring-Opening Polymerization (OROP) of *L*-Lactide and ε-Caprolactone Under Solvent-Free Conditions: from Simplicity to Recyclability

Table of contents

Introduction

In the previous chapter, dibenzoylmethane (DBM) has been evaluated as organocatalyst for the statistical ring-opening-copolymerization (RO*c*P) of *L*-lactide (*L*-LA) and ε-caprolactone (CL) in bulk at 155 °C. Side reactions, such as thermal degradation by hydrolysis of the catalyst as well as side initiation by water, have caused the *in situ* generation of carboxylic acid groups. Unexpectedly, this has enabled to accelerate the DBM-organocatalyzed RO(*c*)P, ORO(*c*)P. This has prompted us to apply different amino acid and acidic organocatalysts for the statistical RO*c*P of *L*-LA and CL and we have discovered that benzoic acid (BA) is particularly efficient to copolymerize both monomers at the same rate. BA thus appears as a promising weak acid-type organocatalyst for P(LA-*stat*-CL) synthesis.

The present chapter proposes to study in-depth the catalytic activity of BA for the bulk OROP of *L*-LA and CL at high temperature. This will allow us to evaluate the bulk ROP of *L*-LA at high temperature which is the other objective of this work. The statistical ORO*c*P of *L*-LA and CL will be then discussed in chapter 4.

As stated in the bibliographic chapter, *L*-LA and CL have a distinct behavior when polymerized by organocatalysts. Strong acidic organocatalysts, such as sulfonic[1]/sulfonimide[2] and phosphoric/phosphoramic acids,[3,4,5] which are known to operate through an activated monomer mechanism (AMM) or a bifunctional mechanism, represent an excellent option to conduct the OROP of CL in solution. In addition, phosphoric acid[6] and boric acids[7] have attracted some interest in the solvent-free OROP of CL (Scheme 1). In contrast, simple amine- and amidine-type catalysts do not enable the OROP of CL and have to be combined with a co-catalyst such as a (thio)urea.[8] Eventually, only "super" strong bases have been successfully used for this purpose; these include phosphazenes (*t*-BuP_2)[9,10,11] or *N*-heterocyclic carbenes (NHCs, Scheme 1).[12,13,14]

Besides, OROP of *L*-lactide (*L*-LA) has been mainly carried out in solution in presence of basic and/or nucleophilic compounds, working through an activated chain end mechanism (ACEM) or *via* bifunctionnal activation (Scheme 1). In contrast, only trifluoromethanesulfonic acid (TfOH)[15,16,17,18] and diphenyl phosphate (DPP),[6] as Bronsted acids, have been successfully applied (Scheme 1). While the former has enabled a controlled ROP of *L*-LA only in solution, the DPP organocatalyst has led to highly isotactic poly(*L*-lactide)(PLLA) in bulk only, but with a very low kinetic. Importantly, basic and or/nucleophilic compounds have met with limited success in conducting the ROP of *L*-LA in solvent-free conditions (Scheme 1).[19,20,21,22] Such structures are generally not thermally stable at high temperatures (140 °C < T < 180 °C), including the highly selective thiourea/amine cocatalalysts,[20] and lead to a poor control during the bulk ROP of *L*-LA. In such conditions, inter- and intra-molecular transesterification and epimerization of *L*-LA are

often noted. This is highly detrimental for optimization of thermal and mechanical properties of the as-obtained poly(*L*-Lactide) PLLA.

Over the last 15 years, weak carboxylic acid catalysts, such as trifluoroacetic acid, or naturally occurring α-hydroxyacids, including lactic acid, citric acid, mandelic acid, tartaric acid,[23,24,25,26,27] and other α-amino acids[26,28,29,30] have also attracted some interest in the OROP of cyclic esters. This is due to their broad availability as well as their air, moisture and thermal stability. Surprisingly, the simplest aromatic carboxylic acid, *i.e.*, benzoic acid (BA), which is a highly thermally stable[31] and naturally occurring compound, has never been investigated as catalyst in bulk OROP. Its high thermal stability, up to 300 °C in subcritical water,[31] is of prime interest for the bulk RO(*c*)P of *L*-LA and CL at high temperature. Another important property of BA is its ability to sublimate, which can be properly exploited during the purification step allowing for its recyclability. Indeed, catalyst recycling represents another challenge that remains to be tackled in polymer synthesis by organocatalysis, and only a handful of reports have addressed this point.[24,26,2,32,12] BA is thus expected to be sufficiently active and thermally stable to trigger the bulk OROP of *L*-LA and CL at high temperature (T > 155 °C). As already emphasized, BA should enable to minimize the epimerization of *L*-LA often observed with basic catalysts.

In the present chapter, we will describe the catalytic activity of BA towards OROP of CL and *L*-LA carried out in bulk in a temperature range of 155-180 °C, and in presence of alcohols as initiators. The kinetic and mechanistic investigations will be carried out and supported by density functional theory (DFT) calculations. The ORO*c*P of *L*-LA and CL is also reported as a means to achieve tribloc copolymers. Moreover, advantage of the capability for BA to sublimate is exploited to recycle and reuse it in further organocatalytic cycles, affording chemically pure PCL- and PLLA-based aliphatic (co)polyesters.

These theoretical calculations have been carried out by Coralie Jehanno, completing her PhD between the institute for Polymer Materials (POLYMAT) at the University of the Basque Country UPV/EHU, in San Sebastian under the supervision of Dr. Fernando Ruiperez and Dr. Haritz Sardon and the School of Chemistry at the University of Birmingham under the supervision of Pr. Andrew Dove.

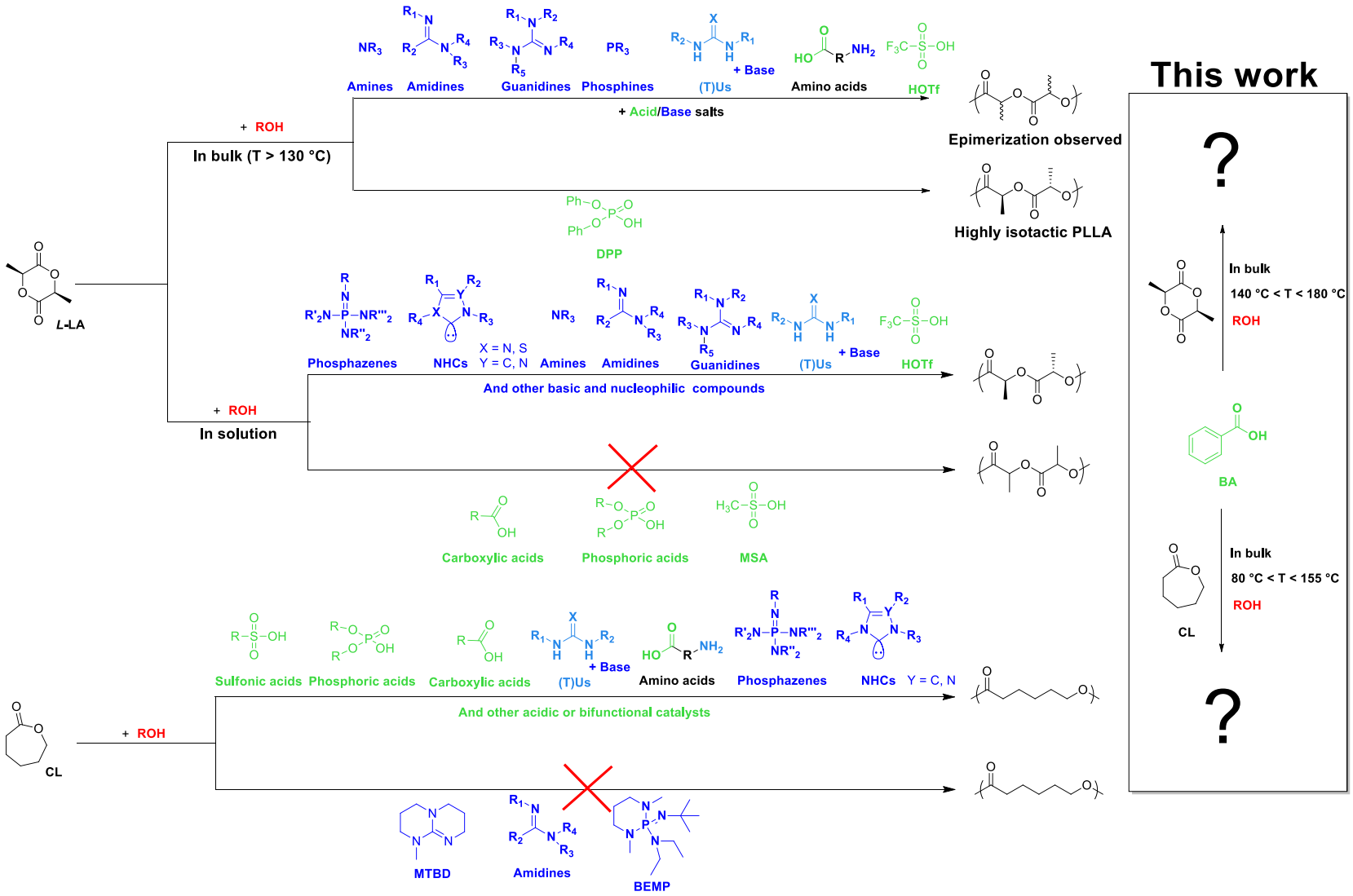

Scheme 1. Organocatalysts already used for the ROP of both *L*-LA and CL in various conditions.

1 Investigations into the BA-OROP of ε-caprolactone (CL) and *L*-lactide (*L*-LA)

1.1 Case of CL

The catalytic activity of BA was first assessed for the OROP of CL, reactions being performed between 80 °C and 155 °C in bulk in presence of butane-1,4-diol (BD), hexane-1,6-diol (HD), benzyl alcohol (BnOH), heptan-1-ol (HepOH) and poly(ethyleneglycol) (PEG_{1000}; M_w= 1000 $g.mol^{-1}$) as initiators.

1.1.1 Diols as initiators for the BA-OROP of CL

Polymerizations were first evaluated with BD targeting a total degree of polymerization ($DP_{tot} = [CL]_0/[BD]_0$) from 25 to 100 in bulk at 155 °C (Scheme 2). The catalytic loading effect was also investigated for a DP of 25 with 2.5-10 mol.% of BA rel. to CL (Table 1, Entries 2 to 6). While no reaction took place in absence of BA (Entry 1), quantitative conversions were reached within less than 7 h, demonstrating the catalytic ability of BA to promote OROP of CL at high temperature under solvent-free conditions. Analyses by ^1H NMR spectroscopy evidenced the formation of α,ω-bis-hydroxy telechelic PCL's, irrespective of the initial experimental conditions (Figure 1). Of particular interest, white semi-crystalline compounds (T_g≈ -60 °C and T_m ranging from 50 °C to 58 °C, as determined by DSC, Figure S 1) were obtained, attesting to the thermal stability of BA as organocatalyst.

Exclusive initiation of the BA-OROP of CL by BD was supported by MALDI-ToF MS analysis. Figure 2a shows the Gaussian-like distribution of a representative PCL with a major population, **A**, corresponding to the expected PCL structure [m/z = 90 (M_{BD}) + m x114 (M_{CL}) + 23 (M_{Na+})]. The other population, **B**, eventually corresponds to PCL chains cationized with Na_2I^+.

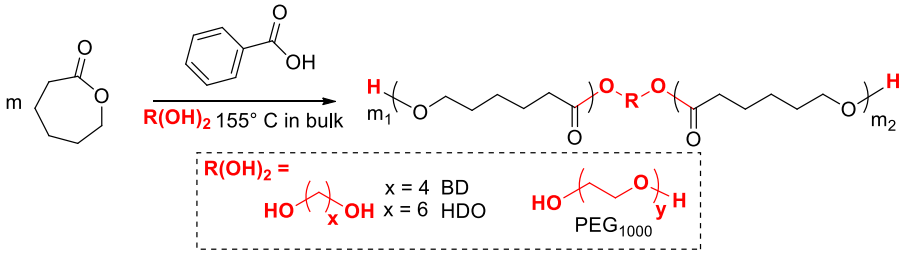

Scheme 2. BA-OROP of CL initiated by diols. With $m = m_1 + m_2$.

Table 1. Results and conditions of the BA-OROP of CL in bulk initiated by different diols.[a]

Entry	I	Cat (%)[b]	$[M]_0/[I]_0$	Time (h)	C_M (%)[c]	$M_{n,SEC}$ (g.mol^{-1})[d]	$Đ$[d]	DP_{th}[e]	DP_{exp}[f]
1	BD	0	25	22	-	-	-	-	-
2	BD	2.5	25	4.5	97	4340	1.17	24.3	23.8
3	BD	5	25	2	93	4170	1.12	23.2	21.3
4	BD	10	25	1.25	94	4180	1.14	23.5	23.0
5	BD	5	50	4	93	8230	1.23	48.3	43.3
6	BD	5	100	7	94	16910	1.33	93.7	93.6
7	HDO	5	25	2	91	4290	1.12	22.8	22
8	PEG	5	50	7.8	95	7780[g]	1.41[g]	47.6	n.a

[a]Reactions were performed in bulk at 155 °C under argon atmosphere with reaction conditions: m_{CL}= 200 mg. [b]Catalyst percent *related to* monomer. [c]CL conversions were determined by ^{1}H NMR analysis. [d]Uncorrected number average molar mass ($M_{n,SEC}$) and dispersity ($Đ$) of crude polymers as determined by SEC chromatography (polystyrene standards) at 313 K and THF as eluent. [e]Theoretical degree of polymerization $DP, th = \frac{[M]_0}{[I]_0} \times C_M$. [f]Experimental degree of polymerization calculated from PCL chain ends as determined by ^{1}H NMR. [g]Determined by SEC chromatography (polystyrene standards) at 308 K and THF/NEt_3(2w%) as eluent. n.a.: not available

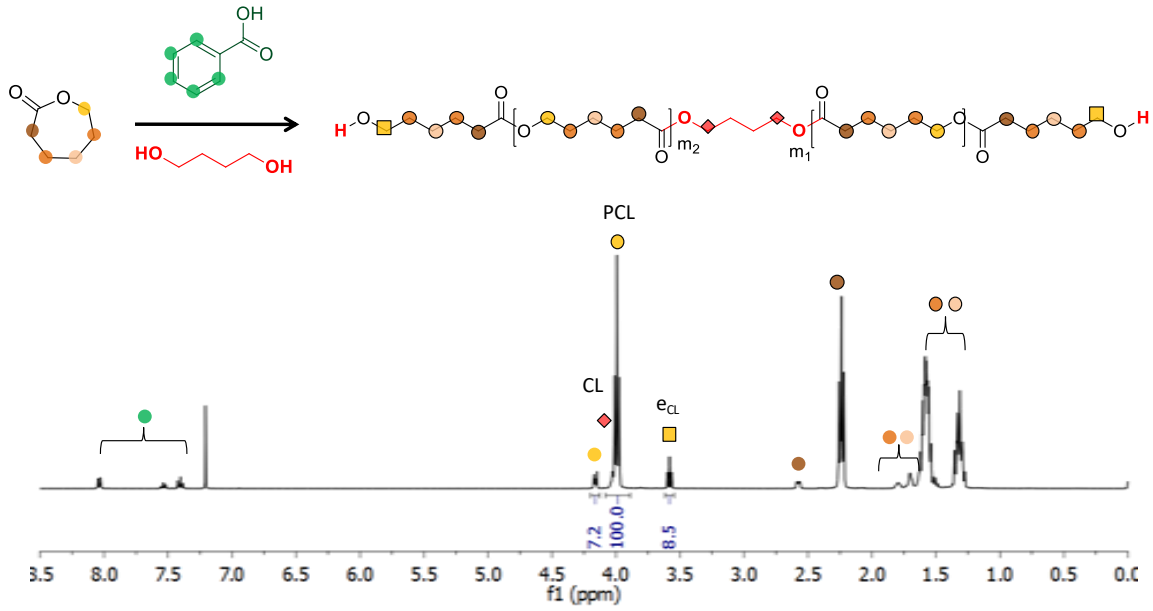

Figure 1. ^{1}H NMR spectrum ($CDCl_3$, 400.2 MHz) of crude PCL obtained by BA-OROP of CL initiated by BD in bulk at 155 °C (Table 1, Entry 3),.

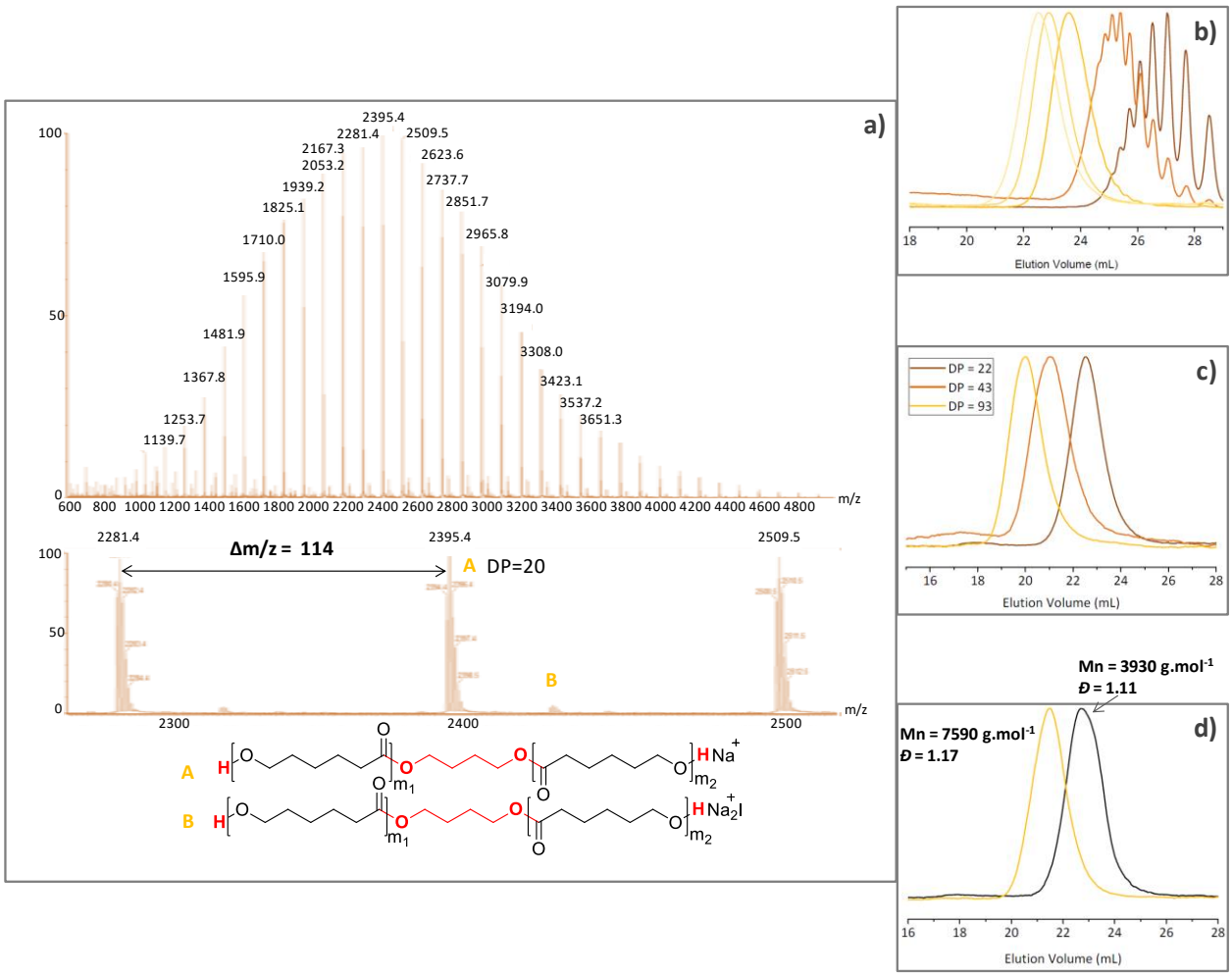

Figure 2. (a) MALDI-ToF mass spectrum of BD-initiated BA-OROP-derived PCL (Table 1, Entry 3) with M_{CL} = 114 g.mol-1; (b) SEC kinetic evolution (Table 1, Entry 3); (c) SEC comparison between entries 3, 5 and 6, Table 1; (d) Chain extension experiments (see main text).

Degree of polymerization, as determined by NMR ($DP_{,exp}$), showed excellent agreement with DP values calculated from the initial $[CL]_0/[BD]_0$ ratio ($DP_{,th}$, Table 1). Additionnally, number average molar masses, as determined by SEC ($M_{n,SEC}$), increasing linearly with monomer conversion (Figure 3a-b) and dispersity values remaining low ($1.12 < Đ < 1.33$; Figure 2 b,c and Figure S 2) were consistent with a controlled ROP process.

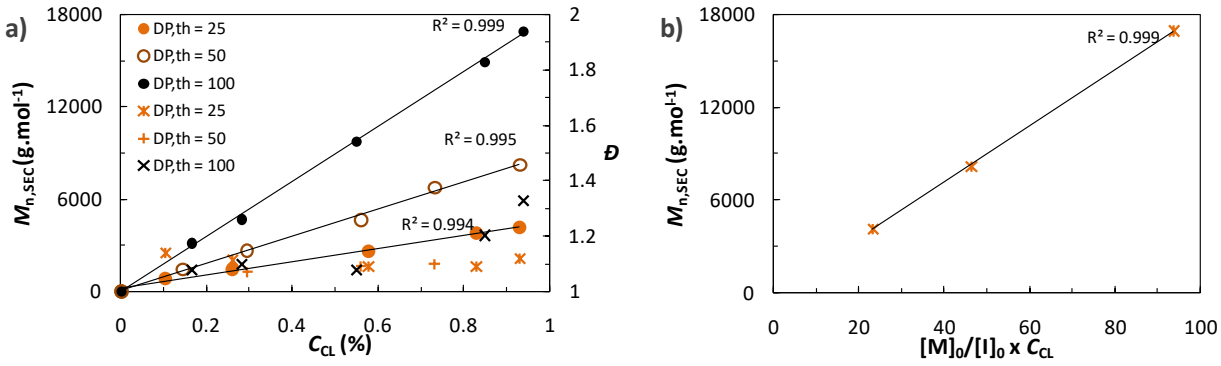

Figure 3. (a) Evolution of uncorrected $M_{n,SEC}$ (•) and dispersity $Đ$ (x) with monomer conversion.(b) Evolution of the uncorrected $M_{n,SEC}$ with monomer-to-initiator ratios multiplied by the monomer conversion (entries 3-5-6, Table 1).

This was also supported by a chain extension experiment, as follows (Table S 1). The BA-OROP of CL in presence of BD at 155 °C ($[CL]_0/[BD]_0/[BA]_0$ = 25/1/1.25) afforded a PCL precursor with $M_{n,SEC}$ = 3900 g.mol^{-1} and $Đ$ = 1.11. Addition of 25 eq. of CL at 155 °C increased the molar mass to $M_{n,SEC}$ = 7600 g.mol^{-1} after 2 h, while maintaining a low dispersity ($Đ$ = 1.17; Figure 2d), confirming an efficient re-initiation from the PCL precursor.

To further demonstrate the versatility of this BA-OROP method, HDO and PEG_{1000} were evaluated as initiators (Table 1, Entries 7-8). Well-defined PCLs samples were also obtained as shown by the observation of monomodal and symmetrical SEC traces (Figure 4a,b). Notably, BA-OROP of CL initiated by BD and HDO were almost completed after 2h of reactions under the same conditions, *i.e.*, in bulk at 155 °C for a $[CL]_0/[BA]_0/[BD]_0$ initial ratio of 25/1.25/1.

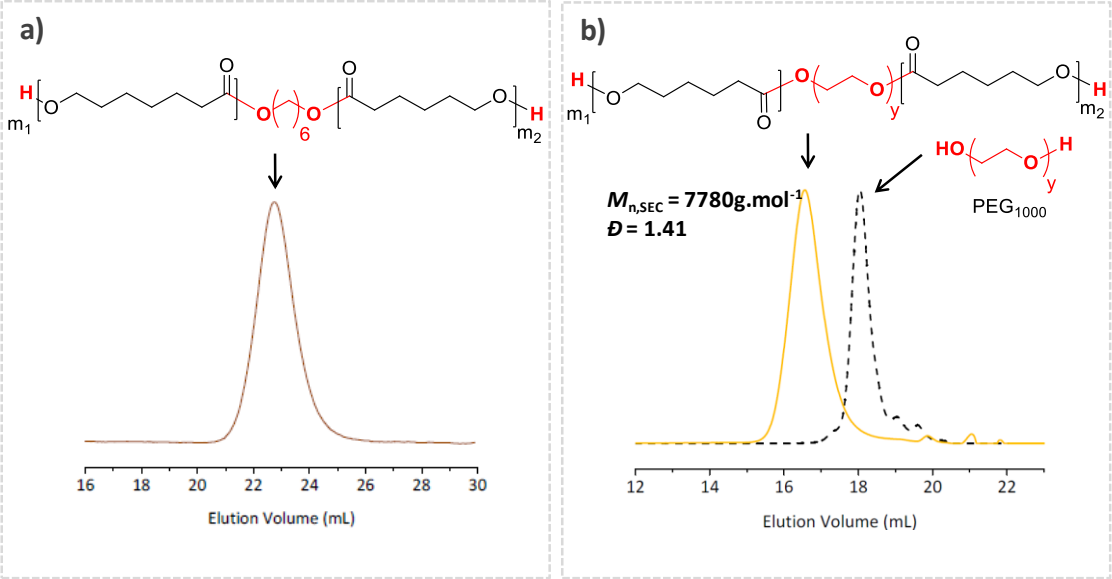

Figure 4. SEC traces of (a) crude PCL obtained from HDO (Table 1, Entry 7), (b) from PEG$_{1000}$ (dashed line) and crude triblock obtained (Table 1, Entry 8, solid line).

1.1.2 Monoalcohols as initiators for the BA-OROP of CL

The polymerization was then evaluated in the presence of two monoalcohols such as BnOH and HepOH targeting a DP between 25 and 50 in bulk at different temperatures ranging from 80 °C to 155 °C (Scheme 3). The results are summarized in Table 2.

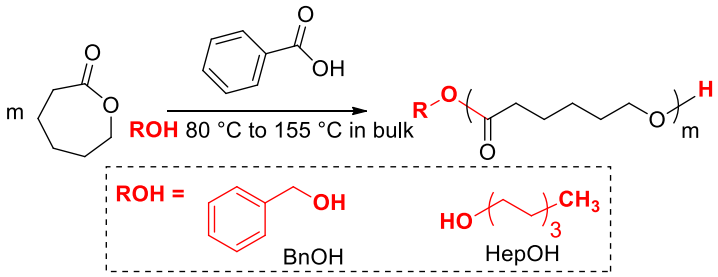

Scheme 3. BA-OROP of CL initiated by monoalcohols.

The BA-OROP of CL was first initiated by BnOH in the same conditions as previously, *i.e.* in bulk at 155 °C for a $[CL]_0/[BA]_0/[BD]_0$ initial ratio of 25/1.25/1 (Table 2, Entry 1). Well defined PCLs were obtained as shown by the linear increase of molar masses with monomer conversion and the observation of monomodal and symmetrical SEC traces (Figure 5a,b).

Table 2. Results and conditions of the BA-OROP of CL in bulk initiated by monoalcohol.[a]

Entry	I	Cat (%)[b]	$[M]_0/[I]_0$	T (°C)[c]	Time (h)	C_{CL} (%)[d]	$M_{n,SEC}$ (g.mol^{-1})[e]	$Đ$[e]	$DP_{.th}$[f]	$DP_{.\omega}$[g]
1	BnOH	5	25	155	3.8	89	4538	1.25	22.2	21.4
2	BnOH	5	50	155	8.2	98	9870	1.7	49.2	50.8
3	HepOH	5	50	155	8	97	9625	1.6	48.7	50.5
4	HepOH	2.5	50	155	16.2	98	8840	1.73	49.3	44
5	BD	5	100	155	7	94	16910	1.33	93.7	93.6
6	HepOH	5	50	80	96	86	8180	1.19	42.8	41.2
7	HepOH	5	50	120	16.3	79	7090	1.23	39.6	32.8
8	HepOH	5	50	140	14.2	86	7480	1.66	42.8	36.6

[a] Reactions were performed in bulk under argon atmosphere with reaction conditions: m_{CL}= 200 mg. [b]Catalyst loading rel. to the monomer; [c] Temperature of the BA-OROP of CL; [d] CL conversions were determined by ^{1}H NMR analysis. [e] Uncorrected number average molar mass ($M_{n,SEC}$) and dispersity ($Đ$) of crude polymers as determined by SEC chromatography (polystyrene standards) at 313 K and THF as eluent. [f] Theoretical degree of polymerization $DP,th = \frac{[M]_0}{[I]_0} \times C_M$. [g] Experimental degree of polymerization calculated from ω-chain ends PCL as determined by ^{1}H NMR. n.a.: not available.

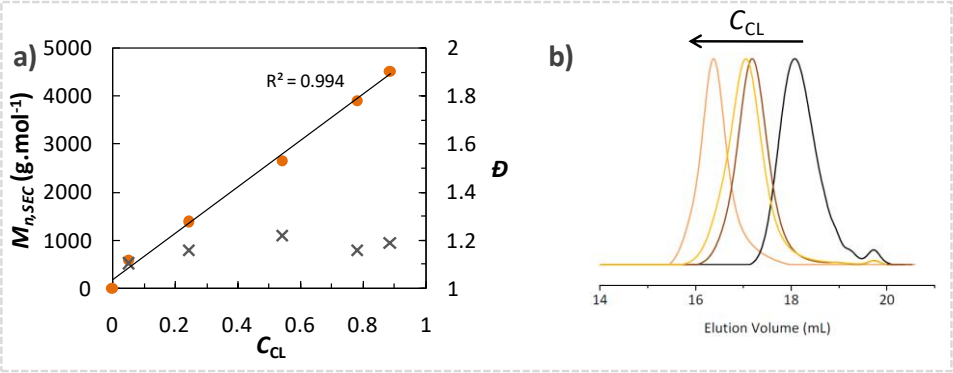

Figure 5. (a) Evolution of the uncorrected $M_{n,SEC}$ of the crude polymers (•), and dispersity $Đ$ (x) with monomer conversion and (b) SEC kinetic evolution (Table 2, Entry 1).

When targeting a DP of 50 using BnOH in the same conditions ($[CL]_0/[BA]_0/[BD]_0$ = 50/2.5/1 in bulk at 155 °C), the $M_{n,SEC}$ was found to evolve linearly with monomer conversion however the dispersity increased up to 1.7 as a result of the apparition of a second population on the SEC chromatograms (Figure 6a, Table 2, Entry 2). When using another monoalcohol such as HepOH in the same conditions, the same bimodal distributions is observed (Figure 6b, Table 2, Entry 3).

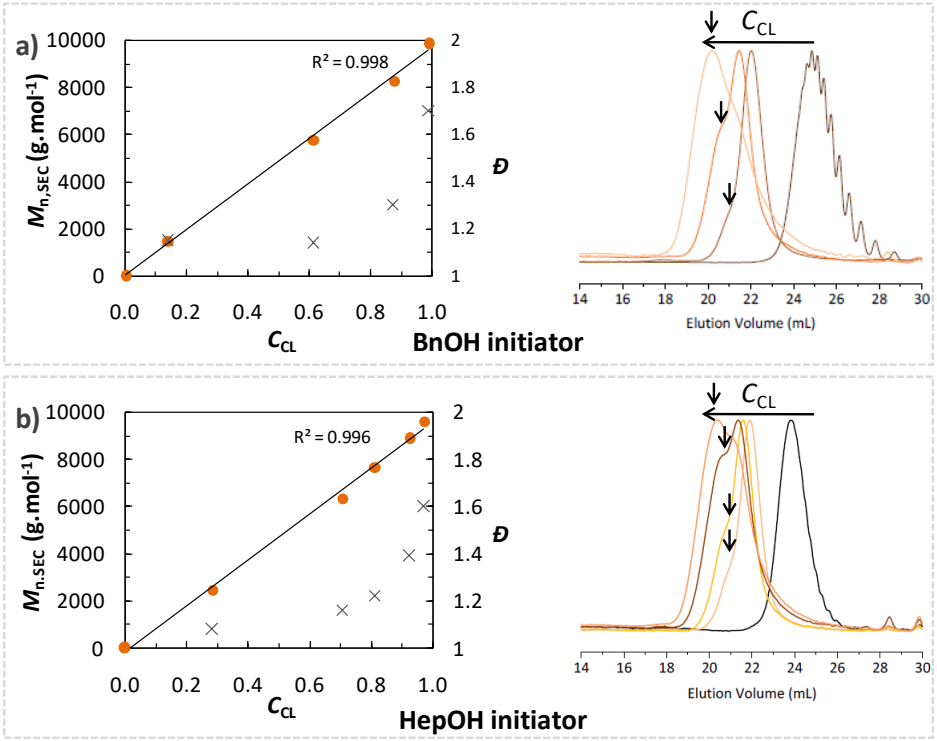

Figure 6. (a) Evolution of the uncorrected $M_{n,SEC}$ of the crude PCLs (•), and dispersity *Đ* (x) with monomer conversion (left) and SEC kinetic evolutions (right) for the BA-OROP of CL initiated by (a) BnOH and (b) HepOH (Table 2, Entries 2 & 3 respectively).

The reagents were thus dried and purified a second time, but nothing changed. We thus decided to decrease the catalyst loading in order to reach a $[CL]_0/[BA]_0/[BD]_0$ initial ratio of 50/1.25/1. However, the bimodal distributions could still be observed in the same conditions (Figure 7b, Table 2, Entry 4). It is worth to mention that this phenomenon has also been observed in other publications reporting the OROP of CL and was not clarified so far.[49,55,56,13,4,27,10,33]

MALDI-ToF MS analysis revealed that the major population of small PCL chains correspond to the expected PCL structure [m/z = 116 (M_{HepOH}) + m x114(M_{CL}) + 23(M_{Na+})] and that the second population, **B**, eventually corresponds to the same PCL chains but cationized with another counterion, *i.e.* Na_2I^+ (Figure 8a). Note that water did not co-initiate the BA-OROP of CL and that cyclic polymers, resulting from intramolecular transesterification reactions, are not observed.

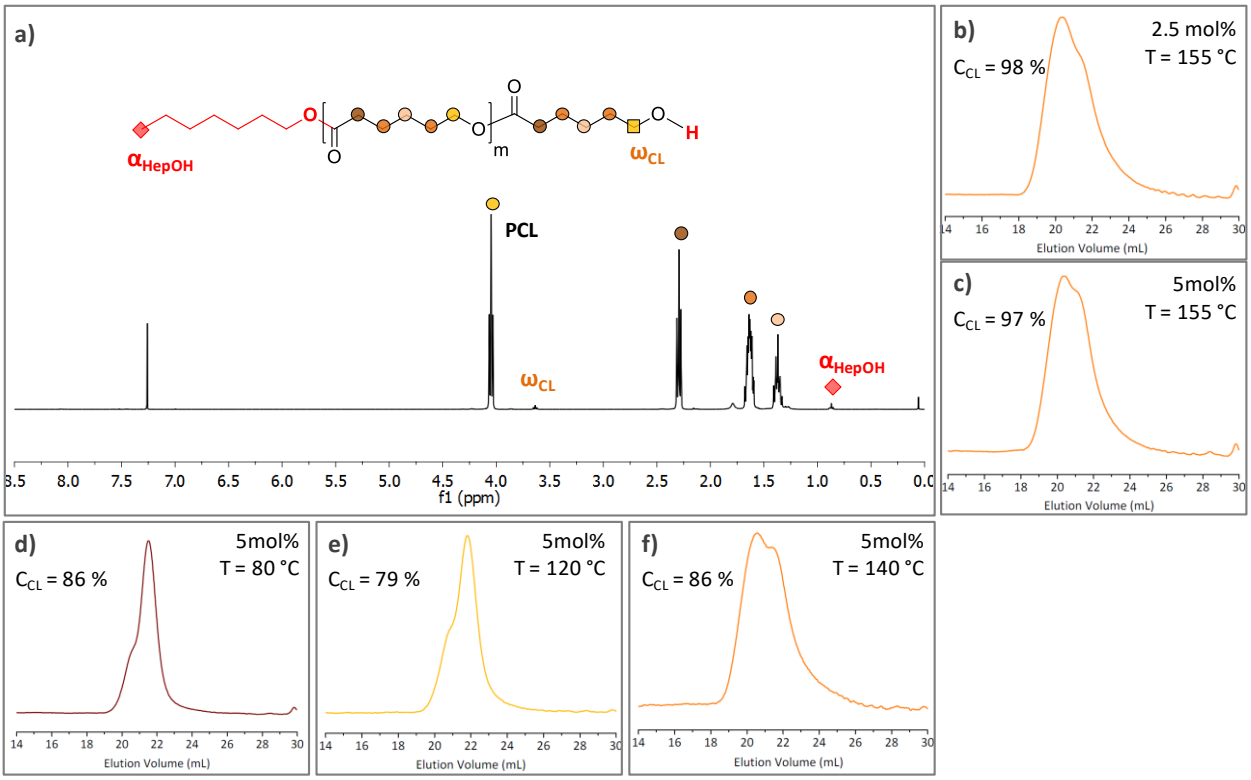

Figure 7. (a) ^{1}H NMR spectrum of pure PCL initiated by HepOH in bulk at 155 °C (Entry 3); SEC traces of PCL (b) Entry 4, (c) Entry 3, (d) Entry 6, (e) Entry 7 and (f) Entry 8, Table 2.

To gain insight into the origin of the shoulder observed in our SEC analyses, samples were fractionated by inverse precipitation (see experimental part) and the high molar masses were studied separately by MALDI-ToF MS analysis. The chains of high molar masses presented a PCL structure similar to the one obtained by initiation from HepOH and present a mass distribution for which m/z = 116 (M_{HepOH}) + m x 114 (M_{CL}) + 23 (M_{Na+}) (Figure 8b, Figure S3, Figure S4). It has to be noted that such high molar mass population has never been observed when the initiator used is a diol, such as BD (Figure 2, Table 1). To our own opinion, such apparition could be explained as follows:

1) The occurrence of a competing mechanism during the BA-OROP of CL as initiated by a monoalcohols. DFT calculations were involved in that problematic but did not provide any proof of such second mechanism (see section 3).

2) The occurrence of prominent intermolecular transesterification reactions. Indeed, when BD is used as initiator a first chain can transesterify only throughout the half of another chain (Figure 9a) while when HepOH is used, the first chain can transesterify throughout the backbone of a second chain (Figure 9b). In the latter case, the two final chains obtained after transfer can present two highly different molar masses (Figure 9b), while in the former case, those two transesterified chains possess relatively close molar masses (Figure 9a).

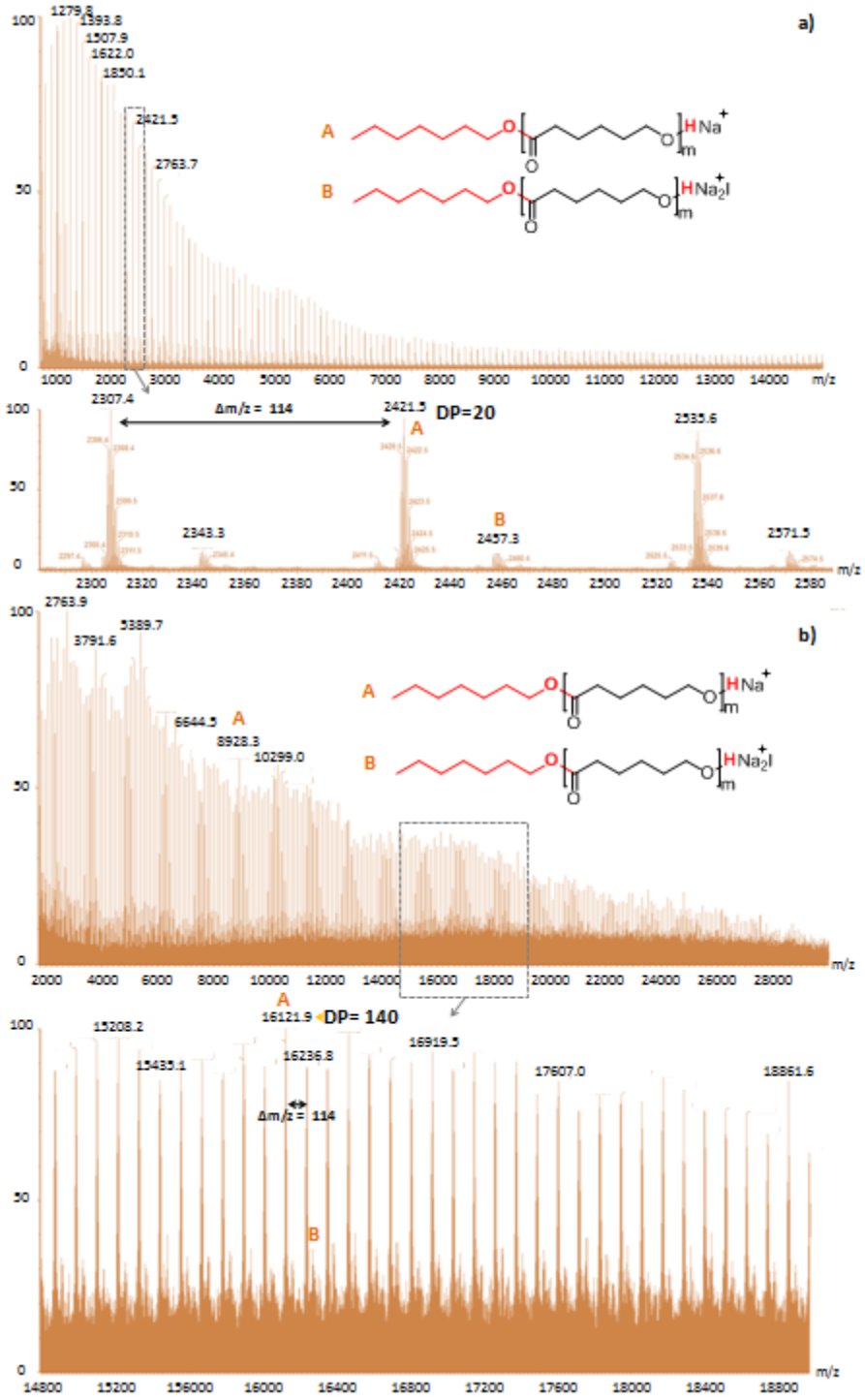

Figure 8. MALDI-ToF mass spectra of (a) PCL initiated from HepOH and of (b) the same PCL of higher molar masses obtained by inverse precipitation (Table 2, Entry 3). With M_{CL}= 114 g.mol^{-1}.

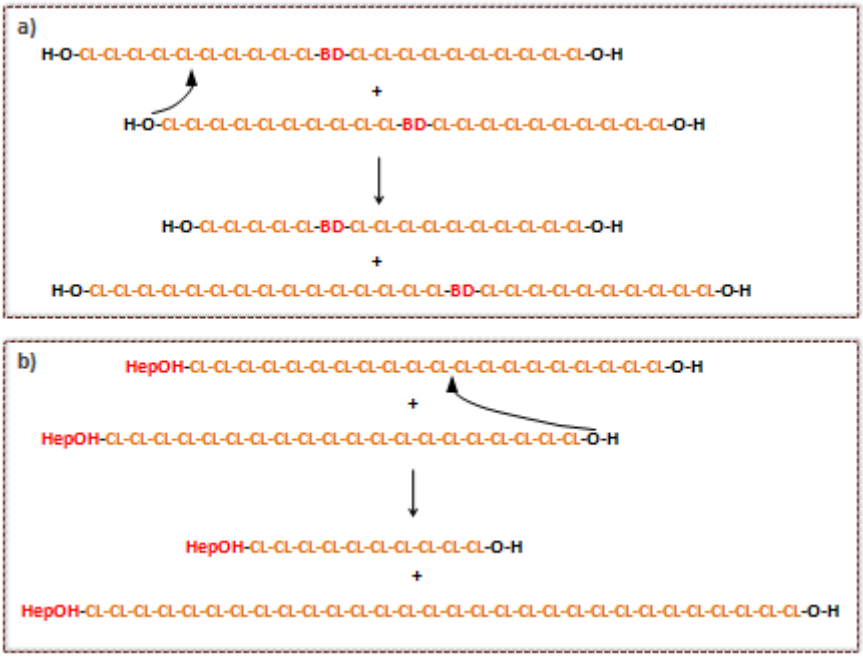

Figure 9. Difference of molar masses of the two PCL chains obtained after intermolecular transesterification between the two PCL chains initiated either from (a) BD or (b) HepOH.

The linear evolution of $M_{n,SEC} = f(C_{CL})$ with the broadening of the dispersity ($Đ$) (Figure 6) and the decrease of the second population of higher molar masses when the reaction temperature was lower, *i.e.* 140 °C, 120 °C and 80 °C supported the occurrence of transesterification reactions (Figure 7 d,e,f, Table 2, Entries 6, 7 & 8). Additionnally, generation of PCL chains of low molar masses can be observed on the SEC kinetic evolutions at higher elution volumes (Figure 6).

In conclusion the OROP of CL catalyzed by BA and initiated by alcohol initiator in bulk between 80 °C and 155 °C may involve the occurrence of transesterification reactions. This side reaction was highlighted by the presence of bimodal distributions in the SEC traces when monoalcohols were used as initiators. Nevertheless, substituted monoalcohols by diols enabled to decrease the principal issue of intermolecular transesterification reactions which is the broadening of the dispersity and the apparition of bimodal distribution. Overall the BA-OROP of CL initiated by diols proved to be relatively well "controlled" as the $M_{n,SEC}$ increased linearly with monomer conversion, the low dispersities obtained ($1.12 < Đ < 1.33$), the high chain end fidelity, the possibility to target the desirable molar masses and to extend the PCL chains.

1.2 Case of *L*-LA

The potential of BA to trigger the OROP of *L*-LA was also investigated (Scheme 4, Table 3, Entries 1-10). The same experimental conditions than those applied to the OROP of CL were first implemented with BD as initiator. The catalyst loading effect was assessed for a DP of 25 with 2.5-10 mol.% of BA rel. to CL (Table 3, Entries 2-4). Several reactions were also carried out in bulk for a DP of 25 and a catalyst loading of 5 mol.% rel. to the monomer at different reaction temperatures ranging from 140 °C to 180 °C (Table 3, Entries 3, 5, 6 and 7).

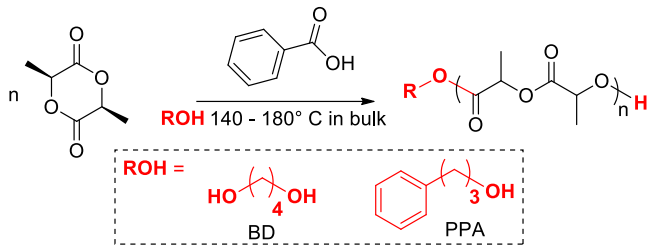

Scheme 4. BA-OROP of LA

Table 3. Results and conditions of BD-initiated BA-OROP of *L*-LA in bulk.[a]

Entry	I	Cat (%)[b]	$[M]_0/[I]_0$	T (°C)	Time (h)	C_M[c] (%)	$M_{n,sec}$[d] (g.mol^{-1})	$Đ$[d]	DP_{th}[e]	DP_{exp}[f]
1	BD	0	25	155	49	69	3660	1.09	17.2	16.5
2	BD	2.5	25	155	46	87	4750	1.17	21.8	23.4
3	BD	5	25	155	36.4	87	4620	1.12	21.8	20.7
4	BD	10	25	155	21	73	4050	1.09	18.2	17.8
5	BD	5	25	140	110.5	91	4140	1.17	22.7	22.5
6	BD	5	25	165	20	85	4160	1.14	21.1	20.4
7	BD	5	25	180	10.1	87	4230	1.13	21.7	21.3
8	BD	5	50	155	69.5	83	8940	1.21	41.4	40.7
9	BD	5	75	155	110	87	14540	1.29	65.2	66.6
10	PPA	5	25	155	87	88	4690	1.34	22	21.6

[a]Reactions were performed in bulk under argon atmosphere with reaction conditions: m_{LA}= 200 mg. [b]Catalyst content rel. to the monomer. [c]*L*-LA conversions were determined by ^{1}H NMR analysis. [d]Uncorrected average molar mass and dispersity ($Đ$) of crude copolymers determined by SEC (polystyrene standards), at 313 K and THF as eluent. [e]Theoretical degree of polymerization $DP,th = \frac{[M]_0}{[I]_0} \times C_M$. [f]Degree of polymerization calculated from the chain ends thanks to ^{1}H NMR.

Remarkably, the BA-OROP of *L*-LA in such conditions, *i.e.* in bulk at 155 °C enabled the synthesis of PLAs of controlled molar masses, with a good concordance between experimental and theoretical values, for initial *L*-LA/BD ratio in the range 25-75. Indeed, $M_{n,SEC}$ values were found to vary linearly with conversion whatever the targeted DP (Figure 10a,b) and dispersities remained low ($Đ$ < 1.29; Figure 10a,c and d, Figure S 5). It is worth mentioning that the reactions seemed also controlled when the temperature and the catalyst contents were varied (Figure S 6, Figure S 7).

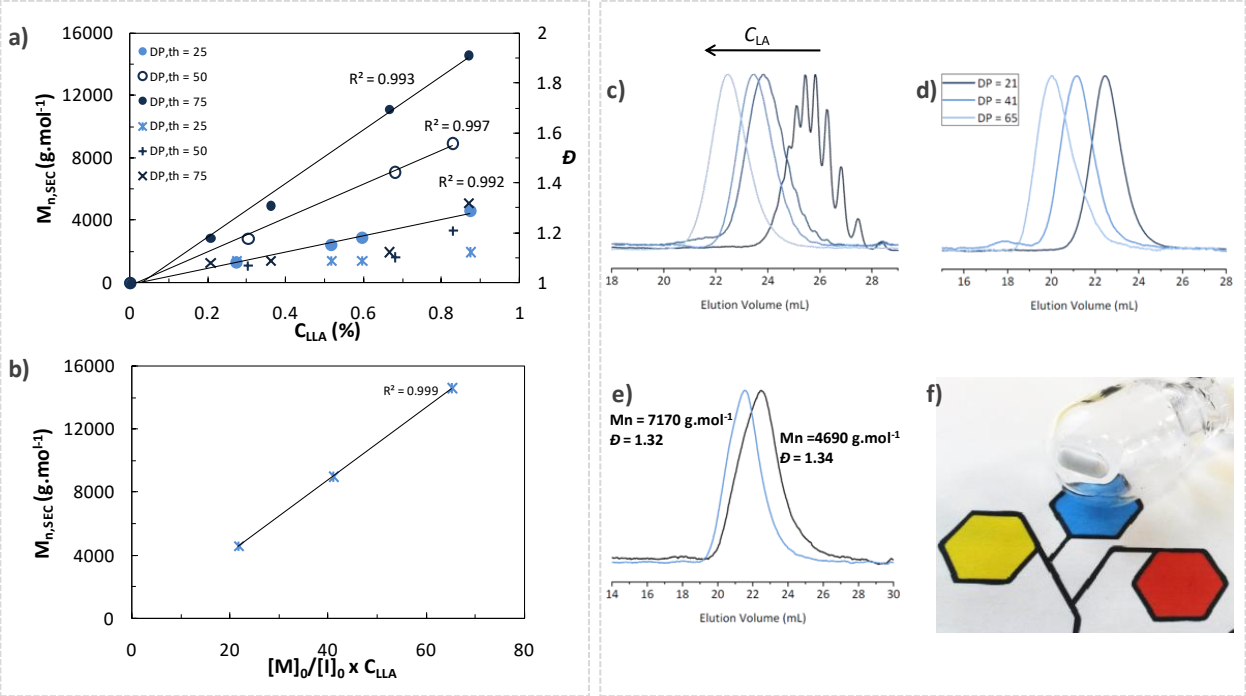

Figure 10. (a) Evolution of uncorrected $M_{n,SEC}$ (•) and dispersity $Đ$ (x) of PLA with monomer conversion; (b) Evolution of $M_{n,SEC}$ of PLAs with the monomer-to-initiator ratios multiplied by the monomer conversion (Table 3, Entries 3, 8 & 9). (c) SEC kinetic evolution (Table 3, Entry 3); (d) SEC comparison of entries 3, 8 & 9, Table 3; (e) Chain extension experiment initiated by PPA (see main text); (f) Picture of a crude PLA obtained after 110 h of reaction at 155 °C (Table 3, Entry 9)

As in the case of BA-derived PCL, ^{1}H NMR analysis of PLA samples showed diagnostic signals arising from the initiator. One initiator fragment per polymer chain was thus determined, attesting to the excellent agreement between DP_{th} and DP_{exp} and to the high end-group fidelity (Figure 11, Table 3).

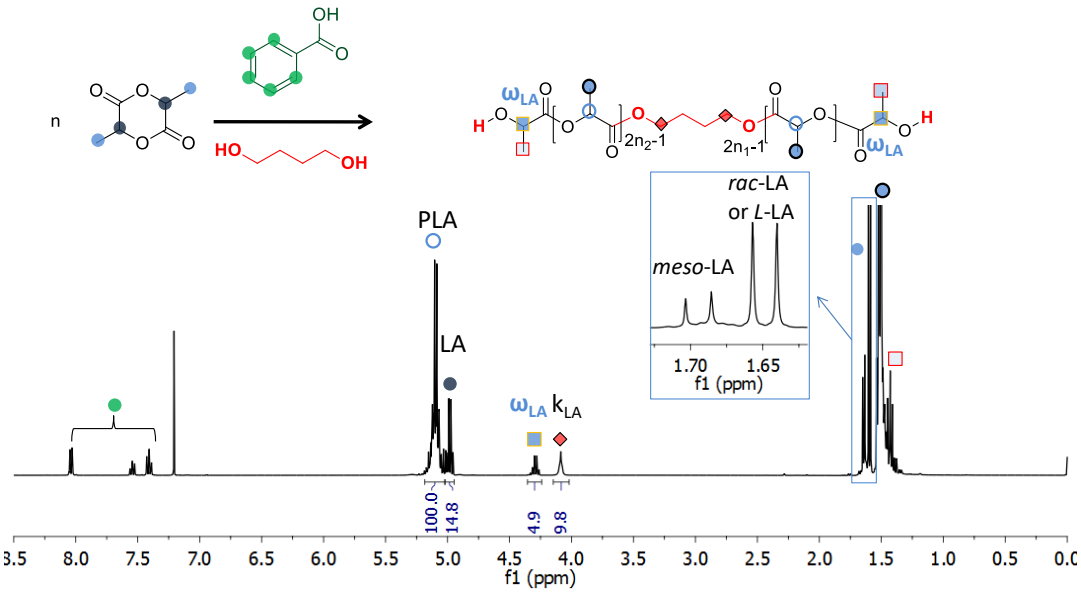

Figure 11. ^{1}H NMR spectrum ($CDCl_3$, 400.2 MHz, r.t) of crude PLA obtained by BA-OROP of *L*-LA initiated by BD in bulk at 155 °C (Table 3, Entry 3).

MALDI-ToF MS analysis of a representative PLA sample also confirmed the incorporation of the BD initiator (Figure 12b, Table 3, Entry 3) with a distribution of peaks consistent with the formation of a α,ω-bis-hydroxy PLA (cationized with sodium), and a peak-to-peak mass increment of 144 g.mol^{-1} corresponding to the molar mass of a *L*-LA monomer unit ($M_{LA,}$ Population **A**). Occurrence of transesterification, *i.e.* intermolecular chain transfer, was however evidenced to some extent, through the presence of signals apart by 72 Da (Population **D**), characteristic of PLAs obtained at high temperature.[34,35] The amount of intermolecular transesterification reactions could be limited by decreasing the polymerization temperature to 140 °C (Figure 12a, Table 3, Entry 5). Water co-initiation could not be evaluated as the peaks consistent with the formation of α-carboxy PLA (cationized with sodium, Population **B**) were under the peak of the population **A.** However, NMR analysis suggested good agreement between $DP_{,th}$ and $DP_{,exp}$ and the α-carboxy PLA cationized with two sodiums were relatively inconspicuous on the MALDI-ToF MS spectra (Population **C**) meaning that most of PLA chains were initiated by BD. Additionally, cyclic PLAs (Population **F**), resulting from intramolecular transesterification reactions could barely be observed on the MALDI-ToF MS spectra (Figure 12a,b).

Surprisingly, while PLAs are generally colored when synthesized in bulk from *N*-containing organocatalysts,[19,35] BA here led to colorless PLAs (Figure 10f) even when performing the OROP reaction at 180 °C.

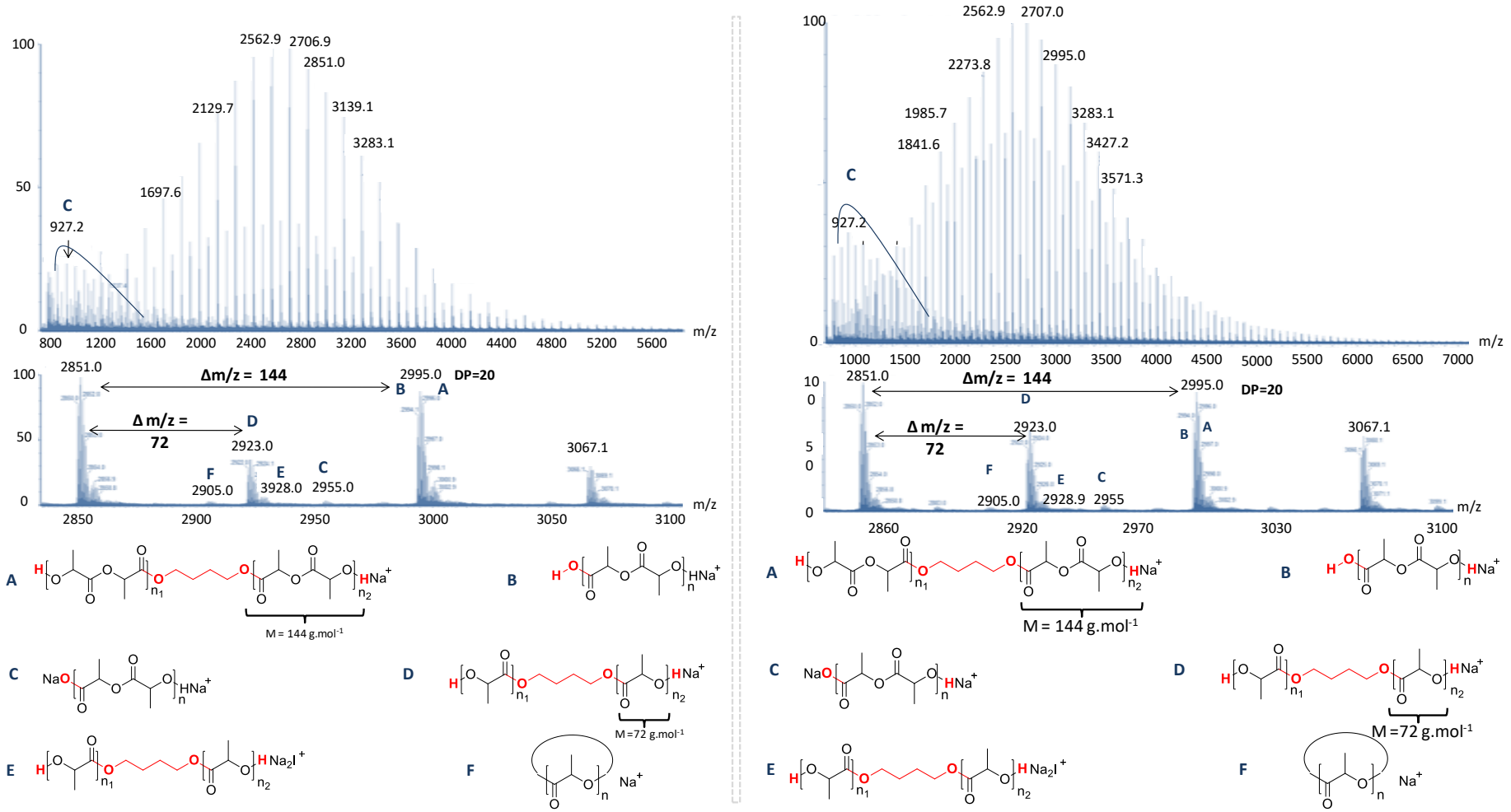

Figure 12. MALDI-ToF MS spectra of pure PLAs initiated from BD synthesized (a) at 140 °C (Table 3, Entry 5) and (b) at 155 °C (Table 3, Entry 3). With M_{LA}= 144 g.mol^{-1}, $M_{LA/2}$ = 72 g.mol^{-1}.

Another side reaction, namely the epimerization of *L*-LA in *meso*-lactide (*meso*-LA) was evidenced by the presence of the peaks assigned to the -CH_3 of *meso*-LA at 1.71 ppm on the ^{1}H NMR of crude PLA obtained by the BA-OROP of *L*-LA (Figure 11).[36] This side reaction, which is generally induced by basic organocatalysts (see Chapter 1 section 1.5),[34,37,28,38,20] is an issue of concern as this leads to the loss of crystallinity of PLA material and thus to the loss of the thermal and mechanical properties. This was supported by the fact that amorphous PLAs, namely without melting points (T_m), were obtained in the present study (Figure S 9).

In order to understand what caused the epimerization, model experiments were carried out. First, *L*-LA was heated alone at 155 °C during 48h in order to discard the possibility of a spontaneous epimerization of *L*-LA under these conditions. Heated alone only 3.2% of *L*-LA was epimerized in *meso*-LA while in the presence of BA, around 17.4% of *L*-LA was epimerized in the same conditions (Figure S 10& Figure S 11). In the sole presence of alcohol initiator less than 8% of *L*-LA was transformed in *meso*-LA (Figure S 12). BA may thus induce an epimerization of *L*-LA and the mechanism will be discussed in the section 3 supported by DFT calculations.

Finally, chain extension experiments were successfully achieved, in this case in presence of 3-phenylpropanol (PPA) as initiator and BA as organocatalyst. The bulk OROP of *L*-LA at 155 °C ($[L\text{-LA}]_0/[PPA]_0/[BA]_0 = 25/1/1.25$) first led to a PLA with a final $M_{n,SEC}$ = 4690 g.mol^{-1} and $Đ$ = 1.34 after 87h, reaching 88% conversion (Table S 2, Entry 1, Figure S 13). After purification, subsequent addition of *L*-LA and BA ($[L\text{-LA}]_0/[PLA]_0/[BA]_0$= 25/1/1.25), and heating the reaction mixture to 155 °C, gave a final PLA of increased molar mass after 55h: $M_{n,SEC}$ of 7170 g.mol^{-1} and a $Đ$ = 1.32 (Figure 10e, Table S 2, Entry 2).

In conclusion the BA-OROP of *L*-LA in bulk at 155 °C was relatively “controlled” yielding colorless PLAs with the expected degree of polymerization and narrow dispersities for bulk polymerization. Furthermore, the $M_{n,SEC}$ was shown to increase linearly with monomer conversion and chain extension experiments were successful. However, side reactions such as intermolecular transesterification reactions and epimerization diminished the level of control of the ROP of *L*-LA catalyzed by BA.

2 Kinetic and mechanism

After BA was demonstrated to efficiently trigger the OROP of the two monomers, reaction kinetics were investigated. Series of BD-initiated BA-OROP experiments were thus conducted at 155 °C using $[Monomer]_0/[BD]_0$ = 25 at three catalytic loadings, namely, 2.5, 5 and 10 mol.% rel. to the monomer. Resulting semi-logarithm plots (Figure 13a,b,c) showed a pseudo

first-order kinetic plot in the case of *L*-LA monomer. As for the OROP of CL, kinetics revealed an inhibition period (Figure 13d).

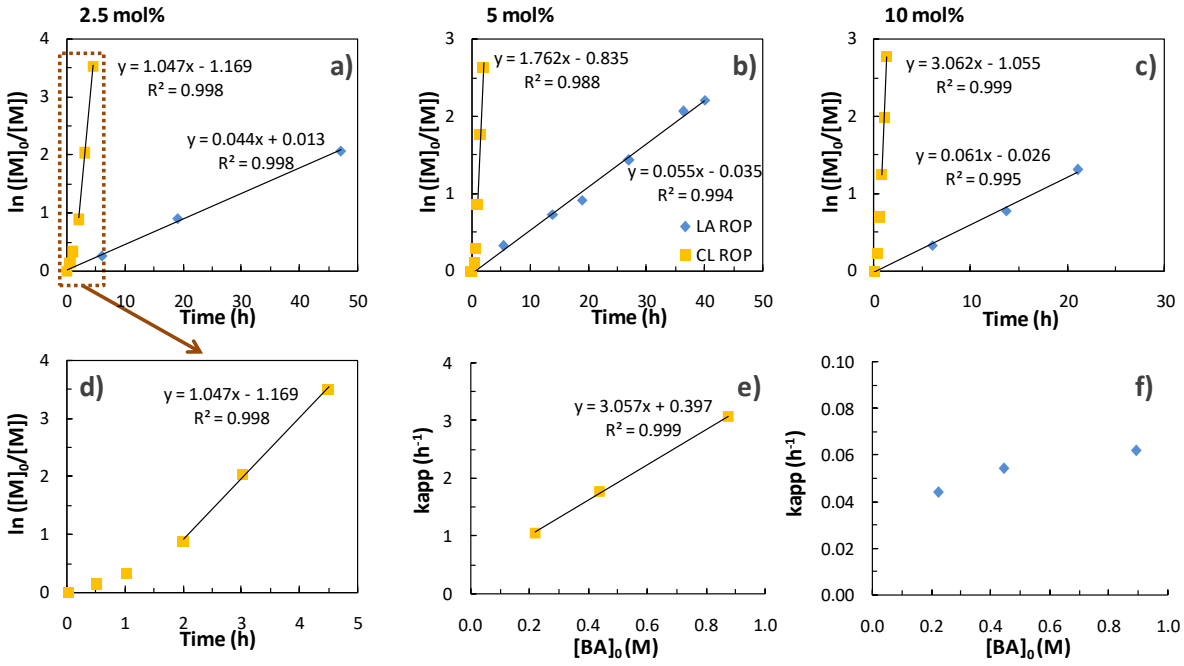

Figure 13. Semi-logarithmic kinetic plots of the BA-OROP of CL (yellow squares) [Table 1, Entries 2 to 4] and *L*-LA (blue diamonds) [Table 3, Entries 2 to 4] using BD as initiator in bulk at 155 °C for $[M]_0/[I]_0$ = 25 and (a) 2.5 mol.%, (b) 5 mol.% and (c) 10 mol.% of BA catalyst rel. to the monomer. (d) Semi-logarithmic kinetic plot of BA-OROP of CL using 2.5 mol% of BA catalyst. The plot of the k_{app} *vs.* the catalyst concentration $[BA]_0$ for the BA-OROP of (e) CL and (f) *L*-LA.

To gain more insight into such kinetics, benzyl alcohol (BnOH) was selected as initiator, probing conversion of the latter by ^{1}H NMR analysis. Methylene protons of BnOH indeed showed a diagnostic signal at 4.68 ppm, while methylene oxycarbonyl-type protons, *i.e.* after initiation, shifted to 5.09 ppm (Figure 14a). The first order kinetic plots, $\ln([M]_0/[M])$ *vs.* time, revealed an induction period that was ascribed to a relatively slow initiation (78% of BnOH was converted after 0.5h, Figure 14b, Table S 3), linear evolution being eventually noted after nearly full conversion of BnOH (98%, after 1.25h).

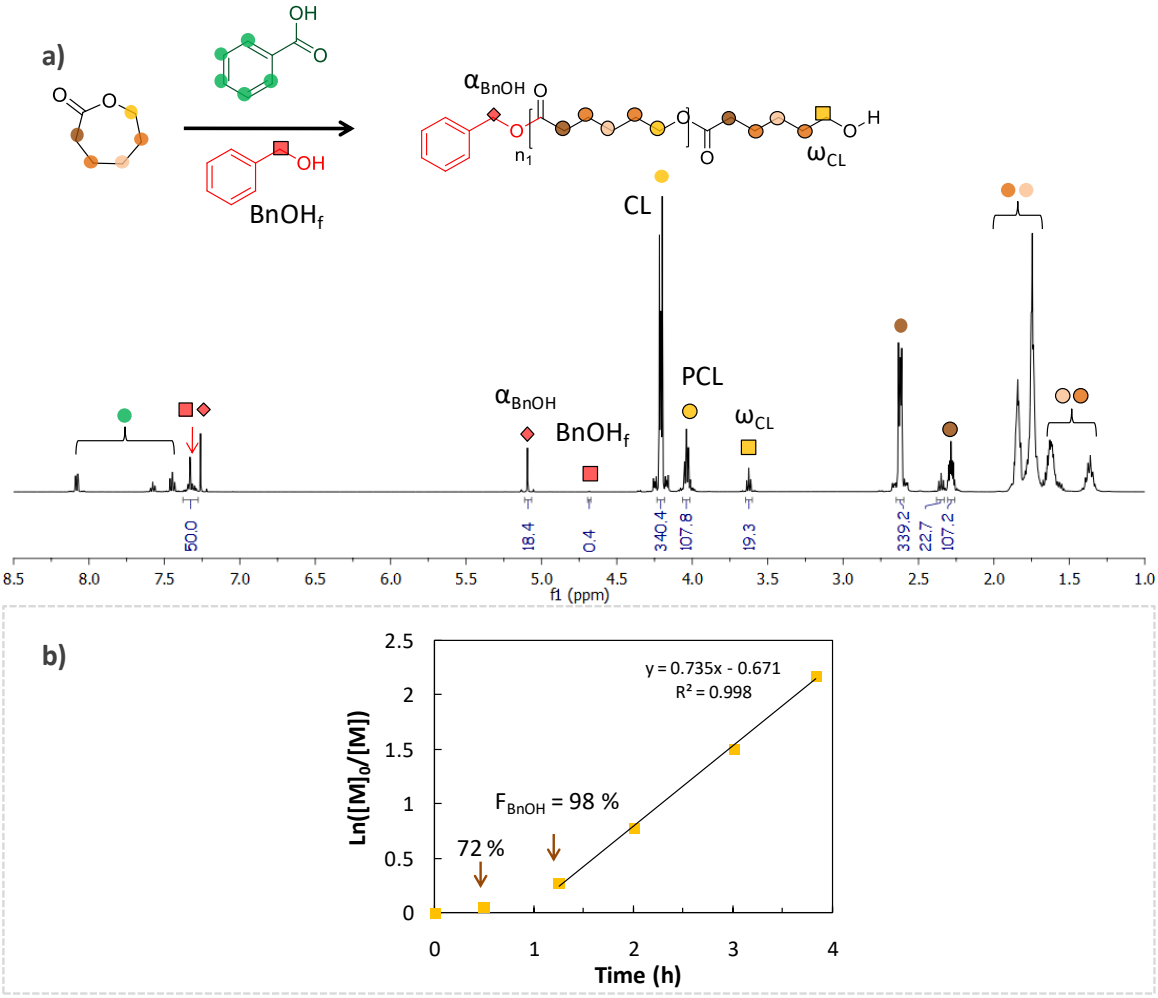

Figure 14. (a) ^{1}H NMR spectrum of crude PCL obtained by BA-OROP of CL initiated by BnOH in bulk at 155 °C (Table S 3, Entry 2) ($CDCl_3$, 400.2 MHz), (b) Semi-logarithmic kinetic plot BA-OROP of CL initiated by BnOH in bulk at 155 °C (Table 2, Entry 1).

Overall, BA-OROP of CL proved faster than that of *L*-LA, consistently with previous findings regarding acidic organocatalyts, namely, TfOH and DPP.[6,39] Model reactions consisting in mixing equimolar amounts of BA and each of the two monomers were analysed by ^{13}CNMR in $CDCl_3$. A clear shift of the carbonyl carbon of CL, from 176.32 to 176.55 ppm, was detected, suggesting CL was activated by BA (Figure 15a). Chemical shift was less clear in the case of *L*-LA (167.51 ppm to 167.56 ppm; Figure 15b), confirming a higher efficacy of acidic catalysts towards OROP of CL. In addition, higher loadings in BA (5-10 mol.% *vs.* 2.5 mol.%) increased the apparent propagation rate constant (k_{app}) of the BA-OROP of CL by a factor of 2 & 3, whereas under the same conditions, the increase of k_{app} was only 1.25 and 1.38 higher for the BA-OROP of *L*-LA. Note that this could mean that the carbonyl group of CL is surely more basic than that of *L*-LA.

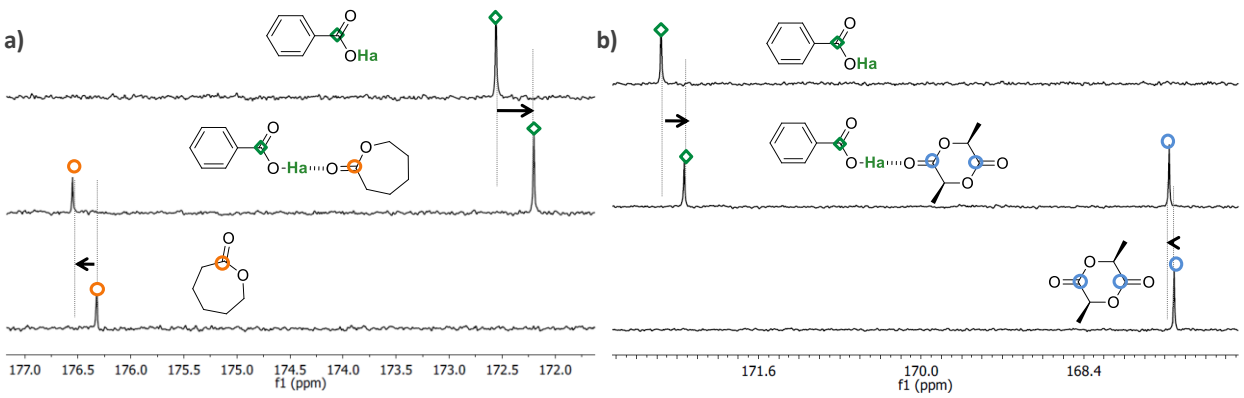

Figure 15. ^{13}C NMR spectra of the carbonyl region of an equimolar mixture of (a) BA and CL and of (b) BA and *L*-LA ($CDCl_3$, 100.6 MHz).

OROP reactions were then conducted by varying the concentration of BD at a constant catalyst concentration of 5 mol.% rel. to the monomer (Figure 16a,b). This allowed us to evidence that $\ln(k_{app})$ varied linearly with $\ln([I]_0)$ (Figure 16c,d, Table S 4, Table S 5).

In other words, the dependence in initiator for both BA-OROPs of CL and *L*-LA was first-order, which allowed us to express the following kinetic equation, where $k_{app} = k_p[BA]_0^Y[BD]_0$ is the apparent rate constant and [M] the monomer concentration:

$$-\frac{d[M]}{dt} = k_{app} \times [M]$$

Furthermore, while k_{app} was found to evolve linearly with $[BA]_0$ in the case of the OROP of CL (Figure 13e), a downward curvature was noted in the case of *L*-LA (Figure 13f). This could be rationalized by the occurrence of competitive interaction/deactivation of PLA hydroxyl chain ends by BA for a high catalyst loading. Similar observations have been made by Bourrissou *et al*. regarding the TfOH-OROP of CL in which the apparent rate constant decreased for high TfOH: initiator ratios.[1]

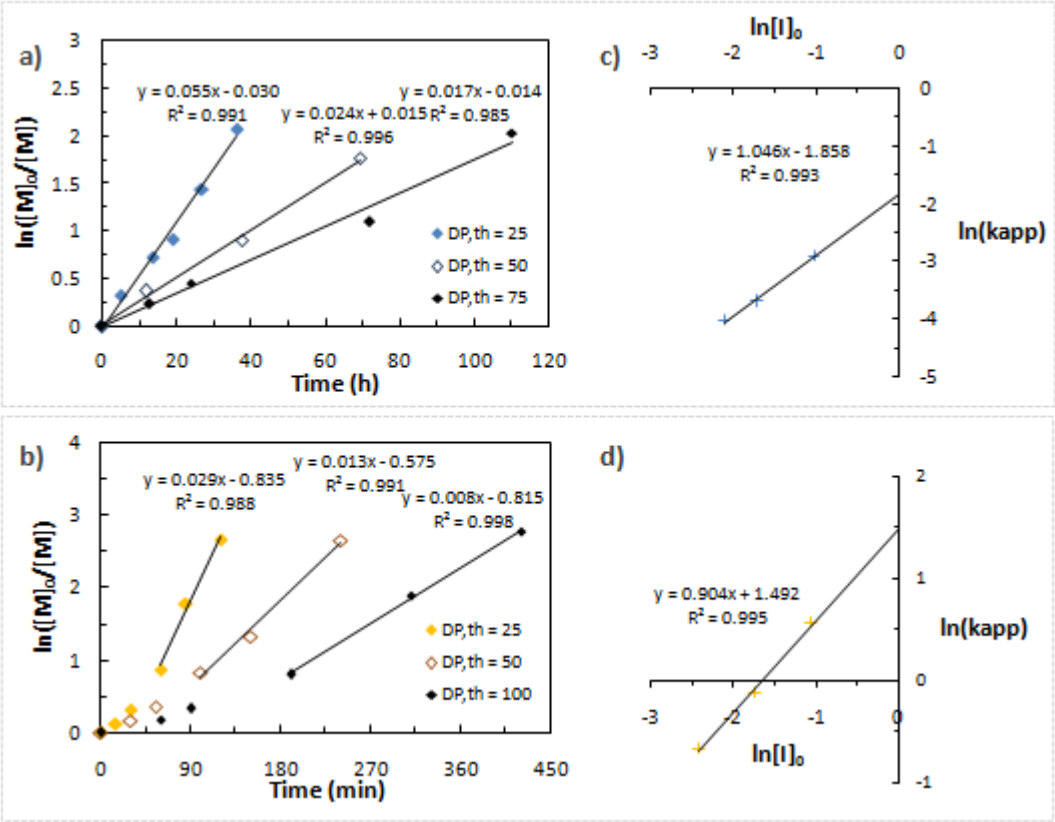

Figure 16. Semi-logarithmic kinetic plots of the BA-OROP of (a) *L*-LA (Table 3, Entries 3, 8 & 9) and (b) CL (Table 1, Entry 3, 5 & 6) initiated by BD in bulk at 155 °C for different targeted degrees of polymerization. $\ln(k_{app}) = \beta \ln([I]_0) + \ln(k_p)$ for the ROP of (c) *L*-LA and (d) CL. With β the kinetic order relative to the initiator.

Model experiments involving this time mixtures of BA and BD in various proportions ($0.5 < [BA]_0/[BD]_0 < 5$) were monitored by ^{1}H NMR spectroscopy in $CDCl_3$. A progressive downfield shift of the hydroxy proton of BD was noted as $[BA]_0/[BD]_0$ increased, demonstrating the existence of the H-bonding between the two components (Figure 17a,b).

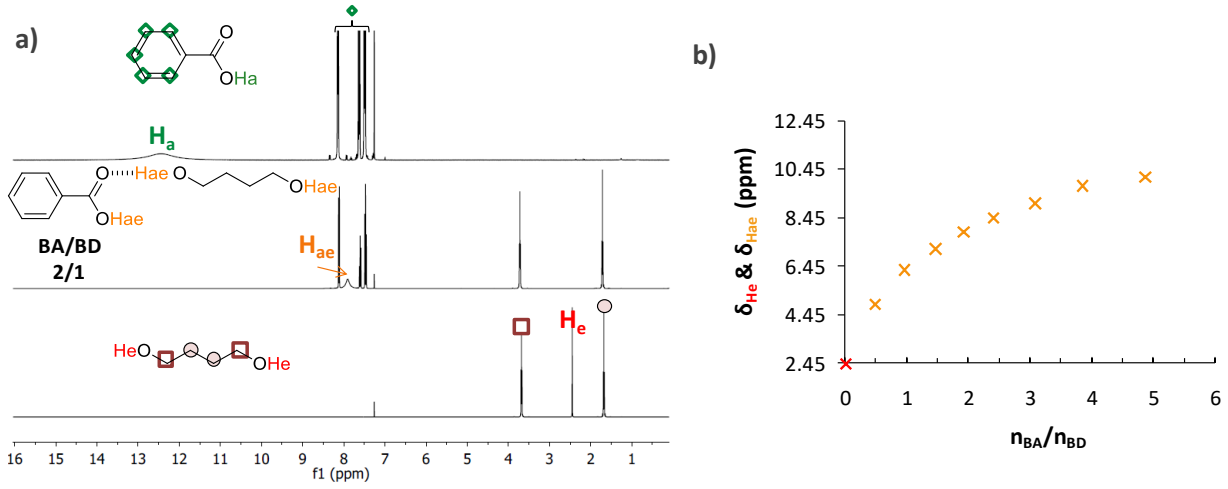

Figure 17. (a) ^{1}H NMR spectra of a mixture of BA and BD (1/2), (b) Chemical shifts of the H_{ae} proton in the ^{1}H NMR spectra observed when BD is mixed with BA in $CDCl_3$ with different n_{BA}/n_{BD} ratios.

All these results appear consistent with the occurrence of a bifunctional mechanism, where both the monomer and the initiator are activated by the organocatalyst, similarly to previous reports utilizing stronger organic acids in OROP of cyclic esters.[3,40,41] The mechanism would thus involve protonation of the carbonyl moiety of the monomer by BA and simultaneous deprotonation of the initiator by the conjugated base of BA enabling the nucleophilic attack (Scheme 5, (**1**)). Ring-opening would be assisted by BA (**2**) leading to a complex between the ring-opened monomer and the catalyst (**3**), as depicted in Scheme 5.

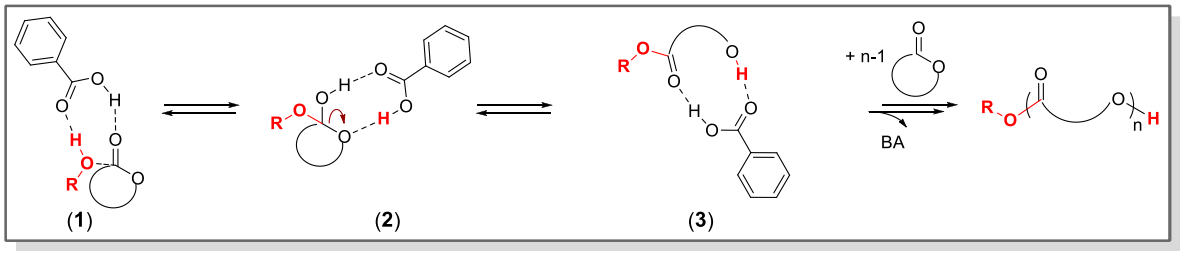

Scheme 5. Bifunctional mechanism proposed for the ROP of lactones catalyzed by benzoic acid (BA).

3 Density functional theory: Toward the reactivity of *L*-LA and CL.

These calculations were performed by Coralie Jehanno, completing her PhD between the Institute for polymer materials (POLYMAT) at the University of the Basque Country UPV/EHU, in San Sebastian under the supervision of Dr. Haritz Sardon and Dr. Fernando Ruipérez and the School of Chemistry at the University of Birmingham under the supervision of Pr. Dove.

All density functional theory (DFT) calculations were carried out with Gaussian 09 suite of programs[42] using the ωB97X-D hybrid functional[43] and with the 6-31+G(d,p) basis set at T =

428 K. To confirm that the optimised structures were minima on the potential energy surfaces, frequency calculations were carried out at the same level of theory and then used to evaluate the zero-point vibrational energy (ZPVE) and the thermal vibrational corrections. The electronic energy was refined by single-point energy calculations at the ωB97X-D/6-311++G(2df,2p) level of theory. All geometry optimisations were performed with the SCRF solvent model and as permittivity of CL is $\varepsilon_{0,CL}$ = 36.5 at room temperature, the SCRF parameter of acetonitrile (ε_0 = 35.6) was used. To our knowledge, the permittivity of *L*-LA is not reported in the literature, then, acetonitrile SCRF parameter was also used. The initiator of the reaction (butane-1,4-diol) have been modeled by an ethanol molecule while the structures of the reagents (*L*-LA and CL) and the catalyst (BA) have been kept.

3.1 Mechanism investigations

Three plausible mechanisms for the BA-OROP of *L*-LA and CL were studied involving two different transition states (TSs, Scheme 6). The bifunctional mechanism (path I) describes a cooperative dual activation of both the initiator/chain end and the monomer carbonyl by BA, while the electrophilic activated monomer mechanism (AMM, path II) describes the activation of the monomer only by BA. Both mechanisms (path I & II) involve first the nucleophilic attack of the initiator/propagating chain on the lactone (TS1), before the ring-opening of the cyclic monomer (TS2).[44,45,46] As for the covalently bound mechanism (path III, Scheme 6), this involves two different TSs, namely the nucleophilic attack of the BA carbonyl on the lactone (TS1) followed by the attack of the initiator/chain end on the ring-opened lactone involving the subsequent BA elimination (TS2).

The bifunctional mechanism (path I), is energetically favored by at least 15.3 kcal.mol^{-1} over the covalently bound mechanism (path III, TS1, Figure 18). In addition, no transition state (TS) could be isolated for the highly reported AMM (path II). The different trials led to the rearrangement of the system to isolate the same TS than for the bifunctional mechanism (path I).

According to calculations the BA organocatalyst may thus follow a bifunctional mechanism for the BA-OROP of *L*-LA and CL. Indeed, the catalyst possesses an acidic moiety (-C-O-H) and a basic moiety (-C=O), in other words the BA catalyst could act as a proton shuttle allowing a fast exchange of protons between the monomer and the initiator/chain ends as explained in Scheme 5 (section 2). These results support our experimental results (section 2) and are consistent with the mechanisms previously reported, by Martin-Vaca, Bourissou and Maron *et al.* for sulfonic acid- and phosphoric acid-OROP of cyclic esters.[40,3]

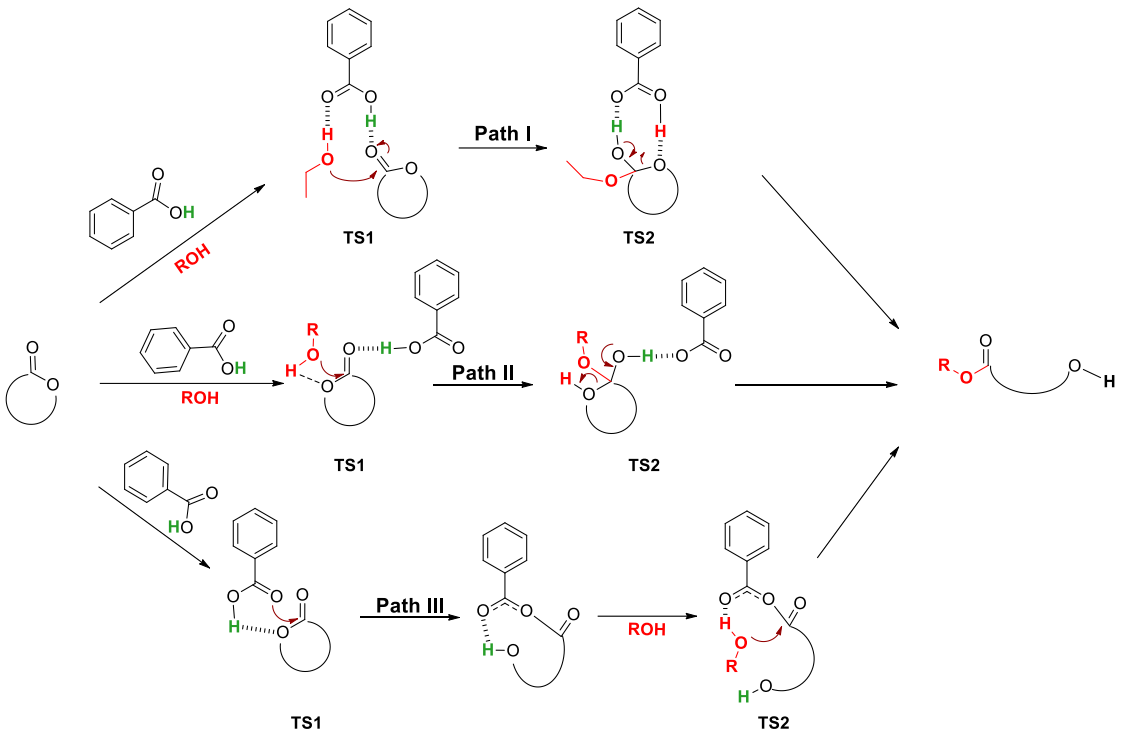

Scheme 6. Plausible mechanisms for the ROP of lactones organocatalyzed by BA. Path I being the bifunctional mechanism, path II the electrophilic AMM and path III the covalently bound mechanism.

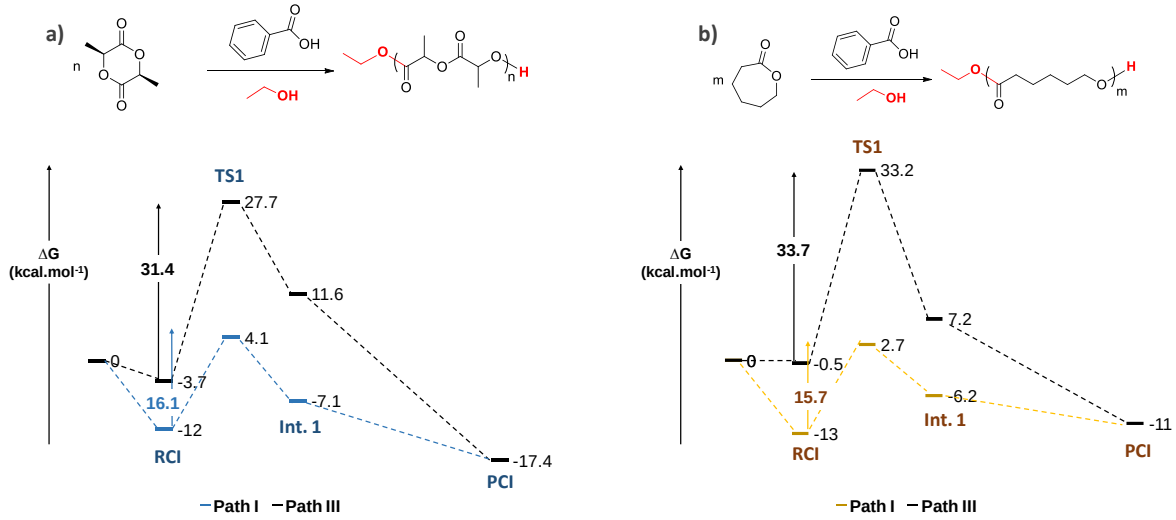

Figure 18. Energetic profiles of the BA-OROP of (a) *L*-LA and (b) CL involving either the bifunctional mechanism (Path I) or the covalently bound mechanism (Path III).

Both initiation (I) and first propagation (P) of the ROP of *L*-LA and CL were then studied and involved two TSs each. Firstly, the nucleophilic attack of the initiator/propagating chain on the lactone (TS1) and, secondly, the ring-opening of the cyclic monomer (TS2, Figure 19).

3.2 Initiation

Calculations predicted that the initiation step of the BA-OROP of *L*-LA and CL did not present significant differences in term of energetic barriers. Indeed, the energetic barriers of the rate determining step, *i.e.* **TS1 I** were 15.7 and 16.1 kcal.mol^{-1} and of the second step, *i.e.* **TS2 I** were 11.8 and 11 kcal.mol^{-1} for ROP of CL and *L*-LA, respectively (Figure 19c). These results were surprising since the carbonyl group of CL was predicted to be more activated by benzoic acid than that of *L*-LA by model experiments using NMR (section 2). We thus expected to observe different behaviors for both monomers. A possible assumption could be that primary alcohol initiators ring-opened more easily the *L*-LA than the CL at high temperature and could offset the higher activation of the carbonyl of CL by BA. Indeed, BD was shown to trigger the bulk ROP of *L*-LA (C_{LA} = 45% in 24 h) on its his own while it could not trigger by itself the ROP of CL at all under otherwise identical conditions (Table 1, Entry 1, C_{CL} = 0%, 22h).

The only noteworthy variation on the energetic profiles for the initiation (Figure 19c) concerned the final product complex **PC I**, far more stable for *L*-LA (-17.4 kcal.mol^{-1}) than for CL (-12 kcal.mol^{-1}).

3.3 Propagation

Contrary to initiation, the propagations involved in the BA-OROP of CL and *L*-LA exhibit energetic differences (Figure 19c). The initial complex involving the catalyst, chain end and the monomer (reagent complex, **RC P**), was much lower in energy during the ROP of *L*-LA than during the ROP of CL (ΔE = 7.3 kcal.mol^{-1}). Moreover, the energetic barrier required to overcome the first transition state of the propagation (**TS1 P**, nucleophilic attack) was higher for the ROP of *L*-LA (21.2 kcal.mol^{-1}) than for the ROP of CL (15.5 kcal.mol^{-1}). The difference between both energetic barriers may first be explained by the difference of propagating alcohols. Indeed, in the case of PCL the active species are primary alcohols while in the case of PLA the active species correspond to more sterically hindered secondary alcohols (Scheme 7a,b). Additionally, one can assume that during the ROP of *L*-LA the nucleophilic attack might also be impeded by steric hindrance of the methyl group in alpha position of the monomer carbonyl (Scheme 7a). These results were consistent with experimental data as the BA-OROP of *L*-LA was slower (Table 3, Entry 3, 40 h) than that of CL (Table 1, Entry 3, 2 h) under otherwise identical conditions. Note that we wanted to compare the ring strain of both monomers but CL being a monolactone and

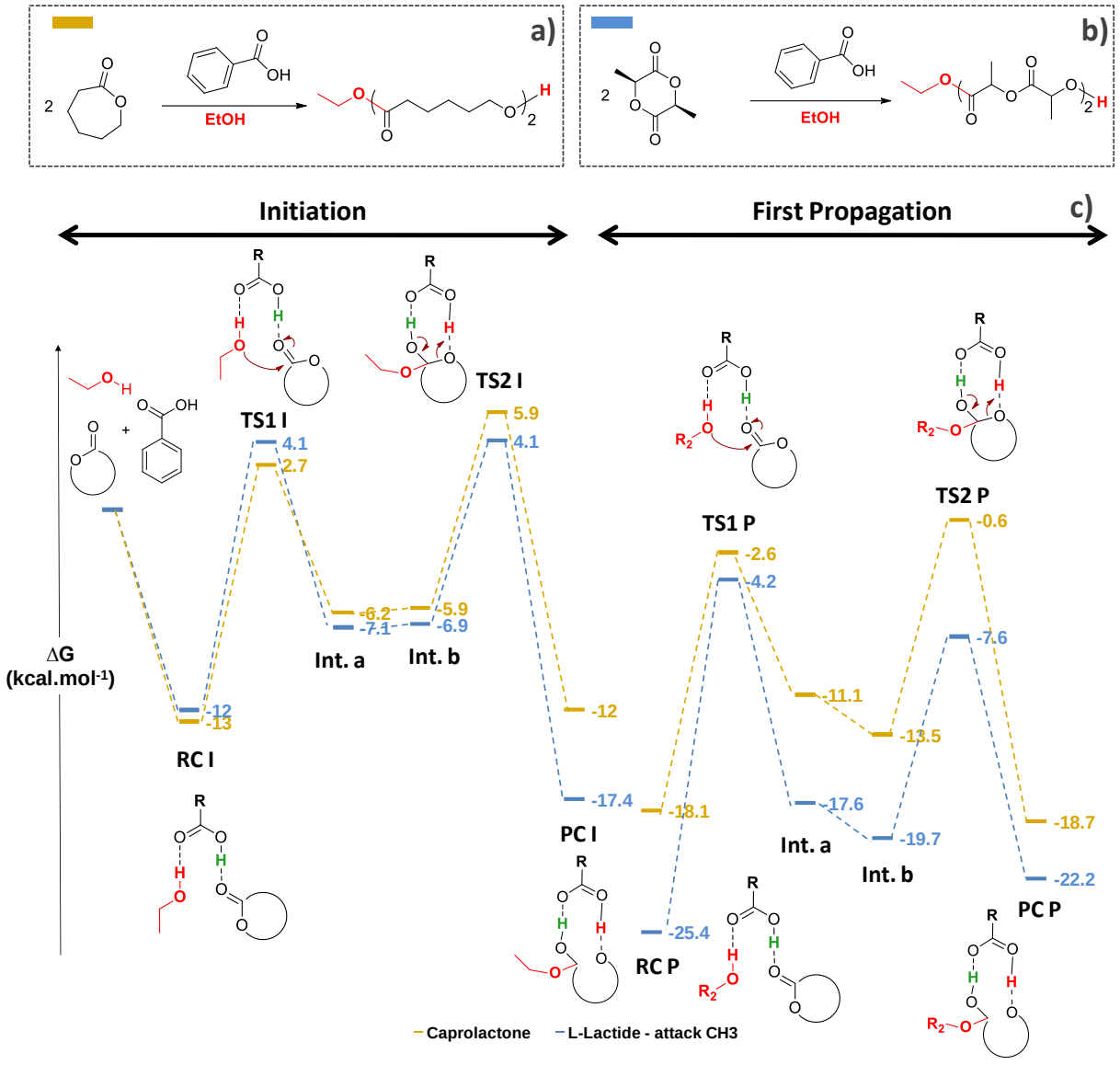

Figure 19. Scheme of the BA-OROP (a) of CL and (b) of *L*-LA modeled by DFT, (c) Gibbs energy profiles of the initiation and the first propagation of the BA-OROP of *L*-LA and CL.

L-LA being a dilactone the ring strain cannot be compared and directly linked to the difference in polymerizability of both monomers.

Additionally, in the case of the ROP of CL, it can be noticed that the energetic barriers for both TS1 and TS2 were very similar for the propagation and the initiation (**TS1 I ≈ TS1 P** and **TS2 I ≈ TS2 P**). These results can mean that initiation rate was not faster than propagation rate ($k_i \approx k_p$ with k_i and k_p the rate constants of initiation and propagation) as it should be in living polymerizations. In section 2 of the present chapter we, indeed, reported an induction period before a linear evolution of $\ln([M]_0/[M])$ *vs.* time during the BA-OROP of CL ascribed to slow

initiation. In contrast during the BA-OROP of *L*-LA, the higher energetic barrier during the propagation than during initiation (**TS1 P** ≈ 21.2 kcal.mol^{-1}, **TS1 I** ≈ 16.1 kcal.mol^{-1}) suggested that k_i is much higher than k_p. The linear evolution of ln($[M]_0$/[M]) *vs.* time during the BA-OROP of *L*-LA verified these calculations.

PC P was also more stable in the case of the ROP of *L*-LA (-22.2 kcal.mol^{-1}, Scheme 7c) than in the case of the ROP of CL (-18.7 kcal.mol^{-1}, Scheme 7d). The complexes of the PLA growing chain with BA are more stable due to the two ester moieties allowing a less constrained conformation of the PLA chains. This particular coiled conformation facilitates the van der Waals interactions and hydrogen bonding between the esters of the penultimate lactidyl unit and BA. In contrast, the PCL growing chain exhibited an extended conformation. These results were consistent with the extended conformation and the coiled conformation found for PCL[47] and PLA[48] as reported by Hall *et al*.

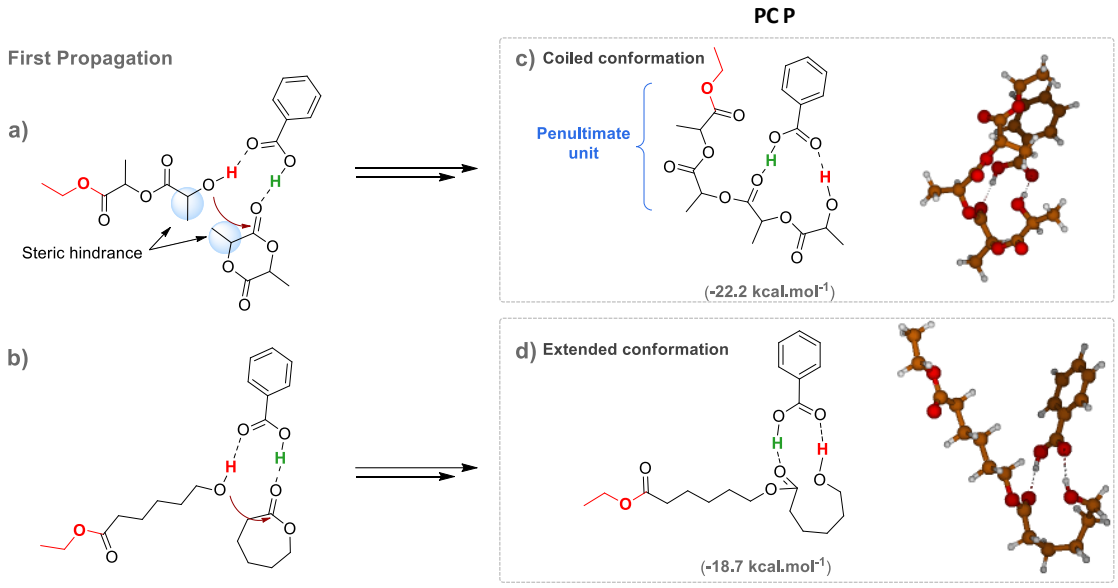

Scheme 7. Nucleophilic attack during the first propagation of the BA-OROP of (a) *L*-LA and (b) CL and the resulting final complexes **PC P** after the ring-opening of (c) *L*-LA and (d) CL units.

3.4 Epimerization

The bifunctional activation of BA can also lead to detrimental side reactions such as epimerization of *L*-LA as observed in our study. BA would thus induce epimerization by protonating the lactide carbonyl with its acidic moiety and by deprotonating the α-methine (CH) group with its basic moiety (**TS1**, Figure 20). A planar enol would result from this reaction, stabilized by mesomeric effect (**1**), the enol moiety would then be protonated back leading to

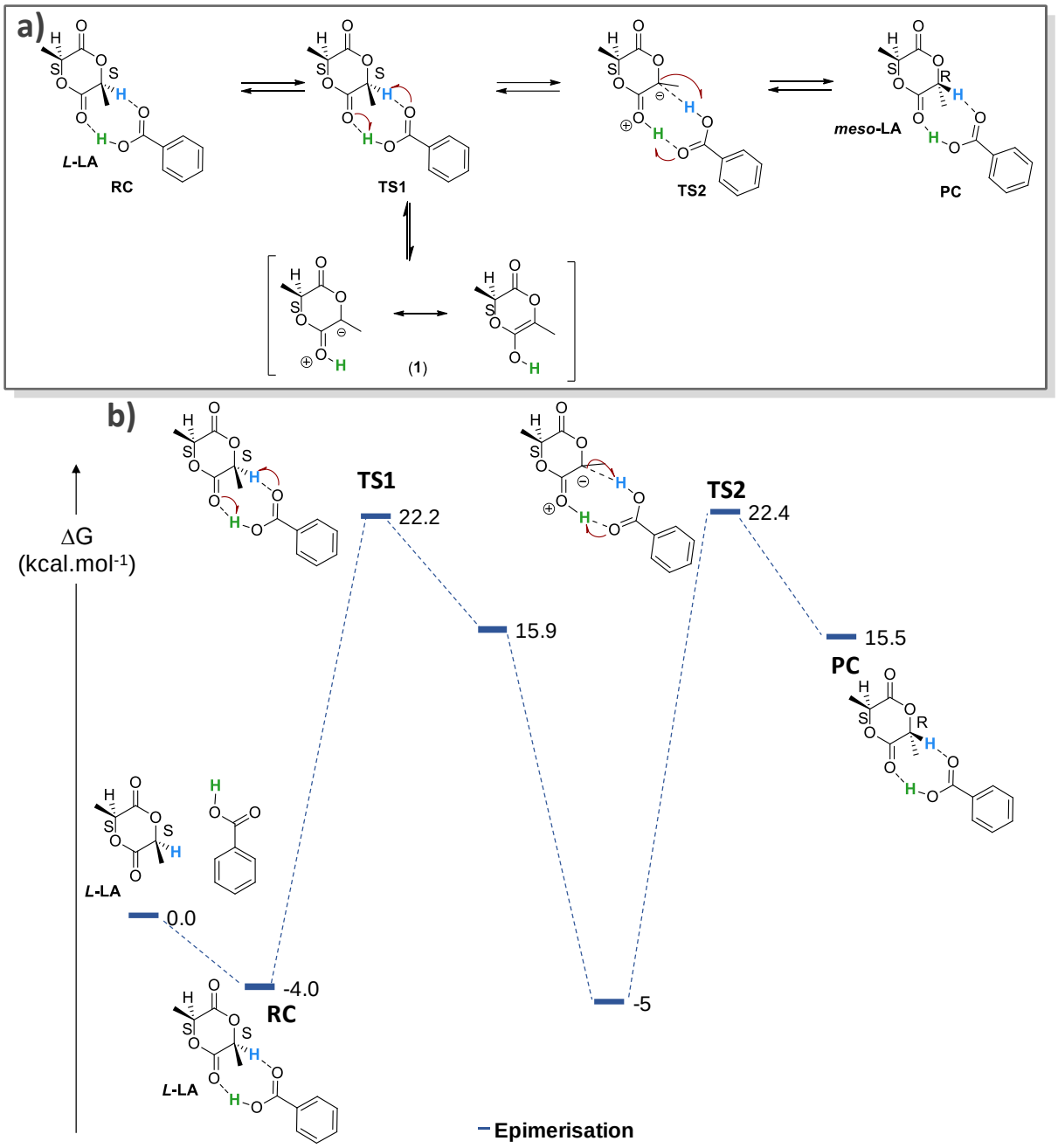

Figure 20. (a) Scheme of the mechanism proposed for the epimerization of *L*-LA as catalyzed by BA. (b) Gibbs energy profiles of epimerization of *L*-LA in *meso*-LA.

meso-LA thanks to BA which deprotonates in the same time the carbonyl oxonium of LA (**TS2**, Figure 20).[34] The computational results suggested relatively high energetic barriers for the transition states involved during the epimerization of *L*-LA (ΔG = 26.4 and 27.4 kcal.mol^{-1} for **TS1** and **TS2** respectively) but not so different from the **TS1 P** (≈ 21.2 kcal.mol^{-1}) of the ROP of *L*-LA. At high temperature (155 °C) such energetic barriers could be overpassed to provide *meso*-

lactide in a small but non- negligible quantity. This is in accordance to the experimental evidences.

In conclusion, BA would activate both the monomer and the initiator/chain end *via* a bifunctional mechanism. The density functional theory calculations supported the experimental data, namely that the ROP of CL is faster than that of *L*-LA, the ignition period observed in the kinetic of the ROP of CL and the epimerization reactions occurring during the ROP of *L*-LA. Furthermore, primary alcohol initiators may ring-opened more easily the *L*-LA than the CL at high temperature and could offset the higher activation of the carbonyl of CL by BA explaining the same energetic barrier during initiation. Finally, these calculations highlighted that the nucleophilic attack during propagation of *L*-LA necessitates a high energetic barrier to be overpassed suggesting that the secondary alcohol at the chain end necessitates a higher activation than that BA carbonyl can provide being a weak base.

4 Catalyst and monomer recycling

Among challenges to address in the developing field of polymer synthesis by organocatalysis, there is still the need for further investigating the toxicity of organocatalytic systems in the one hand. Preliminary studies have shown, for instance, that residual thioureas[49], phosphazenium salt[50] and 4-dimethylaminopyridine[51] (DMAP) exhibit some cytotoxicity. On the other hand, removing the catalyst from the final polymer may be required, as residual catalyst can induce premature degradation after polymerization, in particular during processing.[8,52,53] To prevent hazards due to potentially toxic catalytic species in the final polymers, a purification step is usually implemented -typically by precipitation utilizing a large excess of solvent-, which obviously adds to the cost of the synthesis process. It worth mentioning that Paluch *et al.* developed a solvent-free and catalyst-free ROP of CL under pressure.[54] Here we took advantage of the ability for BA to sublimate enabling its easy removal from the reaction mixture after OROP. As CL and *L*-LA can be also readily removed, respectively, by evaporation and sublimation, this allowed us to achieve highly pure PCL samples (see Chapter 4 for P(LA-*co*-CL)), *i.e.* free of any catalyst and monomer residues. The as-recovered BA could therefore be reused for subsequent organocatalytic cycles, and due to their easy removal, both monomers could be recycled too. The equipment we set-up for both organocatalyst and monomer recycling is displayed in Figure 21a, and practical details are provided in the Experimental Part. Hexane-1,6-diol (HDO) was also evaluated as a potential bio-based initiator for the BA-OROP of CL, using an initial $[CL]_0/[BA]_0/[HDO]_0$ ratio of 25/1.25/1. After reaction at 155 °C for 2h (conv. = 91%) a crude PCL with $M_{n,SEC}$ = 4290 g.mol^{-1} and $Đ$= 1.12 was obtained. After the aforementioned purification step was implemented, a PCL sample free of monomer residues and containing less than

0.15mol.% of BA catalyst was recovered (Figure 21c), the SEC trace of which nearly superimposed that of the crude compound ($M_{n,SEC}$= 4250 g.mol^{-1}, $Đ$= 1.12, Figure 22), indicating absence of transesterification during the workup.

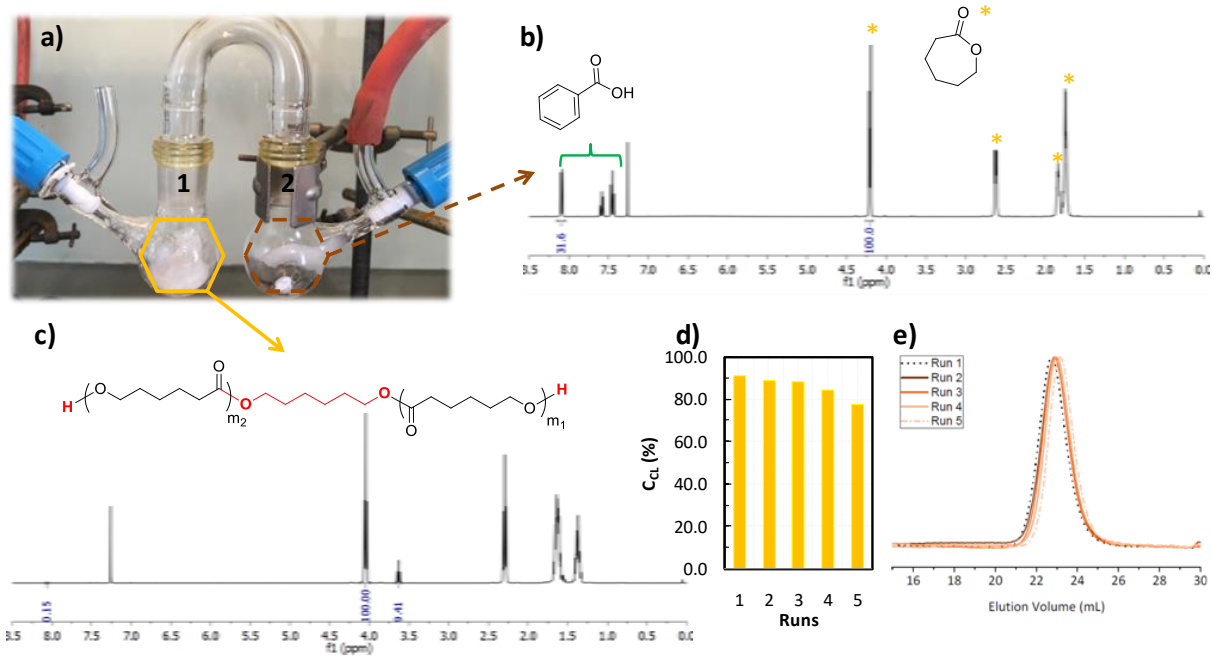

Figure 21. (a) Picture of recycling setup; (b) ^{1}H NMR analysis performed of BA and CL recovered from vacuum treatment (Schlenk 1); (c) ^{1}H NMR analysis performed on the product purified by vacuum treatment: only PCL initiated from the 1,6-hexanediol (Schlenk 2); (d) Bar graph showing the conversion of CL for each run; (e) normalized SEC traces from RI detector of pure PCLs (THF, 313 K, 1mL.min^{-1}).

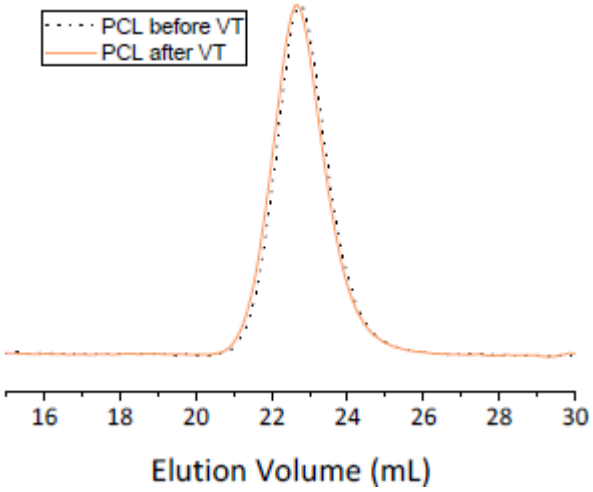

Figure 22. Normalized SEC traces of PCL before and after vacuum treatment (VT) initiated by hexane-1,6-diol of run 1.

Both recovered BA and unreacted CL proved chemically pure (Figure 21b). Hence, they could be reused for a subsequent organocatalytic cycle that was performed under the same conditions by adding appropriate amounts of CL monomer and HDO initiator ($[CL]_0/[BA]_0/[HDO]_0$ = 25/1.25/1). The recycling procedure was thus repeated up to 5 times, providing a PCL always exhibiting very similar features (3740 < $M_{n,SEC}$ < 4290g.mol^{-1}and 1.09 < $Đ$ < 1.12), as summarized in Figure 21e. The slight decrease in the catalytic activity observed after the fifth cycle (Figure 21d) is ascribed to some loss of BA after sublimation during purification. Nonetheless, these results demonstrate that BA can be readily recycled by sublimation and reused without significant loss of its organocatalytic activity. Furthermore, the process is particularly straightforward, fast (5 min.) and does not employ any solvent. This process can be implemented for the controlled synthesis of PCL and for that of BA-derived P(LA-*co*-CL) copolymers (see Chapter 4).

5 Synthesis of triblock copolymers

As "controlled" syntheses of PCL and PLLA, utilizing BA as organocatalyst and BD as initiator, were established, this prompted us to prepare both block copolymers based on PLA and PCL. Synthesis of triblock copolymers was first investigated by sequential BA-OROP in presence of BD as initiator. As depicted in Scheme 8, monomers were introduced either by adding *L*-LA and CL in this order or in the other, *i.e.*CL first then *L*-LA. Results are summarized in Table 4.

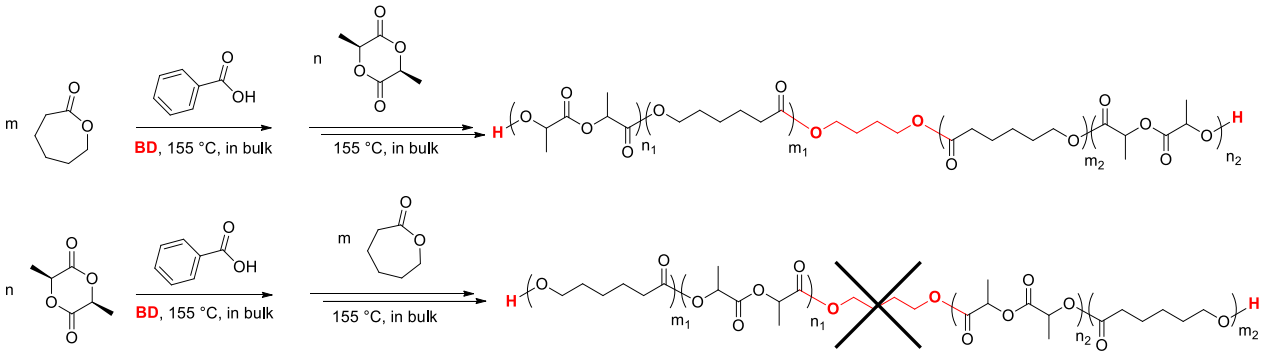

Scheme 8. Synthesis of triblock copolymers by sequential BA-OROP pathway (n= n_1 + n_2 and m = m_1+ m_2).

Table 4. Results and conditions of the triblock synthesis.[a]

Entry	M_1	$[M]_0/[I]_0$	Time (h)	C_1[b] (%)	$M_{n,SEC}$[c] (g.mol^{-1})	$Đ$[c]	M_2	$[M]_0/[I]_0$	Time (h)	C_2[b] (%)	$M_{n,SEC}$[c] (g.mol^{-1})	$Đ$[c]
1	CL	25	2	93	4240	1.12	LA	25	26	75	7730	1.14
2	LA	25	36	90	4200	1.15	CL	25	2	27	n.d	n.d

[a] Reactions were performed in bulk at 155 °C under argon atmosphere with reaction conditions: m_{CL} = 200 mg, m_{LLA}= 253 mg using 5mol% catalyst *vs* monomers and targeted DP of 25 for each monomer; [b]CL and *L*-LA conversions were determined by ^{1}H NMR analysis; [c]Uncorrected average molar mass and dispersity (*Đ*) of crude copolymers determined by SEC chromatography (polystyrene standards), at 40 °C and THF as eluent.

5.1 Synthesis of poly(*L*-lactide)-*b*-poly(ε-caprolactone)-*b*-poly(*L*-lactide)

A very well-defined PLA-*b*-PCL-*b*-PLA triblock copolymer could be obtained as follows. An α,ω-bis-hydroxy PCL ($M_{n,SEC}$ = 4240 g.mol^{-1}, $Đ$ = 1.12, Table 4, Entry 1) was isolated before BA-OROP of *L*-LA ([*L*-LA]$_0$/[BA]$_0$/[PCL]$_0$ = 25/1.25/1) that was conducted at 155 °C for 26h, reaching 75% conversion. Formation of the block copolymer was attested by a clear shift of its SEC trace to the higher molar masses, compared to that of the parent PCL diol ($M_{n,SEC}$ = 7730 g.mol^{-1}; $Đ$ = 1.14; Figure 23c, Table 4, Entry 1). Analysis by ^{1}H NMR confirmed the presence of both PLA and PCL blocks, as illustrated in Figure 23a,b showing the representative protons of both blocks, and protons of hydroxyl-methylene PCL end-groups at 3.6 ppm that totally vanished (Figure 23a), in favor of hydroxyl-end protons in alpha position to the methine end-group of PLLA at 4.36 ppm (Figure 23b).

^{13}C NMR analysis of the carbonyl region also confirmed the formation of triblock copolymers, first by displaying the peaks representative of the carbonyl carbons at 174.49 ppm and at 169.54 ppm of the PCL (CL-CL-CL) and PLA (LL-LL-LL) blocks respectively (Figure 24b). Then the carbonyl carbon representative of the CL-LL-LL sequences **(1),** highlighting the initiation of the PLA blocks from the PCL block, emerged at 170.08 ppm. The characteristic peak of the carbonyl carbon of the lactidyl chain end -identified by HMBC (Figure S 14)- emerged **(2)** with the probable disappearance of the peak characterictic of the carbonyl carbon of the caproyl chain end unit (coc'') **(3)**. Note that the latter peak (coc'') cannot be identified by HMBC.

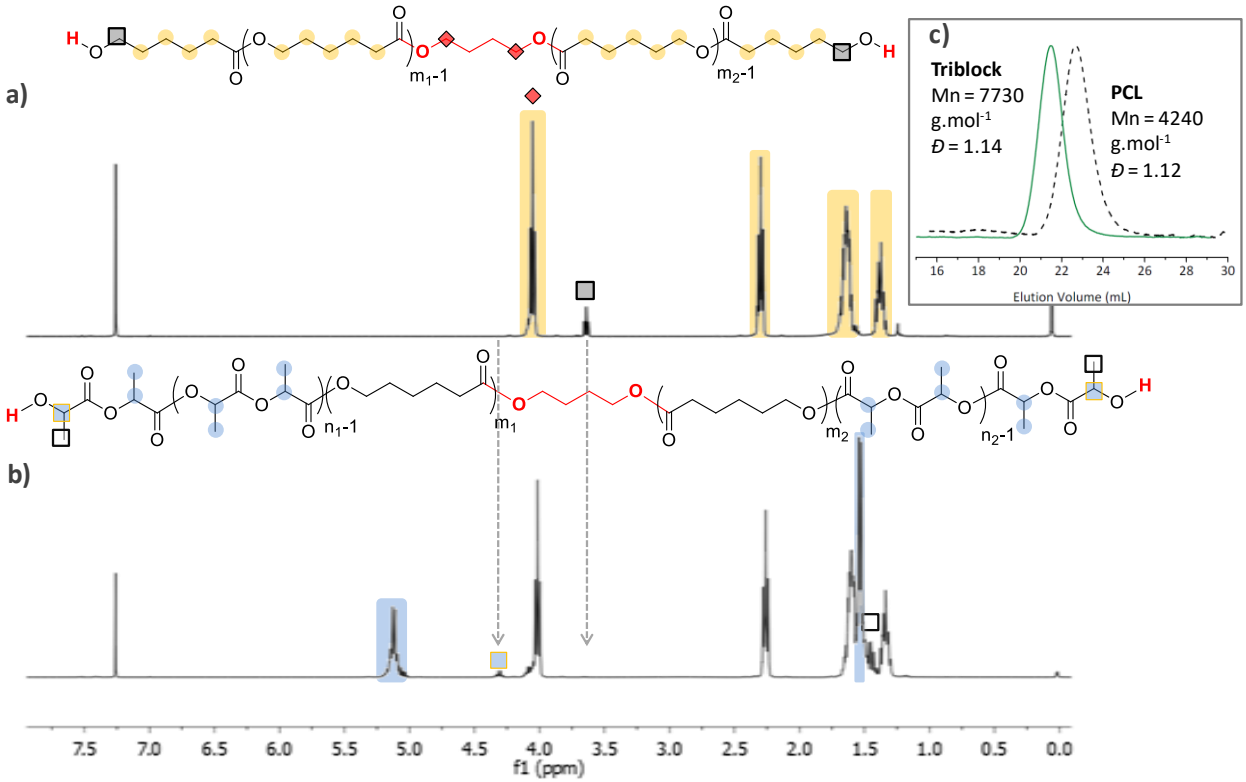

Figure 23. ^{1}H NMR spectra comparing: (a) PCL macroinitiator and (b) PLA-*b*-PCL-*b*-PLA triblock ($CDCl_3$, 400MHz, r.t); (c) Normalized SEC traces from RI detector of PCL (black dashed line) and corresponding triblock copolymer (uncorrected $M_{n,SEC}$ determined by SEC in THF, 313K, 1mL.min^{-1}, PS standards).

Finally, the peak at 170.8 ppm representing "anomalous" CL-L-CL sequences and heterosequences were not observed here signifying that type II transesterification reactions did not occur (Figure 24, **(4)**). [55] Additionnally, the absence of the characteristic peaks of statistical copolymer indicates that transesterification reactions were not occurring suggesting that lactidyl chain end units did not transesterified throughout the PCL backbone.

One point remained unclear, Kasperczyk and Bero attributed the peak at 174.42 ppm to the LL-CL-CL sequence, however in our case, the peak characteristic of CL-CL-LL sequence should appear instead as we are able to see the chain ends **(5)**. We could thus assume that this attribution of Kasperczyk and Bero is maybe not certain. More studies are needed in order to verify our assumption.

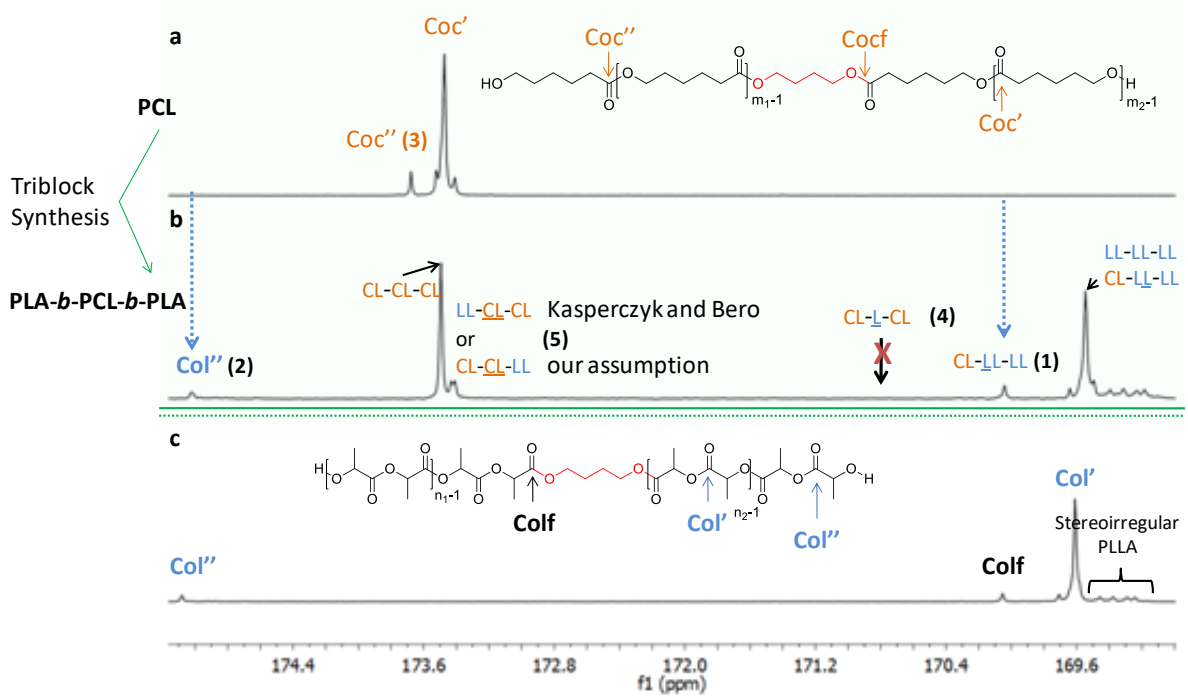

Figure 24. ^{13}C NMR spectra comparing: (a) the PCL macroinitiator,(b) the as-obtained PLA-*b*-PCL-*b*-PLA triblock and (c) a PLA. LL and L refer to lactidyl and lactoyl units, respectively ($CDCl_3$, 100.6 MHz, r.t).

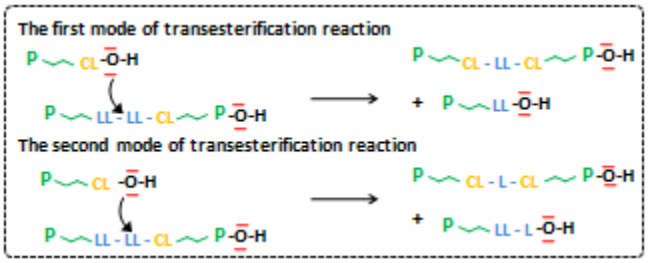

Scheme 9. The two modes of transesterification reaction proposed by Kasperczyk and Bero.[55]

Finally, experimental degree of polymerization ($DP_{,exp}$ = 42.2) were very close to theoretical values ($DP_{,th}$ = 42.1). Thus, triblock copolymer synthesis could be readily accomplished by sequential BA-OROP of CL and *L*-LA in this order, using BD as initiator.

5.2 Synthesis of poly(ε-caprolactone)-*b*-poly(*L*-lactide)-*b*-poly(ε-caprolactone)

In contrast, attempts to reverse the order of the two monomers, *i.e.* by polymerizing *L*-LA first to achieve a PCL-*b*-PLA-*b*-PCL triblock copolymer met with limited success (Table 4, Entry 2). BA-OROP of CL from the α,ω-bis-hydroxy PLA precursor ($M_{n,SEC}$= 4200 g.mol^{-1}; $Đ_M$ = 1.15) proved indeed extremely low conversion (conv. = 27% after 2h). This might be explained by a

slow initiation of CL from the secondary OH end-groups of PLA, as observed by NMR showing indeed a remaining signal due to these protons (e_{LA}, Figure 25). Such hypothesis has been confirmed by initiating the BA-OROP of CL at 155 °C from butane-2,3-diol for an initial monomer-to-initiator of 30 (Table 5). As compared to the same reaction performed from a primary alcohol (Table 5, Entry 1), initiating the BA-OROP from a secondary alcohol reduces considerably the overall polymerization conversion while increases the as-produced PCL dispersity (Table 5, Entry 2 and Figure 26).

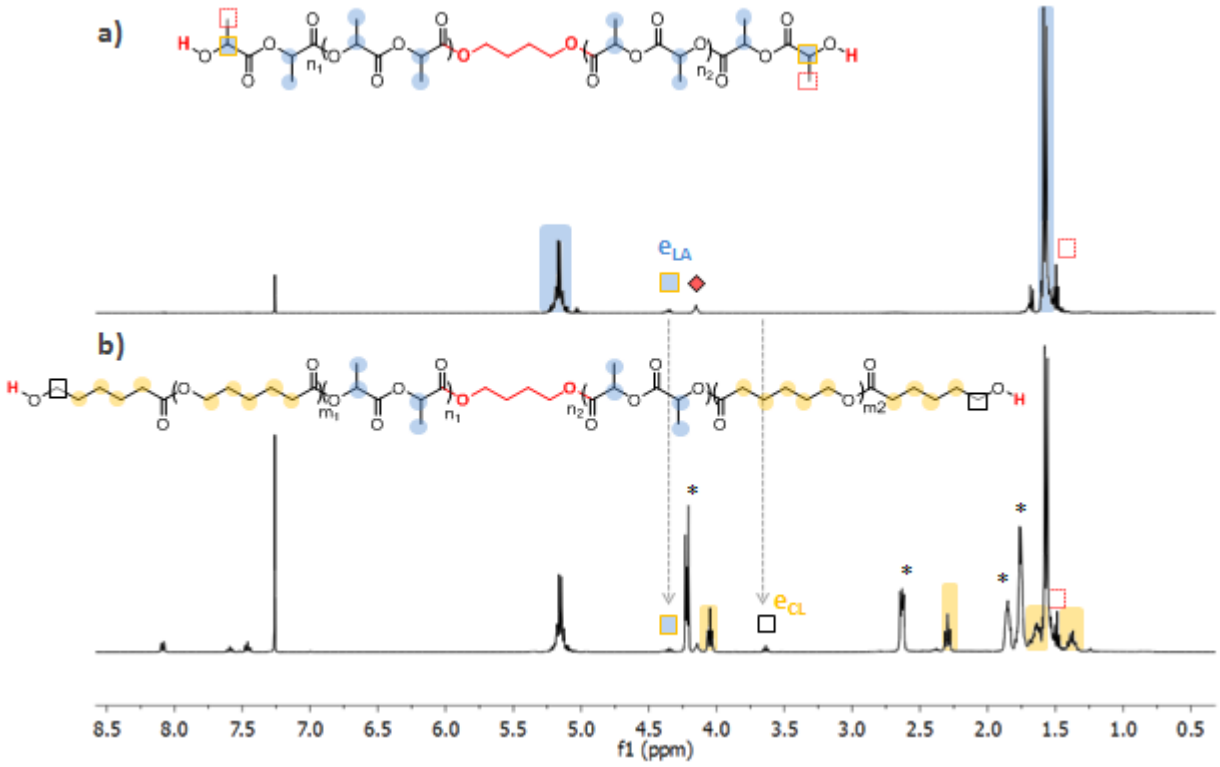

Figure 25. ^{1}H NMR spectra comparison between the PLA macroinitiator (a) and the as-obtained crude PCL-*b*-PLA-*b*-PCL triblock ($CDCl_3$, 400MHz, r.t). * NMR peaks of CL monomer

Table 5. BA-OROP of CL initiated by a primary and a secondary alcohol initiators in bulk at 155 °C.[a]

Entry	I	Cat (%)[b]	$[M]_0/[I]_0$	Time (h)	C_M (%)[c]	$M_{n,SEC}$ ($g.mol^{-1}$)[d]	$Đ$[d]	DP_{th}[e]	DP_{exp}[f]
1	BD	5	30	1.7	78	4360	1.09	23.5	22.3
2	2,3-BD	5	30	1.7	36	2460	1.31	10.9	17.9

[a]Reactions were performed in bulk at 155 °C under argon atmosphere with reaction conditions: m_{CL}= 200 mg $[M]_0/[I]_0$ = 30. [b]Catalyst percent related to monomer. [c]CL conversions were determined by ^{1}H NMR analysis. [d]Uncorrected number average molar mass ($M_{n,SEC}$) and dispersity ($Đ$) of crude polymers as determined by SEC chromatography (polystyrene standards) at 313 K and THF as eluent. [e]Theoretical degree of polymerization $DP,th = \frac{[M]_0}{[I]_0} \times C_M$. [f]Experimental degree of polymerization calculated from PCL chain ends as determined by ^{1}H NMR.

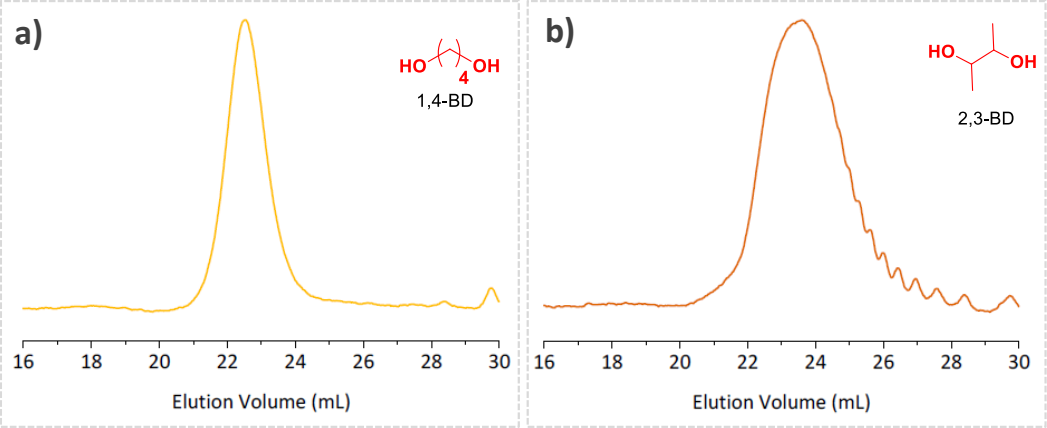

Figure 26. SEC traces of crude PCLs initiated by (a) BD and by (b) 2,3-BD.

Conclusions and outlooks

This study reports the use of benzoic acid (BA) as simple, naturally occurring, cheap, thermally stable and readily recyclable weak acid organocatalyst for the metal-free synthesis of (co)polyesters based on poly(lactide) (PLA) and poly(ε-caprolactone) (PCL). BA is shown to promote the organocatalyzed ring-opening polymerization (OROP) of both ε-caprolactone (CL) and *L*-lactide (*L*-LA) in bulk at a rather high working temperature (80 - 180 °C), in presence of various alcohols as initiators, with an appreciable degree of control over molar masses and dispersities of the resulting aliphatic polyesters when using BD as initiator. However, the presence of epimerization of *L*-LA leading to amorphous PLA and the presence of transesterification reactions decrease the level of control meaning that BA-OROP of *L*-LA and CL are not living.

The good "control" of this BA-OROP process can be exploited to synthesize triblock copolymers by sequential OROP, though only by adding CL and *L*-LA in this order to achieve, for

instance, PLLA-*b*-PCL-*b*-PLLA triblock copolymers, using a diol as initiator without transesterification reactions. The reverse reaction, *i.e*. the synthesis of triblock copolymers by sequential OROP by adding *L*-LA and CL did not afforded the expected material as the secondary alcohol at the chain end of PLA induce a slow initiation of the ROP of CL.

A bifunctional mechanism involving activation by proton exchanges of both the monomer and the alcohol initiator is supported by experimental data and density functional theory (DFT) calculations. Model experiments may suggest that the carbonyl group of CL is more activated by BA than that of *L*-LA surely because the carbonyl group of CL is more basic. Additionally, DFT calculations may suggest that the secondary alcohol at the chain end necessitates a higher activation than that the BA carbonyl can provide being a weak base. These two assumptions could explain the faster propagation rate of the BA-OROP of CL compared to that of *L*-LA

Finally, advantage of the capability for BA to sublimate has been taken to recycle and reuse it in further organocatalytic cycles, without using any solvent, affording highly chemically pure PCL-based aliphatic polyesters.

Part of this work has been published in Green Chemistry.[56]

Overall, these investigations broaden the scope of organocatalysis in macromolecular synthesis, by providing an alternative and green synthetic method to biodegradable, biocompatible and aliphatic (co)polyesters based on PLA and PCL free of catalyst and monomer residues. This can be accomplished through the use of BA as weak acid-type organocatalyst combined with a straightforward purification procedure of the crude (co)polymers. The next chapter will evaluate the synthesis of statistical copolymers using BA as organocatalyst.

Experimental part

Materials

L-Lactide (*L*-LA, 98%, TCI) was recrystallized three times from toluene and dried under vacuum for two days. ε-Caprolactone (CL, 99%, ACROS), benzyl alcohol (BnOH, 99%, ACROS), butane-1,4-diol (BD, 99%, VWR), heptan-1-ol (HepOH, 98%,Sigma Aldrich) and 3-phenylpropanol (PPA, 99%, Alfa aesar) were dried over CaH_2 for 48 hours prior to their distillation under reduced pressure and were stored on molecular sieves. Poly(ethylene glycol) (PEG_{1000}) (Fluka, Mw ~ 1000 $g.mol^{-1}$) and hexane-1,6-diol (HDO, 97%, Alfa aesar) were dried *via* three azeotropic distillations of tetrahydrofuran (THF). Benzoic acid (BA, 99%, ACROS) was recrystallized once and dried *via* two azeotropic distillations using toluene. Compounds were stored in a glove box (O_2 ≤ 6 ppm, H_2O ≤ 0.5 ppm). Tetrahydrofuran solvent was dried using a MBraun Solvent Purification System (model MB-SPS 800) equipped with alumina drying columns. Toluene was dried using a SPS from Innovative technology and stored over polystyrylithium.

Methods

NMR spectra were recorded on a Bruker Avance 400 (^1H,^{13}C, 400.2 MHz and 100.6 MHz respectively) in $CDCl_3$. Molar masses were determined by size exclusion chromatography (SEC) in THF (1ml/min) with trichlorobenzene as a flow marker at 313.15 K, using refractometric (RI) detector. Analyses were performed using a three-column TSK gel TOSOH (G4000, G3000, G2000). The SEC device was calibrated using linear polystyrene (PS) standards. Positive-ion MALDI-Mass Spectrometry (MALDI-MS) experiments were recorded using a Waters QToF Premier mass spectrometer equipped with a Nd:YAG (third harmonic) operating at 355 nm with a maximum output of 65 µJ delivered to the sample in 2.2 ns pulses at 50 Hz repeating rate. Time-of-flight mass analyses were performed in the reflectron mode at a resolution of about 10,000. All samples were analyzed using trans-2-[3-(4-tert-butylphenyl)-2-methylprop-2-enylidene]malononitrile (DCTB) as matrix, which was prepared as a 40 $mg.mL^{-1}$ solution in $CHCl_3$. This solution (1 µL) was applied to a stainless-steel target and air-dried. Polymer samples were dissolved in THF to obtain 1 $mg.mL^{-1}$ solutions and 50 µL of 2 $mg.mL^{-1}$NaI solution in acetonitrile was added to the polymer solution. Therefore, 1 µL of this solution was applied onto the target area already bearing the matrix crystals, and air-dried. For the recording of the single-stage MS spectra, the quadrupole (rf-only mode) was set to pass all the ions of the distribution, and they were transmitted into the pusher region of the time-of-flight analyzer where they were mass analyzed with 1 s integration time. Data were acquired in continuum mode until acceptable averaged data were obtained. Differential scanning calorimetry (DSC) measurements were carried out with a DSC Q100 LN2 apparatus from TA Instruments under helium flow. The PCL samples were heated for the first run from -130 to 100 °C, then cooled again to -130 °C and heated again for the third run to 100 °C (heating and cooling rate 10 °C/min). While PLA samples

undergoes 3 runs between -40 °C and 200 °C and P(LA-*co*-CL) between -70 to 200 °C. Glass transition temperatures (T_g) and melting temperatures (T_m) were measured from the second and first heating run respectively.

General procedure for homopolymerization of CL or *L*-LA.

In a glove box, previously flamed 10 mL Schlenks were charged with the monomer CL or *L*-LA (0.2 g), BA catalyst (2.5, 5 and 10 mol% as compared to the monomer) and a stir bar. Then the initiator (BnOH, HepOH, BD, PPA) was added *via* a 5 or 10 µL syringe and mPEG was directly weighted. Schlenks were carefully sealed before being immersed in an oil bath preheated at the desired temperature (140 °C-180 °C). From time to time, one Schlenk was removed from the oil bath to follow the kinetic of polymerization by ^{1}H NMR and the average molar mass (M_n) and dispersity (*Đ*) by SEC. The purification consists in applying vacuum to the Schlenk at 155 °C with a high stirring rate. The CL monomer can be evaporated while BA catalyst and *L*-LA monomer are sublimated.

The inverse precipitation was carried out as follow: 200 mg of PCL were solubilized by stirring in 2 mL of cold dichloromethane (DCM), and then cold methanol was added drop by drop until the polymer started to precipitate. When the media remained trouble, the sample was centrifuged. After removal of the solvent, the pure polymer is dried at room temperature in an oven overnight. A white powder was obtained and further analyzed by MALDI-ToF MS.

General procedure for block copolymerization of *L*-LA and CL.

In a glove box, previously dried 10 mL Schlenks were charged with the first monomer *L*-LA (0.2 g, 1.4 mmol) or ε-CL (0.2 g, 1.75 mmol), the BA catalyst (5mol% *vs* monomer) and a stir bar. Then the BD initiator ($DP_{,th}$= 25) was added *via* a 10 µL syringes. The Schlenks were carefully sealed before being introduced in an oil bath preheated at 155 °C. After 2h or 36 h of polymerization for CL or *L*-LA monomers, respectively, the Schlenk is introduced in the glove box in order to collect a sample to estimate the conversion *via* ^{1}H NMR and to determine the average molar mass (M_n) and dispersity (*Đ*) by SEC. The polymers were then purified by applying vacuum to the Schlenk at 155 °C with a high stirring rate. The Schlenk is again introduced in the glove box in order to add again the catalyst (5mol.%) and a certain amount of second monomer to target $DP_{,th}$ = 25. The polymerization is restarted by immersing the Schlenks in the oil bath for 2 or 26 hours in the case of CL and *L*-LA OROP, respectively.

General procedure for purification by vacuum.

In a glove box, a previously flamed 20 mL Schlenk was charged with the monomer CL (1 g, 8.76 mmol), BA catalyst (53.5 mg, 4.38 x 10^{-1}mmol), the initiator HDO (41.4 mg, 3.5 x 10^{-}

^{1}mmol) and a stir bar. The Schlenk was then introduced in an oil bath preheated at 155 °C for 2 hours. After the polymerization, the mixture was cooled down and the Schlenk 1 is reintroduced in the glove box in order to collect a sample for ^{1}H NMR and SEC analyses and is then connected *via* a bridge to another flamed Schlenk 2. Schlenk 1 containing the crude polymer was then introduced in an oil bath preheated at 155 °C while vacuum (0.1 – 0.2 mbar) was applied to Schlenk 2 and cooled thanks to liquid nitrogen. After heating the bridge with a heat gun, a high stirring rate (800 rpm) was applied to the Schlenk 1 in order to collect in Schlenk 2, the unreacted CL monomer, the BA catalyst. Overall, the vacuum treatment in the oil bath at 155 °C lasted 5 minutes with some interruptions in order to heat again the bridge. The pure polymer is then cooled down and the assembly is introduced in the glove box. Schlenk 2 containing the unreacted monomer and the catalyst was charged with HDO (41.4 mg, 3.5 x 10^{-1} mmol) and the difference of monomer in order to reach 1g (calculated thanks to the conversion by ^{1}H NMR). Finally, Schlenk 2 was introduced in the oil bath preheated at 155 °C for 2h. The cycle was repeated 5 times.

Detailed calculations for section 1.1.1

The conversion is determined by $C_{CL} = \frac{(I_{PCL}/_2 - I_{eCL}/_4)}{(I_{PCL}/_2 - I_{eCL}/_4) + I_{CL}/_2}$

The degree of polymerization calculated from the chain end$DP, exp = \frac{I_{PCL}/_2 - I_{eCL}/_4}{I_{eCL}/_4}$.

Detailed calculations for section 1.1.2

The conversion is determined by: $C_{CL} = \frac{(I_{PCL}/_2)}{(I_{PCL}/_2) + I_{CL}/_2}$

The degree of polymerization calculated from the chain end: $DP, exp = \frac{I_{PCL}/_2}{I_{\omega CL}/_2}$.

Detailed calculations for section 1.2

The conversion is determined by: $C_{LA} = \frac{I_{PLA}/_2}{I_{PLA}/_2 + I_{LA}/_2}$

The degree of polymerization calculated from the end chain when BD initiated the ROP of *L*-LA $DP, exp = \frac{I_{PLA}/_2}{I_{\omega LA}/_2}$.

Supporting information

BA-OROP of CL

Figure S 1. DSC spectra of the PCL initiated from BD (Table 1, Entries 3-5-6)

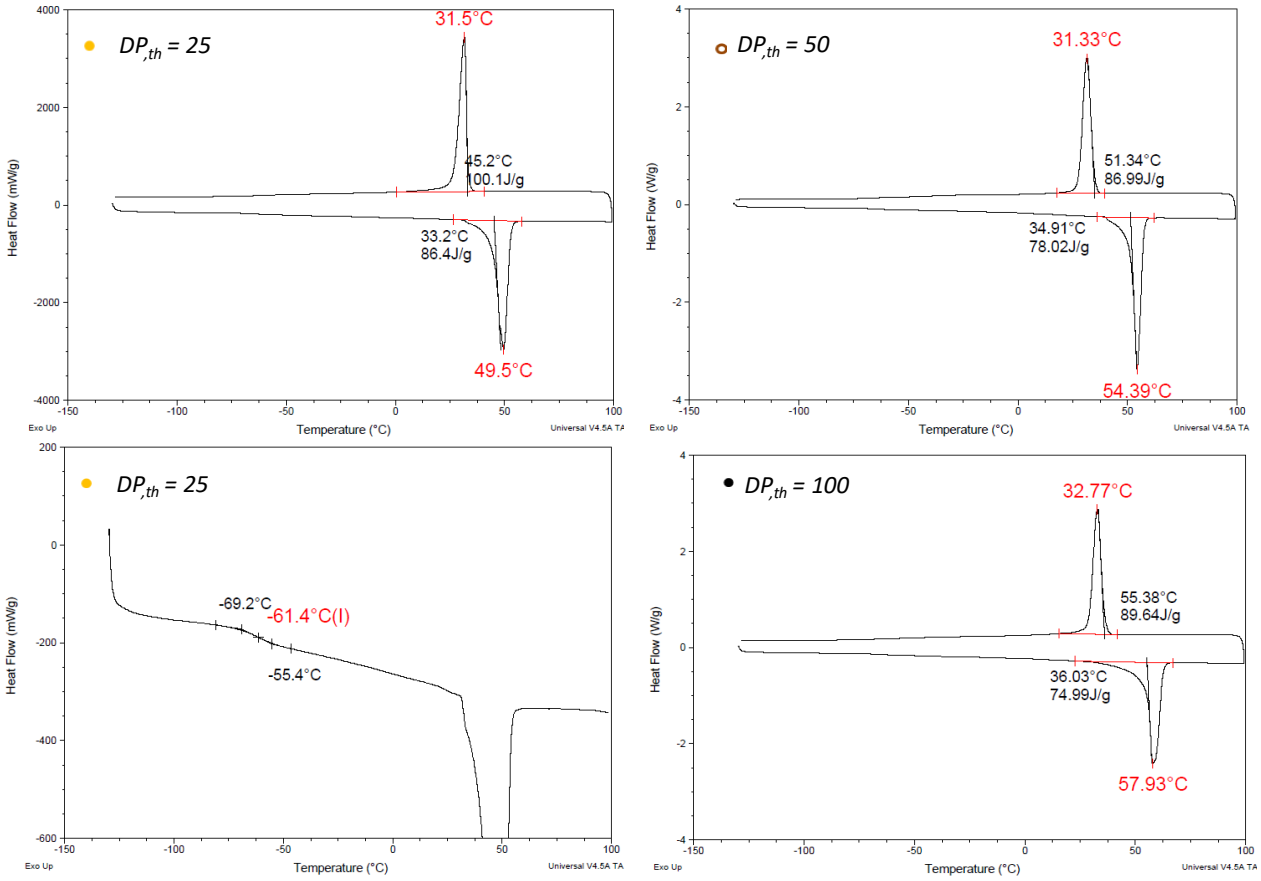

Figure S 2. SEC traces of PCLs obtained by BA-OROP of CL initiated by BD in bulk at 155 °C (Table 1, Entries 5&6) THF as eluent at 313 K.

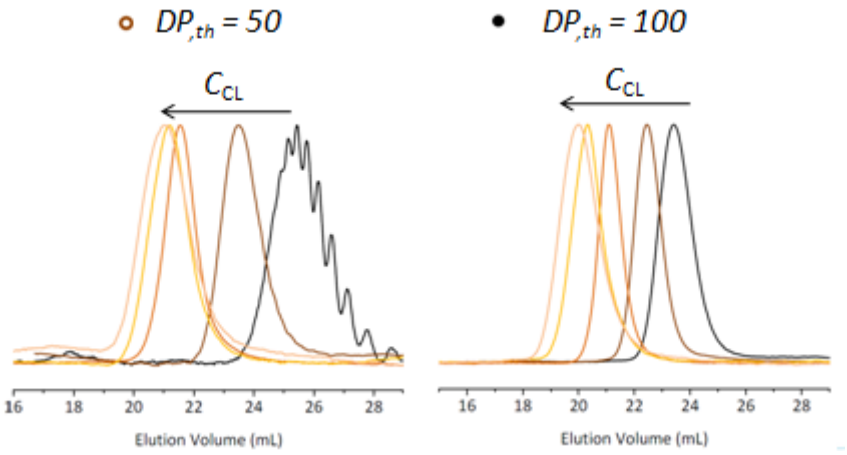

Table S 1. Chain extension experiment for BA-OROP of CL.[a]

Entry	I	$[M]_0/[I]_0$	Time (h)	C_{CL} (%)[b]	$M_{n,SEC}$ (g.mol^{-1})[c]	$Đ^c$
1	BD	25	2	91	3930	1.11
2ce	PCL-entry 1TS1	25	2	n.a	7590	1.17

[a]Reactions were performed in bulk at 155 °C under argon atmosphere with reaction conditions: m_{CL}= 200 mg with a catalyst loading of 5 mol.% rel. to the monomer with BD as initiator. [b]CL conversions were determined by ^{1}H NMR analysis. [c]Uncorrected number average molar mass ($M_{n,SEC}$) and dispersity ($Đ$) of crude polymers as determined by SEC chromatography (polystyrene standards) at 313 K and THF as eluent.

Figure S 3. MALDI-ToF MS of PCL obtained by HepOH-initiated BA-OROP of CL (Table 2, Entry 3).

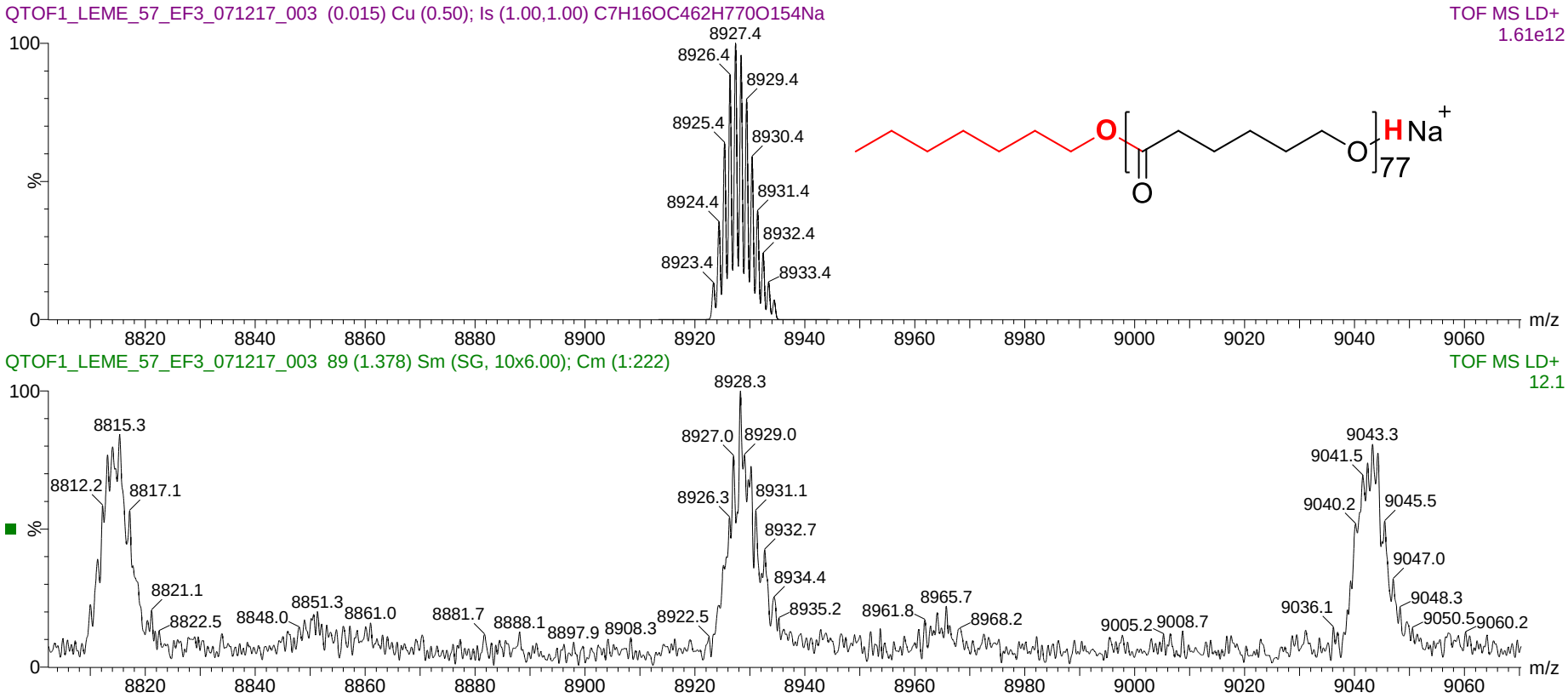

Figure S 4. MALDI-ToF MS of PCL obtained by HepOH-initiated BA-OROP of CL (Table 2, Entry 3).

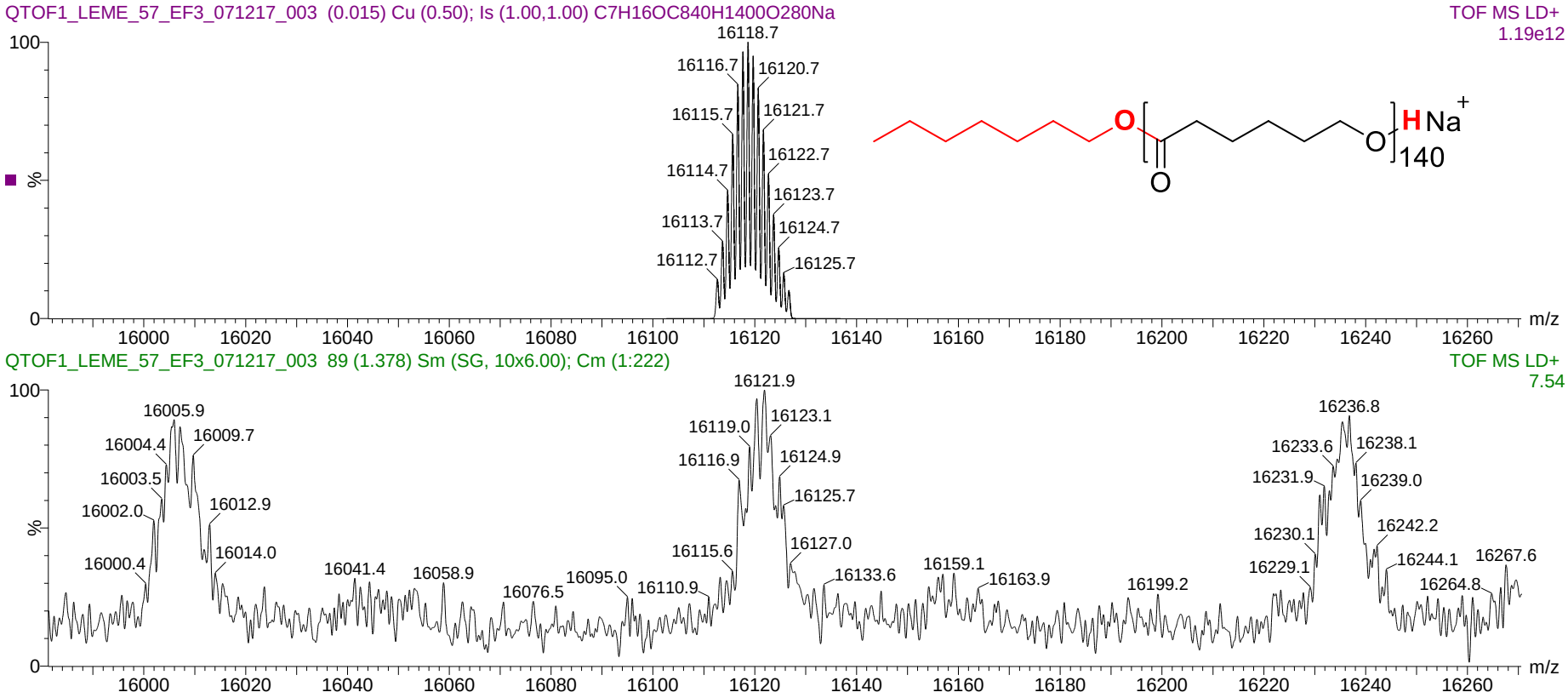

BA-OROP of *L*-LA

Figure S 5. SEC traces of PLA obtained by BA-OROP of *L*-LA initiated by BD in bulk at 155 °C (Table 3, Entries 8-9) THF as eluent at 313 K.

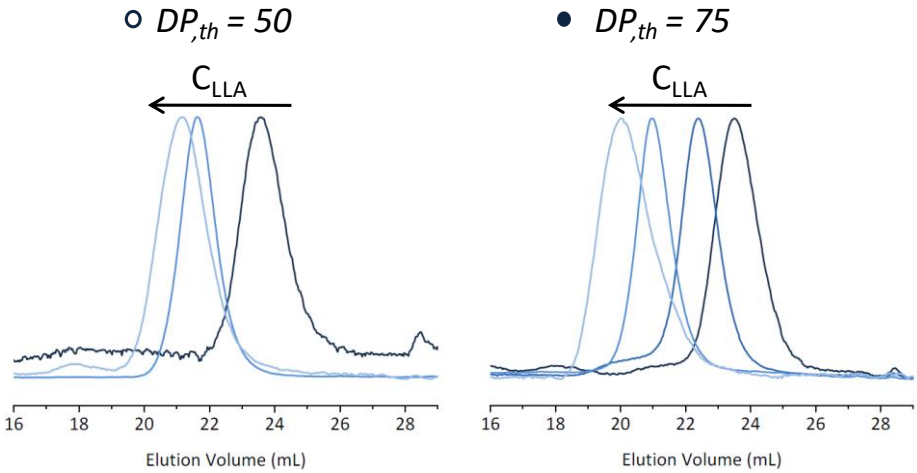

Figure S 6. (a) Evolution of the uncorrected $M_{n,SEC}$ of the crude PLAs (•), and dispersity $Đ$ (x) with monomer conversion and (b) SEC traces for the BA-OROP of *L*-LA initiated by BD at different reaction temperatures (Table 3, Entries 5,6 & 7).

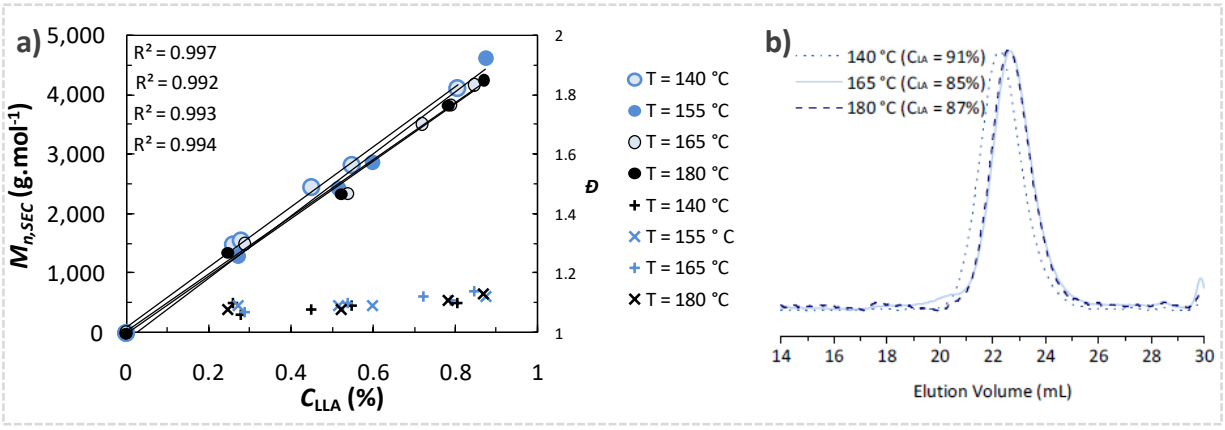

Figure S 7. Evolution of the uncorrected $M_{n,SEC}$ of the crude PLAs (•), and dispersity $Đ$ (x) with monomer conversion (left) and SEC kinetic evolution (right) for the OROP of *L*-LA initiated by BD using (a) 2.5 mol.% and (b) 10 mol/% of BA rel. to the monomer (Table 3, Entries 2 & 4 respectively).

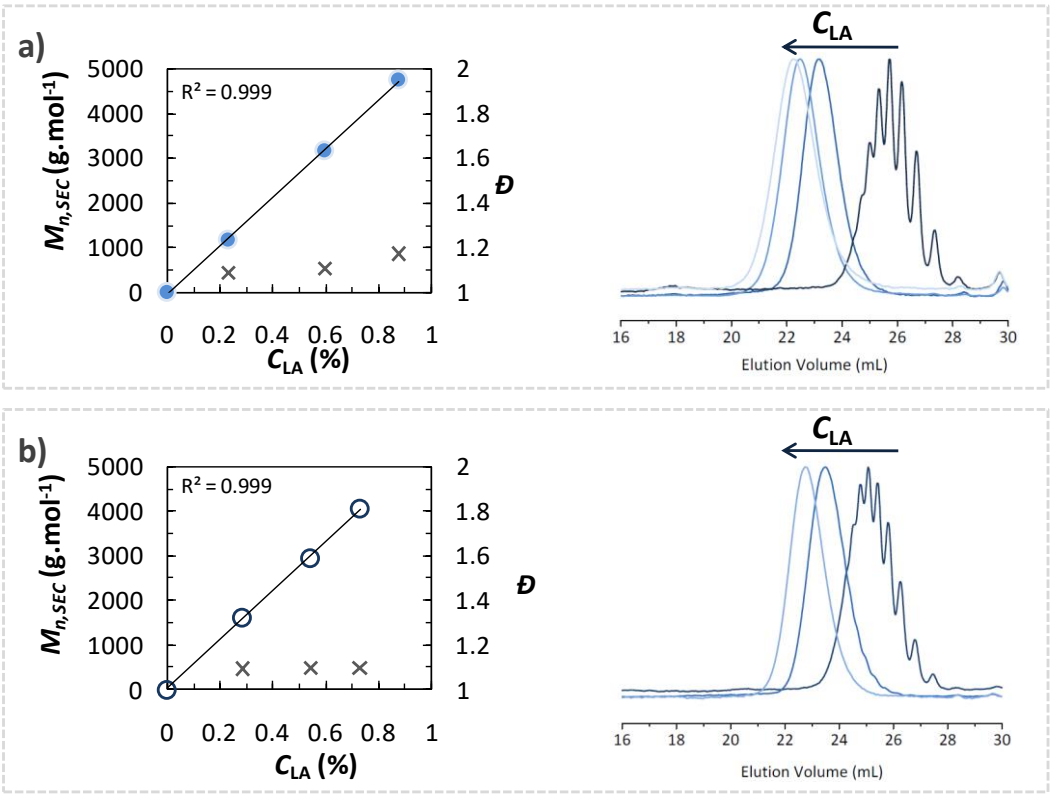

Figure S 8. MALDI-ToF MS spectrum of pure PLAs initiated from BD synthesized at 180 °C (Table 3, Entry 7). With M_{LA}= 144 g.mol^{-1}, $M_{LA/2}$ = 72 g.mol^{-1}.

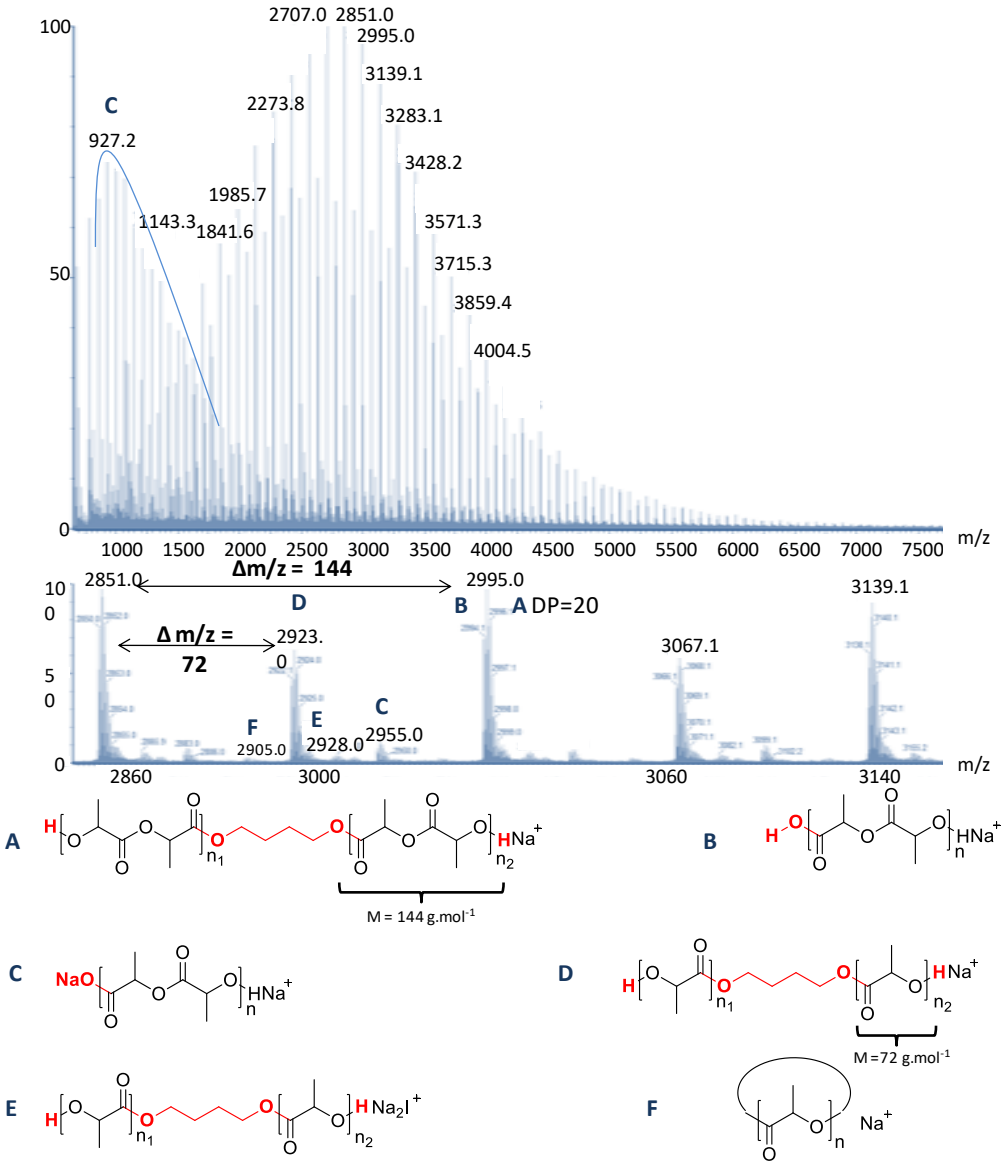

Figure S 9. DSC spectra of the PLAs obtained by BA-OROP of *L*-LA from BD (Table 3, Entries 3, 8 and 9).

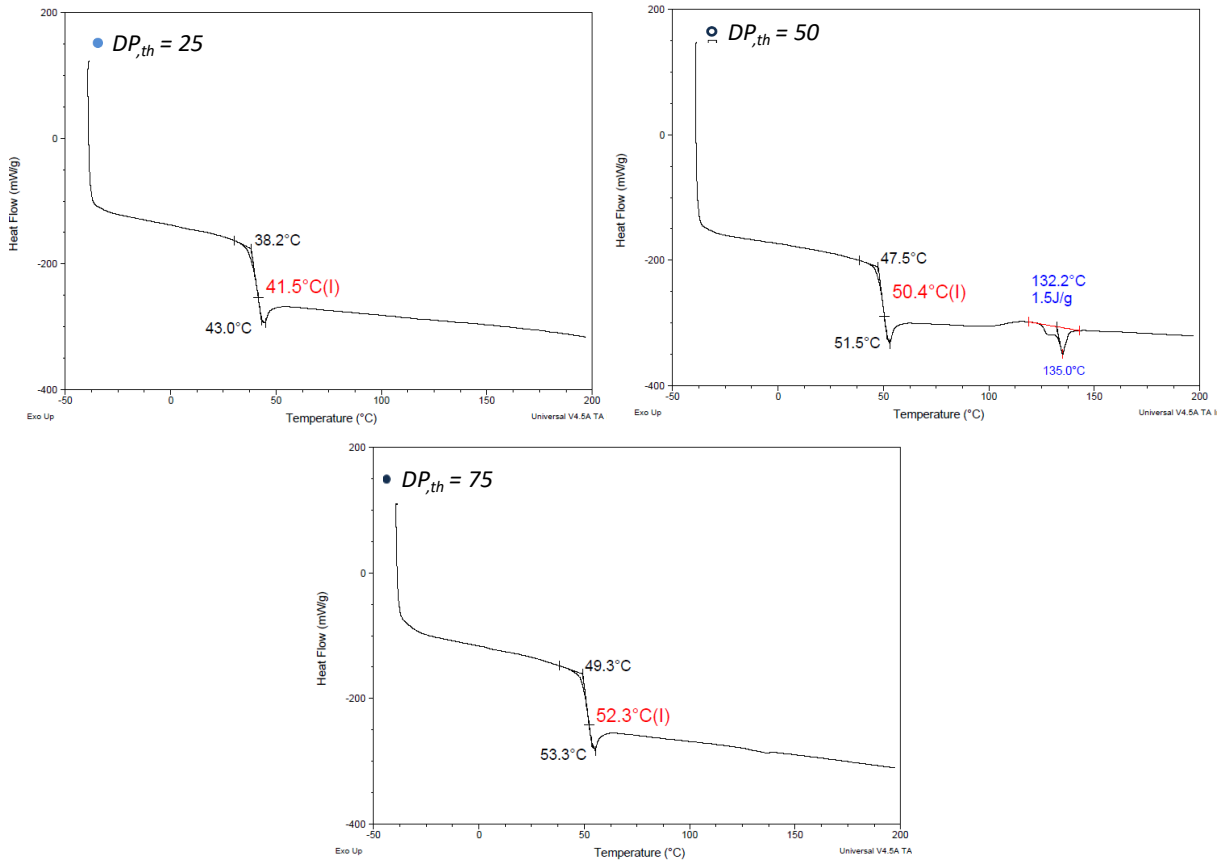

Figure S 10. ^{1}H NMR spectrum of *L*-LA heated during 48 hours at 155 °C (400.2 MHz, $CDCl_3$)

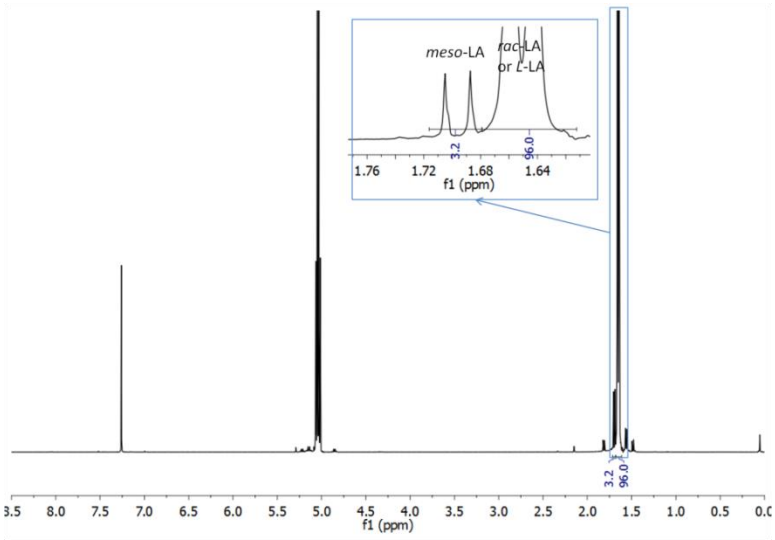

.

Figure S 11. ^{1}H NMR spectrum (400.2 MHz, $CDCl_3$) of *L*-LA heated in the presence of BA catalyst during 48 hours at 155 °C.

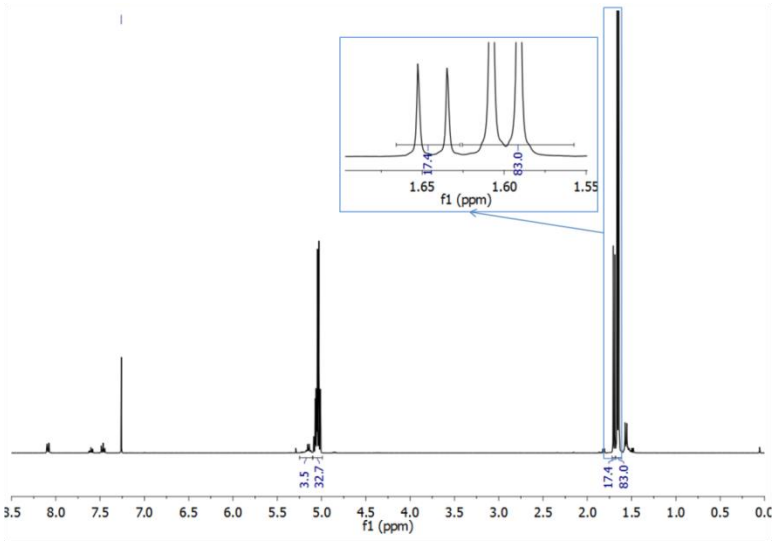

Figure S 12. ^{1}H NMR spectrum (400.2 MHz, $CDCl_3$). of *L*-LA heated in the presence of BD initiator only during 49 hours at 155 °C (Table 3, Entry 1).

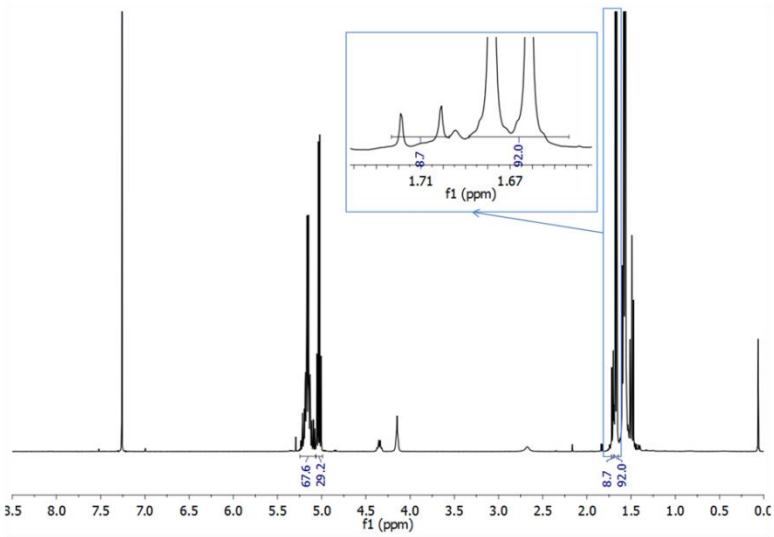

Table S 2. Chain extension experiment for BA-OROP of *L*-LA initiated by PPA (Table 3, Entry 10).[a]

Entry	M	I	Cat (%)	$[M]_0/[I]_0$	T (°C)	Time (h)	Conv (%)	$M_{n,SEC}$ (g.mol^{-1})	$Đ$
1	*L*-LA	PPA	5	25	155	87	88	4690	1.34
2ce	*L*-LA	PLA-entry 1	5	25	155	55	62	7170	1.32

[a]Reactions were performed in bulk at 155 °C under argon atmosphere with reaction conditions: m_{LA}= 200 mg with a catalyst loading of 5 mol.% rel. to the monomer. [b]*L*-LA conversions were determined by ^{1}H NMR analysis. [c]Uncorrected number average molar mass ($M_{n,SEC}$) and dispersity ($Đ$) of crude polymers as determined by SEC chromatography (polystyrene standards) at 313 K and THF as eluent (entry 1, Table S 1= entry 10, Table 3).

Figure S 13. Evolution of the uncorrected $M_{n,SEC}$ of the crude PLAs (•), and dispersity $Đ$ (x) with monomer conversion (left) and semi-logarithmic kinetic plot of the BA-OROP of *L*-LA initiated by PPA (Table 3, Entry 10).

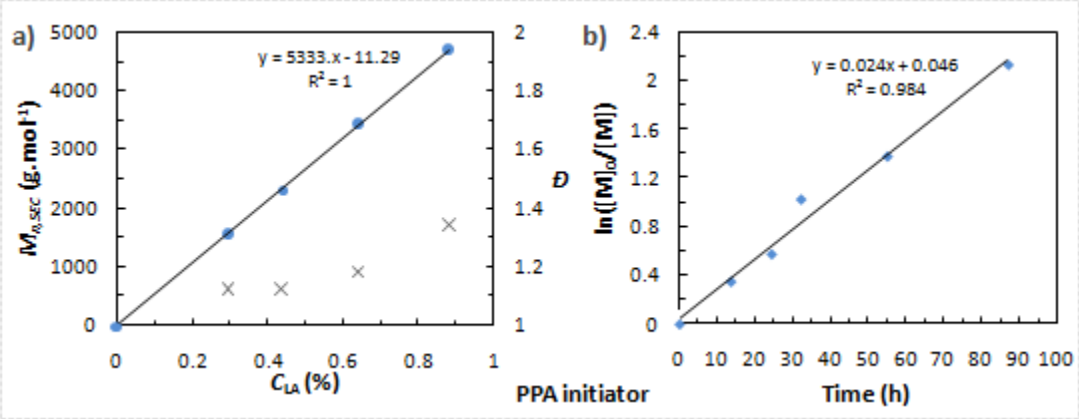

Kinetic and mechanism:

The conversion is determined by $C_{CL} = \frac{I_{PCL/2}}{I_{PCL/2} + I_{CL/2}}$

The degree of polymerization calculated from the ω-chain end $DP,\omega = \frac{I_{PCL/2}}{I_{\omega CL/2}}$.

The degree of polymerization calculated from the ω-chain end $DP,\alpha = \frac{I_{PCL/2}}{I_{\alpha BnOH/2}}$.

Fraction of BnOH which initiated the ROP of CL $F_{BnOH} = \frac{I_{\alpha BnOH}}{I_{BnOHf} + I_{\alpha BnOH}}$

Table S 3. Results and conditions of the BA-OROP of CL with BnOH as initiator at 155 °C.[a]

Entry	$[M]_0/[I]_0$	Time (h)	C_{CL}[b] (%)	$M_{n,SEC}$[c] (g.mol^{-1})	$Đ$[c]	F_{BnOH}[d] (%)	DP,α[e]	DP,th[f]	DP,ω[g]
1	25	0.5	5	600	1.1	72	1.7	1.3	1.6
2	25	1.25	24	1370	1.16	98	5.9	6	5.6
3	25	2	54	2660	1.16	100	13.4	13.4	12.5
4	25	3	78	3910	1.19	100	19.2	19.4	18.5
5	25	3.83	89	4540	1.25	100	22	22.2	21.4

[a] Reactions were performed in bulk at 155 °C under argon atmosphere with reaction conditions: m_{CL} = 200 mg and $([CL]_0/[BA]_0/[BnOH]_0$ = 25/1.25/1). [b] CL conversions were determined by ^{1}H NMR analysis. [c]Uncorrected number average molar mass and dispersities (*Đ*) of crude copolymers determined by SEC chromatography (polystyrene standards), at 308 K and THF/NEt_3 (2w%) as eluent. [d]F_{BnOH} BnOH conversion. [e] Degree of polymerization calculated from the α-chain ends determined by ^{1}H NMR. [f]Theoretical degree of polymerization $DP,th = \frac{[CL]_0}{[I]_0} \times C_{CL}$. [g] Degree of polymerization calculated from the ω-chain ends determined by ^{1}H NMR.

Table S 4. Calculation of β the kinetic order relative to the initiator for the ROP of *L*-LA.

k_{app}	ln k_{app}	$[I]_0$	ln$[A]_0$
0.0542	2.91507437	0.3575	1.02861992
0.0248	3.69691163	0.1816	1.70594881
0.0178	4.02855682	0.1217	2.10619628

Table 3, Entries 3, 8 and 9.

Table S 5. Calculation of β the kinetic order relative to the initiator for the ROP of CL

k_{app}	ln k_{app}	$[I]_0$	ln$[I]_0$
1.76291134	0.56696661	0.3498043	-1.05038142
0.889	-0.11765804	0.17764736	-1.72795484
0.51414331	-0.66525324	0.08952627	-2.41322323

Table 1, Entries 3,5 and 6.

Triblock copolymers

Figure S 14. 1H-13C coupling NMR spectra (HSQC and HMBC) of PLA (Table 3, Entry 3) in $CDCl_3$.

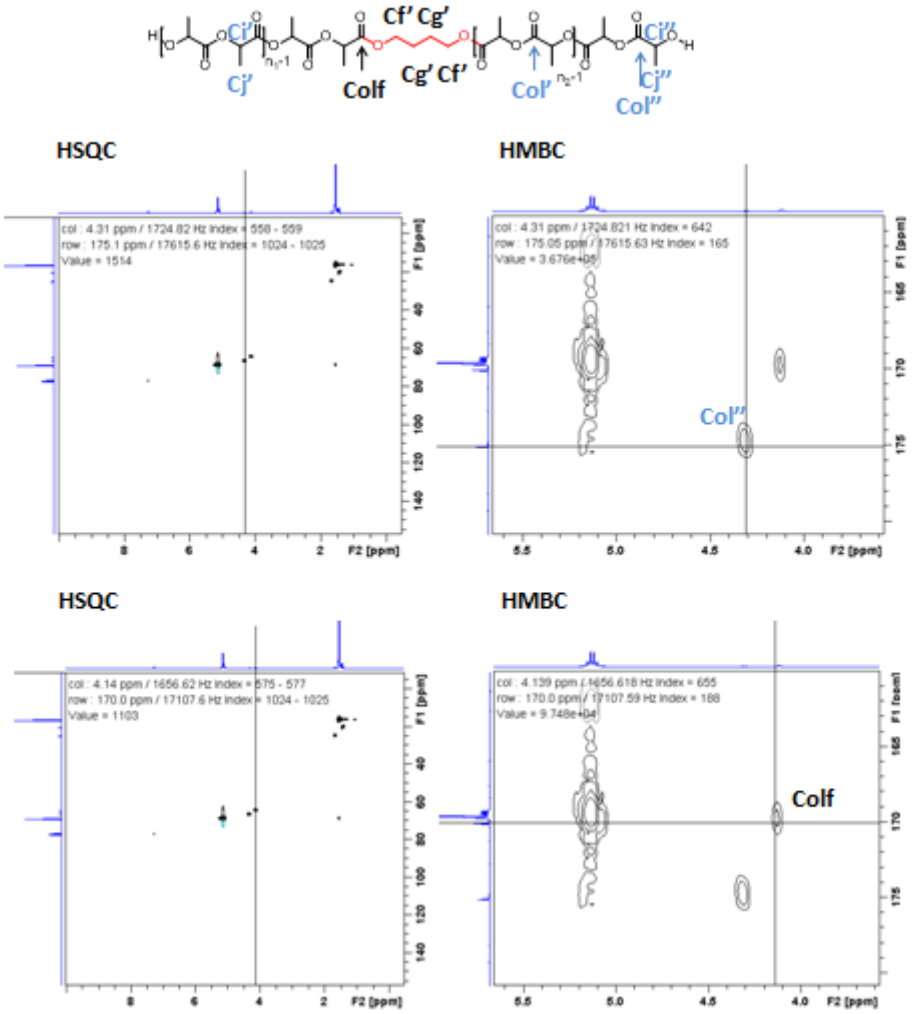

Figure S 15. Thermogravimetric analysis (TGA) of the triblock copolymer (10 °C/min)

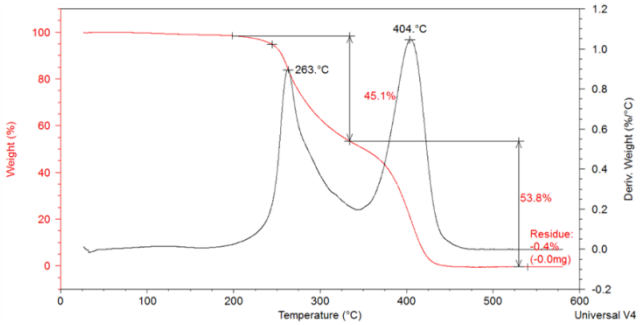

References

1 S. Gazeau-Bureau, D. Delcroix, B. Martín-Vaca, D. Bourissou, C. Navarro and S. Magnet, *Macromolecules*, 2008, **41**, 3782–3784.

2 Y. Jin, Y. Ji, X. He, S. Kan, H. Xia, B. Liang, J. Chen, H. Wu, K. Guo and Z. Li, *Polym. Chem.*, 2014, **5**, 3098–3106.

3 D. Delcroix, A. Couffin, N. Susperregui, C. Navarro, L. Maron, B. Martin-Vaca and D. Bourissou, *Polym. Chem.*, 2011, **2**, 2249–2256.

4 X. Zhou and L. Hong, *Colloid Polym. Sci.*, 2013, **291**, 2155–2162.

5 K. Makiguchi, T. Satoh and T. Kakuchi, *Macromolecules*, 2011, **44**, 1999–2005.

6 T. Saito, Y. Aizawa, K. Tajima, T. Isono and T. Satoh, *Polym Chem*, 2015, **6**, 4374–4384.

7 Y. Ren, Z. Wei, X. Leng, Y. Wang and Y. Li, *Polymer*, 2015, **78**, 51–58.

8 B. G. G. Lohmeijer, R. C. Pratt, F. Leibfarth, J. W. Logan, D. A. Long, A. P. Dove, F. Nederberg, J. Choi, C. Wade, R. M. Waymouth and J. L. Hedrick, *Macromolecules*, 2006, **39**, 8574–8583.

9 H. Yang, J. Xu, S. Pispas and G. Zhang, *Macromolecules*, 2012, **45**, 3312–3317.

10 H. Alamri, J. Zhao, D. Pahovnik and N. Hadjichristidis, *Polym Chem*, 2014, **5**, 5471–5478.

11 H. Alamri and N. Hadjichristidis, *Polym. Chem.*, 2016, **7**, 3225–3228.

12 G. W. Nyce, T. Glauser, E. F. Connor, A. Möck, R. M. Waymouth and J. L. Hedrick, *J. Am. Chem. Soc.*, 2003, **125**, 3046–3056.

13 N. E. Kamber, W. Jeong, S. Gonzalez, J. L. Hedrick and R. M. Waymouth, *Macromolecules*, 2009, **42**, 1634–1639.

14 Y. Wang, J. Niu, L. Jiang, Y. Niu and L. Zhang, *J. Macromol. Sci. Part A*, 2016, **53**, 374–381.

15 D. Bourissou, B. Martin-Vaca, A. Dumitrescu, M. Graullier and F. Lacombe, *Macromolecules*, 2005, **38**, 9993–9998.

16 M. Baśko and P. Kubisa, *J. Polym. Sci. Part Polym. Chem.*, 2008, **46**, 7919–7923.

17 M. Baśko and P. Kubisa, *J. Polym. Sci. Part Polym. Chem.*, 2010, **48**, 2650–2658.

18 M. Bednarek, M. Basko, T. Biedron, E. Wojtczak and A. Michalski, *Eur. Polym. J.*, 2015, **71**, 380–388.

19 L. Mezzasalma, A. P. Dove and O. Coulembier, *Eur. Polym. J.*, 2017, **95**, 628–634.

20 J. U. Pothupitiya, N. U. Dharmaratne, T. M. M. Jouaneh, K. V. Fastnacht, D. N. Coderre and M. K. Kiesewetter, *Macromolecules*, 2017, **50**, 8948–8954.

21 J. Xu, J. Liu, Z. Li, H. Wang, S. Xu, T. Guo, H. Zhu, F. Wei, Y. Zhu and K. Guo, *Polymer*, 2018, **154**, 17–26.

22 H. Li and L. Gu, *J. Polym. Sci. Part Polym. Chem.*, 2018, **56**, 968–976.

23 F. Sanda, H. Sanada, Y. Shibasaki and T. Endo, *Macromolecules*, 2002, **35**, 680–683.

24 P. V. Persson, J. Casas, T. Iversen and A. Córdova, *Macromolecules*, 2006, **39**, 2819–2822.
25 P. V. Persson, J. Schröder, K. Wickholm, E. Hedenström and T. Iversen, *Macromolecules*, 2004, **37**, 5889–5893.
26 J. Casas, P. V. Persson, T. Iversen and A. Córdova, *Adv. Synth. Catal.*, 2004, **346**, 1087–1089.
27 J. Xu, J. Song, S. Pispas and G. Zhang, *J. Polym. Sci. Part Polym. Chem.*, 2014, **52**, 1185–1192.
28 H. Li, S. Zhang, J. Jiao, Z. Jiao, L. Kong, J. Xu, J. Li, J. Zuo and X. Zhao, *Biomacromolecules*, 2009, **10**, 1311–1314.
29 C. Wang, H. Li and X. Zhao, *Biomaterials*, 2004, **25**, 5797–5801.
30 E. Oledzka, M. Sobczak, M. Kolakowski, B. Kraska, W. Kamysz and W. Kolodziejski, *Macromol. Res.*, 2013, **21**, 161–168.
31 E. Lindquist and Y. Yang, *J. Chromatogr. A*, 2011, **1218**, 2146–2152.
32 M. Liras, E. Verde-Sesto, M. Iglesias and F. Sánchez, *Eur. Polym. J.*, 2017, **95**, 775–784.
33 S. García-Argüelles, C. García, M. C. Serrano, M. C. Gutiérrez, M. L. Ferrer and F. del Monte, *Green Chem*, 2015, **17**, 3632–3643.
34 H. R. Kricheldorf, N. Lomadze and G. Schwarz, *Macromolecules*, 2008, **41**, 7812–7816.
35 G. Nogueira, A. Favrelle, M. Bria, J. P. Prates Ramalho, P. J. Mendes, A. Valente and P. Zinck, *React Chem Eng*, 2016, **1**, 508–520.
36 J.-B. Zhu and E. Y.-X. Chen, *J. Am. Chem. Soc.*, 2015, **137**, 12506–12509.
37 P. Lewinski, S. Sosnowski and S. Penczek, *Polymer*, 2017, **108**, 265–271.
38 J. Kadota, D. Pavlović, H. Hirano, A. Okada, Y. Agari, B. Bibal, A. Deffieux and F. Peruch, *RSC Adv.*, 2014, **4**, 14725.
39 M. Baśko and P. Kubisa, *J. Polym. Sci. Part Polym. Chem.*, 2006, **44**, 7071–7081.
40 N. Susperregui, D. Delcroix, B. Martin-Vaca, D. Bourissou and L. Maron, *J. Org. Chem.*, 2010, **75**, 6581–6587.
41 D. J. Coady, H. W. Horn, G. O. Jones, H. Sardon, A. C. Engler, R. M. Waymouth, J. E. Rice, Y. Y. Yang and J. L. Hedrick, *ACS Macro Lett.*, 2013, **2**, 306–312.
42 M. J. Frisch, G. Trucks, H. B. Schlegel, G. E. Scuseria, M. A. Robb, J. Cheeseman, G. Scalmani, V. Barone, B. Mennucci, G. A. Petersson, H. Nakatsuji, M. Caricato, X. Li, H. P. Hratchian, A. F. Izmaylov, J. Bloino, G. Zheng, J. Sonnenberg, M. Hada, M. Ehara, K. Toyota, R. Fukuda, J. Hasegawa, M. Ishida, T. Nakajima, Y. Honda, O. Kitao, H. Nakai, T. Vreven, J. A. Montgomery, J. E. Peralta, F. Ogliaro, M. Bearpark, J. J. Heyd, E. Brothers, K. N. Kudin, V. N. Staroverov, R. Kobayashi, J. Normand, K. Raghavachari, A. Rendell, J. C. Burant, S. S. Iyengar, J. Tomasi, M. Cossi, N. Rega, J. M. Millam, M. Klene, J. E. Knox, J. B. Cross, V. Bakken, C. Adamo, J. Jaramillo, R. Gomperts, R. E. Stratmann, O. Yazyev, A. J. Austin, R. Cammi, C. Pomelli, J. W. Ochterski, R. L. Martin, K. Morokuma, V. G. Zakrzewski, G. A. Voth, P. Salvador, J. J. Dannenberg,

S. Dapprich, A. D. Daniels, O. Farkas, J. B. Foresman, J. V. Ortiz, J. Cioslowski and D. J. Fox, *Gaussian 09 Revision A.1. Gaussian Inc*, Wallingford, CT, 2009.

43 J.-D. Chai and M. Head-Gordon, *Phys. Chem. Chem. Phys.*, 2008, **10**, 6615.

44 I. Nifant'ev, A. Shlyakhtin, V. Bagrov, B. Lozhkin, G. Zakirova, P. Ivchenko and O. Legon'kova, *React. Kinet. Mech. Catal.*, 2016, **117**, 447–476.

45 M. K. Kiesewetter, E. J. Shin, J. L. Hedrick and R. M. Waymouth, *Macromolecules*, 2010, **43**, 2093–2107.

46 A. Chuma, H. W. Horn, W. C. Swope, R. C. Pratt, L. Zhang, B. G. G. Lohmeijer, C. G. Wade, R. M. Waymouth, J. L. Hedrick and J. E. Rice, *J. Am. Chem. Soc.*, 2008, **130**, 6749–6754.

47 C. Alemán, O. Betran, J. Casanovas, K. N. Houk and H. K. Hall, *J. Org. Chem.*, 2009, **74**, 6237–6244.

48 C. Alemán, O. Bertran, K. N. Houk, A. B. Padías and H. K. Hall, *Theor. Chem. Acc.*, , DOI:10.1007/s00214-012-1133-y.

49 A. Nachtergael, O. Coulembier, P. Dubois, M. Helvenstein, P. Duez, B. Blankert and L. Mespouille, *Biomacromolecules*, 2015, **16**, 507–514.

50 Y. Xia, J. Shen, H. Alamri, N. Hadjichristidis, J. Zhao, Y. Wang and G. Zhang, *Biomacromolecules*, 2017, **18**, 3233–3237.

51 Sweet,D.V., *Regist. Toxic Eff. Chem. Subst.*, 1985.

52 O. Coulembier, S. Moins, J.-M. Raquez, F. Meyer, L. Mespouille, E. Duquesne and P. Dubois, *Polym. Degrad. Stab.*, 2011, **96**, 739–744.

53 Y. Fan, H. Nishida, Y. Shirai, Y. Tokiwa and T. Endo, *Polym. Degrad. Stab.*, 2004, **86**, 197–208.

54 A. Dzienia, P. Maksym, M. Tarnacka, I. Grudzka-Flak, S. Golba, A. Zięba, K. Kaminski and M. Paluch, *Green Chem.*, 2017, **19**, 3618–3627.

55 J. Kasperczyk and M. Bero, *Makromol. Chem.*, 1993, **194**, 913–925.

56 L. Mezzasalma, J. De Winter, D. Taton and O. Coulembier, *Green Chem.*, 2018, **20**, 5385–5396.

Chapter 4.

Bulk Organocatalytic Synthetic Access to Statistical Copolyesters from *L*-Lactide and ε-Caprolactone Using Benzoic Acid

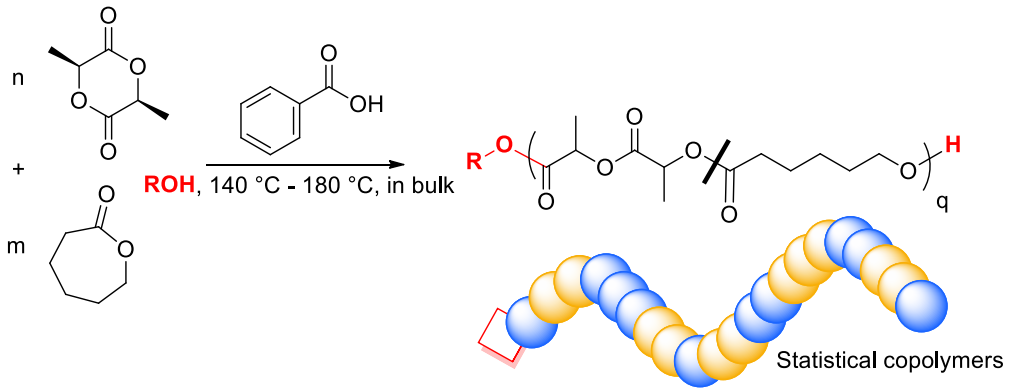

Keywords: organocatalysis, benzoic acid, lactide, caprolactone, copolymerization, bulk, statistical copolymers, ring-opening.

Chapter 4. Bulk Organocatalytic Synthetic Access to Statistical Copolyesters from *L*-Lactide and ε-Caprolactone Using Benzoic Acid

Table of contents

Introduction

As highlighted in the previous chapter, benzoic acid (BA) is a thermally stable organocatalyst that enables the ring-opening polymerization (ROP) of ε-caprolactone (CL) and *L*-lactide (*L*-LA) with a rather good control for such high reaction temperature. A bifunctional mechanism has been proposed to operate in which BA can activate the monomer and the initiator by proton exchanges. The ROP of CL has been shown to be much faster than that of *L*-LA in the same conditions, since the carbonyl group of CL is more activated by BA and thus may be more basic than that of *L*-LA. Another explanation could be that the basic moiety of BA may be too weak to activate efficiently the chain end of *L*-LA. Interestingly, BA has shown, at the end of the second chapter, to catalyze the ring-opening copolymerization (RO*c*P) of *L*-LA and CL in a statistical way.

Such weak carboxylic acids have never been investigated for the organocatalyzed RO*c*P of (lactide) LA and CL maybe because of their low activity. In addition, attempts to design P(LA-*stat*-CL) copolymers by RO*c*P using other organocatalysts have met with limited success.[1,2,3,4,5,6,7,8,9] Basic-type organocatalysts, such as phosphazenes,[2] *N*-heterocyclic carbenes (NHCs),[3,7] 1,5,7-triazabicyclo[4.4.0]dec-5-ene guanidine (TBD) [1]and urea-amine[8] only enable incorporation of LA in the polymer chain, and P(LA-*stat*-CL) copolymer synthesis cannot be achieved in this way (Figure 1a). In contrast, only one Brønsted acid-type catalysts has been shown to perform the statistical organocatalyzed RO*c*P (ORO*c*P) of LA and CL.[4,5,9] Trifluoromethanesulfonic acid (TfOH) has been used in dichloromethane at 35 °C, providing a preferential insertion of LA units in copolymer chains (Figure 1b).[4,5] The same trend has been observed when dibenzoylmethane, investigated in the second chapter, has been used as catalyst for the bulk ORO*c*P of LA and CL at 155 °C, forming gradient to statistical–like copolymers (Figure 1d). Finally, the use of (R)-(−)-1,1'-binaphthyl-2,2'-diyl hydrogen phosphate (BPA) have led to the preferential insertion of CL in the copolymer with only 8% of LA inserted from an equimolar mixture of LA and CL (Figure 1c).[6]

In the present chapter, we provide a complete description of the P(LA-*stat*-CL) copolymer synthesis in solvent-free conditions. In particular, reactivity ratios of co-monomers have been determined, using both the Kelen-Tüdős linear method and a nonlinear method referred to as "the visualization of the sum of squared residuals space" (VSSRS).[10,11] Then, the P(LA-*stat*-CL) statistical copolymers have been characterized by combined analyses, including ^{1}H, ^{13}C and DOSY NMR, DSC and SEC. The rather good control of this BA-ORO*c*P process has been further exploited to achieve PLA-*b*-P(LA-*stat*-CL)-*b*-PLA triblock copolymers, by sequential RO*c*P-mediated synthesis. The ability of BA to conduct the statistical copolymerization of *L*-LA and CL has then been compared to the activity of miscellaneous organocatalysts. Finally, the BA toxicity has been explored by Saad Saba, completing his PhD under the supervision of Pr. Pascal Loyer at the Institute NUMECAN (Nutrition Metabolisms and Cancer) UMR-A 1341, UMR S 1241 at the

University of Rennes. The VSSRS investigations have been conducted in collaboration with Dr. Simon Harrisson at the Laboratoire des Interactions Moléculaires et Réactivités Chimiques et Photochimiques (IMRCP, UMR 5623) in Toulouse.

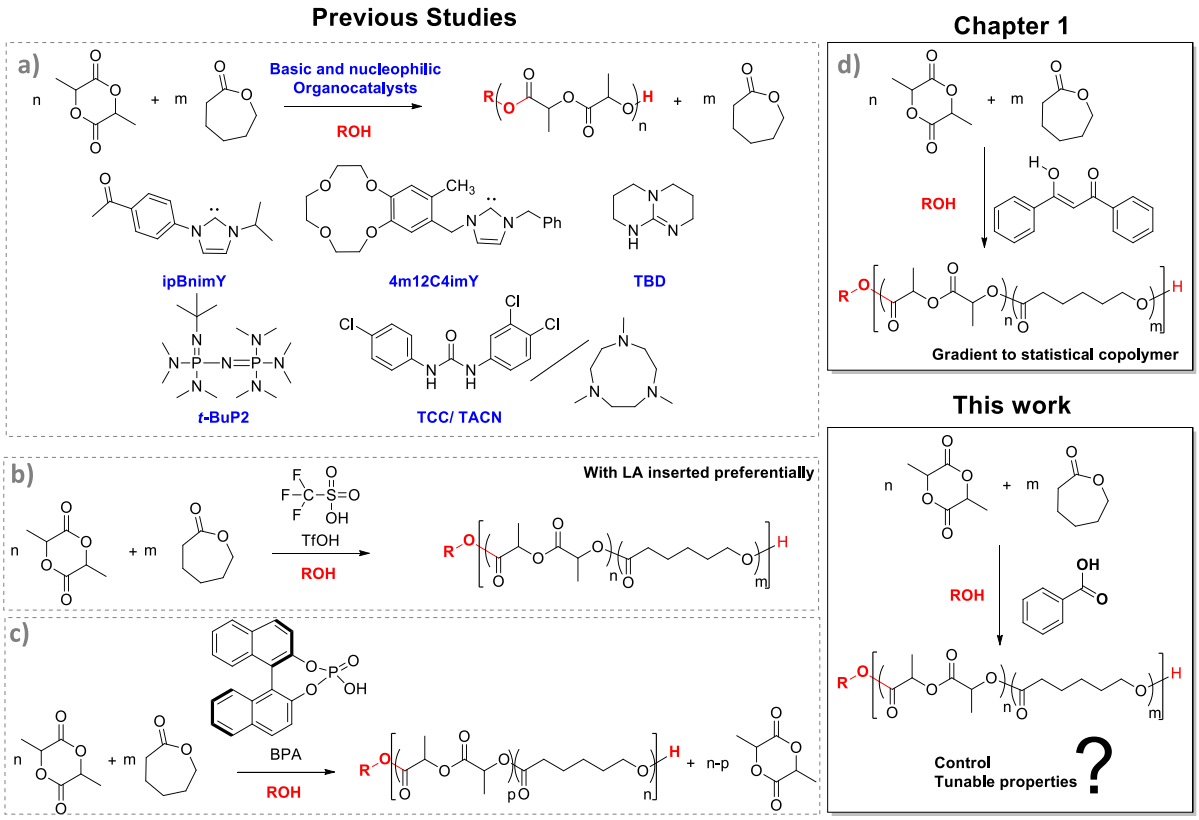

Figure 1. Scope of the organocatalysts applied for the RO*c*P of LA and CL.

1 Investigations into the BA-ORO*c*P of *L*-LA and CL in bulk.

BA was used to catalyze the RO*c*P of *L*-LA and CL in bulk between 140 °C and 180 °C in the presence of the butane-1,4-diol (BD), heptan-1-ol (HepOH) and methoxypoly(ethylene glycol) ($mPEG_{1000}$) as initiators (Scheme 1). Table 1 summarizes the main results obtained.

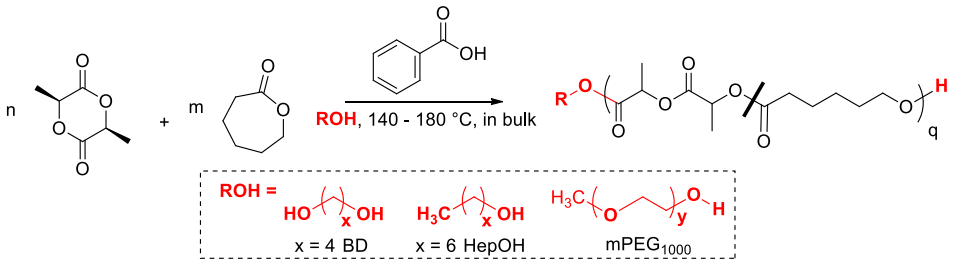

Scheme 1. BA-ORO*c*P of *L*-LA and CL

Table 1. BA-ORO*c*P of *L*-LA and CL in bulk at 155 °C in presence of alcohol initiators (I).

Entry	I	$f_{CL,0}$[b] (%)	BA (mol%)[c]	T (°C)	Time (h)	C_{CL}/C_{LA} (%/%)[d]	F_{CL}[e] (%)	$M_{n,SEC}$[f] (g.mol^{-1})	$Đ$[f]	DP,$_{th}$[g]	DP,$_{exp}$[h]
1	BD	51	0	155	54	15/39	29	2830	1.13	13.4	12.1
2	BD	51	2.5	155	48	85/91	49	7640	1.18	44.2	42.7
3	BD	51	5	155	36	85/87	50	7740	1.15	43	42.0
4	BD	52	10	155	27	92/88	53	8110	1.17	45.1	41.0
5	BD	91	5	155	7.2	82/78	92	7600	1.25	39.9	39.9
6	BD	72	5	155	20.5	84/85	71	7140	1.2	42.3	38.0
7	BD	31	5	155	48	82/80	32	7530	1.11	40.6	38.5
8	BD	21	5	155	66	86/82	22	8040	1.13	42.1	39.1
9[i]	BD	51	5	155	73.6	85/83	52	13820	1.25	83	70.0
10	BD	51	5	140	64	80/79	51	8150	1.15	39.9	42.2
11	BD	51	5	165	20	79/82	50	7080	1.16	40.1	37.1
12	BD	51	5	180	12.4	89/88	51	7720	1.23	44.4	42
13	HepOH	52	5	155	54	87/92	51	8610	1.35	44.8	41.8
14	PEG	94	5	155	24	92/89	94	8790	1.58	45.2	n.a

[a]Reactions were performed in bulk at 155 °C under argon atmosphere with reaction conditions: n_{CL} + n_{LA} = 2.8 mmol; and $[M]_0/[I]_0$ = 50/1 with $[M]_0$ = $[L\text{-LA}]_0$ + $[CL]_0$; [b]CL fraction in the initial feed; [c]mol.% of catalyst loading related to the monomers; [d]CL and *L*-LA conversions were determined by ^{1}H NMR analysis; [e]CL fraction in the pure copolymer; [f]Uncorrected average molar mass and dispersity ($Đ$) of crude copolymers determined by SEC chromatography (polystyrene standards) at 40 °C and THF as eluent. [g]Theoretical degree of polymerization $DP_{,th} = \frac{[L-LA]_0}{[I]_0} \times C_{LA} + \frac{[CL]_0}{[I]_0} \times C_{CL}$. [h]Degree of polymerization calculated from the chain ends determined by ^{1}H NMR; [i]$[M]_0/[I]_0$ = 100/1. n.a: not available.

1.1 Evaluation of the control of the BA-ORO*c*P initiated by butane-1,4-diol

A first series of copolymerization experiments employed different BA catalyst loadings and BD as initiator, with an initial monomer-to-initiator ratio $[L\text{-LA}]_0$:$[CL]_0$:$[I]_0$ of 25:25:1 (Table 1, Entries 2-4). While the reaction proved sluggish in the absence of BA, with *L*-LA being inserted preferentially affording brown copolymers (Table 1, Entry 1, Figure S 1), the copolymerization kinetics could be appreciably enhanced by increasing the BA loading from 2.5 to 10 mol% relative to the monomers, confirming the catalytic role of BA (Entries 2-4). A catalyst loading of 5 mol% relative to the monomers was selected for the rest of the study, as both monomers were consumed at the same rate. The initial co-monomer feed ratio ($f_{CL,0}$ = 0.2, 0.3, 0.5, 0.7, 0.9) was then varied, while maintaining a co-monomers-to-initiator ratio of 50 (Entries 3, 5-8). Finally, the BA-ORO*c*Ps of equimolar amount of *L*-LA and CL were carried out by varying the reaction temperature between 140 °C and 180 °C ($[M]_0/[I]_0$ = 50, Table 1, Entries 3, 10-12). In all

cases, well-defined and transparent α,ω-bishydroxy-P(LA-*co*-CL) copolymers were obtained (Figure 2a & b).

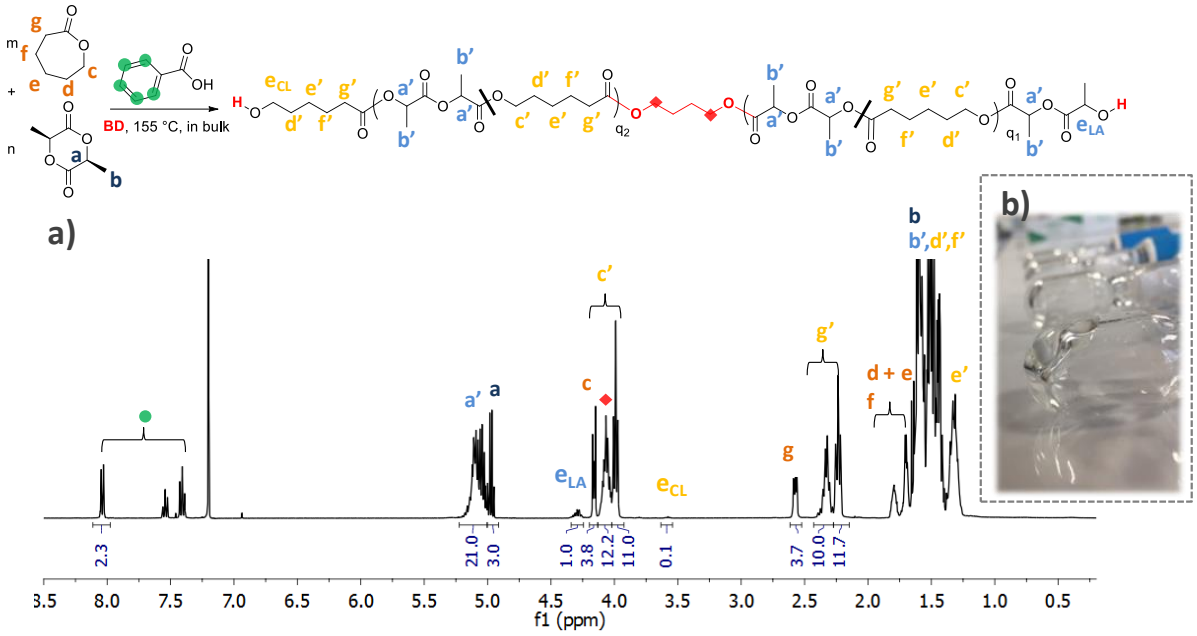

Figure 2. (a) ^{1}H NMR spectrum ($CDCl_3$, 400 MHz, r.t) and (b) picture of the crude P(LA-*co*-CL) obtained by BA-ORO*c*P of LA and CL initiated by BD at 155° C (Table 1, Entry 3).

Experimental degrees of polymerizations ($DP_{,exp}$) were consistent with theoretical values ($DP_{,th}$; Table 1) and molar masses ($M_{n,SEC}$) increased linearly with the overall conversion of the monomers (C_{TOT}, Figure 3a, and Figure S 2 and Figure S 3). Monomodal and symmetrical SEC traces were observed with dispersity remaining low ($1.11 < Đ < 1.25$; Figure 3a-b and Figure S 2, Figure S 3, Figure S 4) confirming the good control over the ORO*c*P process. Similar results were obtained using a co-monomers-to-initiator ratio equal to 100 (Table 1, Entry 9, Figure 3a,c), though a slight discrepancy between $DP_{,exp}$ and $DP_{,th}$ was noted in this case, probably due to side initiation by traces of water. Interestingly, applying a temperature of 180 °C enabled to decrease drastically the reaction time, namely 10h instead of 37h when a temperature of 155 °C was applied (Table 1, Entry 12). At this temperature a good control over the molar masses and the dispersities ($Đ < 1.23$) could be safeguarded (Figure 3d, e).

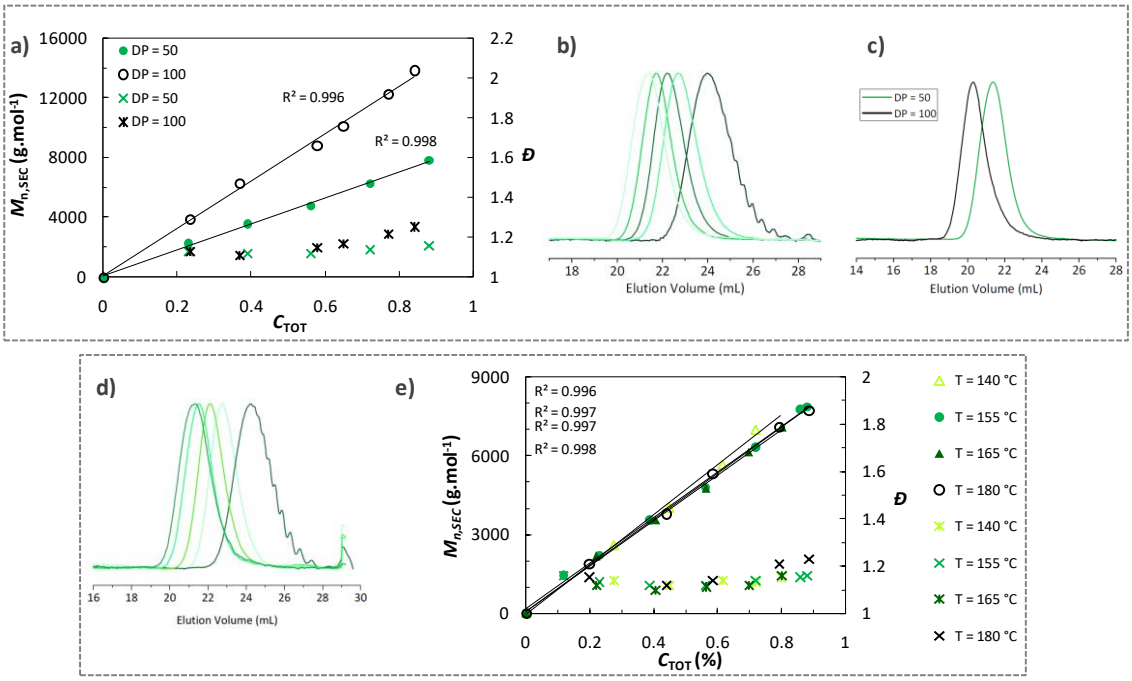

Figure 3. (a) Evolution of uncorrected $M_{n,SEC}$ (•) and dispersity $Đ$ (x) with total monomer conversion (C_{TOT}) of (Table 1, Entries 3 and 9); (b) evolution of SEC molar masses with time (**Table 1**, Entry 3); (c) SEC comparison of entries 3 and 9 (Table 1), (d) evolution of SEC molar masses with time for the BA-ORO*c*P conducted at 180 °C (Table 1, Entry 12), (e) Evolution of uncorrected $M_{n,SEC}$ (•)and dispersity $Đ$ (x) with total monomer conversion (C_{TOT}) of the BA-ORO*c*P of *L*-LA and CL conducted applying different temperatures (Table 1, Entries 3, 10, 11 and 12).

1.2 Catalyst and monomer recycling

As BA organocatalyst remained in the crude copolymers, these were purified to avoid any premature degradation,[1,12] for instance during processing[13] or storage. For this purpose, we exploited the capability of BA and *L*-LA to sublimate and of CL to evaporate following a solvent-free and straightforward purification procedure that was set up in our previous chapter (see experimental part). This also allowed us to recycle and reuse BA for further organocatalytic cycles, leading to chemically pure P(LA-*co*-CL) copolyesters. The recycling procedure was repeated up to 5 times, providing P(LA-*co*-CL) always exhibiting very similar features (5430 < $M_{n,SEC}$ < 6570 g.mol^{-1}and 1.11 < $Đ$ < 1.18), as summarized in Figure 4b. The slight decrease in the catalytic activity observed after the fourth cycle (Figure 4a) is also ascribed to some loss of BA after sublimation during purification. Finally, the SEC trace of the pure P(LA-*co*-CL) obtained after vacuum treatment ($M_{n,SEC}$ = 5960 g.mol^{-1}, $Đ$= 1.2) nearly superimposed that of the crude compound ($M_{n,SEC}$ = 6040 g.mol^{-1}, $Đ$ = 1.18, Figure 4c), indicating absence of transesterification reactions during the workup.

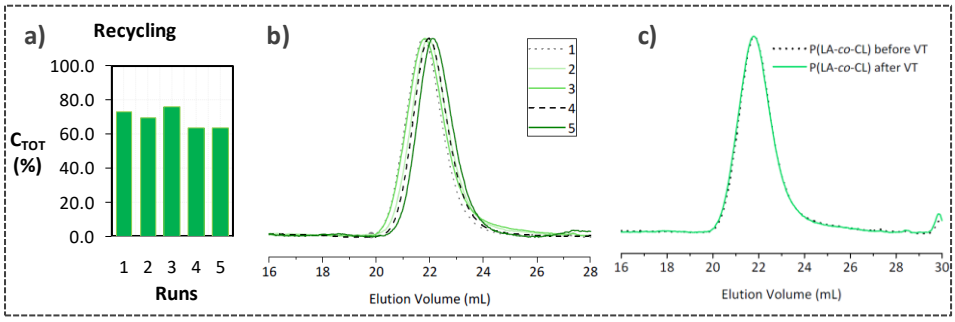

Figure 4. (a) Bar graph showing the total conversion for each run; (b) normalized SEC traces from RI detector of pure P(LA-*co*-CL)s and (c) SEC traces of P(LA-*co*-CL) before and after vacuum treatment (VT) of run 3. (THF, 313 K, 1mL.min^{-1}).

2 Determination of reactivity ratios and analysis of the microstructures

2.1 Determination of reactivity ratios

Analysis by ^{1}H NMR spectroscopy evidenced that both co-monomers were inserted in the copolymer chain throughout this BA-ORO*c*P process, irrespective of the initial co-monomer feed (Figure 5, Figure 6, Table 1).

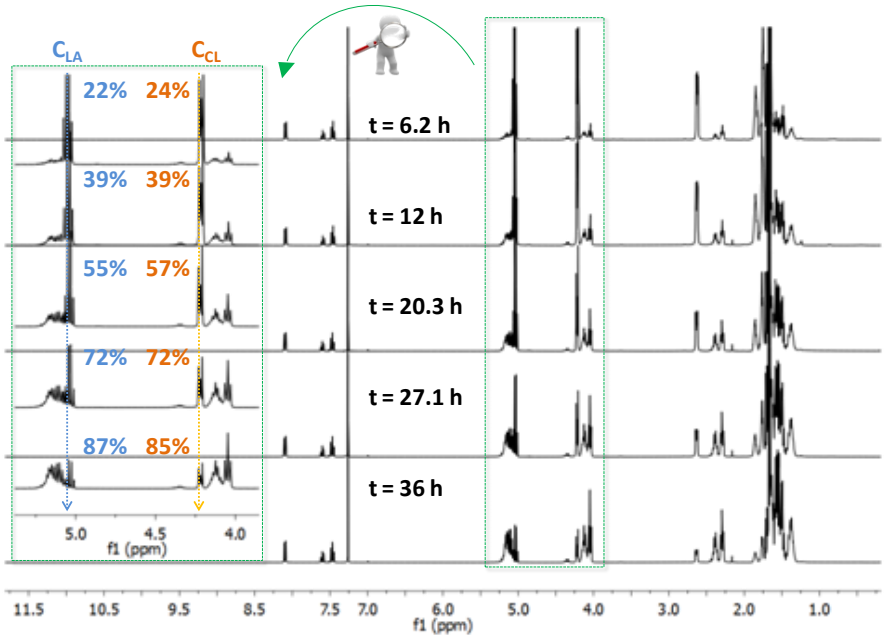

Figure 5. Stack of ^{1}H NMR spectra ($CDCl_3$, 400.2 MHz, r.t) of the crude copolymers obtained during the kinetic of the BA-ORO*c*P of *L*-LA and CL initiated by BD in bulk at 155 °C (Table 1, Entry 3).

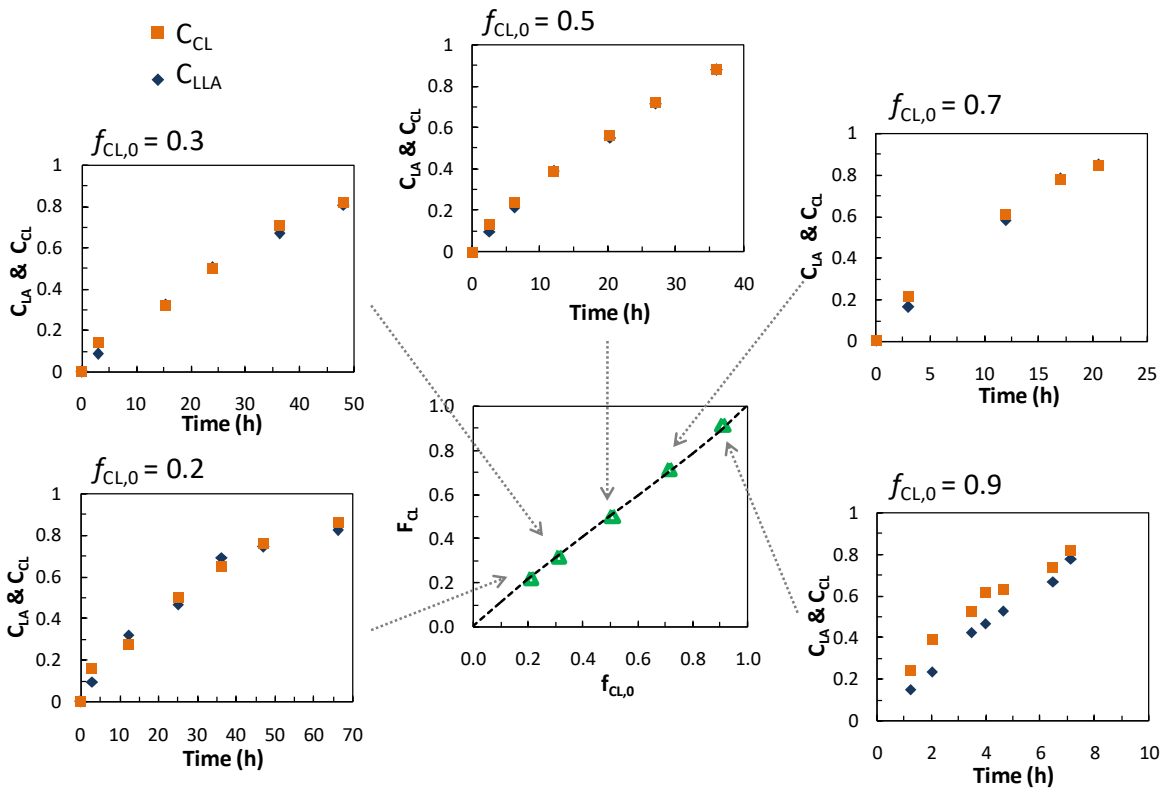

Figure 6. Evolution of the overall monomer conversion *vs.* time for different contents in CL in the initial feed ($f_{CL,0}$ = 0.2, 0.3, 0.5, 0.7, 0.8; Entries 3 and 5 to 8, respectively) and evolution of CL content in the final copolymer (F_{CL}) *vs.* $f_{CL,0}$. Dashed line represents expected F_{CL} for $r_{CL} = r_{LA}$ = 0.86 using the Mayo-Lewis equation (2).

In order to account of the copolymer microstructure, reactivity ratios of *L*-LA (r_{LA}) and CL (r_{CL}) were evaluated using the Kelen-Tüdős method, for the BA-ORO*c*P of *L*-LA and CL carried out in bulk at 155 °C (Figure S 6, Table S 1). These investigations led to the following values: r_{LA} = 0.66, r_{CL} = 0.91. However, linearized methods such as Kelen-Tüdős, which derive from the Mayo-Lewis equation and require that monomer conversion should be kept very low, can distort the error structure of the data and may provide biased estimates of reactivity ratios.

This prompted us to implement a less biased method, the "visualization of the sum of squared residuals space" (VSSRS), a nonlinear method[10,11] developed by Van den Brink *et al.* This VSSRS method not only allows for an estimate of the reactivity ratios at high conversion, but also takes into account errors both on the monomer conversion and the co-monomer ratios, thus providing unbiased estimates of the reactivity ratios as well as joint confidence regions. Data related to monomer conversion, copolymer composition (*F*) and co-monomer ratio (*f*) were fitted to the integrated form of the Mayo-Lewis copolymer composition equation, (**1**):

$$C_{TOT} = 1 - \left(\frac{f_{CL}}{f_{CL,0}}\right)^{\alpha} \times \left(\frac{f_{LA}}{f_{LA,0}}\right)^{\beta} \times \left(\frac{f_{CL,0}-\delta}{f_{CL}-\delta}\right)^{\gamma} \qquad (\mathbf{1})$$

With

$$\alpha = \frac{r_{LA}}{1-r_{LA}} \qquad \beta = \frac{r_{CL}}{1-r_{CL}} \qquad \gamma = \frac{1-r_{CL}\times r_{LA}}{(1-r_{CL})\times(1-r_{LA})} \qquad \delta = \frac{1-r_{LA}}{2-r_{CL}-r_{LA}}$$

The reactivity ratios were found equal to $r_{CL} \approx r_{LA} \approx 0.86$. Figure 7a shows the point estimates and the confidence regions obtained using the VSSRS method. The 95% confidence intervals were almost the same for both r_{CL} (0.74 – 1.01) and r_{LA} (0.75 – 1.00).

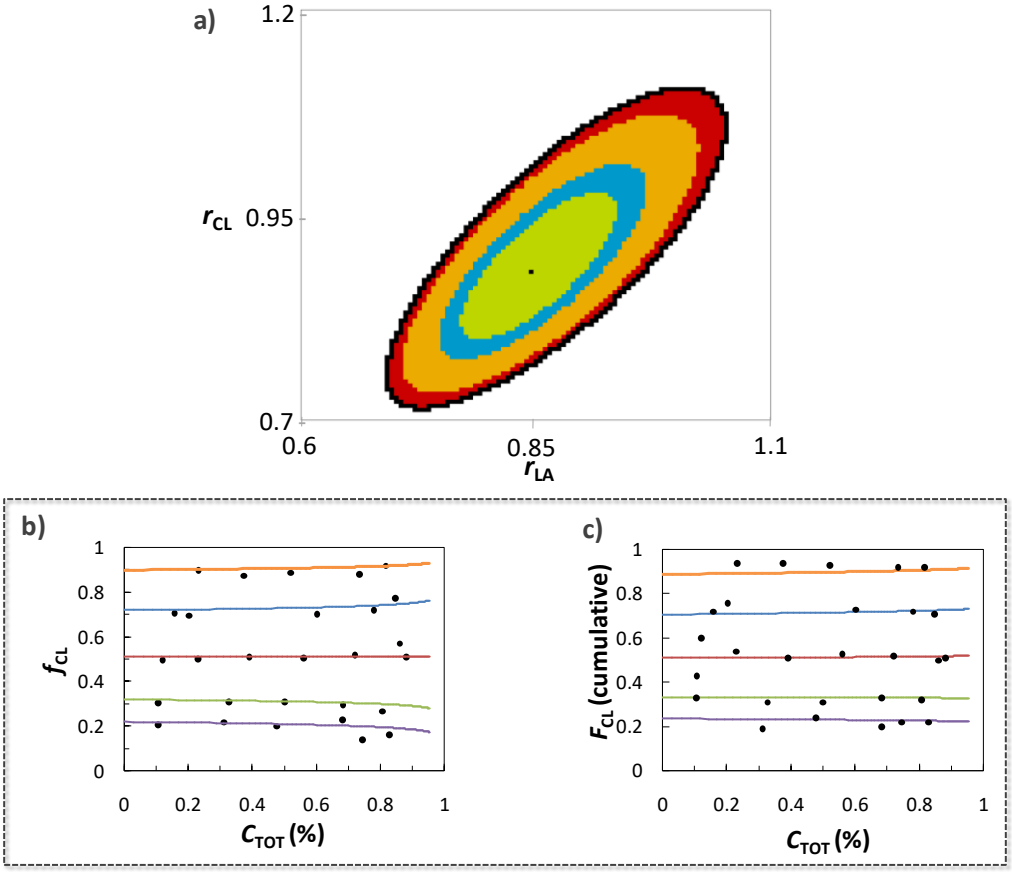

Figure 7. (a) 95% Joint confidence interval (JCI) for reactivity ratios with point estimate ($r_{CL} = r_{LA}$ =0.86). Internal contours indicate 50%, 70%, and 90% JCIs.(b) Prediction of the co-monomer ratio (solid lines) as a function of conversion *vs.* experimental points (black dots). (c) Prediction of the cumulative copolymer composition (solid lines) as a function of conversion versus experimental points (black dots).

Theoretical plots of f_{CL} and F_{CL} as a function of C_{TOT} were then modeled from values of the reactivity ratios obtained by the VSSRS method (Figure 7b&c, solid lines). These plots fit well the experimental data obtained in the course of the bulk BA-ORO*c*P of *L*-LA and CL at 155 °C (Figure 7 b-c, black dots). When plotting $F_{CL,th} = g(f_{CL,0})$ from the reactivity ratios obtained by the VSSRS method (Figure 6, dashed line) using the Mayo-Lewis equation (**2**),[14] we observed a total agreement with experimental data ($F_{CL,exp} = g(f_{CL,0})$, Figure 6). The overall composition F_{CL} was

also found in full accordance with co-monomer contents used in the feed ratio throughout the whole ORO*c*P process, including at low co-monomer conversions. The slight deviation observed at conversion lower than 20% might be due to uncertainties in the NMR measurements. Additionally, these deviations at low conversion account for the difference in estimates of reactivity ratios by the Kelen-Tüdős method and the VSSRS method.

$$F_{CL,th} = \frac{r_{CL} \times f_{CL}{}^{2} + f_{CL} \times f_{LA}}{r_{CL} \times f_{CL}{}^{2} + 2 \times f_{CL} \times f_{LA} + r_{LA} \times f_{LA}{}^{2}} \quad (2)$$

2.2 Analysis of the microstructures

These kinetic results strongly support the formation of statistical copolymers when using BA in ORO*c*P of *L*-LA and CL. Copolymer structures were further analyzed by ^{1}H and ^{13}C NMR spectroscopy from various *L*-LA/CL ratios (Table 1, Entries 3, 5 to 8). The ^{1}H NMR spectrum of the copolymer obtained from BA-ORO*c*P involving an equimolar ratio of LA and CL (Table 1, Entry 3) showed all representative peaks due to homo- and heterodiads, as illustrated in Figure 8a.

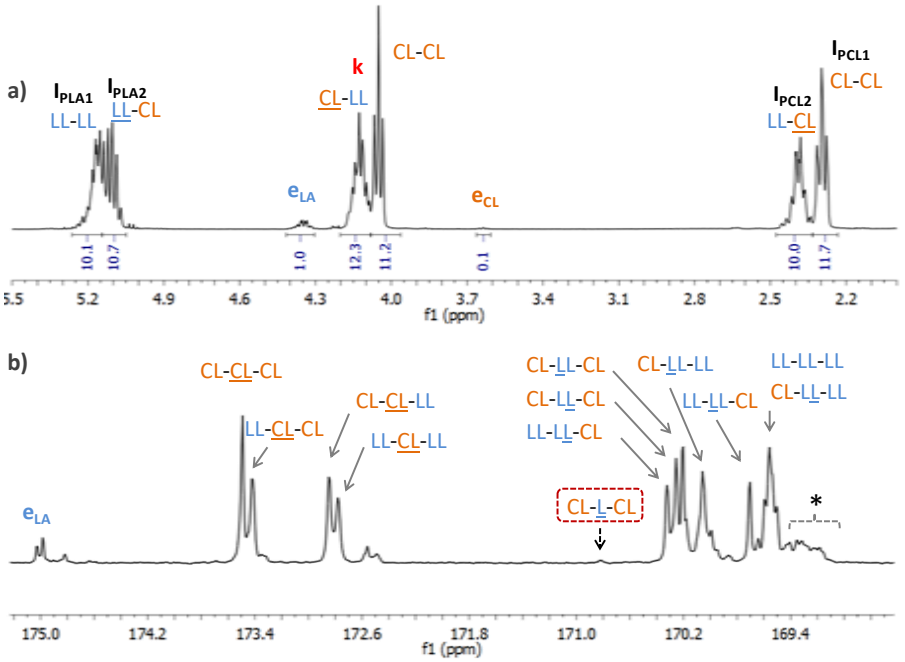

Figure 8. (a)^{1}H (400.2 MHz, r.t.) and (b) ^{13}C (100.6 MHz, r.t.) NMR spectra of a P(LA-*co*-CL) copolymer in $CDCl_3$ (Table 1, Entry 3); LL and L refer to lactidyl and lactoyl units, respectively;* epimerized LL-LL-LL sequences. k being the signal of the characteristic peak of methylene oxycarbonyl-type protons of BD.

As expected for statistical copolymers, integral values of the homosequences closely matched those of the heterosequences for both PLA (10.1/10.7, δ around 5.1 ppm) and PCL (11.7/10.0, δ around 2.35 ppm). Interestingly, the integral value of the terminal lactidyl units (e_{LA}) appearing at 4.36 ppm was ten times greater than that of the terminal caproyl units (e_{CL}) at

3.62 ppm. This might be explained by the higher reactivity of caproyl units at chain-ends, which after fast crossover gave rise to less reactive terminal lactidyl units. This can only be stated because reactivity ratios are close to 1 for both monomers ($r_{CL} \approx r_{LA} \approx 0.86$), and because the BA-OROP of CL is 20 times faster than that of *L*-LA ($k_{CL\text{-}CL} >> k_{LA\text{-}LA}$; see Chapter 3).[15] In these conditions, one can write the following relationships: $k_{CL\text{-}CL} \approx k_{CL\text{-}LA} >> k_{LA\text{-}LA} \approx k_{LA\text{-}CL}$ using equations (**3**):

$$r_{CL} = \frac{k_{CL-CL}}{k_{CL-LA}} \qquad r_{LA} = \frac{k_{LA-LA}}{k_{LA-CL}} \qquad (\mathbf{3})$$

It is worth mentioning that the first inserted monomer into the polymer chain is generally a LA with the methylene oxycarbonyl-type protons of BD, *i.e.* after initiation, at around 4.15 ppm characteristic of BD bound to a lactidyl unit (**k**, Figure 8a). Indeed, methylene oxycarbonyl-type protons characteristic of BD bound to a caproyl unit being at 4.05 ppm.

Analysis by ^{13}C NMR spectroscopy (Figure 8b) also confirmed the microstructure of the copolymer with the expected homo- and heterotriads, as previously reported.[16] Kasperczyk and Bero described two distinct modes of transesterification reactions during the RO*c*P of LA and CL, as depicted in Scheme 2.[17] Here, the "second mode of transesterification reactions", *i.e.* giving rise to the anomalous CL-L-CL sequences (L representing one lactoyl unit) at 170.8 ppm, was barely observed. As the dispersity of the resulting copolymers remained low ($1.11 < Đ < 1.25$), transesterification reactions—if present—occurred to a minor extent during the bulk BA-ORO*c*P process of *L*-LA and CL at 155 °C.

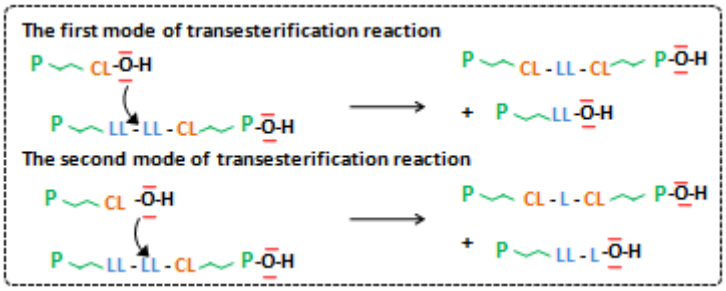

Scheme 2. The two modes of transesterification reactions.

Two series of peaks were also observed at 172.5 ppm and 175 ppm. While after performing HMBC analyses, peaks at 175 ppm could be ascribed to the carbonyl carbon (-C(O)-) of the lactidyl unit at the copolymer chain ends, peaks around 172.5 ppm could not be clearly attributed, and might be the result of minor side reactions occurring at high temperature. In addition, only one diffusion coefficient was determined by DOSY-NMR ($D = 9.24 \times 10^{-11}$ $m^2.s^{-1}$, $DP_{,exp} = 42$, Figure 9a, Figure S 7) that was different from that of PLA ($D = 1.32 \times 10^{-10}$ $m^2.s^{-1}$, $DP_{,exp} = 21$) and of PCL ($D = 5.54 \times 10^{-11}$ $m^2.s^{-1}$; $DP_{,exp} = 21$, Figure 9b,d, Figure S 8, Figure S 9).

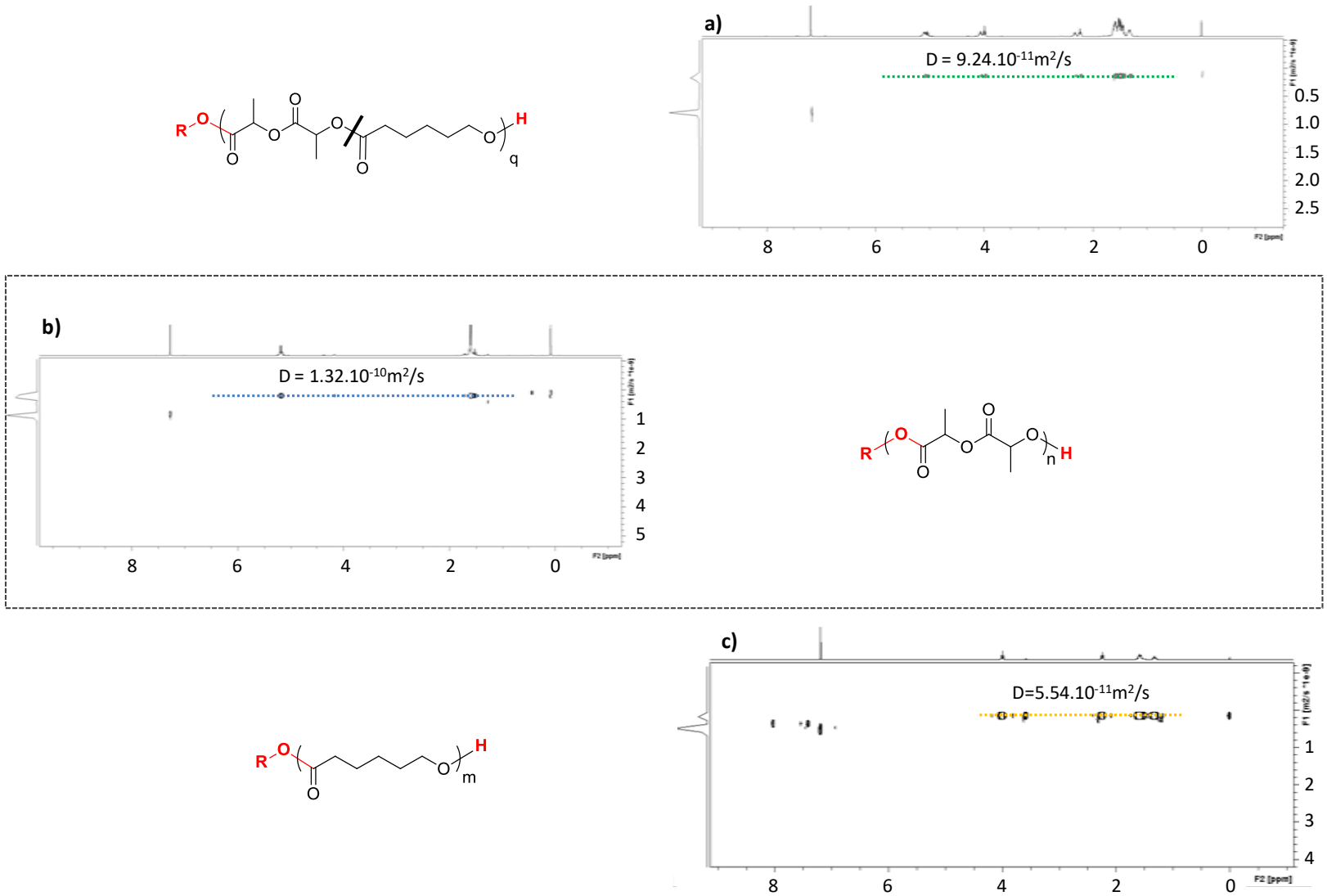

Figure 9. DOSY NMR spectra ($CDCl_3$, 400.2 MHz, r.t) of (a) pure P(LA-*co*-CL) (Table 1, Entry 3), (b) of pure PLA and (c) PCL synthesized by BD-initiated BA-OROP of *L*-LA and CL, respectively (see Chapter 3).

The same peaks of homo- and heterosequences, though of different intensities, were observed for copolymers of differing composition (Figure 10a,b, Table 1, Entries 3 and 5-8). As expected, the content of CL heterodiads ($\mathcal{E}_{CL\text{-}LA}$), in other words the number of links between LA and CL units divided by the total number of links, decreases linearly when the initial feed in CL increases (Figure 10c, Table 2).

Table 2. Characteristics of the copolymers obtained by BA-OROcP of *L*-LA and CL (Table 1, Entries 3, 5-8).

Entry	F_{CL} (%)	$\mathcal{E}_{CL/LA}$ (%)[a]	$L_{CL,th}$[b]	$L_{CL,1H}$[c]	$L_{CL,13C}$[d]	$L_{LA,th}$[b]	$L_{LA,1H}$[c]	$L_{LA,13C}$[d]	$T_{g,Fox}$ (° C)[e]	$T_{g,exp}$ (° C)[f]	T_m (° C)[g]
5	92	8	9.9	12.6	n.d	1.1	n.a	n.d	-54.2	-51.7	46.0
6	71	29	3.2	3.4	n.d	1.3	n.a	n.d	-34.3	-36.5	no
3	50	47	1.9	2.1	2.21	1.8	1.9	2.13	-11.8	-11.6	no
7	32	68	1.4	1.5	n.d	2.9	2.5	n.d	9.5	11.7	no
8	22	78	1.2	1.3	n.d	3.5	3.1	n.d	21.5	24.1	no

[a]Percentage of heterodiads $\varepsilon_{CL-LA} = \frac{I_\varepsilon}{I_\eta + I_\varepsilon}$; the average block length [b] calculated from equations **3**; [c] determined by ^{1}H NMR analyses $L_{CL,1H} = \frac{I_\eta}{I_\varepsilon} + 1$, $L_{LA,1H} = \frac{I_\alpha}{I_\beta} + 1$ (Figure 10); [d] determined by analyses of the ^{13}C NMR, equations in reference [17]; Glass transition temperature; [e] determined by Fox equation with T_g(PLA) = 50 °C and T_g(PCL) = -62 °C, [f] determined from the second cycle of DSC; [g] melting temperature determined by DSC; n.a: not available; n.d: not determined.

The number average block length of the caproyl (L_{CL}) and lactidyl (L_{LA}) units could also be assessed by ^{1}H and quantitative ^{13}C NMR analyses and compared with the theoretical values ($L_{CL,th}$ and $L_{LA,th}$) obtained from equations (**4**) (Figure 11a & Figure S 10).

$$L_{CL,th} = \frac{r_{CL} \times f_{CL} + f_{LA}}{f_{LA}} \qquad L_{LA,th} = \frac{r_{LA} \times f_{LA} + f_{CL}}{f_{CL}} \quad (\mathbf{4})$$

For the pure copolymer of F_{CL} = 0.5 (Table 2, Entry 3), L_{CL} and L_{LA} values determined by ^{13}C NMR ($L_{CL,13C}$ =2.2 and $L_{LA,13C}$= 2.1) were in excellent agreement with the theoretical values ($L_{CL,th}$ = 1.9 and $L_{LA,th}$ = 1.8) and with those determined by ^{1}H NMR spectroscopy ($L_{CL,1H}$ = 2.1 and $L_{LA,1H}$= 1.9). As for the other copolymers of different co-monomer ratios, only the number average block lengths determined by ^{1}H NMR ($L_{LA,1H}$, $L_{CL,1H}$) were determined $L_{CL,th}$ and $L_{LA,th}$ which were in good agreement with the theoretical values (Table 2, Figure 11a).

It worth mentioning that two type of lactidyl chain ends can be observed on the ^{13}C NMR spectra (Figure 10b). Increasing the content of CL in the copolymer, *i.e.* at high $f_{CL,0}$, leads to an increase of the peak at 174.96 ppm which may be ascribed to a lactidyl unit presenting a caproyl unit as penultimate unit ($e_{CL\text{-}LA}$). In contrast, decreasing the content of CL, thus increasing the

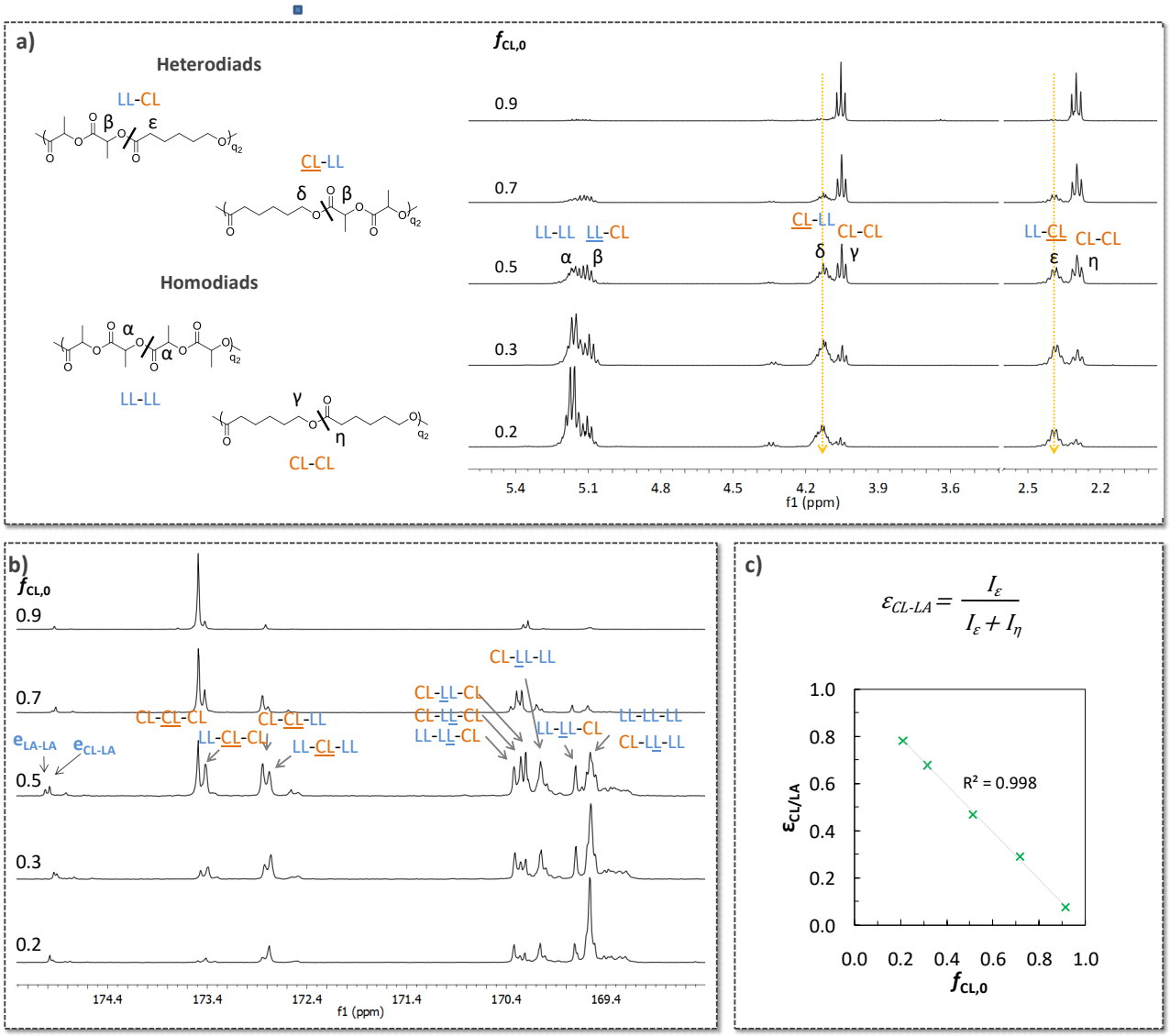

Figure 10. Stack of (a) ^{1}H NMR spectra ($CDCl_3$, 400.2 MHz, r.t) and (b) ^{13}C NMR spectra of pure copolymers of various $f_{CL,0}$ (Table 1, Entries 3, 5 to 8), (c) Percentage of heterodiads ($\mathcal{E}_{CL/LA}$) in the copolymers as a function of f_{CL}.

content of *L*-LA in the copolymer (low $f_{CL,0}$) leads to an increase of the peak at 175.03 ppm which may be ascribed to a lactidyl unit presenting a lactidyl as penultimate unit (e_{LA-LA}).

Finally, glass transition temperatures, as determined from the second run of DSC analyses ($T_{g,exp}$),were consistent with values expected from the Fox equation ($T_{g,Fox}$, Figure 11b, Table 2, Figure S 11).

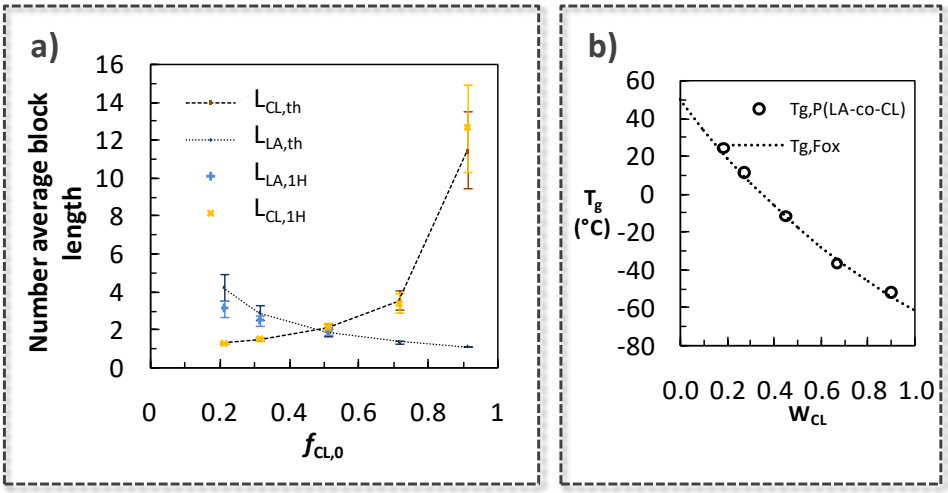

Figure 11. (a) Theoretical number average block lengths ($L_{CL,th}$ and $L_{LA,th}$) as a function of $f_{CL,0}$ and experimental average block length determined by ^{1}H NMR spectroscopy ($L_{CL,1H}$ and $L_{LA,1H}$) for different $f_{CL,0}$. (b) Experimental glass transition temperatures of the P(LA-*co*-CL) copolymers as a function of the weight fraction of CL in the copolymer. Dotted line, theoretical glass transition temperature of the copolymers calculated from Fox equation.

3 BA-ORO*c*P of LA and CL from other initiators and triblock copolymer synthesis

To demonstrate the versatility of BA as an organocatalyst, HepOH and $mPEG_{1000}$ were evaluated as initiators for the bulk ORO*c*P of *L*-LA and CL at 155 °C (Table 1, Entries 13-14) and triblock copolymer was synthesized (Table S 2).

3.1 RO*c*P initiated by heptan-1-ol

Well-defined P(LA-*stat*-CL) could be obtained using HepOH ($[L\text{-LA}]_0/[CL]_0/[HepOH]_0/[BA]_0$ = 25/25/1/2.5, Figure 12a, Table 1, Entry 13), with $M_{n,SEC}$ increasing linearly with $C_{TOT,}$ a theoretical DP in agreement with the experimental one, and monomodal SEC traces with fairly low dispersity ($Đ$ < 1.35) for bulk RO*c*P (Figure 12b,c). The overall composition in the copolymer was in agreement with the initial co-monomer ratio ($f_{CL,0}$ = 0.52, F_{CL} = 0.51).

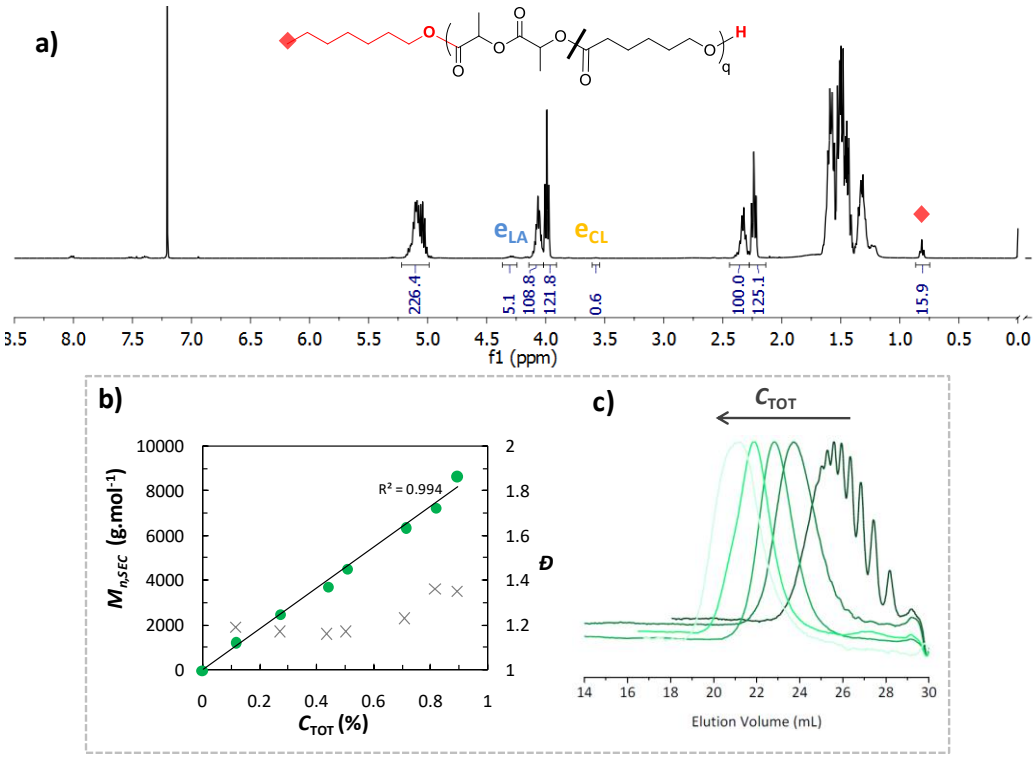

Figure 12. (a) ^{1}H NMR spectrum ($CDCl_3$, 400.2 MHz,r.t) of the pure P(LA-*stat*-CL) synthesized by BA-OROcP of *L*-LA and CL from HepOH (Table 1, Entry 13), (b) Evolution of uncorrected $M_{n,SEC}$ (•) and dispersity *Đ* (x) with total monomer conversion (C_{TOT}) and (c) evolution of SEC molar masses with time (Table 1, Entry 13).

3.2 ROcP initiated by α-methoxy(polyethylene glycol)

Synthesis of mPEG-*b*-P(LA-*stat*-CL) diblock copolymer could also be achieved using commercial $mPEG_{1000}$ as macroinitiator under the same conditions than the ones mentioned before. An initial co-monomer composition of $f_{CL,0}$ = 0.94 was selected to obtain a semicrystalline diblock copolymer (Figure 13a, Table 1, Entry 14, Figure S 12). Efficient crossover from $mPEG_{1000}$ to the targeted diblock was confirmed by the shift to lower elution volume after polymerization with a monomodal SEC trace ($M_{n,SEC}$= 8790 g.mol^{-1}, *Đ* = 1.58, Figure 13b).

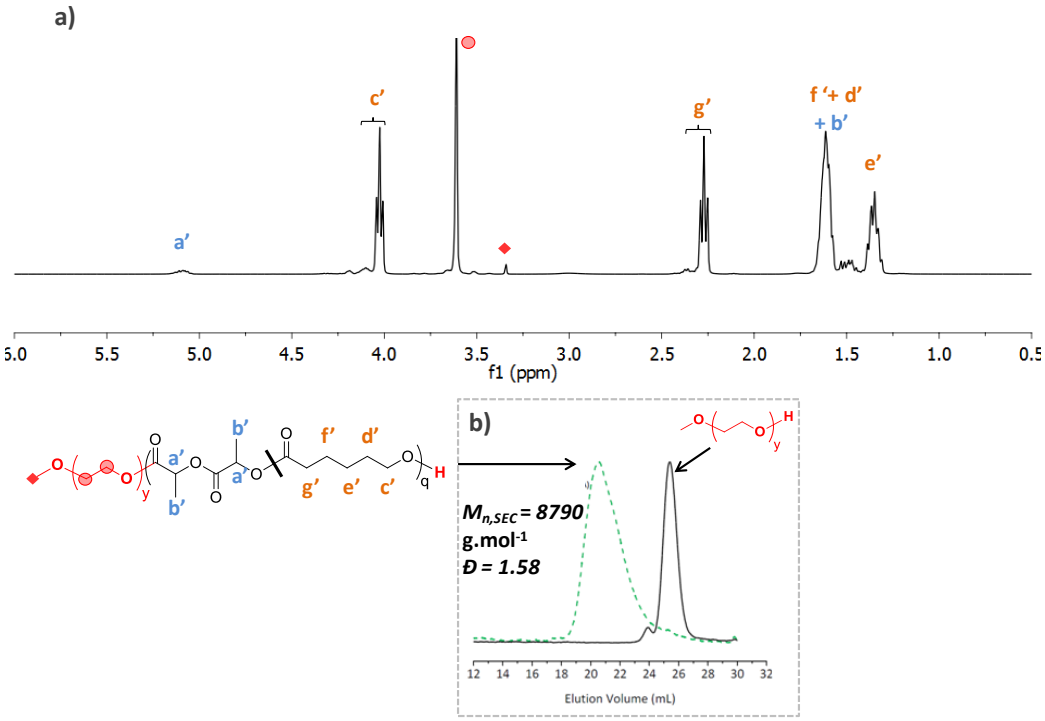

Figure 13. ^{1}H NMR spectrum (400.2 MHz, $CDCl_3$, r.t) of the pure P(LA-*stat*-CL) obtained by BA-ORO*c*P of *L*-LA and CL from $mPEG_{1000}$ in bulk at 155 °C (Table 1, Entry 14) and (b) SEC traces of the pure $mPEG_{1000}$-*b*-P(LA-*co*-CL) (dashed line) and the $mPEG_{1000}$ (solid line).

3.3 Triblock copolymers synthesis

Controlled synthesis of P(LA-*stat*-CL) copolyesters prompted us to derive triblock copolymers by sequential BA-ORO*c*P, using BD as initiator. As depicted in Scheme 3, an α,ω-bis-hydroxy P(LA-*stat*-CL) precursor ($M_{n,SEC}$ = 5480 g.mol^{-1}, $Đ$ = 1.12) was synthesized first, using the conditions described previously ([*L*-LA]$_0$/[CL]$_0$/[BD]$_0$/[BA]$_0$= 25/25/1/2.5; Table S 2).

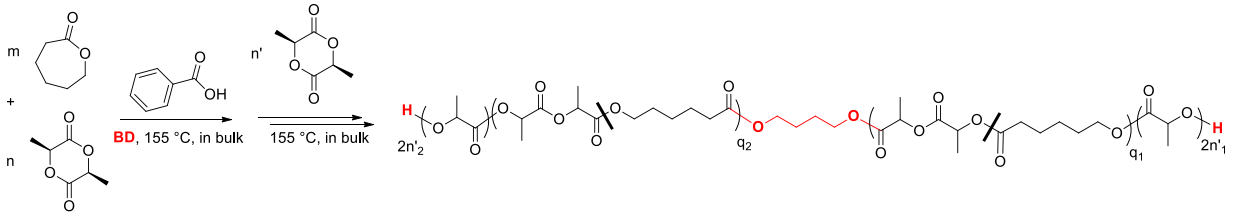

Scheme 3. Synthesis of PLA-*b*-P(LA-*stat*-CL)-*b*-PLA triblock copolymers by sequential BA-ORO*c*P of *L*-LA and CL initiated by BD, followed by a BA-OROP of *L*-LA (q = n + m= q_1 + q_2 and n' = n_1' + n_2').

After 20 hours, extra *L*-LA was added at a [*L*-LA]$_0$/[BA]$_0$/[P(LA-*stat*-CL]$_0$ ratio equal to 25/1.25/1, and the reaction was stirred for 25 hours at 155 °C, reaching a conversion in PLA of 50%. Formation of the PLA-*b*-P(LA-*stat*-CL)-*b*-PLA triblock copolymer was attested by a clear

shift in SEC to higher molar mass ($M_{n,SEC}$ = 8450 g.mol^{-1}, $Đ$ = 1.15) (Figure 14c, Table S 2). Analysis by ^{1}H NMR confirmed the presence of both P(LA-*stat*-CL) and PLA blocks, with representative protons of heterodiads from the statistical central block and increased intensity of PLA homodiads after BA-OROP of *L*-LA (see Figure 14a & b). The proton signals at 3.6 ppm due to hydroxy-methylene PCL end-group of the copolymer precursor totally vanished (Figure 14a) in favor of the methine end-group of PLA at 4.36 ppm (Figure 14b). Furthermore, the experimental degree of polymerization determined by ^{1}H NMR was very close to the theoretical value based on the initial ratio of LA and P(LA-*stat*-CL). The increased intensity of the LL-LL-LL triads in ^{13}C NMR confirmed the triblock copolymer synthesis (Figure 15). Additionally, the peak characteristic of the carbonyl carbon of a lactidyl unit presenting a caproyl as penultimate unit ($e_{CL\text{-}LA}$) at 174.96 ppm totally vanished in favor of the peak characteristic of a lactidyl unit presenting a lactidyl as penultimate unit ($e_{LA\text{-}LA}$) at 175.03 ppm (Figure 15).

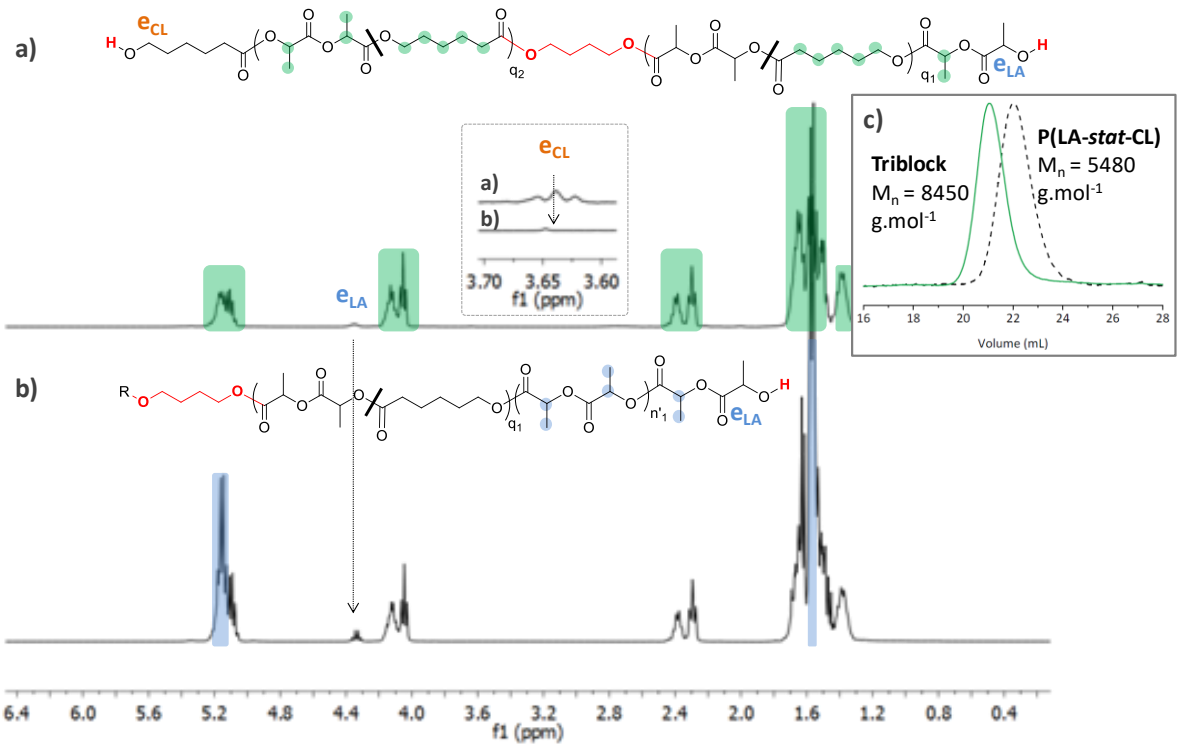

Figure 14. ^{1}H NMR spectra of (a) P(LA-*stat*-CL) macroinitiator and (b) PLA-*b*-P(LA-*stat*-CL)-*b*-PLA triblock copolymer ($CDCl_3$, 400.2 MHz); R represents the second arm of the triblock copolymer; (c) Normalized SEC traces from RI detector of P(LA-*stat*-CL) (black dashed line) and corresponding triblock copolymer ($M_{n,SEC}$ determined by SEC in THF).

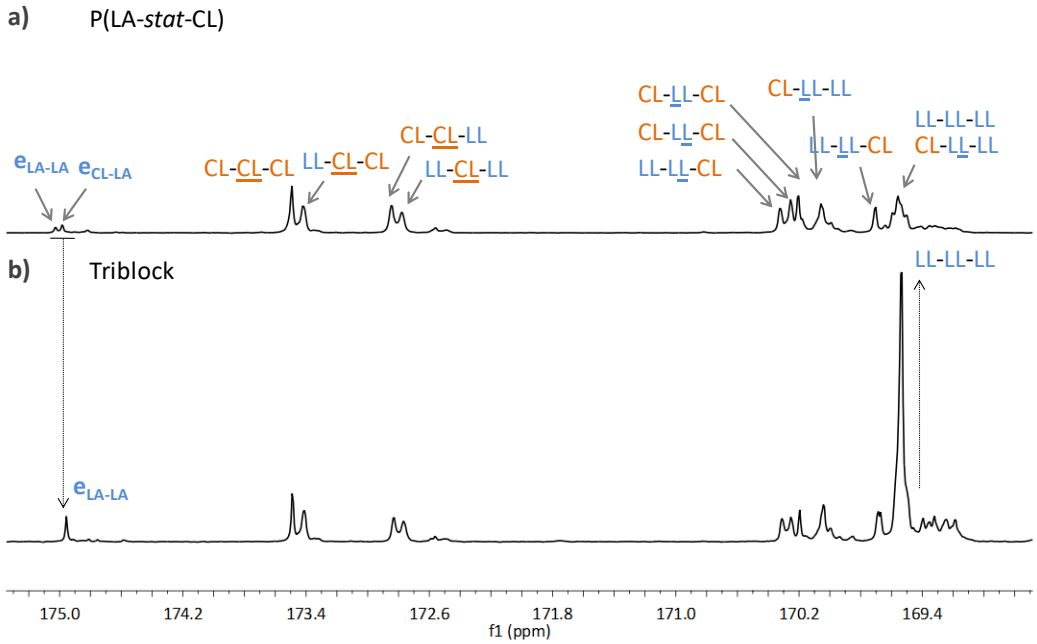

Figure 15. Stack of ^{13}C NMR spectra of (a) the pure P(LA-*stat*-CL) and of (b) the pure triblock copolymer ($CDCl_3$, 100.6 MHz, r.t).

4 ROcP of L-LA and CL using miscellaneous organocatalytic systems

In order to accelerate the ROcP process which require long polymerization time and to deeply understand the key parameters influencing the copolymerization of both *L*-LA and CL, several organocatalysts were studied and compared to the ones reported in the literature. For this purpose, the OROcP of *L*-LA and CL in bulk between 110 °C and 155 °C in the presence of the BD, HepOH or BnOH as initiators and different catalyst. Scheme 4 shows the general synthetic method, Scheme 5 the main catalytic systems used and Table 3 summarizes the main results obtained.

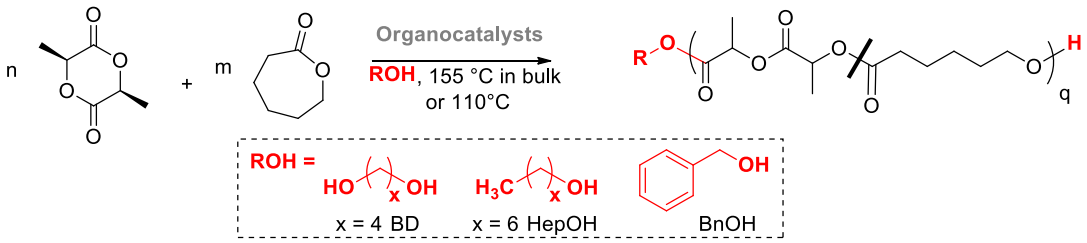

Scheme 4. OROcP of *L*-LA and CL using miscellaneous organocatalytic systems

Table 3. Miscellaneous organocatalysts applied for the bulk RO*c*P of *L*-LA and CL.[a]

Entry	Catalyst	pKa	I[b]	T (°C)	t (h)	C_{CL}/C_{LA}[c] (%/%)	ε_{CL-LA}[e] (%)	$M_{n,sec}$[f] (g.mol^{-1})	$Đ$[f]
1	DPP[g]	1.1	HepOH	155	15	99/72	29	6840	1.85
2	DPP[g]	1.1	HepOH	110	15	99/46	22	6440	1.48
3	2,6-DHBA	1.3	BnOH	155	4	86/22	17	4050	1.53
4	2,6-DHBA	1.3	BnOH	155	24	90/59	19	3550	1.69
5	PFBA	1.48	BD	110	6.1	58/19	12	3390	1.15
6	IPA	3.51	BD	155	12.3	39/18	35	2960	1.17
7	BA	4.2	BD	155	12	39/39	46	3530	1.12
8	DBU[g]	/	BD	155	0.17	0/100	n.a	n.a	n.a
9	DBU/BA[g]	/	BD	155	0.28	1/90	n.a	n.a	n.a
10	DBU/2BA[g]	/	BD	155	0.28	0/86	n.a	n.a	n.a

[a]Reactions were performed in bulk under argon atmosphere with reaction conditions: $n_{CL} = n_{L\text{-}LA}$ = 1.4 mmol; and $[M]_0/[I]_0$ = 50/1, 5mol% catalyst rel. to the monomer; [b] Initiator used, [c]CL and *L*-LA conversions were determined by ^{1}H NMR analysis; [e]Percentage of heterodiads $\boldsymbol{\varepsilon_{CL-LA}} = \frac{I_\varepsilon}{I_\eta + I_\varepsilon}$; [f]Uncorrected average molar mass and dispersity ($Đ$) of crude copolymers determined by SEC chromatography (polystyrene standards) at 40 °C and THF as eluent.; [g] with 1mol% rel. to the monomer.

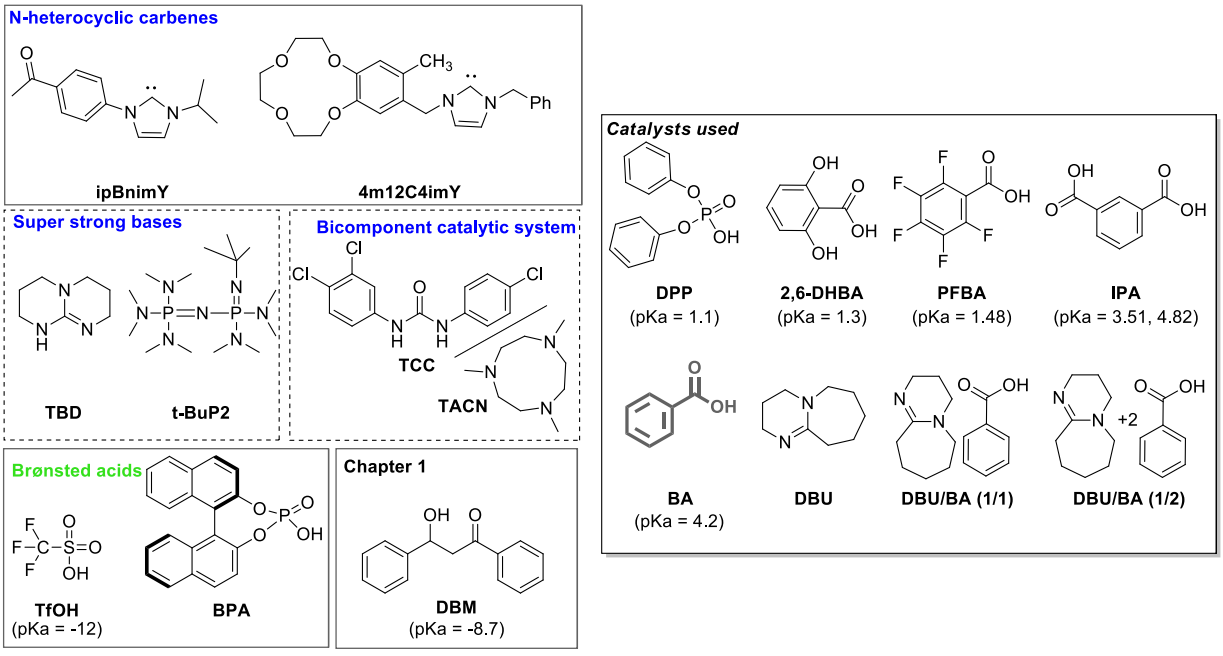

Scheme 5. Miscellaneous organocatalysts employed for the RO*c*P of *L*-LA and CL.

4.1 Basic and nucleophilic catalysts

Study of the previous organocatalysts and the ones applied in the present study (Scheme 5) emphasizes that acidity/basicity of the catalyst could be the principal key parameter influencing the RO*c*P of LA and CL.

When 1,8-Diazabicyclo[5.4.0]undec-7-ene (DBU) was applied for the bulk RO*c*P of *L*-LA and CL at 155 °C, ($[L\text{-LA}]_0/[CL]_0/[DBU]_0/[BD]_0$ = 25/25/0.5/1), *L*-LA conversion reached completion in only 10 min while CL did not start polymerize (Table 3, Entry 8, Figure S 13). Similar trend was observed in the literature, when the RO*c*P of *L*-LA and CL was conducted in the presence of basic and nucleophilic catalysts such as NHCs, TBD, 1-tert-butyl-2,2,4,4,4-pentakis(dimethylamino)-2λ5,4λ5-catenadi(phosphazene) (*t*-BuP2), triclocarban/1,4,7-Trimethyl-1,4,7-triazacyclononane (TCC/TACN). As emphasized previously, these catalysts are known to be more efficient for the ROP of *L*-LA than for the ROP of CL even if the reasons are still not clear.

A salt of DBU with BA (1/1) was then applied with the hope to accelerate the RO*c*P catalyzed by BA alone and to insert more efficiently CL in the polymer chain (Table 3, Entry 9). With this catalytic system, the carboxylate ions was expected to activate less efficiently the initiator/chain end while the protonated DBU would activate the monomer carbonyl *via* the mechanism proposed by Coady *et al.* (Scheme 6a).[18] However, in the same conditions than the ones applied for DBU previously, *L*-LA was completely consumed after 17 min while CL remained in the media.

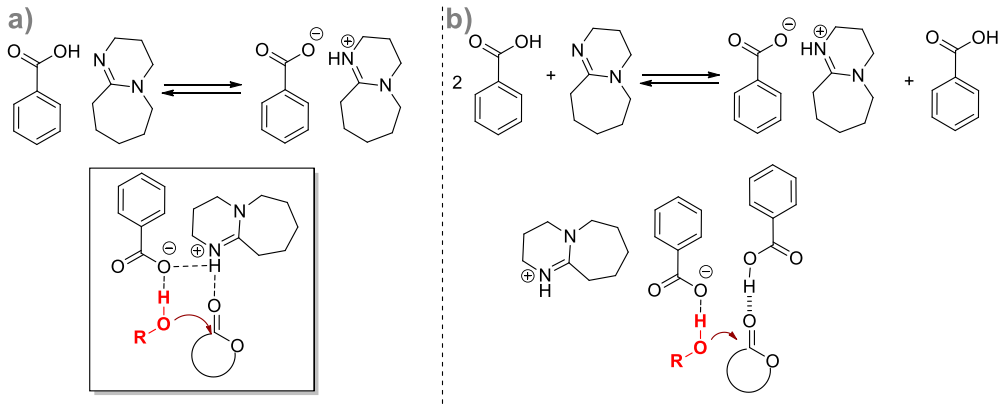

Scheme 6. (a) Bifunctional mechanism proposed by Coady *et al.*[18] (b) Expected mechanism with a DBU/BA salt of 1/2eq.

In order to decrease the activity of DBU we added a second equivalent of BA forming a DBU/BA salt of 1/2eq (Table 3, Entry 10). We expected that the second equivalent of BA catalyst could activate the carbonyl group of CL more efficiently than the protonated DBU (Scheme 6b).

However, in the same experimental conditions, only *L*-LA was consumed after 17 min signifying that DBU.H$^+$ is highly efficient to increase the reactivity ratio of *L*-LA impeding the insertion of CL even if BA is in excess.

4.2 Mild acids

Additionally, when the RO*c*P was conducted in the presence of acidic catalysts such as diphenylphosphate (DPP, pKa = 1.1, Table 3, Entries 1-2,) and 2,6-dihydroxybenzoic acid (2,6-DHBA, pKa = 1.3, Table 3, Entries 3-4), CL was inserted preferentially in the copolymer chain. For instance, when DPP was used for the ORO*c*P of *L*-LA and CL in bulk at 110 °C, CL was completely consumed while the conversion of *L*-LA reached only 56%. A close look to the ^{1}H NMR spectrum bring to light that the percentage of heterodiad units was low ($\mathcal{E}_{CL\text{-}LA}$ = 22%) meaning that the copolymer structure may be a blocky to gradient one. Additionally, the heterodiads observed on the ^{1}H and ^{13}C (Figure S 14) could be due to intensive transesterification reactions mirrored by the high dispersity index obtained at 110 °C ($Đ$ = 1.48) and even higher at 155 °C ($Đ$ = 1.85). Similar observations can be made for 2,6-DHBA. The same trend was reported by Hong *et al.* when using BPA, an acid-type organocatalyst for the RO*c*P of LA and CL. As highlighted in the bibliographic chapter most of the acidic catalysts are, indeed, only efficient for the ROP of CL.

Comparing the results obtained for the bulk RO*c*P of *L*-LA and CL at 155 °C, ([*L*-LA]$_0$/[CL]$_0$/[cat]$_0$/[BD]$_0$ = 25/25/2.5/1), from 2,6-DHBA (pKa = 1.3, 155, Table 3, Entry 3) to a less acidic organocatalyst, *i.e*, isophtalic acid (IPA, pKa$_1$ = 3.51, pKa$_2$ = 5.82, Table 3, Entry 6) highlights the fact that decreasing the acidity increases the content of *L*-LA monomer inserted in the copolymer chain. Indeed, in the case of IPA the copolymer chains contained 35% of heterodiad sequence while only 17% of heterodiads was found in the copolymer obtained with 2,6-DHBA.

Decreasing again the acidity of the catalyst to pKa = 4.2 for BA enable to conduct the statistic BA-ORO*c*P of *L*-LA and CL. Its particular acidity would enable to activate more efficiently the carbonyl group of CL than that of *L*-LA compensating the higher capability of alcohols to polymerize *L*-LA over CL at high temperatures. As an illustration of the latter assumption the bulk copolymerization initiated by BD was conducted in the absence of BA catalyst at 155 °C ([*L*-LA]$_0$/[CL]$_0$/[BD]$_0$ = 25/25/1). *L*-LA was shown to be preferentially inserted in the copolymer chain with the *L*-LA and CL conversions being highly different after 54h of reaction (C_{LA} = 39%, C_{CL} = 15%, Table 1, Entry 1). In the same conditions, introducing 2.5 mol% of BA (rel. to the monomers) enables to decrease the gap between r_{LA} and r_{CL} (C_{LA} = 91%, C_{CL} = 85%, 48h, Table 1, Entry 2). Then, introducing 5mol% of BA led to r_{CL} = r_{LA} (Table 1, Entry 3) and increasing up to 7.5mol% led to slightly higher r_{CL} (C_{LA} = 88%, C_{CL} = 92%, 27h, Table 1, Entry 4).

4.3 Organocatalysts containing fluorine atoms

Taking into account the results obtained when TfOH was applied for the copolymerization of LA and CL, pKa arguments failed to support the previous assumptions. Indeed, when the RO*c*P of *L*-LA and CL was conducted in the presence of this strong acid (pKa ≈ - 12), *L*-LA was strangely inserted preferentially in the copolymer chain.[4] This phenomenon may be first explained by the much higher acidity of TfOH which may not only enable to activate more efficiently the CL carbonyl but also the less basic *L*-LA carbonyls disrupting the balance previously proposed. Additionally fluorine atoms, which are known to be weak hydrogen bond acceptors, may be able to activate the alcohol initiator/chain end *via* ACEM (-C-F···H-O-)[19] favoring *L*-LA insertion (Scheme 7). The combination of both assumptions, *i.e.* the high acidity activating efficiently both the CL and *L*-LA carbonyls and the possible weak hydrogen bond formation with fluorine atoms could be the reason why *L*-LA is inserted preferentially.

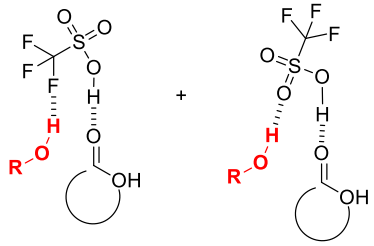

Scheme 7. Two possible modes of bifunctional activation for TfOH catalyst.

Note that the last assumption is plausible as the RO*c*P of *L*-LA and CL conducted by pentaflurobenzoic acid, (PFBA, pKa = 1.48, Table 3, Entry 5) a mild acid containing fluorine atoms, was particularly interesting. When the reaction was performed at 110 °C (to prevent side reactions occurring at 155 °C) with a catalyst loading of 5 mol% and an $[LA]_0/[CL]_0/[BD]_0$ initial ratio of 25/25/1, CL was consumed with a faster polymerization rate in the first stage of the copolymerization up to 50-60% of conversion in CL (Figure 16a, Table S 3). Then, the copolymerization reaction was roughly slowed down with a preferential introduction of *L*-LA in the copolymer chain until the end of the copolymerization with the conversion of CL remaining at a "plateau" of 50-60%. This observation can be explained by the fact that the r_{CL} is very high with a higher propensity of BD to initiate first a CL monomer, then when *L*-LA units are by accident inserted in the copolymer chain the lactidyl unit at the chain end activated by PFBA has a much higher reactivity toward *L*-LA than toward CL. This means that r_{CL} is very high but r_{LA} is much higher. However, more studies are needed in order to completely understand this mechanism. Importantly enough, the $M_{n,SEC}$ evolves linearly with the total conversion until *L*-LA conversion reached 92% with low dispersity values between 1.09 and 1.13 (Figure 16b).

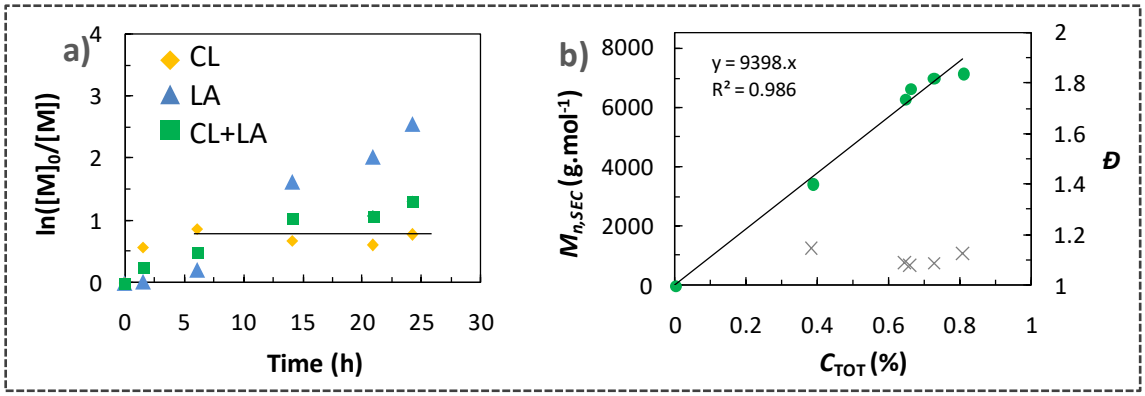

Figure 16. (a) Semi-logarithmic kinetic plots of the BA-ORO*c*P of *L*-LA and CL initiated by BD in bulk at 110 °C (Table 3, Entry 5) and (b) Evolution of uncorrected $M_{n,SEC}$ (•) and dispersity Đ (x) of P(LA-*co*-CL) with monomer conversion.

In conclusion the acidity/basicity of the organocatalyst is surely the main key parameter influencing the RO*c*P of *L*-LA and CL. Indeed, basic and nucleophilic molecules were found to preferentially inserted *L*-LA while the contrary happened when applying acidic compounds. However, the acid/base character of the catalyst is not the only parameter influencing the RO*c*P and some moieties may have an influence such as intermolecular hydrogen bond donors or acceptors: for instance, fluorine atoms.

5 Study of the cytotoxicity of benzoic acid.

The residues of some organocatalysts, such as thioureas[20] and phosphazenium salts,[21] that have been found in synthetic (co)polymers may induce significant cytotoxicity. As our copolymers may contain up to 0.125 mol% residual benzoic acid,[15] it was crucial to study its toxicity. We assessed the cytotoxicity of BA using human HepaRG hepatoma cells. These cells are bipotent hepatic progenitors actively proliferating at low cell density. When these cells are cultured at high cell density, they differentiate into biliary- and hepatocyte-like cells[22] that express all major enzymes involved in xenobiotic metabolism providing a suitable cell model to assess cytotoxicity[23] of xenobiotics. Both progenitor and differentiated cells were incubated in culture media containing BA in a wide range of concentrations from 1 to 300 µM. Benzoic acid was found to be non-toxic for these concentrations (Figure 17).

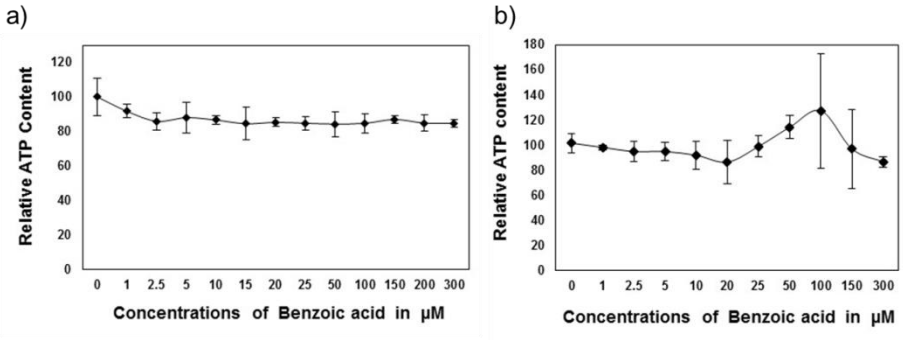

Figure 17. Determination of the relative ATP contents in untreated or treated cultures of progenitor (a) and differentiated hepatocyte-like (b) HepaRGcells. ATP content was arbitrarily set as 100% in untreated cells. No significant alterations of the ATP contents

Conclusion

This work addresses a difficult challenge in polymer chemistry, namely, statistical copolymer synthesis based on poly(ε-caprolactone) and poly(*L*-lactide). Benzoic acid (BA) proves very versatile to this end as it can catalyze the metal-free and statistical ring-opening copolymerization (RO*c*P) of *L*-lactide (*L*-LA) and ε-caprolactone (CL). A library of pure statistical copolymers of varying *L*-LA/CL compositions can thus be synthesized in bulk at 155 °C, in presence of various alcohols as initiators, with a relatively good control over molar masses and dispersities.

The statistical character of the copolymers is supported by ^{1}H and ^{13}C NMR analyses showing homo- and heterosequences and by the glass transition temperatures of the copolymers, that are in good agreement with values calculated from the Fox equation. Moreover, reliable reactivity ratio values of *L*-LA (r_{LA} = 0.86) and CL (r_{CL} = 0.86) have been calculated using "the visualization of the sum of squared residuals space" (VSSRS) method, with a narrow 95% confidence interval for *L*-LA (0.75-1.01) and CL (0.74-1.0). The average block lengths of lactidyl and caproyl units, as determined by ^{1}H NMR and by quantitative ^{13}C NMR spectroscopies, closely match theoretical values.

The quasi "controlled/living" character of this BA-catalyzed process is further demonstrated through the synthesis of PLA-*b*-P(LA-*stat*-CL)-*b*-PLA triblock copolymers, using butane-1,4-diol as initiator.

Benzoic acid could then be readily removed and reused in further organocatalytic polymerization using the solvent-free process set up in the previous chapter affording highly chemically pure P(LA-*stat*-CL). Importantly, benzoic acid, which can remain in the final copolymers after the purification, has been shown to be non-toxic on HeparG hepatoma cells.

Finally, the acid/base character of the miscellaneous organocatalysts applied for the RO*c*P of *L*-LA and CL has a major influence on their reactivity. While basic- and nucleophilic-type organocatalysts increase the reactivity of *L*-LA monomer by activating the initiator/chain end, mild acid organocatalyst increase the reactivity of CL by activating more efficiently the carbonyl group of the monomer. However, other factors may influence the reactivity of both monomers such as for instance the functional group providing hydrogen bonding.

This work thus expands the scope of organocatalyzed polymerization reactions, by providing a straightforward and metal-free synthetic alternative to biodegradable, biocompatible and aliphatic statistical copolyesters based on PLA and PCL, thanks to the use of BA as a weakly acidic and non-toxic organocatalyst.

Experimental Part

Materials

L-Lactide (*L*-LA, 98%, TCI) was recrystallized three times from toluene and dried under vacuum for two days. ε-Caprolactone (CL, 99%, ACROS), butane-1,4-diol (BD, 99%, VWR) and heptan-1-ol (HepOH, 98%,Sigma Aldrich) were dried over CaH_2 for 48 hours prior to distillation under reduced pressure and were stored on molecular sieves. Methoxypoly(ethylene glycol) ($mPEG_{1000}$, 98%, TCI, M_n ~ 1000 $g.mol^{-1}$) was dried by three azeotropic distillations using tetrahydrofuran (THF). Benzoic acid (BA, 99%, ACROS) was recrystallized once and dried by two azeotropic distillations using toluene. Pentafluorobenzoic acid (PFBA, 99%, Alfa aesar), isophtalic acid (IPA, 99%, sigma) and 2,6-dihydroxybenzoic acid (2,6-DHBA, 98%, TCI) were dried by three azotropic distillations using toluene. Diphenylphosphate (DPP, 99%, Sigma) and 1,8-diazabicyclo[5.4.0]-7-undecene (DBU, 98%, TCI) were used as received. Compounds were stored in a glove box (O_2 ≤ 6 ppm, H_2O ≤ 0.5 ppm). THF and toluene were dried using an SPS from Innovative technology and stored over sodium benzophenone and polystyrylithium respectively and distilled prior to use.

Methods

NMR spectra were recorded on a Bruker Avance 400 (^1H,^{13}C, 400.2 MHz and 100.6 MHz, respectively) in $CDCl_3$ at 298K. Quantitative ^{13}C NMR was performed on copolymer samples (60 mg in 0.6 mL) using the "INVGATE" sequence with a pulse width of 30°, an acquisition time of 0.7 s, a delay of 4s between pulses and 6144 scans in order to investigate the co-monomer distribution within copolymers.[24] Diffusion Ordered Spectroscopy (DOSY)[25,26] measurements were performed at 298K on a Bruker Avance III 400 spectrometer operating at 400.33 MHz and equipped with a 5mm Bruker multinuclear z-gradient direct cryoprobe-head capable of producing gradients in the z direction with strength 53.5 G cm^{-1}. The sample was dissolved in 0.4

mL of $CDCl_3$for internal lock and spinning was used to minimize convection effects. The sample was thermostated at 298 K for at least 5 minutes before data accumulation. The DOSY spectra were acquired with the *ledbpgp2s* pulse program from Bruker topspin software. The duration of the pulse gradients and the diffusion time were adjusted in order to obtain full attenuation of the signals at 95 % of maximum gradient strength. The values were 2.4 ms for the duration of the gradient pulses and 100 ms for the diffusion time. The gradients strength was linearly incremented in 16 steps from 5% to 95% of the maximum gradient strength. A delay of 5 s between echoes was used. The data were processed using 8192 points in the F2 dimension and 128 points in the F1 dimension with the Bruker topspin software. Field gradient calibration was accomplished at 25 °C using the self-diffusion coefficient of H_2O+D_2O of19.0 x 10^{-10} $m^2.s^{-1}$.[27,28]

Molar masses were determined by size exclusion chromatography (SEC) in THF (1mL.min^{-1}) with trichlorobenzene as a flow marker at 313K, using refractometric (RI) detector. Analyses were performed using a three-column TSK gel TOSOH (G4000, G3000, G2000).The SEC device was calibrated using linear polystyrene (PS) standards.

Differential scanning calorimetry (DSC) measurements were carried out with a DSC Q100 LN2 apparatus from TA Instruments under helium flow. The PCL samples were heated for the first run from -130 to 100 °C, then cooled again to -130°C and heated again for the third run to 100°C (heating and cooling rate 10 °C/min). While PLA sample undergoes 2 runs between -40°C and 200°C and P(LA-*co*-CL) between -70 to 200 °C. Glass transition temperatures (T_g) and melting temperatures (T_m) were measured from the second and first heating run, respectively.

General procedure for statistical copolymerization of *L*-LA and CL in presence of BA or other organocatalysts

In a glove box, previously flamed 10 mL Schlenks were charged with the appropriate amount of *L*-LA and CL, the catalyst (2.5, 5 and 10 mol.% relatively to the monomer) and a stir bar. The initiator (BD or HepOH) was added *via* a 5 or 10 µL syringe while $mPEG_{1000}$ was charged directly in the Schlenk. The Schlenks were sealed before being introduced in an oil bath preheated at the desired temperature (110 - 180 °C). At specified times, one Schlenk was removed from the oil bath to monitor the reaction by ^1H NMR. The as-obtained copolymers were purified by applying vacuum (0.1-0.2 mbars) to the Schlenk at 155 °C with a high stirring rate (800-1000 rpm) for 5 minutes. The number average molar mass ($M_{n,SEC}$) and the dispersity (*Đ*) were determined by SEC.

General procedure for purification by vacuum.

In a glove box, a previously flamed 20 mL Schlenk was charged with LLA (0.6 g, 4.163 mmol) and CL (0.475 g, 4.163 mmol) monomers, BA catalysts (51 mg, 4.16 x 10^{-1}mmol), BD

initiator (15 mg, 1.67 x 10^{-1}mmol) and a stir bar. The Schlenk was then introduced in an oil bath preheated at 155 °C for 27 hours. After the polymerization, the mixture was cooled down and the Schlenk 1 is reintroduced in the glove box in order to collect a sample for ^{1}H NMR and SEC analyses and is then connected *via* a bridge to another flamed Schlenk 2. Schlenk 1 containing the crude copolymer was then introduced in an oil bath preheated at 155 °C while vacuum (0.1 – 0.2 mbar) was applied to Schlenk 2 and cooled thanks to liquid nitrogen. After heating the bridge with a heat gun, a high stirring rate (800 rpm) was applied to the Schlenk 1 in order to collect in Schlenk 2, the unreacted CL and LA monomers and the BA catalyst. Overall, the vacuum treatment in the oil bath at 155 °C lasted 5 minutes with some interruptions in order to heat again the bridge. The pure copolymer is then cooled down and the assembly is introduced in the glove box. Schlenk 2 containing the unreacted monomer and the catalyst was charged with BD initiator (15 mg, 1.67 x 10^{-1}mmol) and the difference of monomer (calculated thanks to the conversion by ^{1}H NMR). Finally, Schlenk 2 was introduced in the oil bath preheated at 155 °C for 27h. The cycle was repeated 5 times.

General procedure for triblock synthesis

In a glove box, a previously flamed 10 mL Schlenk was charged with *L*-LA (0.200 g, 1.4 mmol) and CL (0.158 g, 1.4mmol), the BA catalyst (5mol% rel. to monomers) and a stir bar. The BD initiator ($DP_{,th}$= 25 for each monomer) was added *via* a 10 µL syringe. The Schlenk was then sealed before being introduced in an oil bath preheated at 155 °C. After 20h of reaction, the Schlenk was introduced in the glove box in order to estimate the monomer conversion *via* ^{1}H NMR spectroscopy and to determine the average molar mass (M_n) and the dispersity ($Đ$) by SEC. The as-obtained copolymer was purified by applying vacuum at 155 °C with a high stirring rate. The Schlenk was again introduced into the glove box in order to add more BA catalyst (5mol% rel. to *L*-LA) and the *L*-LA monomer (0.200 g; 1.4 mmol) to target $DP_{,th}$≈ 25. The polymerization could be restarted by immersing the Schlenk in the oil bath for 25 hours. A sample was collected to estimate conversion by ^{1}H NMR spectroscopy prior to the purification. The as-obtained triblock copolymer was analyzed by SEC, ^{1}H NMR and ^{13}C NMR spectroscopy, DSC and TGA.

Toxicity of BA catalyst

Cytotoxicity was assessed using progenitor and differentiated HepaRG cells incubated for 48 h with various concentrations of BA ranging from 1 to 300 µM**.** HepaRG cells were seeded at a density of 2.6 × 10^{4} cells/cm^{2} and cultured in William's E medium supplemented with 10% FBS, 100 units/ml penicillin, 100 µg/ml streptomycin, 2 mM glutamine, 5 µg/ml insulin, and 50 µM hydrocortisone hemisuccinate. After 2 weeks, cell differentiation was further enhanced by maintaining the cells in the same medium supplemented with 2% DMSO for 2 more weeks. Cell viability was evaluated in progenitor and differentiated cell cultures at day 2 and 30 after plating, respectively, by measuring the intracellular ATP content using the CellTiter-Glo®

Luminescent Cell Viability Assay (Promega, Charbonnières, France) according to the manufacturer's instructions. Briefly, untreated and treated HepaRG cells were first incubated with the CellTiter-Glo® reagent for 10 min at 37 °C. Cells were then transferred in opaque-walled 96-well plates and the luminescent signal was quantified at 540 nm with the POLARstar® Omega microplate reader (BMG Labtech). ATP levels in treated cells were expressed as the percentage of the ATP content measured in untreated cells.

Supporting information

Figure S 1. Picture of the crude P(LA-*co*-CL) obtained by RO*c*P of *L*-LA and CL initiated by BD without BA catalyst in bulk at 155 °C (Table 1, Entry 1).

Figure S 2. BA-ORO*c*P of LA and CL initiated by BD in bulk at 155 °C ($[LA]_0/[CL]_0/[BA]_0/[BD]_0$ = 25/25/X/1, Table 1, Entries 2 and 4). Evolution of the uncorrected $M_{n,SEC}$ (•), and of the dispersity $Đ$ (x) of the crude copolymers with monomer conversion using (a) 2.5 mol% catalyst and (b) 10 mol% catalyst rel. to the monomers.

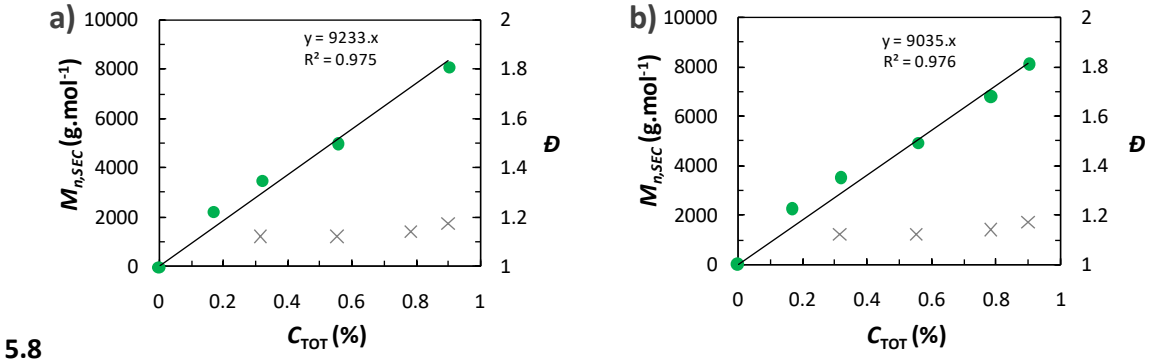

5.8

Figure S 3. BA-ORO*c*P of LA and CL initiated by BD in bulk at 155 °C ($[LA]_0/[CL]_0/[BA]_0/[BD]_0$ = X/Y/2.5/1, Table 1, Entries 5, 6, 7 and 8).Evolution of the uncorrected $M_{n,SEC}$ (•), and of the dispersity $Đ$ (x) of the crude copolymers with monomer conversion for different initial feed ratios ($f_{CL,0}$ = 0.9, 0.7, 0.3, 0.2).

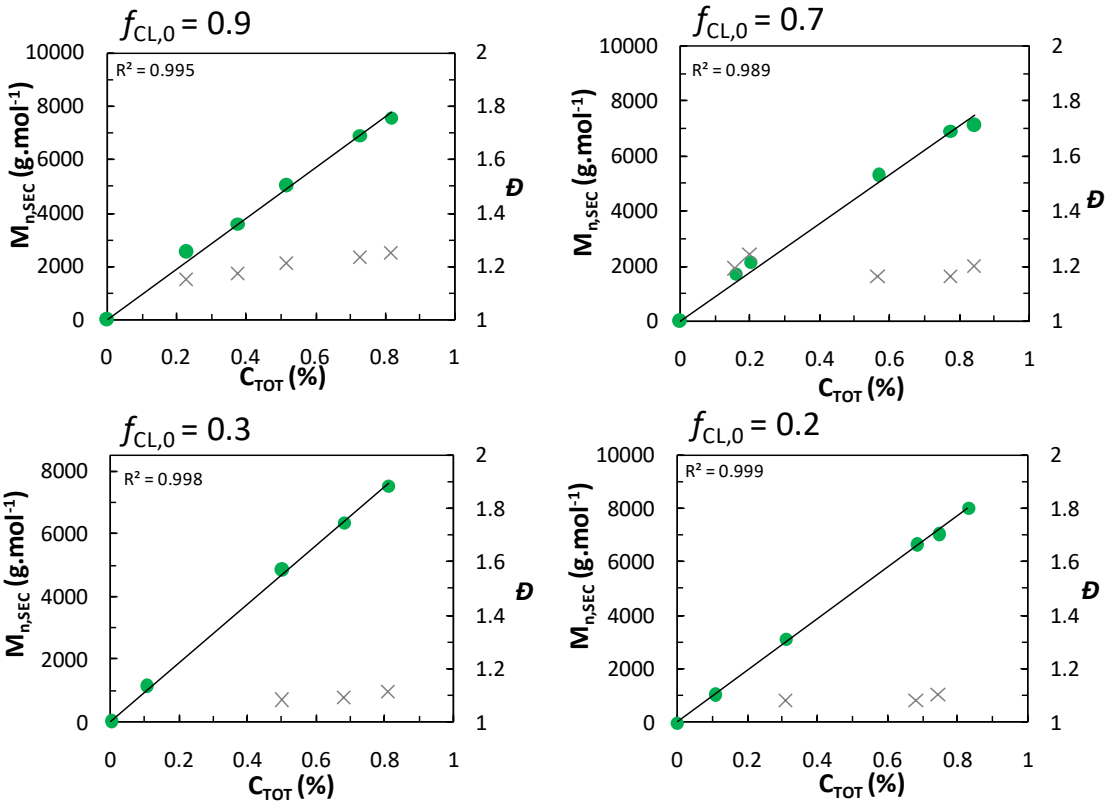

Figure S 4. Evolution of the SEC traces of P(LA-*co*-CL) with different co-monomer ratios (Table 1, Entries 5 to 8), (SEC in THF, 313 K, 1mL.min^{-1}, polystyrene standards).

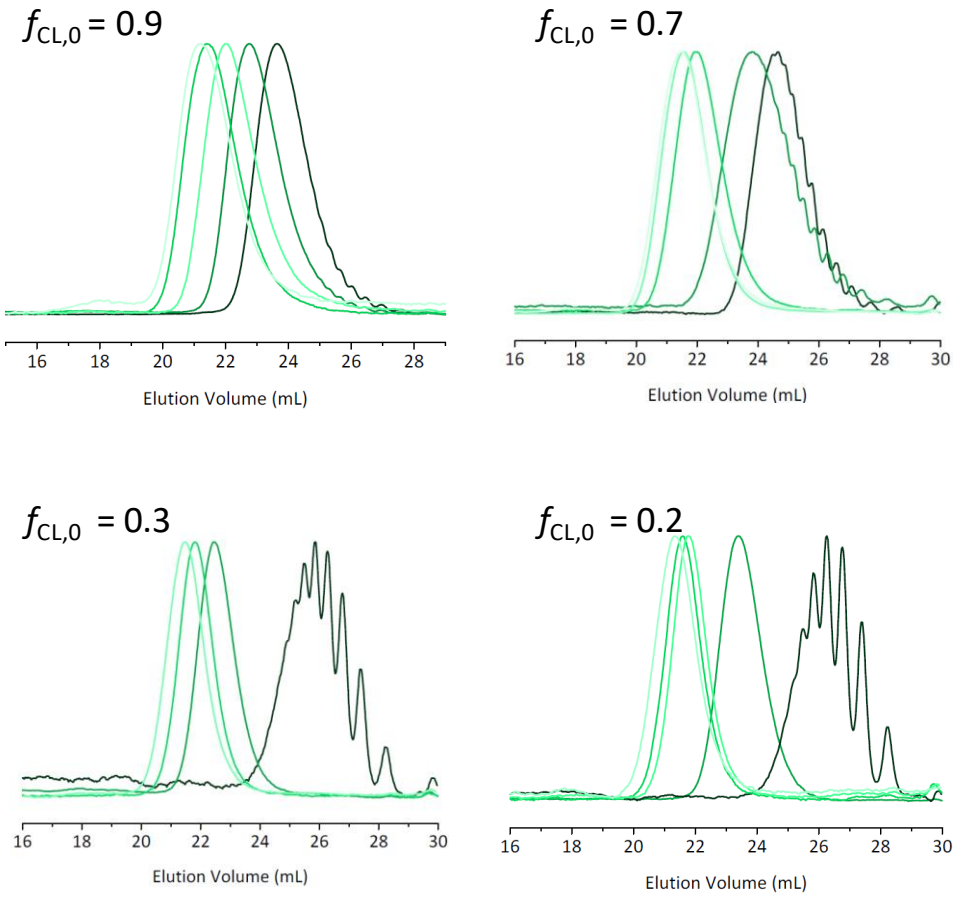

Determination of reactivity ratios

The following equations define the relationship between reactivity ratios and the different rate constants (k_{ij}) of the four propagation reactions represented in Figure S 5.

$$r_{CL} = k_{CL-CL}/k_{CL-LA} \quad \text{and} \quad r_{LA} = k_{LA-LA}/k_{LA-CL}$$

Figure S 5. Rate constants in the ROcP of *L*-LA and CL.

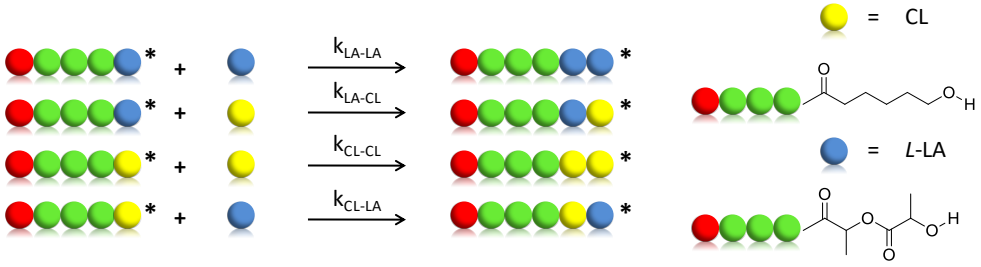

The reactivity ratios were calculated using the Kelen-Tüdős[29] linear method which can be used in ROP[30]. For this purpose, the copolymerization of the comonomers with different chosen compositions ($f_{LA,0}$ and $f_{CL,0}$ ≈ 0.2, 0.3, 0.5, 0.7) were performed and the monomer compositions (F_{LA} and F_{CL}) in the obtained oligomers were examined at low conversion.

Kelen-Tüdős: Where $x = \frac{f_{CL,0}}{f_{L-LA,0}}$, $y = \frac{F_{CL}}{F_{L-LA}}$

$$G = \frac{x\,(y-1)}{y}, \quad F = \frac{x^2}{y}$$

$$\eta = \frac{G}{\alpha + F}, \varepsilon = \frac{F}{\alpha + F} \text{ with } \alpha = \sqrt{F_{min}.F_{max}}$$

$$\eta = \left(r_{CL} + \frac{r_{LA}}{\alpha}\right) \quad \varepsilon - \frac{r_{LA}}{\alpha}$$

Table S 1. Mole fraction of CL monomer in the initial reaction mixture ($f_{CL,0}$) and in the copolymer (F_{CL}) and the total conversion (C_{TOT}).

$f_{CL,0}$	C_{TOT} (%)	F_{CL}
0.71	16	0.72
0.52	14	0.55
0.31	9	0.35
0.22	11	0.28

Figure S 6. Kelen-Tüdős linear method.

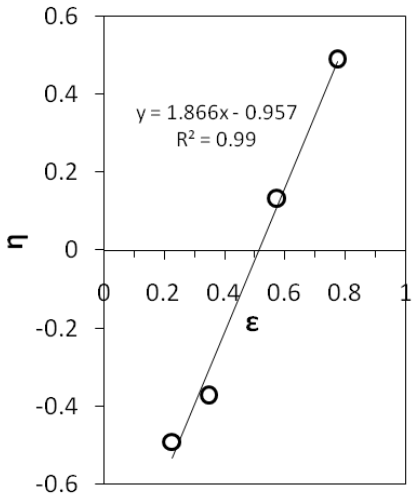

The visualization of the sum of squared residuals space (VSSRS):

Easy to implement in Microsoft Excel software the method was totally described by Van den Brink *et al*.[10] This method consists in minimizing the sum of squares (SS) as described in equation S1.

Equation S1 $$SS(r_{CL}, r_{LA}) = \sum_{i=1}^{n} w_i \times \left(z_{i,exp} - z_{i,th}\right)^2$$

In equation S1, w_i are the weighting factors (here a constant absolute error was considered, i.e. w_i = 1), $z_{i,exp}$ are the experimental values of the variable z for the experiment i and $z_{i,th}$ are the theoretical values of the variable z for the experiment i. The best estimate for the reactivity ratios is set for the minimum value of SS.

Analysis of the microstructures

Figure S 7. DOSY-NMR calibration curve for P(LA-*co*-CL) sample (400.2 MHz, $CDCl_3$, r.t).

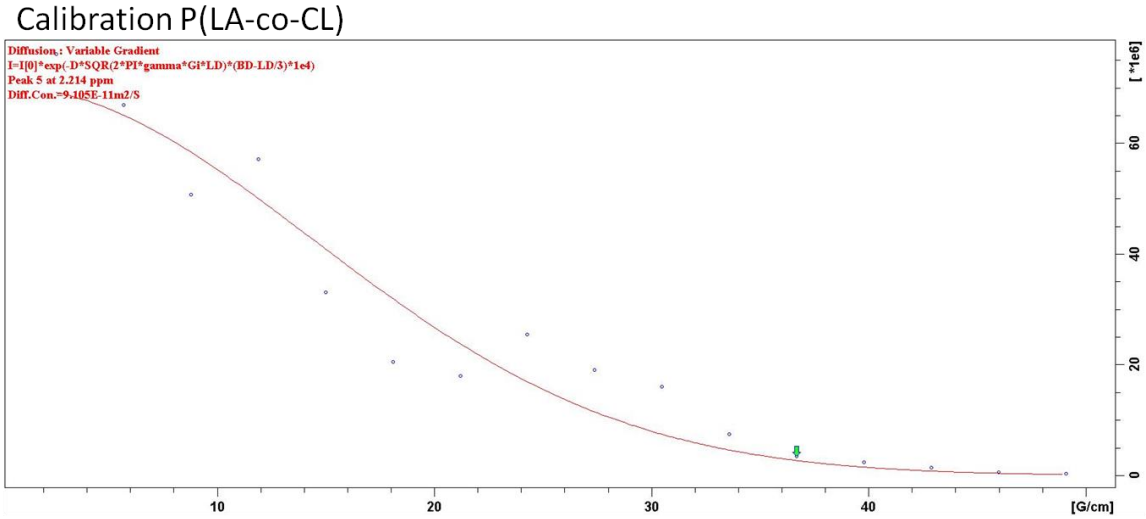

Figure S 8. DOSY-NMR calibration curve for PLA sample (400.2 MHz, $CDCl_3$, r.t).

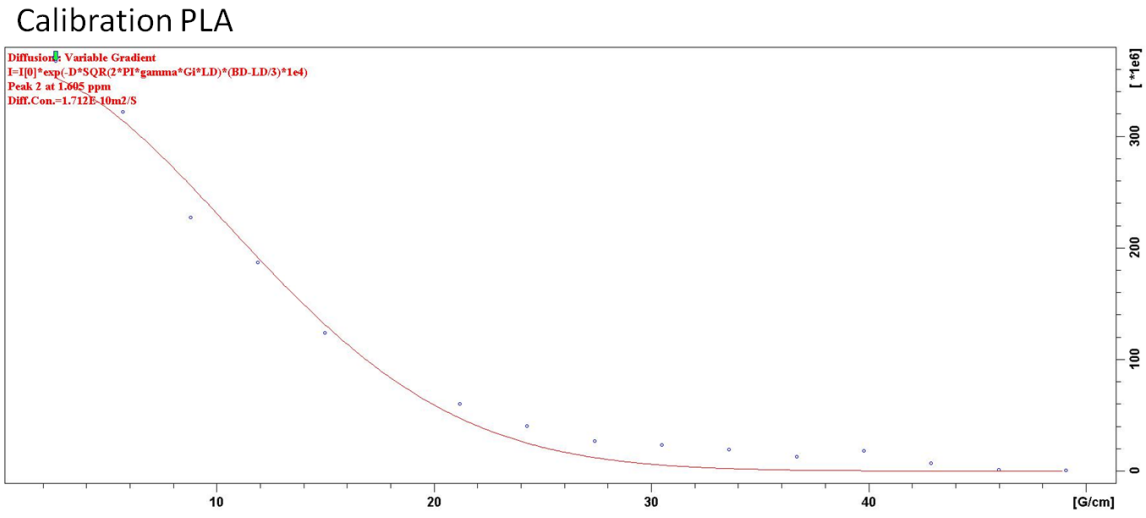

Figure S 9. DOSY-NMR calibration curve for PCL sample (400.2 MHz, $CDCl_3$, r.t).

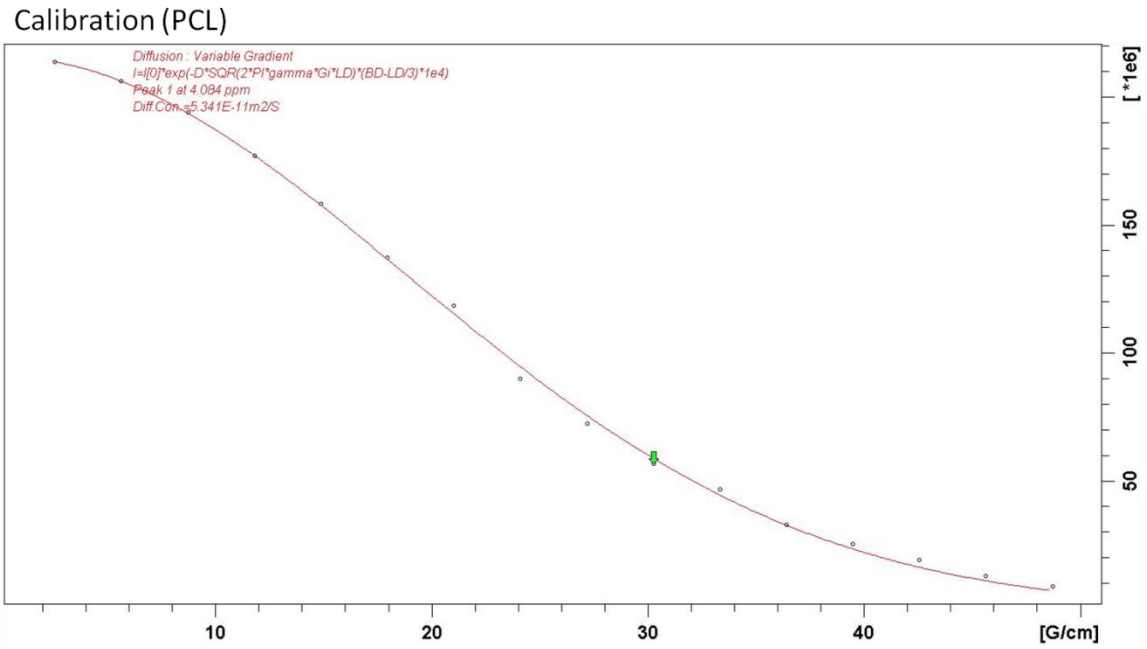

Figure S 10. Determination of the number average block length by ^{1}H NMR.

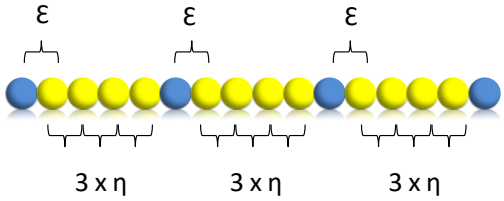

$$L_{CL,1H} = \frac{I_\eta}{I_\varepsilon} + 1 = \frac{9}{3} + 1 = 4$$

Figure S 11. DSC chromatograms of the statistical copolymers, second run (10 °/min in N_2).

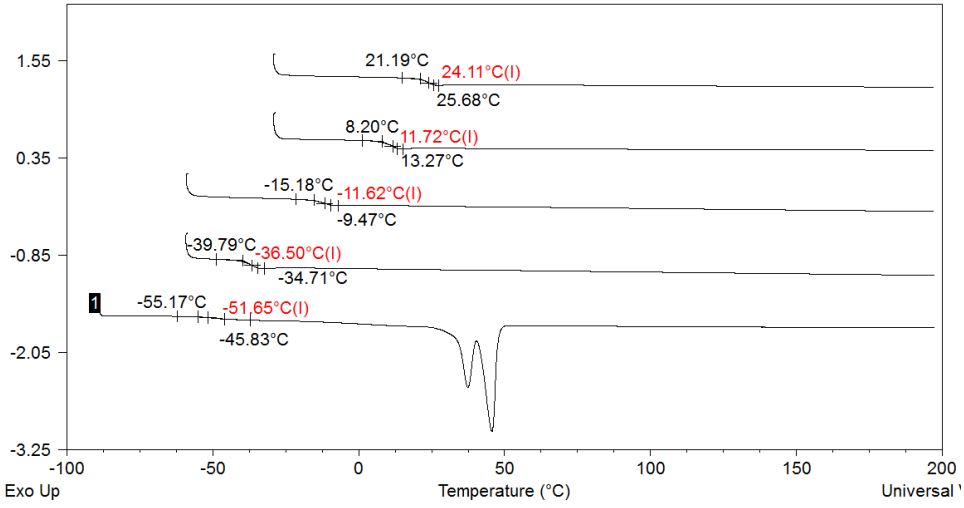

ROcP initiated by α-methoxy(polyethylene glycol)

Figure S 12. DSC spectrum of the P(LA-*stat*-CL) initiated from $mPEG_{1000}$ (Table 1, Entry 14).

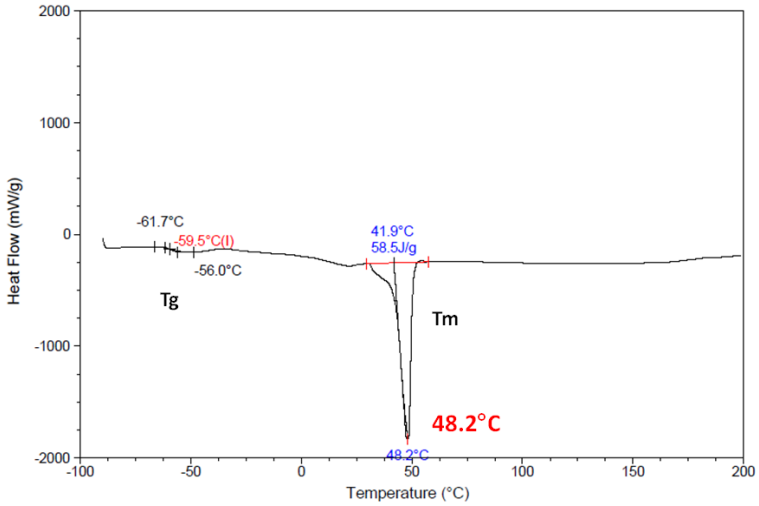

Triblock copolymers synthesis

Table S 2. Results and conditions of triblock synthesis.[a]

run	M	$[M]_0/[I]_0$	Time (h)	C_{TOT}[b] (%)	$M_{n,SEC}$[c] (g.mol^{-1})	$Đ$[c]	M_2	$[M]_0/[I]_0$	Time (h)	C_2[b] (%)	$M_{n,SEC}$[c] (g.mol^{-1})	$Đ$[c]
1	CL + LA	50	20	62.5	5480	1.12	LA	25	25	50	8450	1.15

[a] Reactions were performed in bulk at 155 °C under argon atmosphere with reaction conditions: m_{CL} = 158 mg, m_{LA}= 200 mg using 5mol% catalyst *vs.* monomers. [b] Total and *L*-LA conversions were determined by ^{1}H NMR analysis. [c] Average molar mass ($M_{n,SEC}$) and dispersity ($Đ$) of crude copolymers determined by (SEC chromatography in THF at 313 K using polystyrene standards.

Figure S 13. (a) ^{1}H NMR ($CDCl_3$, 400 MHz) spectrum and (b) picture of the crude PLA obtained by DBU-OROcP of an equimolar mixture of LA and CL initiated by BD in bulk at 155 °C. With e_{LA} the lactidyl chain end unit.

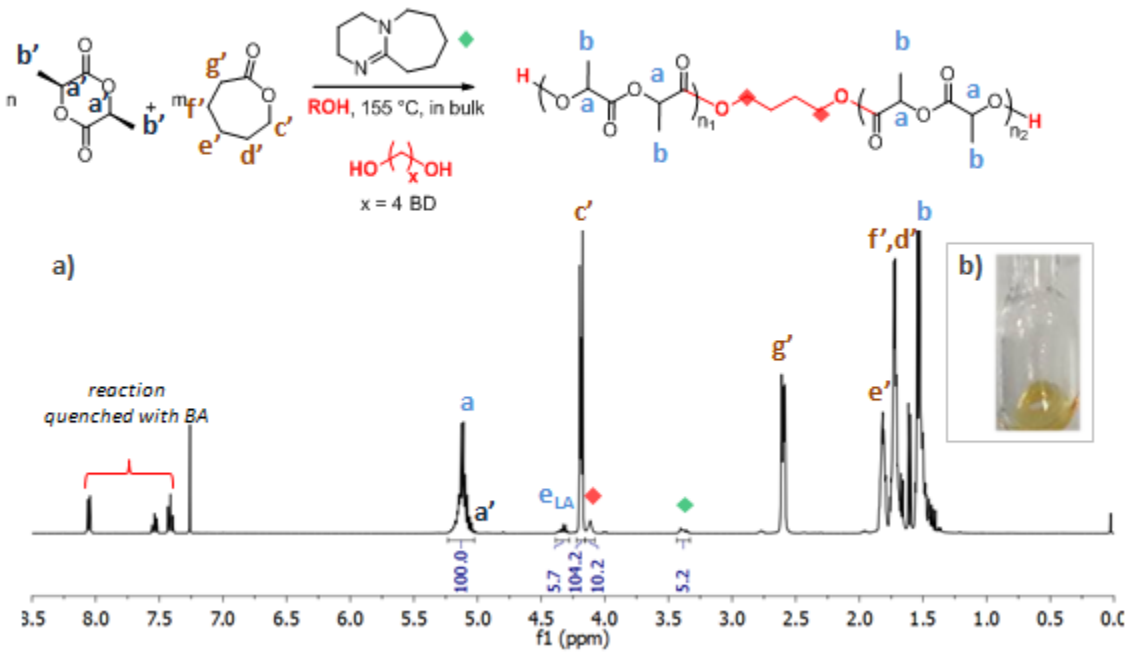

Figure S 14. (a) SEC trace and (b) ^{1}H NMR spectrum of crude P(LA-*co*-CL) obtained by DPP-OROcP of *L*-LA and CL initiated by HepOH (Table 3, Entry 2).

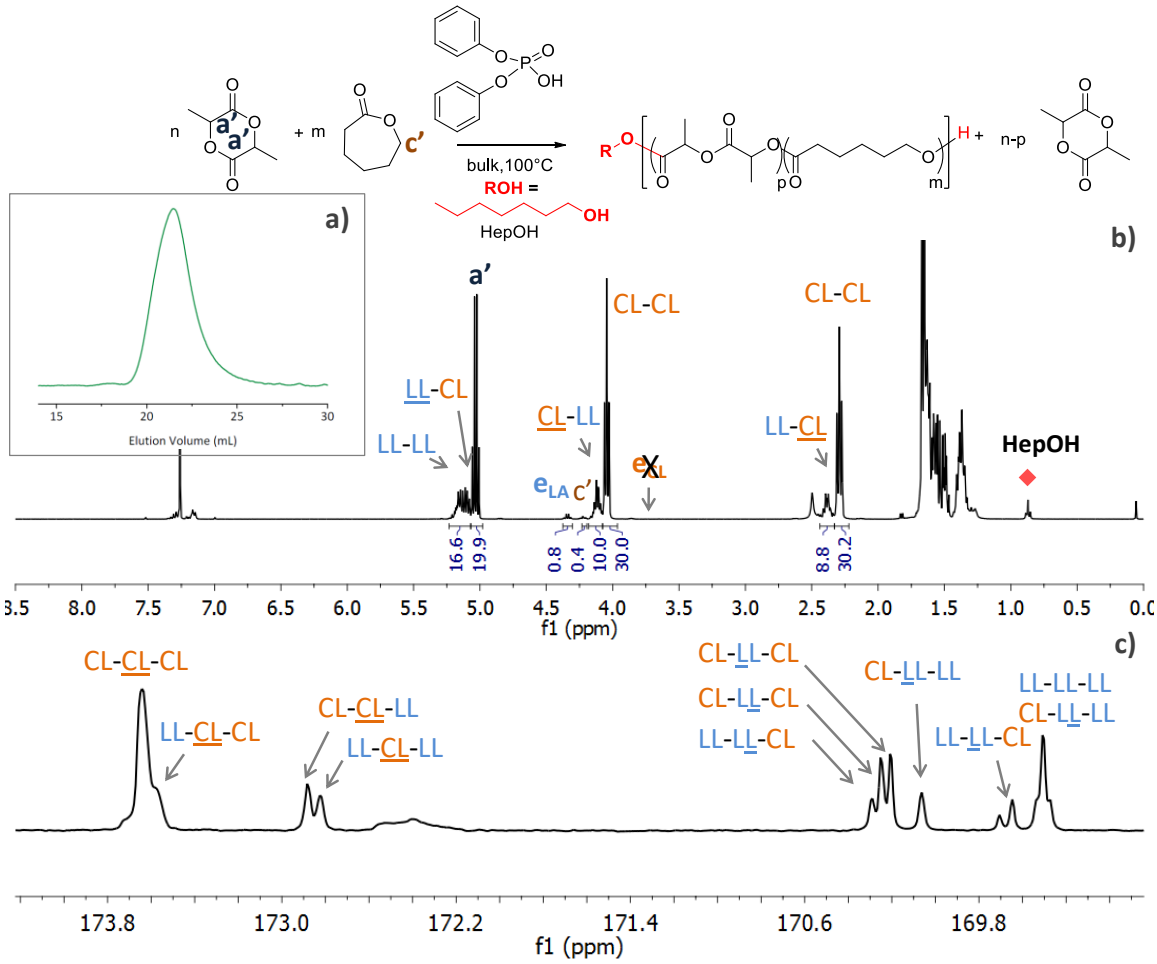

Table S 3. Results and conditions of the PFBA-RO*c*P of *L*-LA and CL.[a]

Entry	f_{CL} (%)[b]	time (h)	C_{CL}/C_{LA} (%/%)[c]	F_{CL} (%)[d]	$M_{n,SEC}$ (g.mol^{-1})[e]	$Đ^e$	$DP_{,th}$[f]	$DP_{,exp}$[g]
1	48	6.1	58/19	74	3386	1,13	19,3	15.12
2	49	14.1	49/80	37	6274	1,09	32,3	30,38
3	51	20.9	45/87	35	6630	1,08	33,1	31,37
4	49	24.3	54/92	36	6989	1,09	36,5	31,67
5	53	48.1	65/97	43	7106	1,13	40,5	n.a

[a]The reactions were performed in bulk at 110 °C under an argon atmosphere with m_{CL}=158 mg, m_{LA}=200 mg. [b] the initial comonomer ratio of CL f_{CL}; [c]The monomer conversions were determined by ^{1}H NMR; [d] CL content in the copolymer; [e] Uncorrected average molar mass ($M_{n,SEC}$) and dispersity ($Đ$) determined by SEC chromatography (polystyrene standards) at 40 °C and THF as eluent. [f]Theoretical degree of polymerization $DP_{,th} = \frac{[L-LA]_0}{[I]_0} \times C_{LA} + \frac{[CL]_0}{[I]_0} \times C_{CL}$. [g]Degree of polymerization calculated from the chain ends determined by ^{1}H NMR; n.a: not available.

References

1 B. G. G. Lohmeijer, R. C. Pratt, F. Leibfarth, J. W. Logan, D. A. Long, A. P. Dove, F. Nederberg, J. Choi, C. Wade, R. M. Waymouth and J. L. Hedrick, *Macromolecules*, 2006, **39**, 8574–8583.

2 H. Alamri, J. Zhao, D. Pahovnik and N. Hadjichristidis, *Polym Chem*, 2014, **5**, 5471–5478.

3 Y. Wang, J. Niu, L. Jiang, Y. Niu and L. Zhang, *J. Macromol. Sci. Part A*, 2016, **53**, 374–381.

4 M. Baśko and P. Kubisa, *J. Polym. Sci. Part Polym. Chem.*, 2006, **44**, 7071–7081.

5 M. Baśko and P. Kubisa, *J. Polym. Sci. Part Polym. Chem.*, 2007, **45**, 3090–3097.

6 X. Zhou and L. Hong, *Colloid Polym. Sci.*, 2013, **291**, 2155–2162.

7 L. Zhang, N. Li, Y. Wang, J. Guo and J. Li, *Macromol. Res.*, 2014, **22**, 600–605.

8 J. U. Pothupitiya, N. U. Dharmaratne, T. M. M. Jouaneh, K. V. Fastnacht, D. N. Coderre and M. K. Kiesewetter, *Macromolecules*, 2017, **50**, 8948–8954.

9 L. Mezzasalma, J. De Winter, D. Taton and O. Coulembier, *J. Polym. Sci. Part Polym. Chem.*, 2018, **56**, 475–479.

10 M. Van Den Brink, A. M. Van Herk and A. L. German, *J. Polym. Sci. Part Polym. Chem.*, 1999, **37**, 3793–3803.

11 S. Harrisson, F. Ercole and B. W. Muir, *Polym Chem*, 2010, **1**, 326–332.

12 O. Coulembier, S. Moins, J.-M. Raquez, F. Meyer, L. Mespouille, E. Duquesne and P. Dubois, *Polym. Degrad. Stab.*, 2011, **96**, 739–744.

13 Y. Fan, H. Nishida, Y. Shirai, Y. Tokiwa and T. Endo, *Polym. Degrad. Stab.*, 2004, **86**, 197–208.

14 F. R. Mayo and F. M. Lewis, *J. Am. Chem. Soc.*, 1944, **66**, 1594–1601.

15 L. Mezzasalma, J. De Winter, D. Taton and O. Coulembier, *Green Chem.*, 2018, **20**, 5385–5396.

16 J. Kasperczyk and M. Bero, *Makromol. Chem.*, 1991, **192**, 1777–1787.

17 J. Kasperczyk and M. Bero, *Makromol. Chem.*, 1993, **194**, 913–925.

18 D. J. Coady, K. Fukushima, H. W. Horn, J. E. Rice and J. L. Hedrick, *Chem. Commun.*, 2011, **47**, 3105–3107.

19 H.-J. Schneider, *Chem. Sci.*, 2012, **3**, 1381.

20 A. Nachtergael, O. Coulembier, P. Dubois, M. Helvenstein, P. Duez, B. Blankert and L. Mespouille, *Biomacromolecules*, 2015, **16**, 507–514.

21 Y. Xia, J. Shen, H. Alamri, N. Hadjichristidis, J. Zhao, Y. Wang and G. Zhang, *Biomacromolecules*, 2017, **18**, 3233–3237.

22 V. Cerec, D. Glaise, D. Garnier, S. Morosan, B. Turlin, B. Drenou, P. Gripon, D. Kremsdorf, C. Guguen-Guillouzo and A. Corlu, *Hepatology*, 2007, **45**, 957–967.

23 R. Josse, C. Aninat, D. Glaise, J. Dumont, V. Fessard, F. Morel, J.-M. Poul, C. Guguen-Guillouzo and A. Guillouzo, *Drug Metab. Dispos.*, 2008, **36**, 1111–1118.

24 P. Vanhoorne, P. Dubois, R. Jerome and P. Teyssie, *Macromolecules*, 1992, **25**, 37–44.
25 P. Stilbs, *Anal. Chem.*, 1981, **53**, 2135–2137.
26 C. S. Johnson, *Prog. Nucl. Magn. Reson. Spectrosc.*, 1999, **34**, 203–256.
27 L. G. Longsworth, *J. Phys. Chem.*, 1960, **64**, 1914–1917.
28 M. Holz and H. Weingartner, *J. Magn. Reson. 1969*, 1991, **92**, 115–125.
29 T. Kelen and F. Tüdös, *J. Macromol. Sci. Part - Chem.*, 1975, **9**, 1–27.
30 A. Duda and A. Kowalski, in *Handbook of Ring-Opening Polymerization*, eds. P. Dubois, O. Coulembier and J.-M. Raquez, Wiley-VCH Verlag GmbH & Co. KGaA, Weinheim, Germany, 2009, pp. 1–51.

General conclusions and outlooks

In less than a century, plastic materials have become indispensable in our daily life. Their applications are now generalized to all essential sectors generating a huge amount of waste in cities, countries, forests, mountains and oceans, disturbing the life of our entire ecosystem. In that respect, chemical industries endeavor to limit their impact by substituting polymers from non-renewable resources by biosourced and biodegradable polyesters such as poly(lactide) (PLA) and poly(ε-caprolactone) (PCL).

This work aimed at developing innovative and sustainable synthetic strategies to lactide-based (*co*)polymers. The ring-opening (*co*)polymerization (RO(*c*)P) reactions have been catalyzed by natural or "copy-paste" from nature, cheap, commercially available and biocompatible organic molecules.

The **bibliographic chapter** has emphasized that organocatalysts have been highly studied over the last 20 years for the ring-opening polymerization (ROP) of *L*-lactide (*L*-LA) and ε-caprolactone (CL), however, some challenges remain to be tackled:

1) The first challenge consists in the organocatalyzed ROP (OROP) of *L*-LA in bulk requiring high temperature up to 180°C. Most of the organocatalysts attempted to fulfill this task have, indeed, met with limited success in part due to the thermal degradation of the basic-type catalysts traditionally used for this ROP in solution. Important side reactions, such as epimerization, that decrease the thermal and mechanical properties of the obtained poly(*L*-lactide) (PLLA), can occur as well. Diphenylphosphate (DPP), an acidic-type molecule, has shown to be the only organocatalyst to produce highly isotactic PLLA in bulk at high temperature but with a slow kinetic.

2) The second challenge is the discovery of organocatalysts able to conduct a truly statistical ring-opening copolymerization (RO*c*P) of lactide (LA) and CL in a controlled manner. Only a handful of organocatalysts has been attempted leading to either a faster kinetic rate of CL or LA in the course of the copolymerization. Indeed, basic-type organocatalysts lead to the generation of PLA free of CL unit, while acidic compounds have different behaviors depending on their nature.

Organocatalysts such as weak carboxylic acids have never been investigated to perform either the ROP of *L*-LA in bulk nor the RO*c*P of *L*-LA and CL. This work has thus evaluated this class of catalysts.

In the **second chapter**, dibenzoylmethane (DBM), a weak acidic, non-toxic and naturally occurring compound has been evaluated as organocatalyst for the statistical ring-opening copolymerization (RO*c*P) of *L*-LA and CL at 155 °C in presence of various alcohol initiators (Figure

1). A relatively good control has been achieved as attested by the linear evolution of the average molar mass determined by SEC ($M_{n,SEC}$) in function of the total monomer conversion (C_{TOT}) and the relatively low dispersity values. However, copolymer of high co-monomers–to-initiator ratios could not be afforded.

To gain insight into the copolymer structure, the reactivity ratios of both *L*-LA (r_{LA}) and CL (r_{CL}) have been determined by the Kelen-Tüdős linear method (KT) and the nonlinear method called "the visualization of the sum of squared residual space" (VSSRS). The structures of the copolymers have also been assessed by ^{1}H and ^{13}C NMR and differential scanning calorimetry (DSC). These combined analyses have revealed that a gradient-like copolymer is obtained at the early stage of the RO*c*P process, a statistical copolymer being formed at the later stage (Figure 1).

Investigation into the OROP of *L*-LA and CL and their kinetic have emphasized that DBM is a poor monomer and chain end activator, the acceleration of the RO*c*P process being eventually explained by the occurrence of side reactions. The carboxylic acids formed *in situ* by thermal degradation of the reagents and by the co-initiation by water may catalyze the DBM-ORO(*c*)P processes which can be viewed as self-catalyzed reactions.

Finally, application of miscellaneous carboxylic acids for this copolymerization has highlighted that benzoic acid (BA) is very interesting to trigger the statistical RO*c*P of *L*-LA and CL.

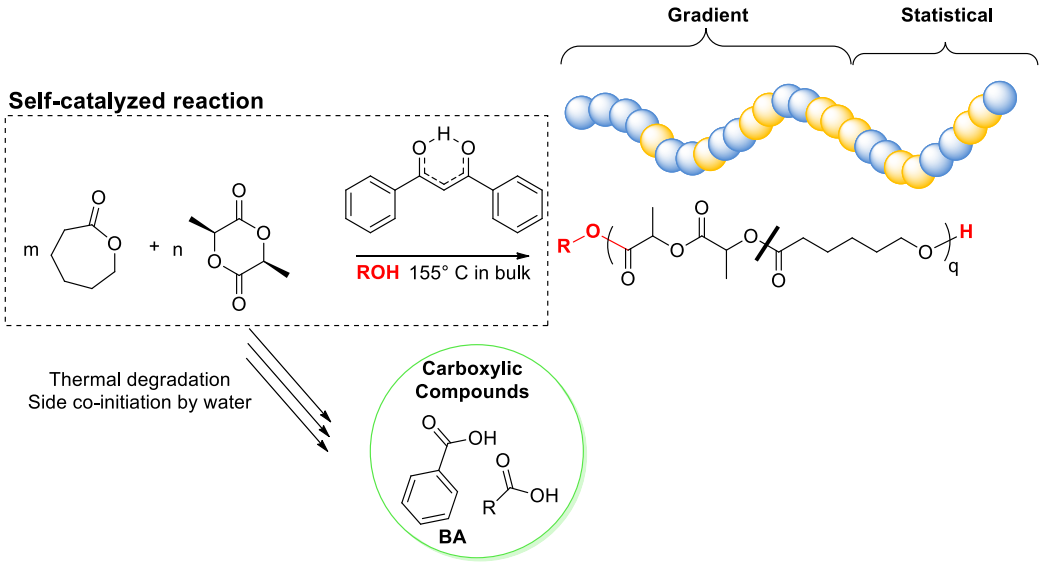

Figure 1. Self-catalyzed DBM-RO*c*P of *L*-LA and CL - **Chapter 2**.

The **third chapter** has thus been focused on the evaluation of BA for the OROP of *L*-LA and CL as preliminary investigations before conducting the BA-ORO*c*P of *L*-LA and CL in order to evaluate the control and the mechanism of these processes. This has been a good opportunity to evaluate the activity of BA for the bulk ROP of *L*-LA, which is also one of the challenges of this work.

The bulk BA-OROP of CL initiated by diols at 155°C exhibits a good control as attested by the linear evolution of $M_{n,SEC}$ in function of conversion, the narrow dispersity obtained, the high chain end fidelity and the possibility to extend the polymer chains (Figure 2, **2**). Initiating this ROP process with monoalcohol initiators between 80 and 155°C has, however, pointed out that some transfer reactions such as intermolecular transesterification may occur (Figure 2a, **8**). The use of diols has nevertheless limit the inconvenience of such transfer, *i.e.*, the increase of the dispersity values and the apparition of a second population in SEC analyses.

The BA-OROP of *L*-LA initiated by diols and monoalcohols at temperature up to 180°C exhibited a good control over the molar mass and the dispersity affording totally transparent PLAs (Figure 2, **6**). However, high molar masses cannot be achieved, and epimerization of *L*-LA has been shown to occur in the course of the ROP process leading to amorphous PLAs.

The possibility to extend the polymer chains has then been properly exploited in order to synthesize triblock copolymers, namely PLA-*b*-PCL-*b*-PLA from butane-1,4-diol (BD, Figure 2, **1**). This synthesis highlighted that no transfer reactions of the lactidyl chain end take place on the first PCL block precursor. In contrast, the reverse reaction, *i.e.* initiating the ROP of CL from a PLA precursor has not been successful as the secondary alcohol at the chain end of PLA could not efficiently initiate the ROP of CL (Figure 2, **5**).

Finally, kinetic studies and density functional theory (DFT) calculations have shown that BA is a monomer and chain end activator working *via* a bifunctional mechanism. Overall, BA is twenty times more efficient for the bulk ROP of CL than for the bulk ROP of *L*-LA. Such a trend was hypothetically explained by a more efficient activation of the carbonyl group of CL (as compared to the *L*-LA ones) potentially ascribed to the higher basicity of the former. A second explanation could be that the conjugated base of BA is too weak to efficiently activate the less nucleophilic and sterically hindered secondary alcohol at the chain end of PLA.

The first challenge, consisting in the controlled ROP of *L*-LA in bulk without occurrence of epimerization, has not been achieved. One can imagine that the highly thermally stable BA organocatalyst can also be combined with appropriate Brønsted base in order to form a salt which could efficiently trigger the bulk ROP of *L*-LA without epimerization.

However, organocatalysts being poorly efficient for the bulk ROP of *L*-LA, application of non-toxic metal-based catalysts, such as magnesium-, zinc-, potassium- or sodium-based, can be a good alternative.

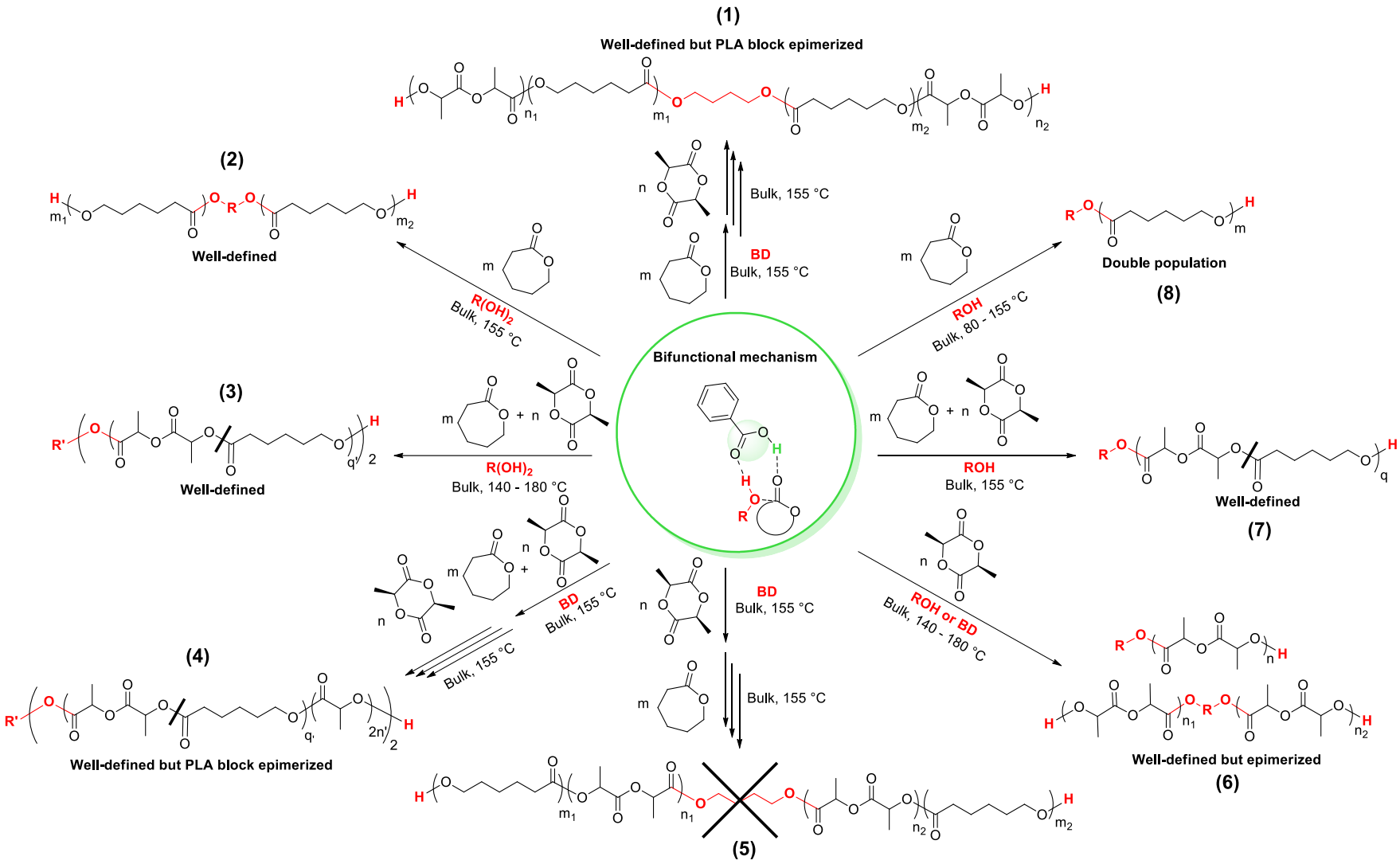

Figure 2. BA-ORO(*c*)P of CL and *L*-LA in bulk -**Chapters 3 and 4** - with q = n + m and n = n_1 + n_2 and m = m_1 + m_2 and 2q' = q and 2n' = n. R' = -CH_2-CH_2-CH_2-CH_2-.

In the **fourth chapter**, the bulk RO*c*P of *L*-LA and CL at high temperature (140 to 180° C) has been investigated in the presence of benzoic acid and various initiators, leading to a good level of control over the molar mass and the dispersity (Figure 2, **3** and **7**). A library of copolymers of varying *L*-LA/CL compositions have been synthesized in bulk at 155 °C. The statistical character of the as-obtained copolymers has been assessed by combined characterization techniques such as ^{1}H, ^{13}C and DOSY-NMR spectroscopy and by DSC. Application of the VSSRS method enabled to determine more reliable reactivity ratio values in disagreement to the one obtained using the KT linear method surely due to uncertainties in the NMR measurements at low conversions. The calculation of the reactivity ratios obtained by the VSSRS method has provided further proof of the statistical nature of the copolymers. The possibility to extend the copolymer chains has then been properly exploited in order to synthesize triblock copolymers, namely PLA-*b*-P(LA-*stat*-CL)-*b*-PLA (Figure 2, **4**).

Importantly, a new solvent-free purification method has been set up in chapter **3** and **4** in order to achieve highly pure PCL and P(LA-*stat*-CL) samples. The as-recovered BA could therefore be reused for subsequent organocatalytic cycles, and due to their easy removal, both monomers could be recycled too.

Finally, the reactivity of *L*-LA and CL in presence of different organocatalysts has been evaluated. This study has pointed out that the acidity/basicity of the organocatalyst is surely the main key parameter influencing the RO*c*P of *L*-LA and CL. Indeed, basic and nucleophilic molecules were found to preferentially inserted *L*-LA while the contrary happened when applying acidic compounds. The particular acidity of BA would activate more efficiently the carbonyl group of CL than those of *L*-LA compensating the higher capability of alcohol to polymerize *L*-LA over CL at high temperatures enabling this RO*c*P process. However, the acid/base character of the catalyst is not the only parameter influencing the RO*c*P and some moieties may have an influence such as intermolecular hydrogen bond donors or acceptors: for instance, fluorine atoms.

The second challenge, consisting in conducting the statistical RO*c*P of *L*-LA and CL has been successfully achieved using BA as organocatalyst. Some improvements should however be carried out such as the increase of the reaction kinetics. One can imagine that combining the proper Brønsted/Lewis base with the proper Brønsted/Lewis acid with precise molar ratio would enable to achieve statistical copolymers based on *L*-LA and CL. The (*co*)polymerization kinetic could maybe be increased, by transposing bulk copolymerization in reactive extrusion.

Additionally, BA has been shown to be very versatile, one can imagine that various structures such as star shaped or functionalized PLAs, PCLs, P(LA-*b*-CL)s and P(LA-*stat*-CL)s could be obtained applying this recyclable catalyst. Also, BA could be applied for the solvent- and metal-free ROP of other cyclic esters or cyclic carbonates, namely δ-valerolactone or

trimethylene carbonate, in order to carry out solvent- and metal-free ROP affording highly pur polymers

Finally, this work shows in background the difference of reactivity of *L*-LA and CL depending on the organocatalyst used. On the one hand, we showed that the ROP of *L*-LA is arduously conducted in presence of mild and weak acids maybe because its carbonyl groups are not enough basic to be activated. Another possible explanation could be that, the sterically hindered and less nucleophilic secondary alcohol may be highly activated to efficiently attack the sterically hindered carbonyl group of LA. On the other hand, it would be interesting to understand why the ROP of CL is hardly conducted without the presence of monomer activators. It would be interesting to determinate the basicity of the carbonyl groups of *L*-LA and CL or to evaluate the copolymerization propagation by DFT calculations. More studies are needed in order to better understand the reactivity of *L*-LA and CL monomers

Publications

- L. Mezzasalma, A.P. Dove, O. Coulembier, Organocatalytic ring-opening polymerization of l -lactide in bulk: A long standing challenge, European Polymer Journal. 95 (2017) 628–634. doi:10.1016/j.eurpolymj.2017.05.013.

- L. Mezzasalma, J. De Winter, D. Taton, O. Coulembier, Extending the Scope of Benign and Thermally Stable Organocatalysts: Application of Dibenzoylmethane for the Bulk Copolymerization of L-Lactide and ε-Caprolactone, Journal of Polymer Science Part A: Polymer Chemistry. 56 (2018) 475–479. doi:10.1002/pola.28921.

- L. Mezzasalma, J. De Winter, D. Taton, O. Coulembier, Benzoic acid-organocatalyzed ring-opening (co)polymerization (ORO(c)P) of L-lactide and ε-caprolactone under solvent-free conditions: from simplicity to recyclability, Green Chemistry. 20 (2018) 5385–5396. doi:10.1039/C8GC03096K.

- L. Mezzasalma, S. Harrisson, S. Saba,‖ P. Loyer,‖ O. Coulembier, D. Taton, Bulk Organocatalytic Synthetic Access to Statistical Copolyesters from *L*-Lactide and ε-Caprolactone Using Benzoic Acid, submitted to biomacromolecules.

- Another publication concerning the mechanistic aspect of the BA-OROcP of *L*-lactide and ε-caprolactone is in progress.